STRUCTURAL ~~AND~~/THERMODYNAMIC STUDIES OF POLYANIONIC MELTS.

Thesis

presented for the degree

of

DOCTOR OF PHILOSOPHY

in the

University of London

by

RAMAMRITHAM SRIDHAR

Nuffield Research Group,
Department of Metallurgy,
Royal School of Mines,
Imperial College of Science and Technology,
London, S.W.7.

June 1967.

ABSTRACT

The distributions of polyanions in binary phosphate glasses of sodium, cadmium, magnesium and lead oxides were determined by a paper chromatographic technique. The effect of making these glasses with rigid exclusion of moisture and the effect of quenching rates on the constitution of these glasses were investigated. The results indicate that the distributions are a function of cation and the mean chain length $\bar{n}$. The breadth of these distributions is directly related to the shape of the heat of formation curve for the glasses (from the constituent oxide), and to the cation radius to charge ratio of the cation to the extent this determines the heat of formation. The glasses made under dry conditions and also by fast quenching had anion distributions the same as those made in the conventional manner.

The thermodynamic properties of PbO, PbO+SiO_2, PbO+P_2O_5, PbO+B_2O_3 and PbO+PbF_2 melts were obtained by measuring the emf of the cell,

Pb / PbO containing melts / O_2 : Pt

The measurements were usually carried out in the temperature range 850°C to 1050°C. From the emf and its dependence on temperature the activities of PbO, and the partial free energies, heats and entropies of solution of PbO in PbO + SiO_2, PbO + P_2O_5, PbO + B_2O_3 and PbO + PbF_2 melts were derived .The corresponding

thermodynamic properties of the other components in these binary were derived using the Gibbs-Duhem relationship and these were combined with those for PbO to obtain the integral thermodynamic properties.

The interpretation of observed PbO activities for the lead borate and Phosphate melts, more basic than the ortho composition, in terms of structural models seems to indicate the presence of three and four co-ordinated boron atoms in the borates and the possible existence of five co-ordinated Phosphorus atoms in the phosphate. The structural information gained on the phosphate glasses has been extended to the silicate and borate systems. Various available models, which relate the thermodynamic properties andstructure of these polyanionic melts are assessed;It seems that Meadowcroft and Richardson's model is the only one capable of relating quantitatively the structure and thermodynamic properties of such melts. The thermodynamic data obtained for PbO + PbF_2 melts shows these to be regular solutions, with an ideal entropy of mixing as defined by Temkin.

Unsuccessful attempts to study the anionic distribution in silicate glasses by a chromatographic separation technique are described in the appendix.

TABLE OF CONTENTS

PART - A

GENERAL INTRODUCTION

PART - B

STRUCTURAL STUDIES OF PHOSPHATE GLASSES

PART - C

THERMODYNAMICS OF PbO, $PbO-SiO_2$, $PbO-B_2O_3$ and $PbO-PbF_2$ MELTS

PART A

GENERAL INTRODUCTION

Chapter 1

(i) Introduction:

The structural and thermodynamic aspects of slags are of interest to glass technologists and in particular to the metallurgists. Since the majority of slags encountered in extraction metallurgy are silicates, in recent years much research has been directed towards understanding the structure and thermodynamics of these systems.

First studies on the activities of oxides in complex slags were made by Chipman and co-workers[1,2]. These were then extended to binary[3,4,5,6], ternary[7,6] and multicomponent[8] oxide-silica melts to understand the thermodynamics of one or more oxide additions to silica. On the other hand the work of Bockris and co-workers on the electrochemistry of silicates[9,10] showed these melts to be ionic in character. Further work on the transport properties including viscosity[11] yielded a picture of molten silicates as ionic melts, with cations responsible for carrying the current and moving through a large network of silicate anions - which are responsible for the high viscosity. Studies on borate[12] and phosphate[13] melts and glasses have shown these solutions to be polyanionic in nature - resembling the silicates. A systematic

study of silicate, phosphate and borate systems was necessary to understand more fully their thermodynamic and structural behaviour and more so the inter-relation of these two properties for such polyanionic melts.

(ii) Some Theories Concerning Activities in Melts:

The following theories applicable to ionic salt mixtures are of interest in view of the ionic nature of these oxide solutions.

(a) Herasymenko Model

The first attempt at introducing the concentrations of a particular ion, rather than that of a neutral molecule, in ionic melts is due to Herasymenko[14]. He defined the activity of a component in an ideal ionic mixture as follows:-

$$a_{M_1A_1} = \frac{n_{M_1^+}}{\Sigma n_{M_1^+} + \Sigma n_{A_1^-}} \cdot \frac{n_{A_1^-}}{\Sigma n_{M_1^+} + \Sigma n_{A_1^-}}$$

Where $n_{M_1^+}$ is the number of M_1^+ cations, $n_{A_1^-}$ is the number of A_1^- anions and $\Sigma n_{M_1^+}$ and Σn_{A^-} are the total number of cations and anions respectively in the mixture.

This requires the cations and anions to be randomly distributed. For this to happen the heat movements should be so vigorous, that they overcome the electrostatic binding energy between oppositely charged particles. Flood, Forland and Grjotheim[15] have pointed out that for sodium chloride, this energy requirement will not be met below 100,000°C. Thus Herasymenko's model is considered unreasonable.

(b) Temkin Model

Temkin[16] formulated the activity of the component M_1A_1 of an ionic mixture as:-

$$a_{M_1A_1} = \frac{n_{M_1^+}}{\Sigma n_{M_1^+}} \cdot \frac{n_{A_1^-}}{\Sigma n_{A_1^-}} = N_{M_1^+} \cdot N_{A_1^-}$$

Where $N_{M_1^+}$ and $N_{A_1^-}$ are the cation and anion fractions.

According to this model, cations are surrounded by anions only and vice versa, while the cations as well as the anions are randomly distributed among themselves. This is energetically more reasonable to expect than Herasymenko's model.

Temkin's model can be applied to a binary silicate melt containing 0 to 33% (mole) SiO_2 (i.e. up to orthosilicate composition). If the breakdown of the silicate network follows the pattern established in the solids (cf Chaper 2(a)), the melt in this range would contain M^{2+}, SiO_4^{4-} and O^{2-} ions, except at and beyond $N_{SiO_2} = 0.33$ when the amount of free O^{2-} ions should become zero. The activity of metal oxide will be given by:-

$$a_{MO} = N_{M^{2+}} \cdot N_{O^{2-}}$$

$$= N_{O^{2-}}$$

since the cationic mole fraction $N_{M^{2+}} = 1$

also,

$$N_{O^{2-}} = \frac{n_{O^{2-}}}{n_{O^{2-}} + n_{SiO_4^{4-}}}$$

This would give a metal oxide activity in a binary silicate melt at and above $N_{SiO_2} = 0.33$ to be zero. However, in practice this is never the case because of the equilibria between the various silicate and oxygen anions and these have to be precisely known before the Temkin model can be applied to such melts.

(c) Flood, Forland and Grjotheim[17] Model

These authors based their model on the similarity between the solid and liquid states for the salt mixtures. They formulated the activity of a component in the salt mixture to be:-

$$a_{M_1A_1} = N^1_{M_1^+} \cdot N^1_{A_1^-}$$

Where $N^1_{M_1^+}$ and $N^1_{A_1^-}$ are equivalent ionic fractions. For example, $N^1_{Na^+}$ is defined in a $NaCl-CaCl_2$ mixture as:-

$$N^1_{Na} = \frac{n_{Na^+}}{n_{Na^+} + n_v + n_{Ca^{2+}}} = \frac{n_{Na^+}}{n_{Na^+} + 2n_{Ca^{2+}}}$$

because $2Na^+$ ions can be replaced by one vacancy and one Ca^{2+} ion.

This model over-emphasizes the similarity between the solid and liquid and one would expect it to be less applicable far from the melting point. [17a]

(d) Flood, Forland and Grjotheim[18] Regular Solution Model

In this model the mixture of ionic solutions is considered to be regular, that is to say, ideal entropy of mixing with some heat of mixing. The activity of component M_1A_1 in a mixture is given by:-

$$a_{M_1A_1} = N_{M_1^+} \cdot N_{A_1^-} \gamma$$

Where $N_{M_1^+}$ and $N_{A_1^-}$ are ionic fractions defined by Temkin.

From electrostatic considerations for a solution containing Na^+, Cl^- K^+, Br^- ions (e.g. KBr + NaCl mixture), Flood et al derived the following expression for the activity coefficient γ

$$\gamma NaCl = \exp. N^1_{K^+} . N^1_{Br^-} \frac{\Delta G_{KBr}}{RT}$$

Where $N^1_{K^+}$ and $N^1_{Br^-}$ are the equivalent ion fractions (would be the same as Temkin mole fraction for mixtures of ions of same valency) and ΔG is the standard free energy of the reaction:-

$$NaBr(l) + KCl(l) = NaCl(l) + KBr(l)$$

Flood, Forland and Grjotheim[15] applied this theory to basic open-hearth slags; it was assumed that the principal ions in solution are Ca^{2+}, Mg^{2+}, Fe^{2+}, SiO_4^{4-} and O^{2-}. In this case γFeO is given by:-

$$RT \ln \gamma FeO = N_{Ca^{2+}} . N_{SiO_4^{4-}} (-\Delta G^\circ_1) + N_{Mg^{2+}} . N_{SiO_4^{4-}} (-\Delta G^\circ_2)$$

Where ΔG°_1 and ΔG°_2 are the free energy changes for the exchange reactions.

$$FeO + \tfrac{1}{2} Ca_2 SiO_4 = \tfrac{1}{2} Fe_2 SiO_4 + CaO$$

and $$FeO + \tfrac{1}{2} Mg_2 SiO_4 = \tfrac{1}{2} Fe_2 SiO_4 + MgO$$

When applied to experimental data this theory fits observed values for FeO in such melts up to $N_{SiO_2} = 0.25$ but above this the deviation is high. This is understandable since O^{2-} and SiO_4^{4-} would cease to be the only main constituent anions in these melts because more complex silicate anions would be present as the mole fraction of silica is increased.

(e) Richardson's Ideal Mixing Theory

Richardson[19] has extended Temkin's type approach to predict activities in ternary silicate melts from available binary data. This treatment assumes that the free energy of mixing of a binary silicate melt (such as $CaO-SiO_2$) with another (such as $FeO-SiO_2$) of similar metal oxide to silica ratio is ideal, i.e. the heat of mixing is zero and that the entropy of mixing is only the configurational one of mixing the cations in a constant anionic matrix. It is then possible to calculate the free energy of mixing of these two silicates from the pure component oxides. From these integral curves, for example at a constant CaO/SiO_2 ratio, the partial free energy and hence the activity, a_{FeO} can be obtained by the tangent intercept method.

Because of the difficulty in drawing accurate tangents, an alternative approach has been used by Richardson in which the activity of SiO_2 in the ternary is extrapolated as follows:-

$$\log (a_{SiO_2})_{\text{ternary}} = \frac{N_{CaO}}{N_{CaO} + N_{FeO}} \log (a_{SiO_2})_{CaO-SiO_2} + \frac{N_{FeO}}{N_{FeO} + N_{CaO}} \log (a_{SiO_2})_{FeO-SiO_2}$$

From the assumption of ideal mixing,

$$a_{(x\ FeO.SiO_2)} = N^{x}_{(x\ FeO.SiO_2)}$$

and also,

$$a_{(x\ FeO.SiO_2)} = \frac{a^{x}_{FeO} \cdot a_{SiO_2}\ (\text{ternary})}{a^{x}_{FeO} \cdot a_{SiO_2}\ (\text{Binary})} = N^{x}_{(x\ FeO.SiO_2)}$$

The only unknown is a^{x}_{FeO} in the ternary which can be readily calculated.

This model fits well with experimental data in the metasilicate region but not so well near the orthosilicate region. This has been explained as due to the possible reactions of the type:-

$$3\ Ca_2SiO_4 + Fe_2SiO_4 = 2\ Ca_3Si_2O_7 + 2\ FeO$$

This again points towards the need for the better understanding of the anion equilibria in these silicate melts.

(f) Lumsden's Theory

Lumsden[20] has shown that the heat of mixing in a molten mixture of alkali halides (with a common anion) can be calculated by estimating the polar interactions, giving a polarisation energy and an energy term due to non-polar London forces. For a mixture of NaCl and KCl this can be expressed as:-

$$RT\ \ln\ \gamma_{NaCl} = K\ N^2_{KCl}$$

Where $K = K_L + K_p$ which are determined from the London forces and polarisation forces respectively. This theory is in good agreement, for simple alkali halide mixtures, with available data, but is not easily applicable for complex melts such as the silicates and phosphates for which the London and polarisation force constants are difficult to estimate.

Lumsden[21] has used a similar approach for calculating activities in the system FeO-$FeO_{1.5}$-SiO_2 by assuming the binary and ternary solutions to be regular. Here he has calculated the interaction paramer 'K' from available experimental data instead of estimating it

as in the case of alkali halides. In calculating these parameters Lumsden considers the silicate anions to be present as Si^{4+} and O^{2-} ions, though the existence of Si^{4+} ions in the silicate melts is improbable. The values obtained for the ternary are in good agreement with observed data, but this approach gives the melting point of silica to be 4,700°K, whereas the known value is 1980°K. To explain this discrepancy Lumsden has postulated a standard state of silica in which Si^{4+} ions and O^{2-} ions are distributed at random. Besides this limitation it is doubtful whether the regular solution approach will be applicable to systems like $CaO-SiO_2$ with very high interaction parameters, in which the ions cannot be considered as mixing randomly.

In general it can be seen that a better knowledge of the anionic structure of these polyanionic melts is essential for applying the various thermodynamic models of ionic solutions discussed above.

Chapter 2

Structure of Crystalline Silicates, Phosphates and Borates

(a) Silicates [22,23]

In silicates the silicon is tetrahedrally co-ordinated with oxygen. A convenient way of classifying these silicates is according to the arrangement of the SiO_4 tetrahedra. Silicates with an unshared SiO_4^{4-} tetrahedron are called orthosilicates. These occur in minerals such as divine which have the general formula M_2SiO_4, where M is a divalent metal (Mg, Fe, Mn) or a mixture of such metals. The SiO_4^{4-} has been diagramatically represented in fig. 1 (a).

When one of the oxygen ions is shared between two SiO_4 tetrahedra, the pyrosilicate ($Si_2O_7^{6-}$, fig. 1 (b) ion results which has been characterised for example in $SC_2Si_2O_7$. The sharing of two oxygens of a SiO_4 tetrahedron with two other tetrahedra would result either in closed rings or infinite chains of general formula $(SiO_3)_n^{2n-}$. Of the cyclic silicon-oxygen complexes only the $Si_3O_9^{6-}$ (fig. 1 (c)) and $Si_6O_{18}^{12-}$ ions are known to exist as discrete ions in crystalline silicates. On the other hand a large variety of chain type structure are known. They are the pyroxenes fig. 1 (d), amphibole double chains, fig. 1 (e), Mica networks with $[Si_2O_5]_\infty$ with hexagonal rings, wollastonite chains $[Si_3O_9]_\infty$, xonotlite ribbons $[Si_6O_{17}]_\infty$, okenite networks with alternating 5 and 8 membered rings and finally apophyllite networks with alternating 4 and 7 membered rings.

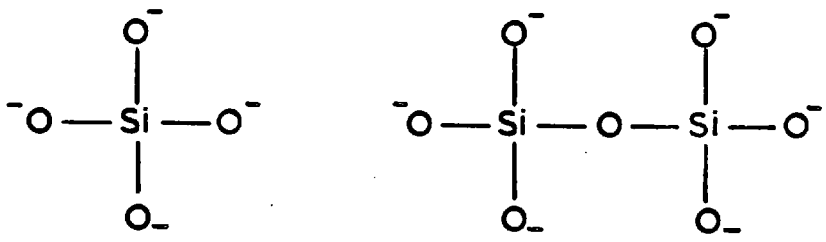

(a)

(b)

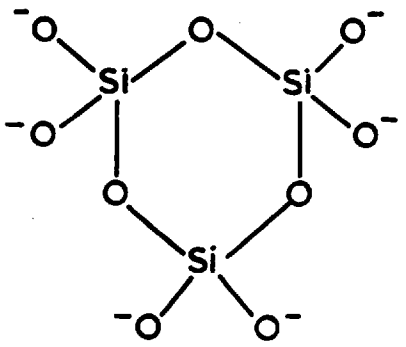

(c)

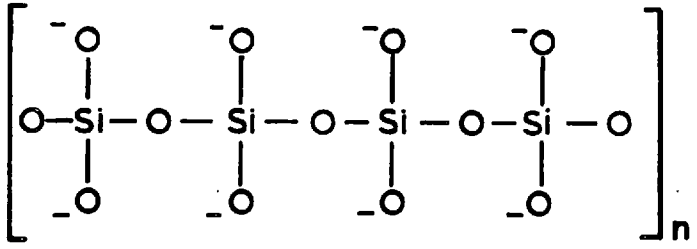

(d)

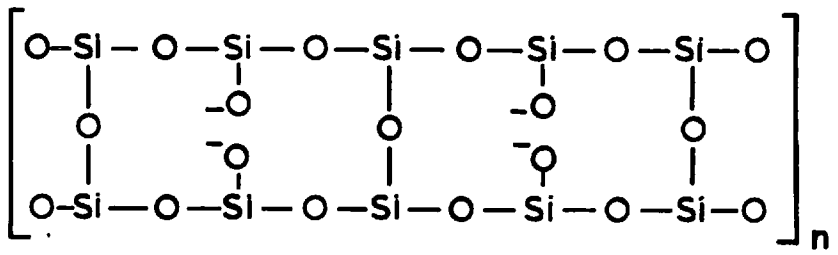

(e)

FIG. 1 DIAGRAMATIC REPRESENTATION OF ANIONIC STRUCTURES IN SILICATES

The sharing of three O atoms of each SiO_4 tetrahedron with other tetrahedra give systems of compositions $(Si_2O_5)_n^{2n-}$. These could be finite or infinite in one, two or three dimensions. Though no finite ions of the type $(Si_2O_5)_n^{2n-}$ have been isolated, many crystalline silicates of this formula with layer structure have been identified. Finally the sharing of all corners of each SiO_4 tetrahedron leads to infinite three dimensional frameworks as in the various forms of silica.

(b) Phosphates[13,22]

Phosphorus, even though has one more electron in its outter shell than silicon, is mainly tetrahedrally co-ordinated with oxygen in phosphates, which makes the structural chemistry of phosphates similar to silicates. Thus, similarly we can consider the phosphates according to the arrangment of PO_4 tetrahedra. The phosphates with discrete PO_4^{3-} ions (fig. 2 (a)) are termed orthophosphates and numerous crystalline orthophosphates, example, Na_3PO_4, Li_3PO_4, YPO_4 have been structurally investigated. The sharing of one O atom between two PO_4 tetrahedra leads to the formation of pyrophosphate ($P_2O_7^{4-}$) anion (fig. 2 (b)). The existence of various crystalline pyrophosphates example ZrP_2O_7, $Na_4P_2O_7$ have been confirmed. The sharing of two O atoms of a PO_4 tetrahedra with two other tetrahedra can either lead to ring phosphates or infinite chains of formula $(PO_3)_n^{n-}$. In case of rings, $P_3O_9^{3-}$ (fig. 2 (c)) and $P_4O_{12}^{4-}$ are known as discrete ions in the crystalline phosphates, whereas $Si_3O_9^{6-}$ and $Si_6O_{18}^{12-}$ occur in the case of crystalline silicates. The long chain phosphates of general formula $(PO_3)_n^{n-}$ (fig. 2 (d)) have been crystallised in the form of

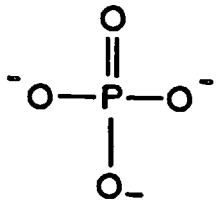

(a)

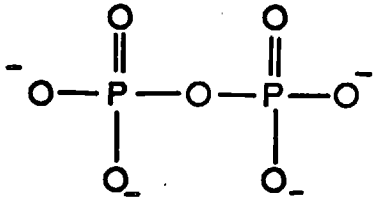

(b)

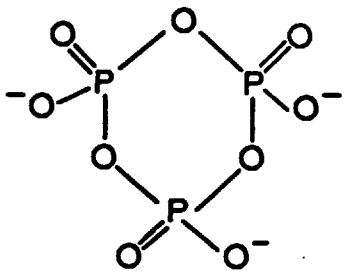

(c)

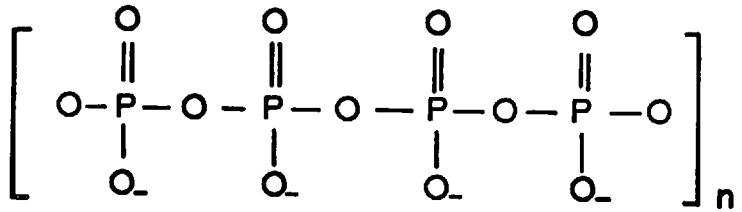

(d)

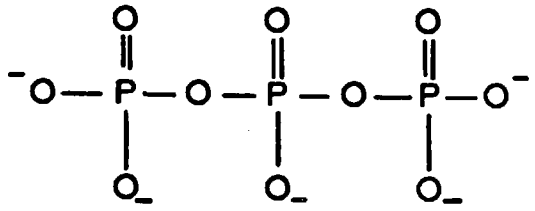

(e)

FIG. 2 DIAGRAMATIC REPRESENTATION OF ANIONIC STRUCTURES IN PHOSPHATES

Kurrol and Mandrell salts.

Though the existence of chain silicates in the composition range of pyro to metasilicate have been postulated, only in the case of the phosphates the crystalline varities have been isolated in this composition range. The crystalline tripoly phosphate, $P_3O_{10}^{5-}$ (fig. 2 (e) occurs in the sodium system, whereas the tetrapoly $P_4O_{13}^{6-}$ and pentapoly $P_5O_{16}^{7-}$ have been reported in the lead and calcium respectively.

Finally, sharing of all three available O atoms in each PO_4 tetrahedron results in the formation of P_2O_5 which occurs as P_4O_{10} molecules or as an infinite array of PO_4 tetrahedra forming rings to build up a three dimensional network. The availability of one oxygen less in case of PO_4 tetrahedra, because of one double bonded oxygen, restricts the number of arrangements when compared to those of SiO_4 tetrahedra. Thus in general leads to a less complex structure in the phosphate when compared to the silicate of same basicity.

(c) Borates[22]

The structural chemistry of borates when compared to the silicates and phosphates is more complex due to the possibility of both three and four co-ordination of Boron in these compounds. No general rule has been established for the preferential stability of three or four co-ordinated borons. To take first the borates with boron in three fold co-ordination with oxygen, these can again be considered according to the arrangement of the BO_3 groups. The orthoborates with BO_3^{3-} groups (fig. 3 (a)) have been isolated, for example $ScBO_3$,

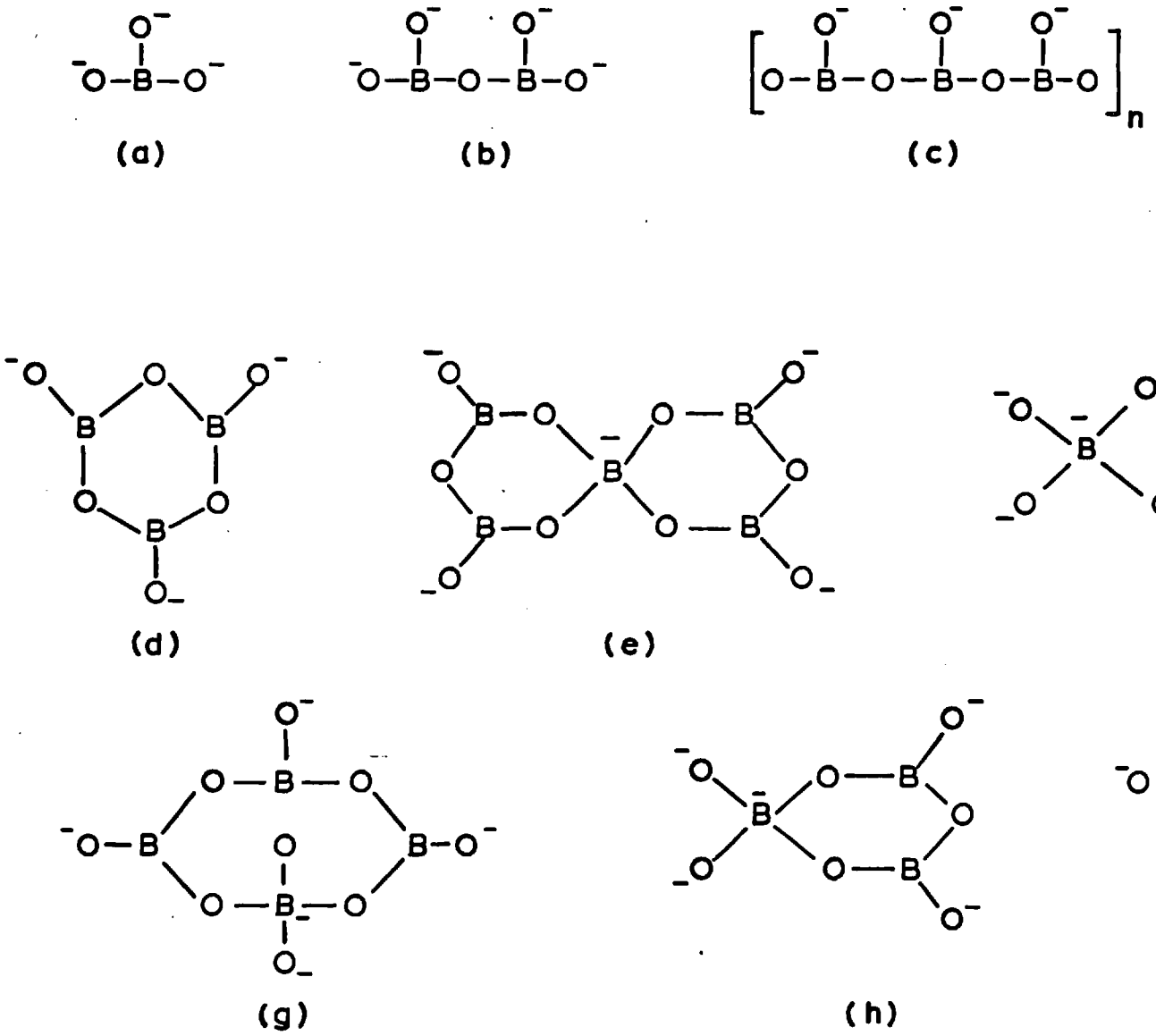

FIG.3 DIAGRAMATIC REPRESENTATION OF ANIONIC STRUCTURES IN BORATES

YBO_3; the pyroborates, with two BO_3 groups sharing an O atom (forming the $B_2O_5^{4-}$ ion, (fig. 3 (b)) have been found as the cobalt and magnesium salts. The metaborates in which two O atoms of BO_3 groups are shared, with a general formula $(BO_3)_n^{n-}$ exist both as long chain polymer (fig. 3 (c)) as in CaB_2O_4, and in the ring structure (fig. 3 (d)) as in $Na_3B_3O_6$. In B_2O_3 it is generally believed that all the three O atoms in three co-ordinated BO_3 groups are shared amongst themselves leading to a three dimensional network.

Some cyclic borate ions can be built from planar BO_3 and tetrahedrally co-ordinated BO_4 groups. The main examples of crystalline borates of this type are the various hydrated borates, but tetrahedral co-ordination may well also occur in anhydrous borates, for which the studies are limited. The Spiro ion, $B_5O_{10}^{5-}$ (fig. 3 (e))occurs in $KH_4B_5O_{10}\cdot 2H_2O$ which contains one BO_4 group and four BO_3 groups. When these join into a helix this leads to the crystalline borate KB_5O_8. Two BO_4 groups and one BO_3 gives the ion $B_3O_8^{7-}$ (fig. 3 (f)) which occurs as $CaH_5B_3O_8.H_2O$. Joining of two BO_4 and two BO_3 groups give the ion $B_4O_9^{6-}$ (fig. 3 (g)) occuring naturally as borax $Na_2.H_4B_4O_9.8H_2O$. The three dimensional frame work ion occur in $C_sB_5O_8$ in which a unit containing one BO_4 and two BO_3 (fig. 3 (h)) form rings which are joined together as a helix. There are also examples of borates which contain only tetrahedrally co-ordinated boron (fig. 3 (i)), for example in BPO_4, $BAsO_4$.

Chapter 3

Structure of Molten Silicates, Phosphates and Borates

Crystalline structures and that in the liquid state differ in the thermal energy involved in the latter. This energy can be high enough to make and break the oxygen to Silicon, Phosphorus or Boron bonds and rearrange the ions to give a completely different structure from that in the crystal. This was first postulated for silicates by Richardson[24] and has been shown to be the case in the phosphates[25]. For example when crystalline $Na_5P_3O_{10}$ with $P_3O_{10}^{5-}$ ion is melted and quenched rapidly to a glass, and the resulting glass analysed paper chromatographically, the anion distribution has been found to be:-

	Ortho.	Pyro.	Tripoly.	Tetrapoly.	Pentapoly.	Hexapoly.
	PO_4^{3-}	$P_2O_7^{4-}$	$P_3O_{10}^{5-}$	$P_4O_{13}^{6-}$	$P_5O_{16}^{7-}$	$P_6O_{19}^{8-}$
%	0.00	22.69	49.36	21.48	5.48	0.93

instead of being 100% $P_3O_{10}^{5-}$ as in the room temperature crystal. Using ion-exchange chromatography range of chain anions containing up to 15 Phosphorus atoms per chain, have been isolated in glassy phosphoric acid[26] and sodium metaphosphate[27].

Because of this difference between the solid and liquid state, to gain a knowledge of the structure of the liquid silicates, borates or phosphates, it is desirable to determine the exact amounts of various anions present in these melts. Unfortunately no direct method exists for doing this at the present time. Hence, we have

to resort to some indirect method to get an idea about the structure in the liquid state. One of the methods by which we can do this .. in the case of phosphates, is to study the anion distribution in the quenched glass using the chromatographic technique. (This method has been employed in this study and would be described fully in Part B). Here it is assumed that structure of the liquid is frozen in the phosphate glass. Unfortunately however, no such method exists for silicates and borates. In the case of the silicates, Lentz[28] has attempted to extract the structure from crystalline mineral silicates but there are inherent difficulties in the method (which are dealt with in the appendix) and it does not yield any useful results. Hence, at the present time, there is only the possibility of extending our observations on the phosphates to the silicate and borate systems.

A different approach to this problem of structure is by interpret ing the available thermodynamic data in terms of structural models. As these models will be dealt with in detail in Part D only they are briefly mentioned here. Richardson[29] has suggested that in a silicate melt an equilibrium of the type:-

$$2(\gtrless Si\text{-}O^-) = \gtrless Si\text{-}O\text{-}Si\lessgtr + O^{2-}$$

or $2\,O^- = O^0 + O^{2-}$

between the doubly bonded, singly bonded and non bonded oxygen can occur. The equilibrium constant for such a reaction will be given by:-

$$K = \frac{a_{O^{\circ}} \cdot a_{O^{2-}}}{a^2_{O^-}} \qquad (A.1.)$$

The K varies with temperature and is characteristic of the cations present in any binary or ternary silicate melt. The existence of such an equilibrium would correspond to the equilibrium existing between various anions in the melt. In terms of free energy of mixing curves for MO and SiO_2 this would mean that for a system with a shallow ΔG^M curve, the distribution will be wider than for a system with a peaked ΔG^M curve. This can be seem with the help of fig. 4. in which curves 1 and 2 represent the free energy of mixing for two binary silicate melts. For the purpose of argument, let a melt of composition $N_{SiO_2} = 0.5$ dissociate into a distribution which can be represented by a mixture of anions at A and B. The increment in energy in the two cases will be G_1 and G_2. That is to achieve the same distribution in system 2 as in system 1, we need a bigger energy change for the former. Conversely for a given energy change (supplied by the thermal energy) a wider distribution of anions will be formed in system 1 with a shallower free energy of mixing curve than that in system 2, when there is a possibility of forming a distribution. This approach gives us only a qualitative idea of the anionic distribution but more recently Meadowcroft and Richardson[25] have put forwared somewhat different model which seemsto be more valuable in understanding the relation between the thermodynamics and structure of such melts. Their treatment will be discussed in detail in Parts B and D.

Toop and Samis[30] have used Richardson's older

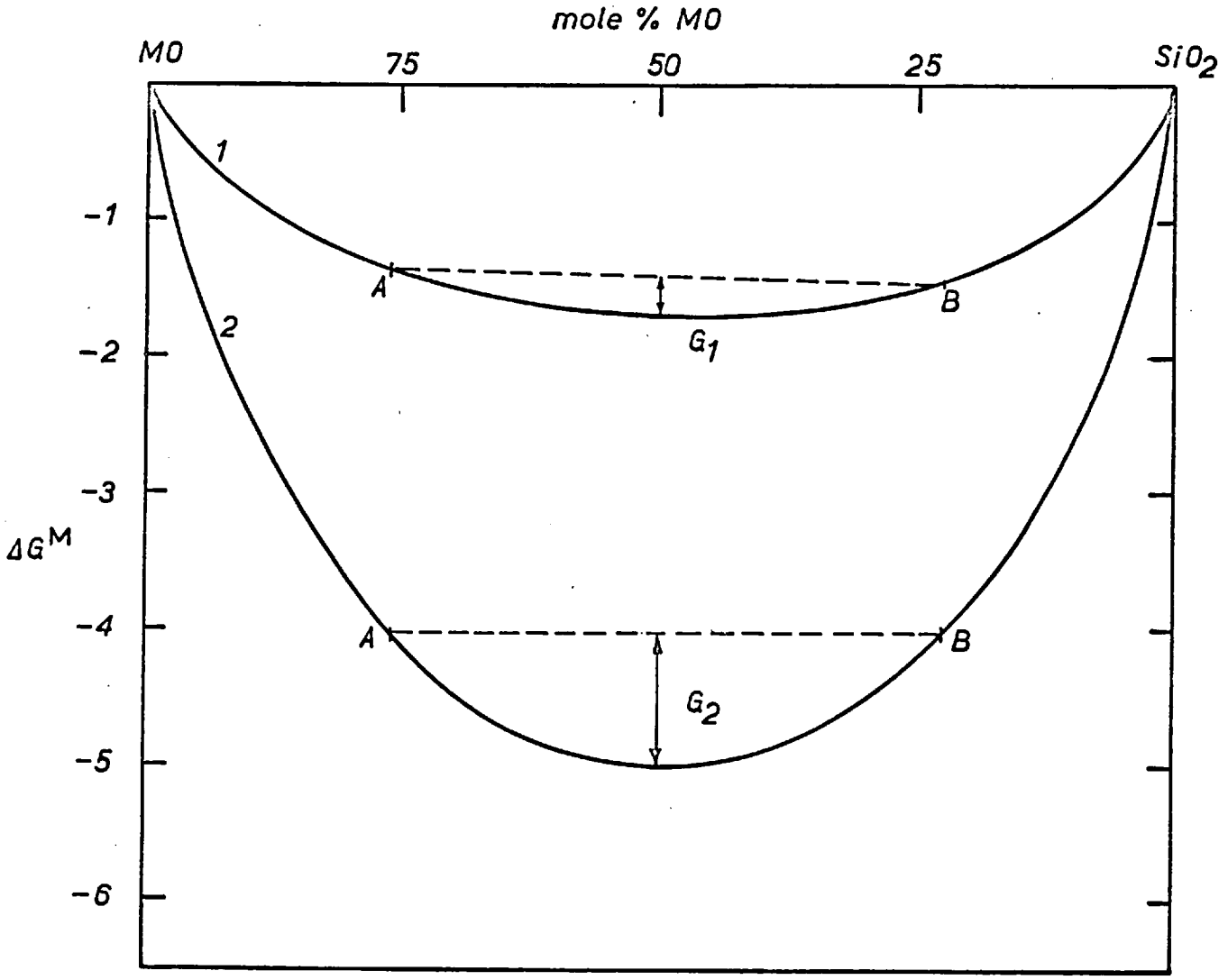

FIG.4 ΔG^M CURVE FOR TWO BINARY SILICATES

approach and have substituted values for K in equation A.1 and derived free energy versus composition curves, which they claim have a similar shape to the integral free energy of mixing curves for the binary silicates. From this they have concluded that the ΔG^M in silicate melts is due to interaction between oxygen ions and silica only. They have also tried to inter-relate the values of K silica molefraction and the average number of Si atoms per ion in these melts.

More recently Masson[31] has used a model which is similar to Richardson's newer approach, specially for considering silicate melts in the basic region where crosslinking may be regarded as relatively unimportant. Some attempts have also been made by Flood and co-workers[32,33] to infer the type of anions present in borate and silicate melts, using the depression in freezing point from the phase diagrams. Also Flood and Knapp[34] have tried to fit activity data in $PbO-SiO_2$ melts assuming the anions present to be O^{2-}, SiO_4^{4-}, $(SiO_3)_3^{6-}$ and $(SiO_{2.5})_6^{6-}$. It seems unlikely that only these four anions will be present in lead silicate melts. As mentioned before these models and their merits and demerits will be discussed in detail later in part D.

Chapter 4

Object and Scope of this Investigation

From the preceding chapters it can be seen that we need to have a better knowledge of the structure of these polyanionic liquids not only to understand their structural chemistry but also to be able to apply the various available thermodynamic models of melts.

In this direction it was decided to attempt to elucidate the silicate structures from the corresponding glass by a chemical treatment followed by a chromatographic separation as has been done previously with phosphates. In case of phosphates an extension of Meadowcroft and Richardson's[25] work was thought desirable. A possible criticism of their work could be the effect of small amounts of water dissolved in these melts. This could be tested by preparing these glasses under dry conditions and to check the difference, if any in the anionic distributions. Extending their study to other binary phosphate systems was necessary to have a better understanding of the effect of various cations on the anionic distributions. Further the influence of cooling rate on the chain distribution need to be investigated to show up any differences in structure corresponding to changes produced in glass temperatures by this means.

On the other hand the lack of thermodynamic data on molten phosphates made it difficult to understand the relationship

between the structural data available for these systems and the thermodynamic properties. In order to overcome this to a degree it was decided to study activities of PbO in PbO-P_2O_5 melts together with anion distributions in the corresponding glasses. To do this the applicability of the e.m.f. technique employed by Ito and Yanagase[35] for lead silicates using the cell

$$Pb \mid PbO\text{-}SiO_2 \text{ melts} \mid O_2:Pt$$

was interesting to investigate. Also it was useful to extend the work of Ito and Yanagse on lead silicates over a wider range of compositions and temperatures. The determination of lead oxide activities in these melts from the e.m.f. of the above cell requires a knowledge of the thermodynamics of PbO in the same temperature range. Since there is a disagreement between the reported thermodynamic data for liquid PbO, it was necessary to determine these values using lead oxide as the electrolyte in the above cell.

The possibility of the use of similar cells to investigate the thermodynamics of other polyanionic melts containing lead oxide led to the study of PbO-B_2O_3 and PbO-PbF_2 melts. Here again attempts have been made to relate the thermodynamic data obtained in terms of structural models, based on available data, and to make comparisons between the four binary systems containing PbO which have been investigated.

PART B

STRUCTURAL STUDIES OF PHOSPHATE GLASSES

Chapter 5

(i) Introduction

Like the silicates, phosphates can be obtained as glasses, merely by quenching the melts sufficiently fast, and thereafter the glasses are stable at room temperature. As mentioned briefly in Chapter 3, the study of phosphate glasses is of interest in understanding the structure of these and other polyanionic melts like the silicates and borates.

The phosphate glasses and the corresponding crystals can be dissolved in water (either simply or in the presence of agents to complex the cations), without the lengths of phosphate chain anions being altered. The resulting solution can then be analysed chromatographically and the proportion of different anions (hereafter referred to as the anionic distribution) thereby determined. Determination of anionic distribution of alkali phosphate glasses using filter paper chromatography have been reported by Westman and Gartaganis[36]. Meadowcroft and Richardson[25] confirmed their results for the alkali phosphate glasses and extended the study to alkaline earth glasses. Recently Cripps-Clark has studied more completely the $ZnO-P_2O_5$ system and made some preliminary investigations in the $PbO-P_2O_5$

system. These studies showed that not only the metal oxide to phosphorus pentoxide ratio but also the identity of the cations had a pronounced influence on the anionic distributions in these glasses.

One possible criticism of these studies is the chance of dissolution of small amounts of water in the glasses, since these were made by melting in air and subsequent quenching. Meadowcroft and Richardson observed that, in their experimental distributions the number of anions was in no case greater than 8%. They pointed out that the extra anions could be caused by the presence of small amounts of water in the melt, which would mean that the distributions obtained would correspond to a ternary glass with small amounts of H_2O and not to a binary. To clarify this uncertainty an apparatus was designed in which the glass could be melted and quenched under controlled atmospheres with the rigid exclusion of moisture.

In all these cases, the anionic distributions obtained were those corresponding to the glass transition temperatures, which are the temperatures at which the glasses are in internal equilibrium with corresponding supercooled liquids. Cripps Clark[37] determined these temperatures using a D.T.A. technique and found that they varied from 270°C, for Na_2O-P_2O_5 system, to 550°C for the CaO-P_2O_5 system, but did not vary much with the composition within a particular binary. Since, however, the object was to investigate the structures in the melt, it would be desirable to know the change in distribution for a system at a given composition at higher glass temperatures nearer the temperature of the melt. Usually for

polymer systems, the glass temperatures are increased with increasing quenching rates, and it was, therefore, decided to investigate the change in distributions resulting from increased quenching rates.

It was also interesting to study the effect of different cations on the distributions as a direct extension of earlier work. For this the studies were extended to the $PbO-P_2O_5$, $CdO-P_2O_5$ and $MgO-P_2O_5$ systems. Before describing the results of the present investigation the various theories put forward to fit the data obtained previously for phosphate glasses are summarised and their merits and demerits discussed.

(ii) Theories on Anionic Distribution in Phosphate Glasses

The theoretical distributions proposed have been mainly for linear chain anions since the investigations so far have been carried out in the composition regions where linear chains are predominant with negligible amounts of ring and branched-chain anions - because of the ease of analysing linear chain anions chromatographically and the relative instability of the branched chain anions in aqueous solutions.

(a) Flory Distribution

Most of the theories applied to phosphate glasses have been based on Flory's[38] approach to organic polymers. Flory was the first to propose a molecular size distribution of linear polymers resulting from the condensation of bifunctional monomers. The principle of equal reactivity of all functional groups, that is to say that equal opportunity for reaction is available to each func-

tional group of a particular chemical type irrespective of the size of the molecule to which it is attached, is the basis of Flory's derivation. We can apply this approach to the reorganisation process taking place in the phosphate melts in terms of the polymerisation and depolymerisation of the PO_4 tetrahedra (ignoring the charges attached to the oxygens). It follows from the principle of equal reactivity that the probability that a given functional group has reacted will be equal to the fraction 'p' of all functional groups of the same type which has condensed. The signifcance of this statement lies in the fact that if a given unit is known to be attached through one of its functinnal groups to a sequence of 'x' consecutive units combined in a linear polymer chain, the probability that the other functional group of the unit also has reacted is still exactly equal to 'p' and is independent of the length of the chain indicated by 'x'.

Now let us examine the probability of finding an x-mer, composed of x-units.

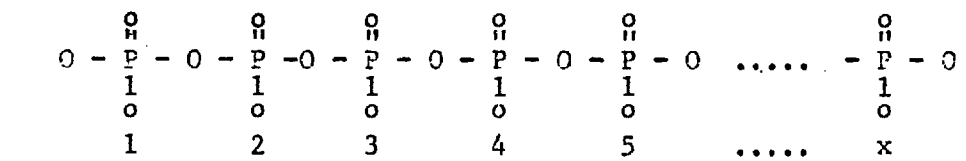

The probability that the first unit has polymerised is 'p'. The probability that the second unit has polymerised is also 'p' as is independent of whether or not a linkage 1 has formed. The probability that this sequence continues for x-1 linkages is the

product of separate probabilities or p^{x-1}. This is the probability that the molecule contains at least x-1 P - O - P linkages or at least x units. The probability that the xth unit has unreacted so that the chain is limited to x units is 1-p. Hence the probability of finding an x-mer is

$$N_x = p^{x-1} (1-p) \qquad \text{B-1}$$

This probability that the unit selected at random consists of x-units must be euqd to the molefraction of x-mers.

Now if we fix the composition of the melt by fixing the metal oxide to P_2O_5 ratio, we define the mean chain length $\bar{n}$; which is given in terms of metal oxide to P_2O_5 ratio for linear chain phosphates by the relation.

$$\bar{n} = \frac{2}{\left(\frac{M_2O}{P_2O_5} - 1\right)} \qquad \text{B-2}$$

This number average degree of polymerisation or the mean chain length $\bar{n}$ is also given by the expression,

$$\bar{n} = \sum_1^\infty x N_x \qquad \text{B-3}$$

Substituting for N_x from equation B-1,

$$\bar{n} = \sum_1^\infty x p^{x-1} (1-p)$$

$$= (1-p) \sum_1^\infty x p^{x-1}$$

This summation can be evaluated as follows:-

$$\frac{dp^x}{dp} = x\,p^{x-1}$$

$$\text{therefore} \qquad x\,p^{x-1} = \frac{d\sum_{o}^{\infty} p^x}{dp} = \frac{d}{dp} \cdot \left[\frac{1}{1-p}\right] = \frac{1}{(1-p)^2} \qquad \text{B-4}$$

$$\text{or} \qquad p = \frac{\bar{n} - 1}{\bar{n}} \qquad \text{B-5}$$

Substituting for p and 1-p in equation B-1,

$$Nx = \frac{1}{\bar{n}} \cdot \left(\frac{\bar{n} - 1}{\bar{n}}\right)^{x-1} \qquad \text{B-6}$$

This expresses the Flory distribution mathematically and has found wide applicability for organic polymers.

(b) Van Wazer's Theories

Van Wazer[13, 39, 40] was the first to apply the Flory type model to the phosphate systems. In his first model, he considered the random reorganisation of flexible chains in the absence of rings and orthophosphate. The assumption of the absence of orthophosphate anions was based on the information then available for alkali phosphate glasses and the model was to fit the data. However, Meadowcroft and Richardson[25] have since shown the presence of appreciable amounts of orthophosphate anions in alkaline-earth glasses.

Though he used a statistical approach like Flory,

he used a completely different derivation for the distribution function based on the probabilities of finding end and middle groups. An end group was the pyrophosphate anion and the middle was of the formula $\left(O - \overset{\overset{O}{\|}}{\underset{\underset{O}{|}}{P}} - O - \overset{\overset{O}{\|}}{\underset{\underset{O}{|}}{P}} - O\right)_n^{n-}$

He derived the probability of finding an x-mer as,

$$N_x = \frac{1}{\bar{n} - 1} \left(\frac{\bar{n} - 2}{\bar{n} - 1}\right)^{x-2} \qquad \text{B-7}$$

Where the symbols are the same as defined in Flory's derivation.

Alternatively, the same distribution can be derived in an analogous manner to that detailed in the last section. If the ortho ions are absent, the probability of finding an x-mer as given by equation B-1 will become,

$$N_x = p^{x-2} (1-p) \qquad \text{B-8}$$

Also themean chain length in this case will be defined as,

$$\bar{n} = \sum_{x=2}^{\infty} x \, N_x \qquad \text{B-9}$$

Then from equation B-8 above,

$$\bar{n} = \sum_{x=2}^{\infty} x \, p^{x-2} (1-p)$$

$$= (1-p) \, p^{-1} \sum_{2}^{\infty} x \, p^{x-1}$$

$$= \frac{1-p}{p} \left[\left(\sum_{x=1}^{\infty} x\, p^{x-1} \right) - \left(x\, p^{x-1} \right)_{x=1} \right]$$

The summation $\sum_{x=1}^{\infty} x\, p^{x-1} = \frac{1}{(1-p)^2}$. (c.f. B-4)

$$\therefore \quad \bar{n} = \frac{1-p}{p} \left[\frac{1}{(1-p)^2} - 1 \right]$$

$$= \frac{2-p}{1-p}$$

Simplifying,

$$\bar{n} - 1 = \frac{1}{1-p}$$

and

$$p = \frac{\bar{n} - 2}{\bar{n} - 1}$$

Substituting for p and 1-p in equation B-8

$$N_x = \frac{1}{\bar{n} - 1} \left(\frac{\bar{n} - 2}{\bar{n} - 1} \right)^{x-2}$$

which is the same as equation B-7 derived by Van Wazer.

This distribution was broader than the experimentally determined ones. Parks and Van Wazer[40] interpreted this as due to the polyelectrolytic nature of these phosphate anions i.e. the charges had to be taken into account. On the evidence of the work of Van Wazer, Goldstein and Farber[41] they considered these anions to be a "brush heap" of rigid rods and derived a distribution with the

help of the 'information theory'. This results in complicated expression which gives a distribution somewhat steeper than the earlier flexible chain model, as can be seen from fig. 5, which is a histogram for $\bar{n} = 4$.

Derivation of the above model of Parks and Van Wazer[40] and the following model by Matula, Groenweghe and Van Wazer[42] are based on specialised mathematical theories, which will not be given in detail here. Matula, Groenweghe and Van Wazer have used the "stochastic graph theory"to interpret equilibria resulting from scrambling reactions whichlead to size distribution of molecules. To apply this theory to vitreous phosphates they have derived an equilibrium constant,

$$K = \left[\frac{X_{(em_\ell)}}{X_{(em_{\ell-1})}}\right]^2 \qquad \frac{X^{2\ell}_{(m_\ell)}}{X^{\ell+1}_{(m_{\ell+1})}\, X^{-1}_{(m_{\ell-1})}}$$

where X is the abundance of graphs, ℓ is the reorganisation heat order and e and m the end and middle units. They determine the values of K for various θ values (defined as the order of the environment). This could be solved by a Fortan programme, and on application to phosphate data they find K is unity for values of θ greater than about three for all systems. This approach of K to unity is interesting to note, since this has been observed for the Meadowcroft and Richardson's equilibrium constants(this model described in Section (d)) when applied to available data.

FIG. 5 DISTRIBUTION FOR A GLASS OF $\bar{n}=4$.

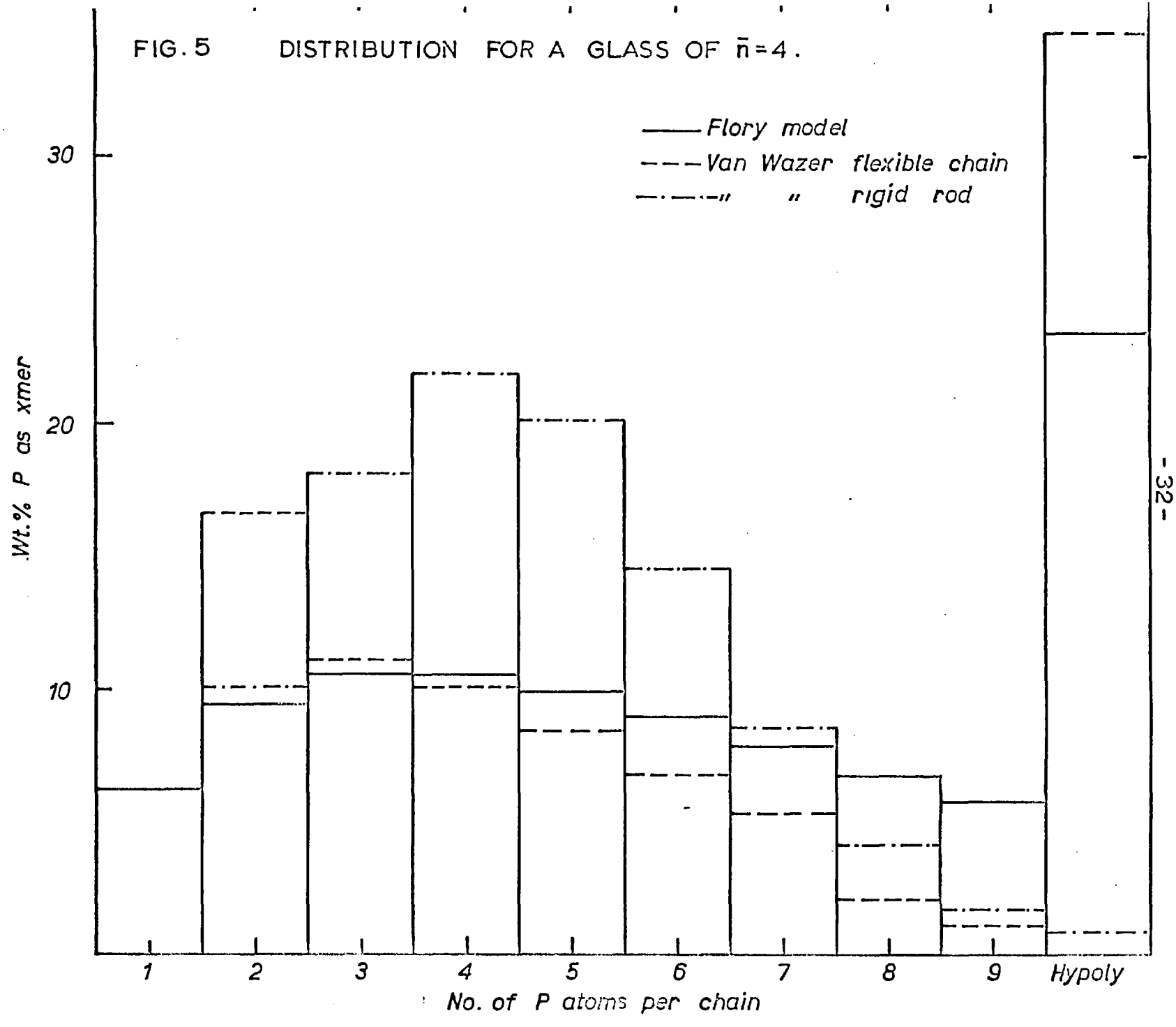

(c) Jost and Wodcke's Theory

Jost and Wodcke[43] have introduced multipliers to the probability 'p' in the Flory theory. Westman and Beatty[44] have termed these "probability coefficients", by analogy with activity coefficients, since they modify an ideal situation. Jost and Wodcke have also assumed the absence of the ortho phosphate anions and derived equations

$$N_x = (x-1)\ (ap)\ p^{x-3}\ (1-p)^3 \quad \text{for } x \geq 3$$

and $$N_2 = (1-p)\ (1-ap)$$

where the coefficient should meet the condition $1 \leq a \leq 1/p$. They found that two coefficients were sufficient to fit the data examined. Westman and Beatty[44] have shown that this can be written as

$$Nx = a_1\ a_2\ p^x\ (1-p) \qquad x \geq 2$$

where a_1 and a_2 are the two multipliers and have derived the relationship between p and $\bar{n}$ as

$$a_1\ (a_2 - 1)p^2 + (a_1 + \bar{n})p - \bar{n} = 0$$

(d) Meadowcroft and Richardson's[25] Model

They consider that in the melt random reorganisation of the anions occurs and in the ideal case this would lead to the distribution predicted by Flory. These reorganisations can be considered in terms of equilibria of the type,

$$2\ P_nO_{3n+1}^{-n-2} = P_{n-1}O_{3n-2}^{-n-1} + P_{n+1}O_{3n+4}^{-n-3} \qquad (2-10)$$

with an equilibrium constant,

$$K_n = \frac{N_{(P_{n-1}O_{3n-2})}^{-n-1} \quad N_{(P_{n+1}O_{3n+4})}^{-n-3}}{N^2_{(P_nO_{3n+1})}^{-n-2}}$$

However, for the Flory distribution (c.f. equation B-6)

$$N_{(P_nO_{3n+1})}^{-n-2} = \frac{1}{\bar{n}} \left(\frac{\bar{n}-1}{\bar{n}}\right)^{n-1}$$

and, applying this expression to the above equation, a value of $K_n=1$ is obtained for all values of n and $\bar{n}$.

The experimental distributions did not correspond to Flory, and they found that values of kn were dependent on the cation present, on the value n and to an extent on $\bar{n}$. At higher values of n, and usually if $n > 4$, $K_n = 1$ and was constant at unity up to $n = 14$, which is the upper limit to which data are available for the H_2O-P_2O_5 system[26]. The tendency of K_n to approach zero as n becomes small was attributed to the coulombic energy change involved in the above reactions at lower chain lengths (i.e. small values of $\bar{n}$).

Meadowcroft and Richardson consider that the anion mixing is ideal, but the enthalphy and free energy changes for the disproportionation reactions (like equation B-10) are not necessarily zero as is the case for Flory distribution. If the entropy change is zero, then ΔH_n (heat of disproportionation) is equal to the free energy change and is related to Kn by the expression,

$$\Delta H_n = - RTg \ln K_n$$

where Tg is the glass temperature (the temperature at which the glass is in internal equilibrium with the super cooled liquid). Hence this model gives a thermodynamic reason for the observed deviation from the statistically derived Flory distribution.

(e) Westman and Beatty's[44] Approach

Westman and Beatty have summarised the various models available for calculating chain length distributions in polyphosphoric acid and polyphosphate glasses. They arrived at the conclusion that the useof "probability coefficients" by Jost and Wodcke[43] and the equilibrium constant approach of Meadowcroft and Richardson[25] are the best available methods for altering the ideal Flory distribution to fit phosphate glass data.

They have combined the probability coefficients of Jost and Wodcke and the first two equilibrium constants of Meadowcroft and Richardson to give,

$$K_1 = a_2 (1-a_1 p) (1-p) \;/\; a_2 (1-p)$$

Although for a system with k different polymer chain lengths, k-2 independent equilibrium constants must be defined, in a practical application to data, they agree with Meadowcroft and Richardson, that perhaps not more than 3 K's have to be defined for a system because those values after K_4 are experimentally found to be unity. Also they have recalculated Jameson's[26] data, taking into account the amount of free water present, and evaluated the K's for the H_2O-P_2O_5 system; they find that K_1 and K_2 vary linearly with $\bar{n}$

for this system. Similar trend was found for K_3 in $Na_2O-P_2O_5$ system based on Westman and Gartagnis's[36] results.

(f) Discussion of the Theories

Flory's theory serves as a useful basis for considering distributions of phosphate anions. The modifications of this distribution by Van Wazer and later by Parks and Van Wazer, which neglect the ortho ions to obtain a steeper distribution, seem to be incorrect because appreciable amounts of orthophosphate have been found by Meadowcroft and Richardson and in the present investigation (described later). Also Van Wazer does not take into account the different distributions corresponding to different cations.

Matula, Groenveghe and Van Wazer's model need a computer programme to arrive at the results. Also their equilibrium constant becomes unity at higher values of 'θ' (order of environment) the behaviour similar to that observed for Meadowcroft and Richardsons's equilibrium constant K_n which reach unity at higher values of 'n'. However, Matula et al do not give any reason for deviation of K from unity at small values of "θ". It is considered therefore, that this complex theory does not have many advantages over the simpler approach of Meadowcroft and Richardson,

Jost and Wodcke's model takes into account the deviations from the ideal Flory distributions, by reducing the probabilities of formation of smaller chains. This suffers from the same

drawbacks as Van Wazer's first theories by not considering ortho ions. Also they do not give any physical reason for reducing the probability of finding the small chain anions.

Only Meadowcroft and Richardson have attempted to explain the deviations of observed distributions from ideal Flory in terms of the endothermic heats involved in the equilibrium (equation B-10) at low values of 'n'. Also their model is a simple one to apply to experimental data, unlike Matula et al's model.

Westman and Beatty find Meadowcroft and Richardson's approach easiest to apply to data, and, though they mention that a modified Jost-Wodcke approach, considering also the ortho ions, can fit data, they only use the equilibrium constant approach in their application of models to data. Because of this advantage of Meadowcroft and Richardson's model over the others and the possibility of relating thermodynamic properties to the observed distribution this has been used in this investigation to interpret the experimental results.

Chapter 6

EXPERIMENTAL

(a) Materials

The following raw materials were used to make the phosphate glasses:-

$Na_4P_2O_7$ -------- very pure anhydrous sodium pyrophosphate supplied by Albright and Wilson analysing not less than 99.9% $Na_4P_2O_7$.

$Na_3(PO_3)_3$ ------- crystalline sodium trimeta phosphate was made by heating analar grade $NaH_2PO_4.2H_2O$ at 150°C and then at 550°C for one week. Paper chromatographic analysis showed less than 0.5% P as ortho and pyrophosphate.

Analar $NH_4H_2PO_4$ -------- this looses ammonia and water on heating and was, therefore, used as the source of P_2O_5 since it could be weighed and handled easily.

Analar PbO, Analar MgO and G.P.R. grade CdO were used after drying for making their respective glasses.

(b) Preparation of Glasses

(i) Sodium Phosphate Glasses Under Dry Condition:-

For melting and quenching a glass in the absence of moisture under controlled atmospheres the apparatus shown in fig. 6 was designed. It consisted of a cylindrical water cooled brass

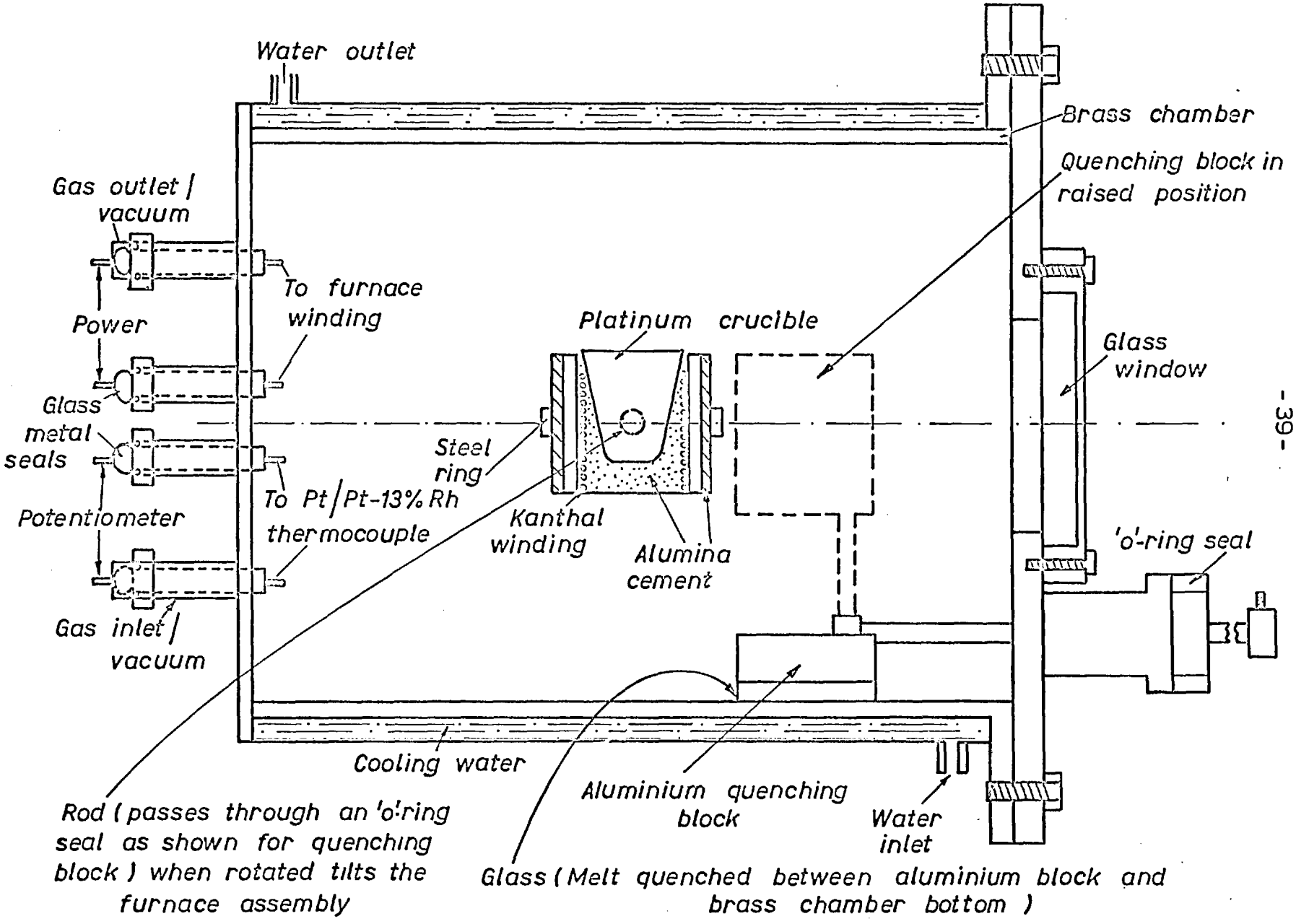

FIG. 6 APPARATUS FOR MELTING AND QUENCHING GLASSES UNDER CONTROLLED ATMOSPHERES

chamber, inside which was a specially designed crucible-shaped heater which could accommodate a 25 ml platinum crucible. Due to the small area which had to be heated, difficulty was found in designing the heater which could operate up to 1000°C. This was overcome by using thin Kanthal-A wire (0.02" dia.) which was coiled in sections. This was wound on a 2" section of alumina tubing of 1½" diameter, in such a way that the coiled portions of the wire faced each other inside, whereas the straight portions were on the outside. This was then set, using pure alumina cement, which was also used to close the bottom and to shape the inside to fit the platinum crucible snugly, so that it would not fall out when the crucible assembly was tilted. This assembly was mounted on a steel ring which was screwed onto the end of a rod, which therefore when rotated tilted the crucible assembly, could be manipulated from outside via an O-ring seal.

The power for the crucible assembly was conducted through an end of the brass furnace chamber via tungsten sealed in glass. Thick tungsten wire was used in order to have the low resistance necessary to prevent heating of the O-ring and glass to metal seals. Similarly platinum wire sealed in glass was used to connect the Pt/Pt-13% Rh thermocouple which was employed to measure the temperature of the crucible. At the otherside was fitted a glass window, and an O-ring seal through which passed a rod attached to a quenching block which formed one part of the quenching system:

the other being the water cooled brass chamber bottom. The quenching block was made of aluminium and shaped to fit the curvature of the brass chamber. Usually the aluminium block was kept raised and the arrangement was such, when the rod was rotated from outside the block slapped onto the brass bottom.

The raw materials, namely anhydrous $Na_4P_2O_7$ and $Na_3P_3O_9$, were first separately dried inside this furnace for 16 hrs at 200°C under vacuum. These were then weighed and mixed in the correct ratio and then placed inside the platinum crucible. This was heated and maintained at 400°C for 16 hrs under vacuum (1×10^{-3} mm. of Hg) to eliminate last traces of moisture either inside the furnace atmosphere or in the raw materials. Then high purity Argon dried by passing through magnesium perchlorate and phosphorus pentoxide was let inside the chamber and the temperature raised to 50-100°C above the melting point of the phosphate. Melting could not be done under vacuum because of the possibility of volatilization of the components and the change in composition resulting from it. The molten phosphate was poured onto the bottom of the brass chamber by tilting the crucible assembly by means of the rod outside and quenched by slapping the aluminium block on to the bottom. The glass thus obtained was at once stored in a P_2O_5 desiccator.

(ii) Lead, Cadmium and Magnesium Phosphate:

As will be seen later, the sodium phosphate glasses made under normal and dry atmosphere conditions, did not have sig-

nificantly different chain distributions. For this reason, and because the phosphates of lead, cadmium and magnesium melt at higher temperatures which were not attainable with the small furnace, these latter glasses were made in the conventional way by melting in platinum crucibles in a muffle and quenching between two aluminum blocks.

The required amounts of pure oxide and ammonium dihydrogen orthophosphate ($NH_4H_2PO_4$) were weighed and mixed thoroughly. The initial step of eliminating NH_3 and H_2O from these mixtures was performed by slow heating over a bunsen flame. Great caution had been exercised during this step to get a correct final composition. Vigorous heating initially led to spurting of the particles due to violent escape of NH_3 and H_2O from the mixture. After slow initial heating, a thorough heating with bunsen was necessary to eliminate all last traces of ammonia and water before the crucible is introduced into the muffle at temperature $\geq 1000^{\circ}C$. This was becuase any trace of ammonia could reduce any unreacted oxide to the metal which would result in the alteration of the composition of the mixture and also the metal could attack the platinum. This difficulty was first observed in case of the lead phosphates, and is understandable since PbO is easily reducable by hydrogen which could be produced from traces of ammonia. (Jeffes and Mekerrel[45] report a p_{H_2} of 8×10^2 in equilibrium with NH_3 at $1000^{\circ}C$). This difficulty was avoided in other cases by taking adequate precautions.

Usually glasses were made in all these systems in the composition range of $^{5}/3$ to $^{7}/5$ metal oxide to phosphorus pentoxide ratios. In most of the phosphate systems a glass could not be obtained for compositions more basic than $^{5}/3$. However, recently Cripps-Clark has obtained glasses at the pyrophosphate composition, ($MO/P_2O_5 = {}^{4}/2$) in the zinc phosphate system. Similarly it was found that in the lead and cadmium system, glasses could be obtained up to this composition. The lower limit of $^{7}/5$ for MO/P_2O_5 ratio is set by the increasing amounts of ring anions present in more acid glasses, which connot be separated by the one dimensional chromatographic technique used in this investigation. In the case of magnesium phosphates, glasses of MgO/P_2O_5 ratio $^{5}/3$ could not be obtained free of crystals because of the high melting points in this system since it was difficult to attain high enough temperatures above the melting point ($\sim$ 1400°C) to enable us to quench it into a complete glass. In all cases the glasses were checked for crystallinity under a microscope with the help of polarised light. Samples with crystals were discarded.

(e) Fast Quenching of Phosphate melts

In an attempt to freeze these liquids into glass at various temperatures by varying the quenching rate a fast quenching apparatus was constructed. This was basically similar to the one used by Duwez and Willens[46] for quenching molten metals at rates up to 250000°C/sec. Even a fraction of this rate would be several orders

of magnitude faster than quenching between two aluminium blocks, and it was interesting to study the difference it produces on the distribution.

This apparatus, shown in fig. 7, consists of a shock tube, using helium as the driving gas, driven into Argon. The shock tube was made of stainless steel and consisted of a high pressure section which was one third the length of the low pressure section, as was required for production of a shock wave.(47) The choice of the two inert gases of different densities, and hence velocities of sound, was also essential for the production of an ideal shock wave(47). (Inert gases were chosen to avoid any reactions at high temperatures with other materials.) "Mylar" of 0.001" thickness were used as diaphragm. To increase the bursting pressures up to three diaphragms were used to increase the effective thickness to 0.003". This allowed the bursting pressures to be varied from 150 psi to 500 psi. The melt was contained in a small platinum insert fitting into the graphite container which also acts as susceptor in a high frequency field. To have an idea of temperature of the melt before the shock wave "splats" the liquid on to the quenching plate, it was necessary to do a prior calibration of the melt temperature, the power setting on the H.F. set and the optical temperature of the graphite susceptor. For quenching, once the temperature was attained, the pressure valve connecting the helium cylinder and the high pressure section of the shock tube was opened. When a pressure over the bursting pressure was developed in this section, the diaphragm burst and the

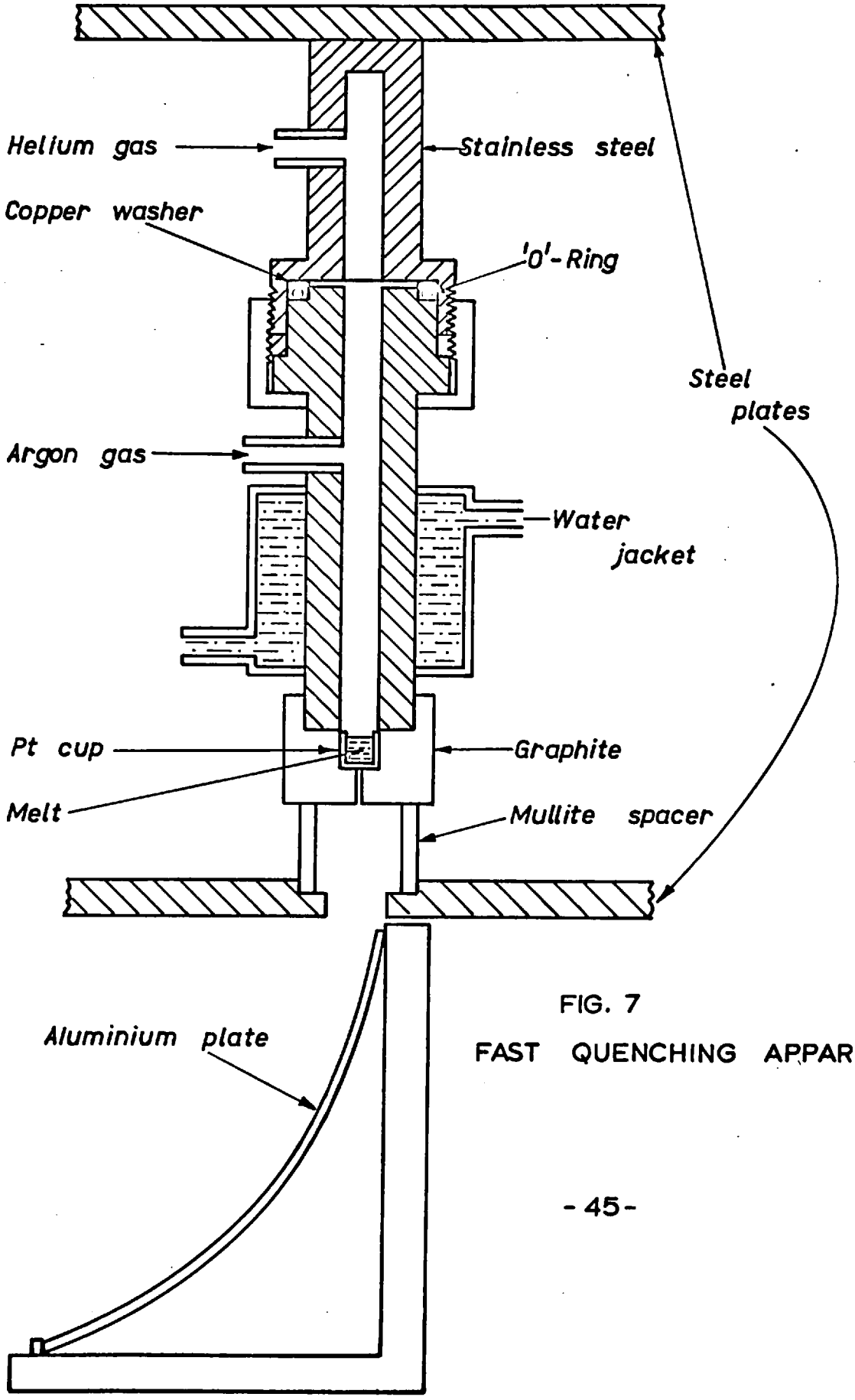

FIG. 7

FAST QUENCHING APPARATUS

melt was ejected on to the cooling plate. During the initial experiments a small hole was made in the bottom of the platinum cup, in addition to the one already present in the graphite container (c.f. fig. 7). Later, howerver, it was found that it was not necessary since the shock wave could burst a small hole in the cup and to "splat" the liquid through it.

When higher bursting pressures (400-500 psi) were used the products produced were usually very thin fibres like fluffy material, especially with longer chain length glasses. Hence lower bursting pressures were generally empolyed for most runs. Also the glass produced by liquid splashed on to the cooling plate would immediately crack up and shatter around the plate due to the quenching stresses. This made it impossible to recover the whole amount of glass produced.

(d) Chromatographic technique

Earlier workers have employed both upflow and downflow chromatographic techniques and a variety of solvents have been used for the anionic separation of the phosphates. The first studies on phosphate glasses were made at the Ontario Research Foundation by Westman and co-workers[36,48,49]. In the present study the technique reported by Smith[50] of the Ontario Research Foundation was used.

The paper for chromatography was the Schliecher and Schull No. 2043B, corresponding to the American 589 green ribbon,

used by Smith[50]. The filter paper wick needed for equilibrating the solvent in the chromatographic tank was Whatman No. 1 paper. The solvent used for the separation was the modified Ebel's acid solvent, used by Smith. It consisted of 70 ml of isopropyl alcohol, 20 ml of 25% trichloroacetic acid and 0.3 ml of 28% ammonia solution in 100 ml of the solvent. It was found that the pH of the solution so prepared was between 1.2 and 1.8 and it must be in this range to get a good separation. The R_f values, defined as the ratio of the distance moved by the solvent to that by the ion, were determined for chain anions from one to seven using a phosphate glass.

The glass obtained from the quenching operation was ground to a fine powder in an agate motor. About 100 m.g. of the glass was dissolved in 5 ml of a neutral solvent. Sodium and other alkali phosphates could be dissolved in distilled water. For lead, cadmium and magnesium a five percent solution of E.D.T.A. (Ethylene diamine tetra-acetic acid - disodium salt) neutralised with ammonia was used.

In the case of lead phosphates the resulting solution was treated with Na_2S to precipitate Pb^{2+} ions as PbS. This was found necessary, because in the preliminary runs there was no movement of the anions on the chromatogram and it was found that this could be rectified by this procedure. This peculiarity in the lead system is thought to be due to the precipitation of lead chloride on the paper, due to the presence of Cl^- ions in the chromatographic

solvent. To check whether the precipitation of Pb^{2+} by Na_2S and the presence of $S^{"}$ ions in solution would effect the chromatographically obtained distribution, some runs were carried out with crystalline lead phosphates. These confirmed that the treatment did not affect the accuracy of the method.

At first, from the stability constant data, it seemed that DCYTA (1,2, Diamino-cyclohexane tetra-acetic acid) would be a better complexing agent than E.D.T.A. for magnesium and other alkaline earth phosphates. This can be seen from the table below:-

Table B.1

Stability Constants of Ligands of:

	Ba^{2+}	Mg^{2+}	Sr^{2+}	Ca^{2+}	Cd^{2+}	Zn^{2+}	Pb^{2+}
E.D.T.A.	7.76	8.49	8.88	10.59	16.46	16.46	18.30
DCYTA	7.99	10.45	9.36	12.50	12.50	19.23	20.33

where the stability constant is defined as

$$K = \frac{(ML_n)}{(M)(L^n)}$$

where M is the metal and L is the ligand.

When solution of magnesium phosphate was attempted in 5% solution a disodium salt of DCYTA neutralised to pH-7, the rate of solution was no greater than in E.D.T.A. solution. These similar rates of dissolution could be due to either of two reasons. (1) The increase in stability constants are not large enough to

appreciably enhance the rates of solution. (2) The stability constants apply at best conditions of complexing which is near pH 7 for E.D.T.A. complexes and near and above pH 10 for DCYTA. Since it was important that the pH should be near pH 7 to avoid any hydrolysis, dissolutions of all phosphates were, therefore, carried out in E.D.T.A. solutions. To overcome the slow dissolution, it was found necessary to grind the samples (especially magnesium phosphates) to less than 300 mesh and dissolve with the help of a mechanical shaker if necessary. In case of magnesium small amounts were dissolved to reduce the dissolution time with this procedure magnesium glasses could be dissolved in comparable times to that required for calcium phosphate glasses studied earlier by Meadowcroft.(51)

The solution was then painted on to the chromatogram using a small bore capillary whose end was ground flat. Usually for sodium phosphate glasses one or two applications of the solution were enough to give sufficient amount of phosphorus in the bands for an analysis. However, in the case of lead phosphates, the use of Na_2S solution to precipitate PbS diluted the solution and in the case of magnesium the solution was also made dilute to dissolve in reasonable time. Furthermore, with the heavier cations about 100 mg of the initial glass taken for dissolution gives lesser amounts of phosphorus in solution than would a sodium phosphate glass. Hence in all cases except sodium three or more applications were needed. When repeated applications had to be done the second and subsequents had to be performed after the previous one had dried. This ensured

that the band of solution applied was always within about $\frac{1}{8}$" broad. If this became broader or smeared instead of a uniform line, the bands obtained were not straight and the separation, especially of the higher fractions, would become increasingly difficult.

The chromatograms were run at 4°C for at least 16 hrs, but sometimes longer times up to 24 hrs were necessary to allow high polymer fractions to be separated. The chromatograms were then dried at 110-120°C for 10 minutes and sprayed with a fine mist of ammonium molybdate solution (1)gm $(NH_4)_6\ Mo_7O_{24}.^4\ H_2O$ 5 ml 37% $HClO_4$, 1 ml conc HCl in 100 ml of solution). It was important that the atomizer delivers a fine mist rather than large drops, since the latter tended to spread over the paper carrying phosphate with them. The paper was then dried with the help of infra-red lamps, to prevent any charring which would occur if it were dried at a temperature above 80°C, because of the presence of $HClO_4$ in the spray solution. The chromatograms were then exposed to ultra-voilet light until the ammonium-molybdate blue complex was observed.

(e) Analysis for Phosphorus

The method used for analysis of phosphorus was the method of Lucenda-Conde and Pratt which has been modified by Smith[50]. The reagent used was made as follows: 8.15 gm of $(NH_4)_6\ Mo_7C_{24}\cdot 4H_2O$ were dissolved in 60 ml of distilled water. To 30 ml of this

solution was added 50 ml of 12N.HCl and 56 ml of 36N.H_2SO_4. The volume was then brought up to 136 ml by the addition of 12N.HCl. A further 25 ml of the initial molybdate solution was then shaken vigorously for at least five minutes with 12.5 ml of 12N.HCl and 10 ml of distilled mercury. This solution was then filtered to give 40 ml of a ruby red solution which was added to the previous solution to give an emerald green reagent. The total volume was then made up to 200 ml by the addition of water.

Because of the high cost of mercury it was desirable to recover the amount used in the above operation. This was carried out by vigorous shaking of the black precipitate in the above operation with acetone for about 20-30 minutes. This caused the black mercury to coagulate and when all the mercury had a metallic lustre as before, it could be cleaned using dilute HNO_3. However, use of any acid before cleaning with acetone always resulted in the formation of a precipitate presumably calomel (due to the presence of abundant cl' ions), and metallic mercury was difficult to recover fromit.

The individual components of the chromatograms were cut out with scissors and put in dry 50 ml Erlenmeyer flasks. The phosphorus was then extracted by shaking with 25 ml of 0.1N. NH_4OH for at least ten minutes. A 20 ml aliquot of solution was then transferred to a 50 ml volumetric flask and 3 ml of molybdate reagent was added. The flasks were then heated in a boiling water bath for one hour. After boiling, the solution was cooled slowly

and made up to 50 ml with water. It was important that all the phosphate strips from any one chromatogram be analysed together to minimise the errors. A filter paper blank from a clear part of the chromatogram was also run with each analysis.

The phosphorus content of each sample was then determined colorimetrically on a Unicam SP 600 Spectrophotometer set at 8300 Angstroms. The optical density is a linear function of concentration in the range studied, the ratio of a single component to the sum of the optical densities of all components on the chromatogram was equal to the weight fraction of phosphorus in that component. For all the readings either a matched set of Spectrophotomer cells were used or the cell correction was taken into account.

Chapter 7

Results

The paper chromatographic technique can be employed to separate the first seven chain anions, for example anions with values of n from one to seven in the general formula $P_nO_{3n+1}^{-n-2}$. Because of the very low mobility of higher chain length ions these could not be separated and were grouped together as hypoly and analysed as the eighth fraction. Previous work by Westman and Crowther [48] and Meadowcroft [51] indicates that the amount of phosphorus occuring as rings would be less than 1% of the total and that in most cases there would be no rings in the composition range MO or M_2O/P_2O_5 of 5/3 to 7/5. Since the present work was carried out in this and more basic composition range, in all cases the amount of rings present have been assumed as negligible.

From the positions of the anions on the chromatogram, the R_f value defined as the ratio of the distance travelled by the ion to that by the solvent, can be calculated for each anion. The R_f values are characteristic of the anion and the solvent used and are plotted as a function of chain length in fig. 8.

One of the sources of error in chromatography is the hydrolysis of pyro and longer chain phosphates to orthophosphate. This could take place during the dissolution of the glass painting on the chromatogram and during the chromatographic

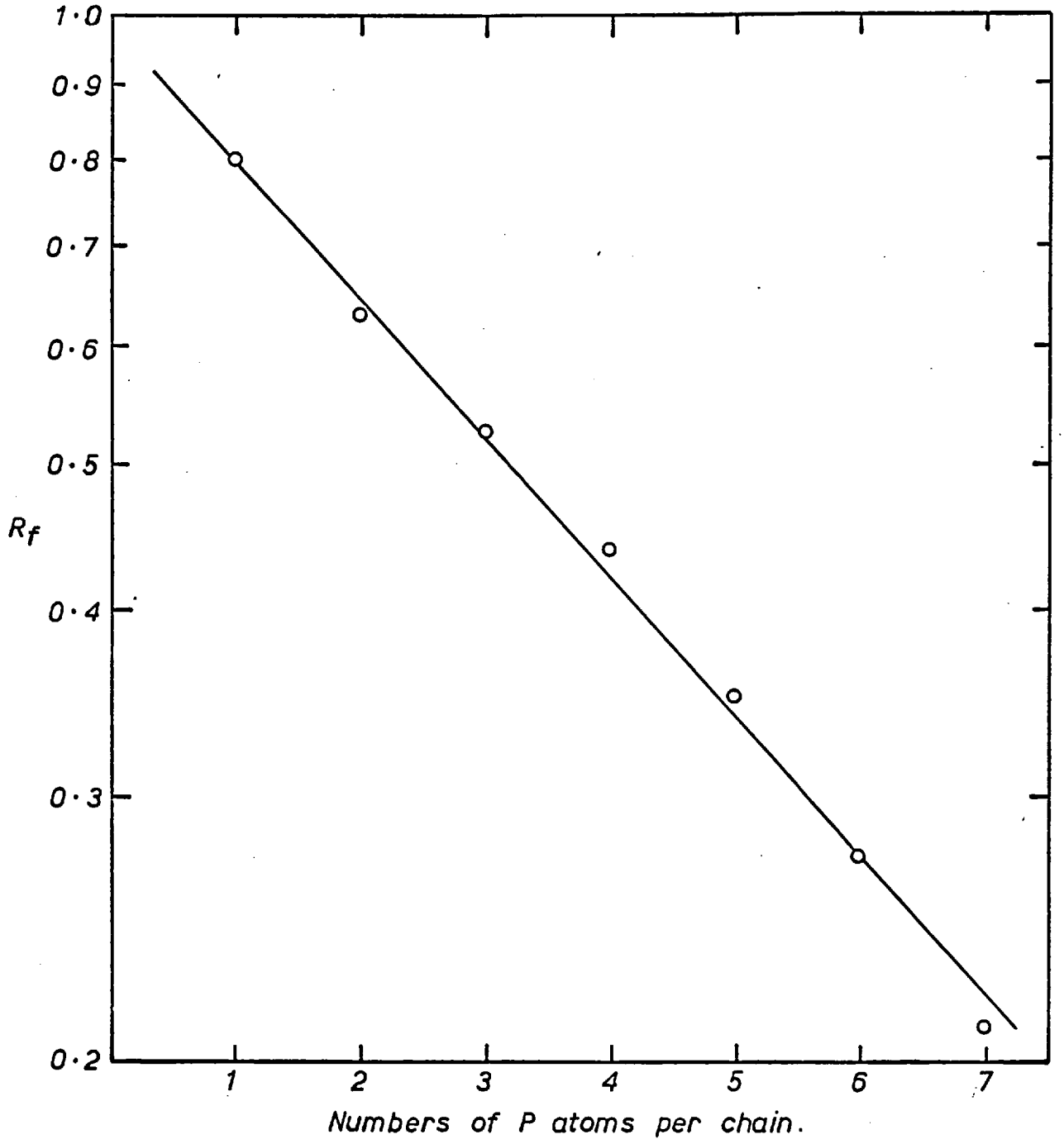

FIG 8 R_f VALUES FOR THE CHROMATOGRAPHIC COLUMN TECHNIQUE USED

separation on the paper. Cripps-Clark[37] found that hydrolysis taking place during the solution and painting steps is immeasurably small. Meadowcroft and Richardson[25] have suggested that the hydrolysis during the chromatographic separation can be corrected by subtracting 0.6%(wt) from the ortho value and then adjusting the other analyses by multiplying by 100/99.4. This was based on the fact that in chromatograms from crystalline pyro and triphosphates 0.6 $\pm$ 0.4% of the total phosphorus was found as orthophosphate. The hydrolysis taking place can be written as :-

$$(P_n O_{3n+1})^{-n-2} = (P_{n-1} O_{3n-2})^{-n-1} + PO_4^{3-} + 2H^+$$

which would mean that each orthophosphate ion produced by hydrolysis, is accompanied by another phosphate ion containing one phosphorus atom less than it held originally. If all the P-O-P links are liable to hydrolysis, the proportion of phosphorus found in each anion should be increased by the hydrolysis of the longer anions and decreased by its own hydrolysis. The two effects tend to cancel, and it is therefore sufficient to correct, for the hydrolysis, in the above manner.

Since exactly the same chromatographic technique was used in this investigation, the hydrolysis during the chromatographic separation could be corrected in the same way as by Meadowcroft and Richardson. This correction was applied to all the distributions reported here and the corrected distributions are given in tables B-2 to B-4.

Table B.2

Distribution of Sodium Phosphate Glasses Made Under Dry Condition

Na_2O/P_2O_5	Ortho	Pyro	Tri	Tetra	Penta	Hexa	Hepta	Hypoly	no. of chains per 100 P atoms	$\bar{n}$
6/4	0	6.04	28.84	27.73	17.04	9.06	5.42	5.96	25.90	3.86
6.25/4.25	0	5.26	2.467	25.13	16.60	9.66	5.63	13.05	24.32	4.11
7/5	0	2.82	15.17	20.55	16.84	12.04	9.32	23.26	20.89	4.79

Distribution of Sodium Phosphate Glasses Made By Melting in Air (Meadowcroft & Richardson)

6/4	0	5.96	28.76	26.98	16.90	9.58	5.52	6.31	25.69	3.89
7/5	0	3.19	15.45	19.59	17.47	12.43	9.07	22.89	21.03	4.76

Table B.3

Distribution in Lead Phosphate Glasses

PbO/P_2O_5	Ortho	Pyro	Tri	Tetra	Penta	Hexa	Hepta	Hypoly	no. of chains per 100 P atoms	$\bar{n}$
2/1	12.04	63.25	17.45	4.58	1.13	-	-	1.54	51.05	1.96
5/3	3.01	32.45	25.01	15.39	9.77	5.61	3.36	4.40	35.52	2.81
6/4	2.83	16.31	17.26	15.71	13.22	10.68	8.38	15.61	28.02	3.57
6.4/4.4	2.62	12.48	13.34	12.69	11.50	9.80	8.63	28.94	24.86	4.02
7/5	2.08	9.96	10.67	10.71	9.07	8.47	7.69	41.35	22.21	4.50

Table B.4

Distribution in Cadmium Phosphate Glasses

CdO/P_2O_5	Ortho	Pyro	Tri	Tetra	Penta	Hexa	Hepta	Hypoly	no. of chains per 100 P atoms	$\bar{n}$
2/1	13.10	56.16	17.37	5.21	1.60	-	-	6.56	49.41	2.02
5/3	2.20	30.01	24.81	15.99	10.22	6.22	3.61	6.94	33.83	2.96
6/4	1.40	15.80	16.10	14.54	12.04	9.54	7.41	23.17	25.93	3.86
7/5	1.01	12.59	11.16	10.16	9.48	8.23	6.86	40.51	22.31	4.48

Distribution in Magnesium Phosphate Glasses

6/4	2.87	12.21	13.63	13.24	10.81	8.52	6.42	32.35	24.92	4.01
7/5	1.08	5.43	8.29	9.00	8.98	8.29	7.86	51.07	18.78	5.32

In table B-2 the distributions obtained for sodium phosphate glasses made under dry conditions are compared with those of Meadowcroft and Richardson,[25] who made their glasses by melting in air and subsequent quenching. In tables B-3 and B-4 the distribution obtained for lead, cadmium and magnesium glasses are given. All the distributions have been given in terms of weight per cent total phosphorus of each component. In these tables the number of chains per hundred phosphorus atoms is calculated by dividing the weight per cent of the total phosphorus corresponding to each chain length by the number of phosphorus atoms in that chain and summing these numbers. For hypoly fraction the average number of phosphorus atoms per chain has been taken as nine for these calculations. From the total number of chains per hundred phosphorus atoms the mean chain length '$\bar{n}$' was derived by dividing hundred by this number. The metal oxide to phosphorus pentoxide ratio given in these tables refer to the composition in the starting material.

The distributions are represented graphically in figures 9 to 16. Though the more correct way of representing distributions is by histograms, they are represented in the manner shown in the following figures because of the clarity of such a plot. In fig.9 to 12 the distributions for sodium, lead, cadmium and magnesium phosphates are shown. In figure 13 to 16 the distributions of various phosphates at constant ratios of M_2O or MO/P_2O_5 from $2/1$ to $7/5$ are compared with each other and that of Flory.[38]

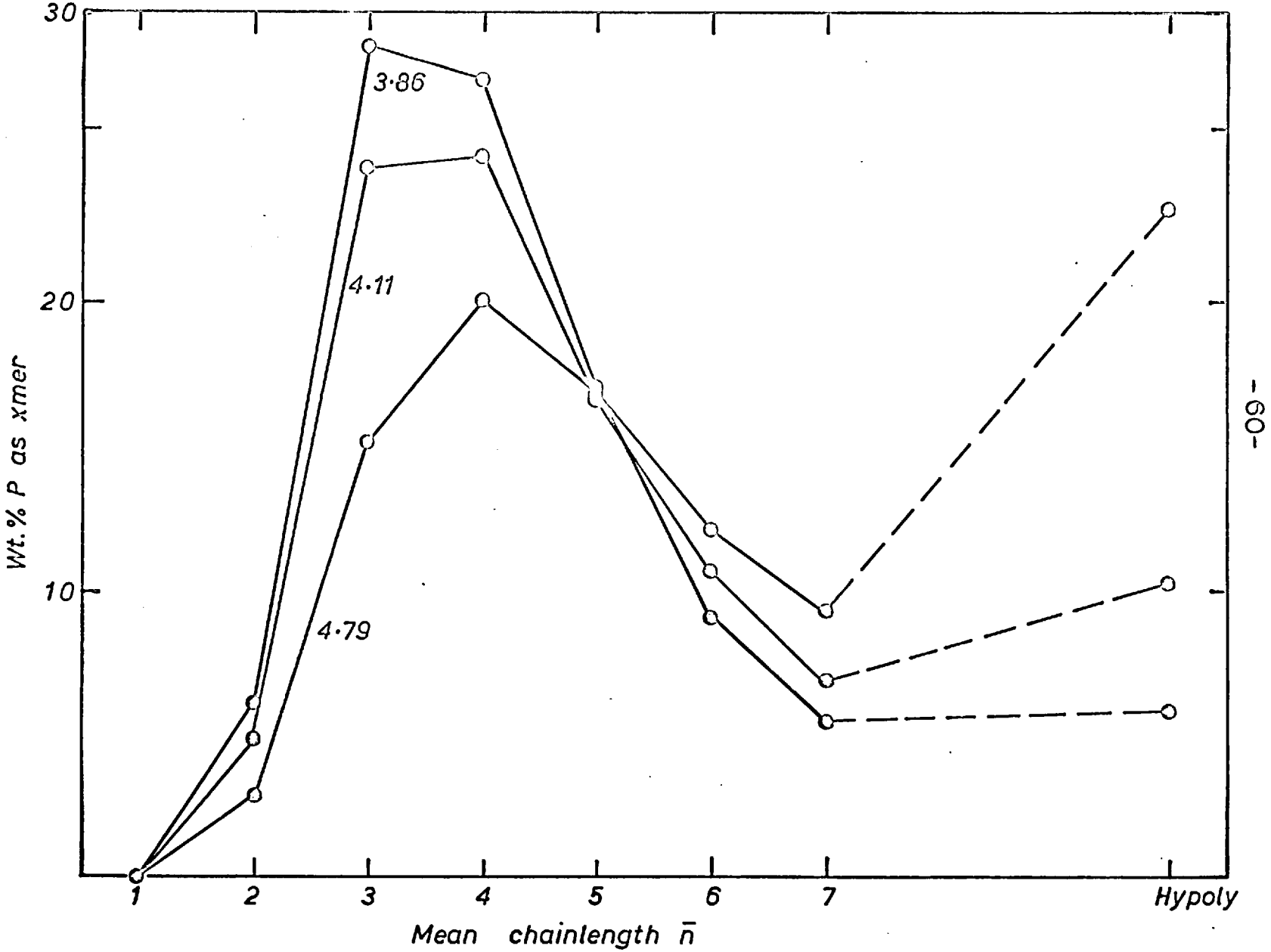

FIG.9 ANION DISTRIBUTION IN SODIUM PHOSPHATES OF VARIOUS MEAN CHAINLENGTHS

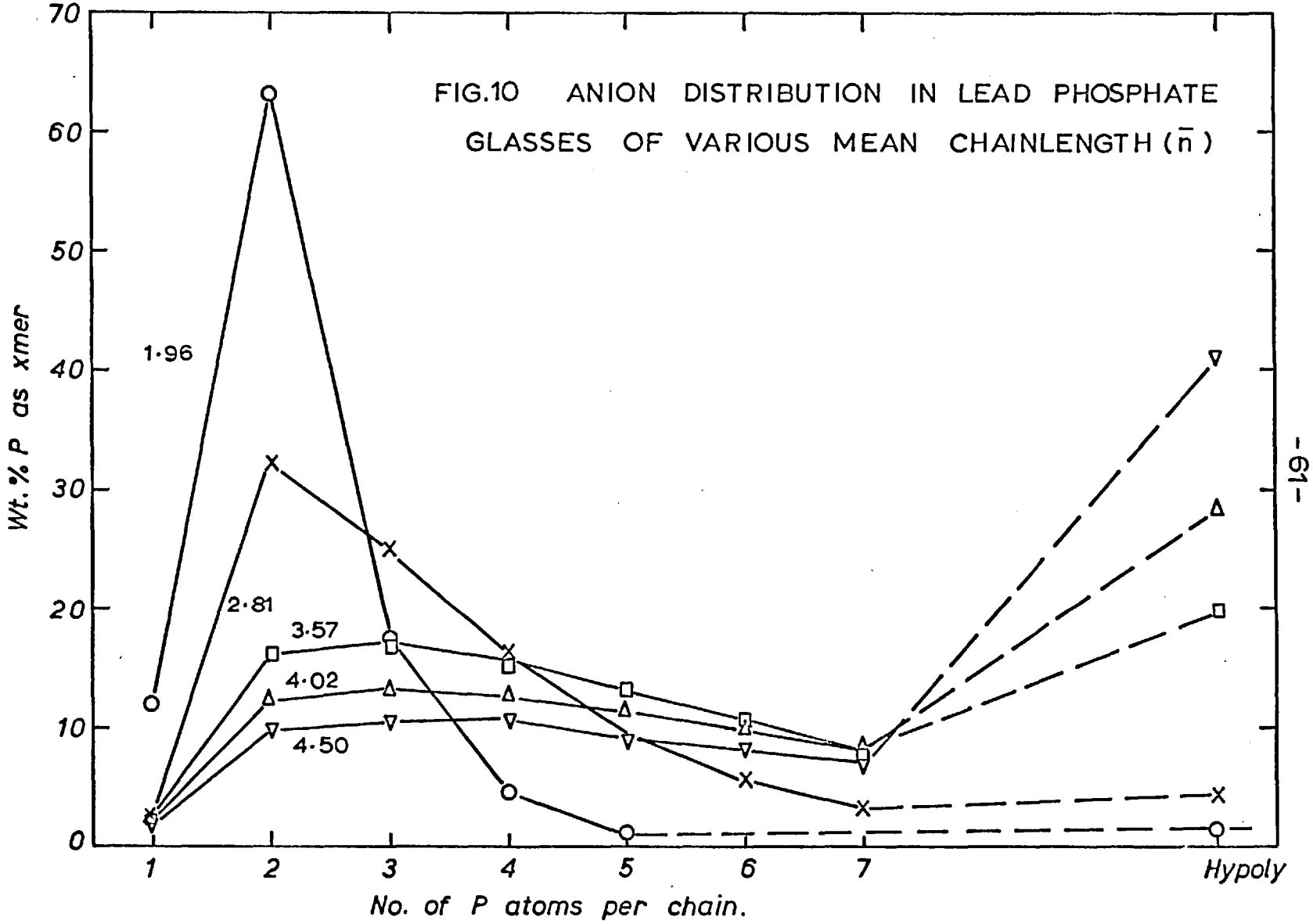
FIG.10 ANION DISTRIBUTION IN LEAD PHOSPHATE GLASSES OF VARIOUS MEAN CHAINLENGTH ($\bar{n}$)
Wt. % P as xmer
No. of P atoms per chain.
1·96
2·81
3·57
4·02
4·50
0
10
20
30
40
50
60
70
1
2
3
4
5
6
7
Hypoly

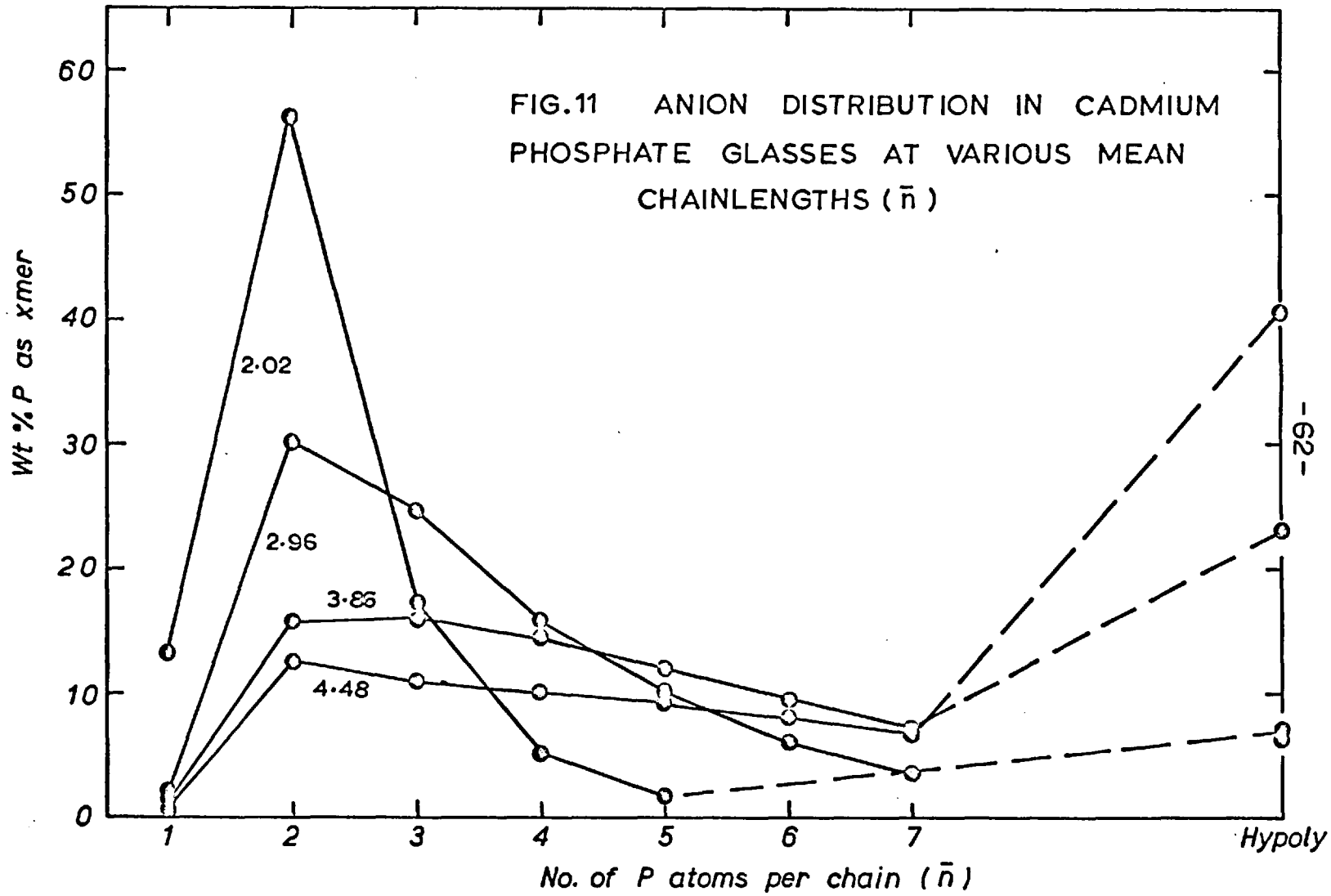
FIG.11 ANION DISTRIBUTION IN CADMIUM PHOSPHATE GLASSES AT VARIOUS MEAN CHAINLENGTHS (n̄)
Wt % P as xmer
No. of P atoms per chain (n̄)
2·02
2·96
3·86
4·48
Hypoly
0
10
20
30
40
50
60
1
2
3
4
5
6
7

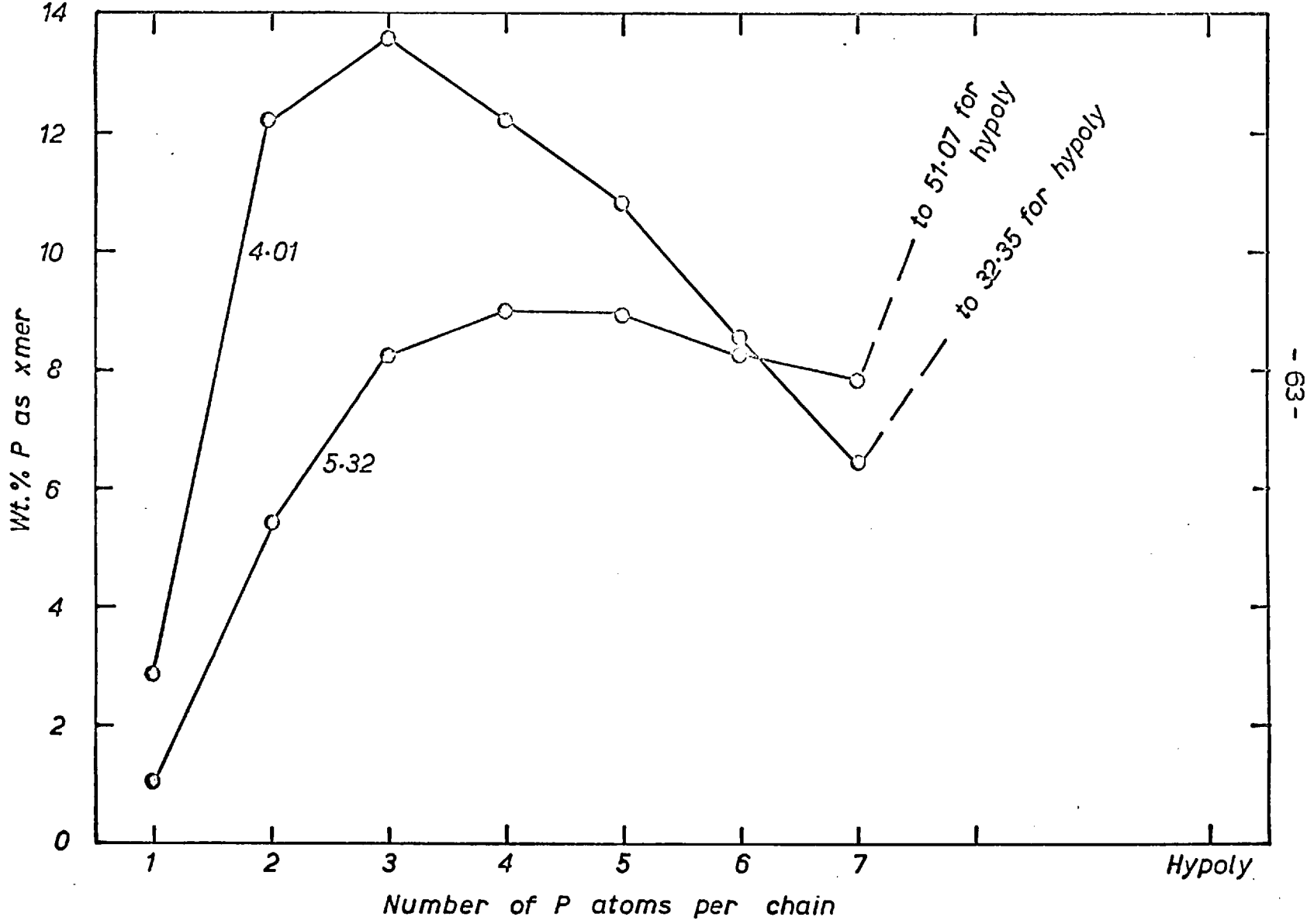

FIG 12 ANION DISTRIBUTION IN MAGNESIUM PHOSPHATE GLASSES OF MEAN CHAINLENGTH 5·32 & 4·01

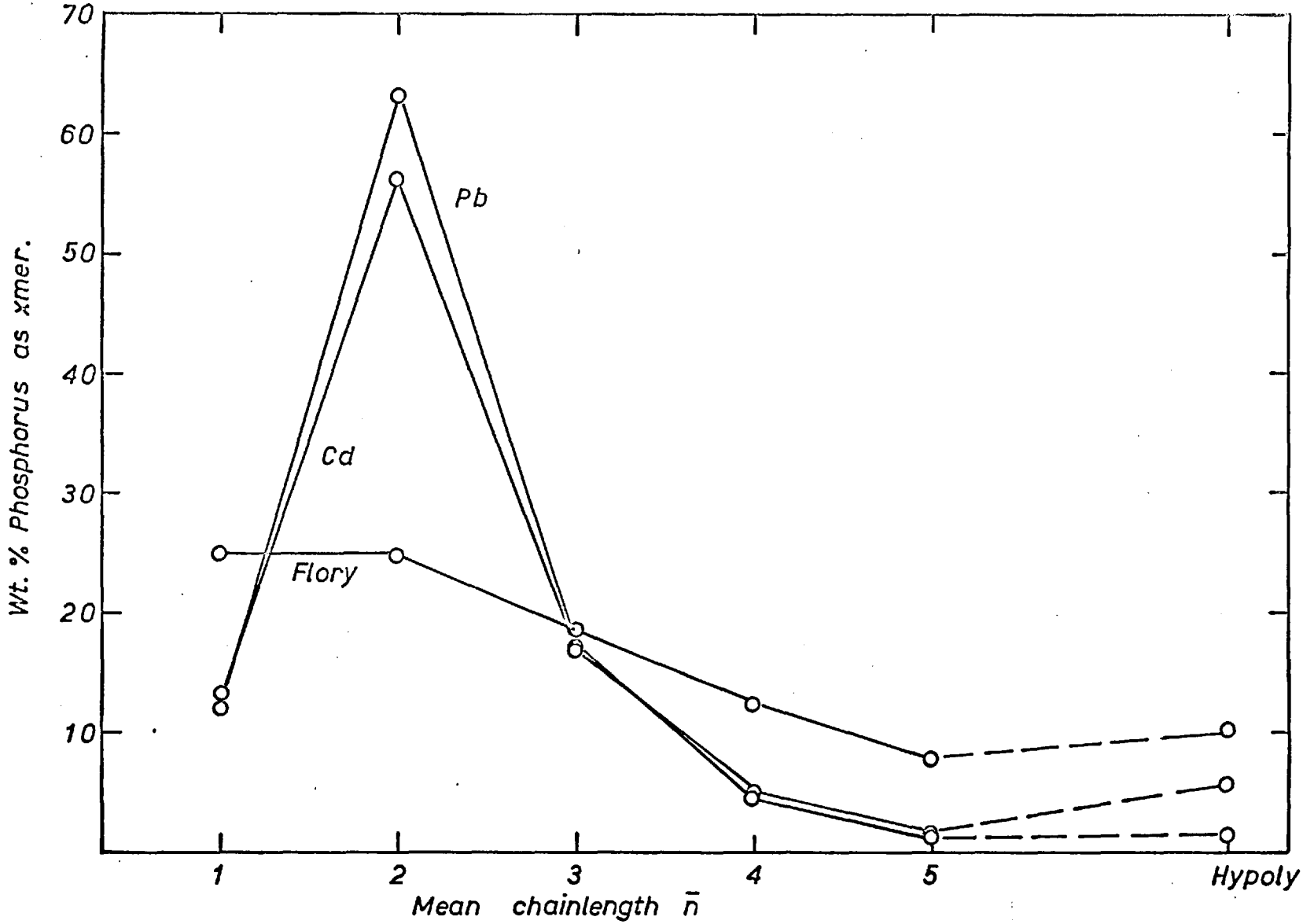

FIG.13 ANION DISTRIBUTION FOR $MO/P_2O_5 = {}^{2}/_{1}$ GLASSES

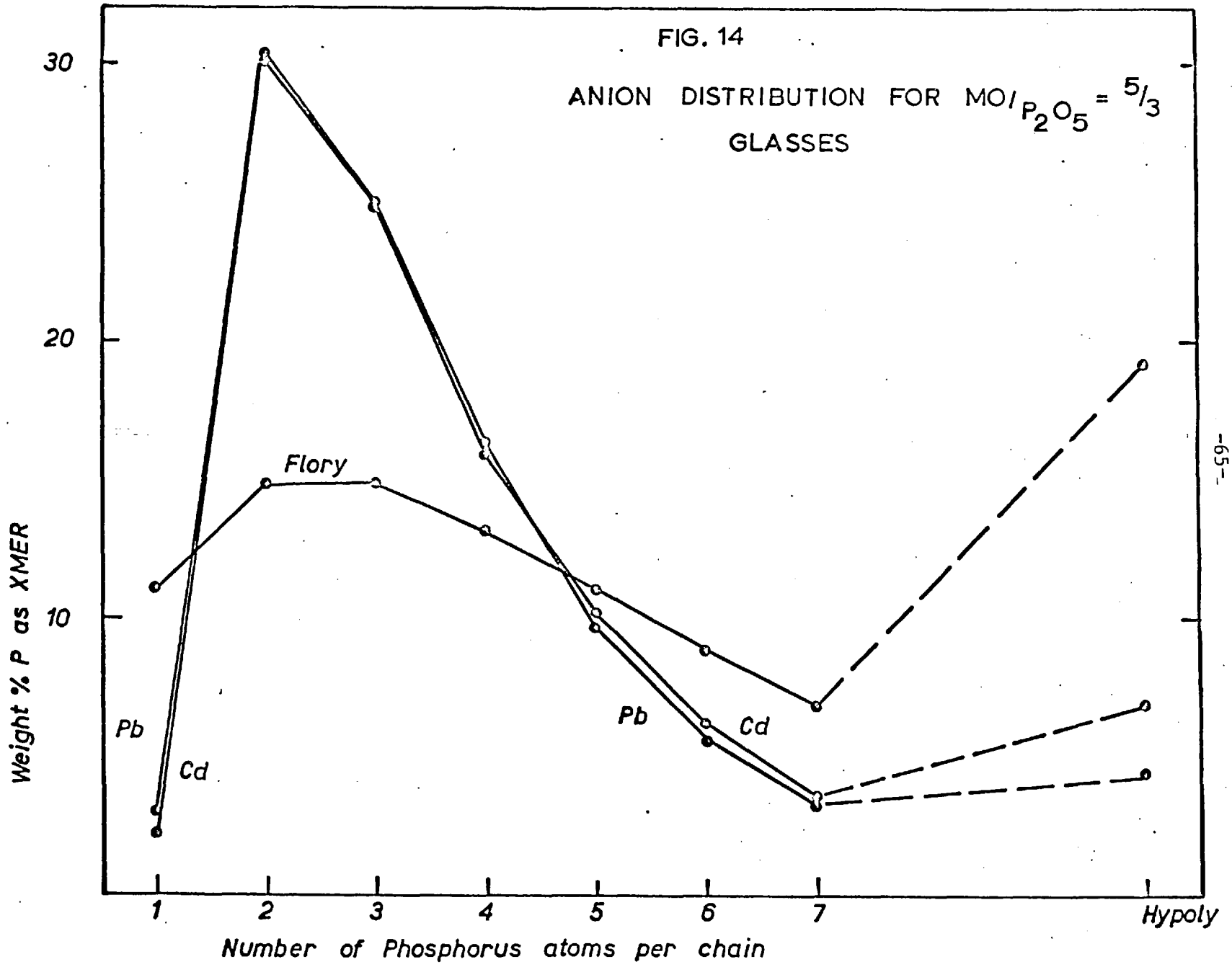
FIG. 14
ANION DISTRIBUTION FOR $MO/P_2O_5 = 5/3$ GLASSES
30
20
10
Weight % P as XMER
Flory
Pb
Cd
Pb
Cd
1
2
3
4
5
6
7
Hypoly
Number of Phosphorus atoms per chain

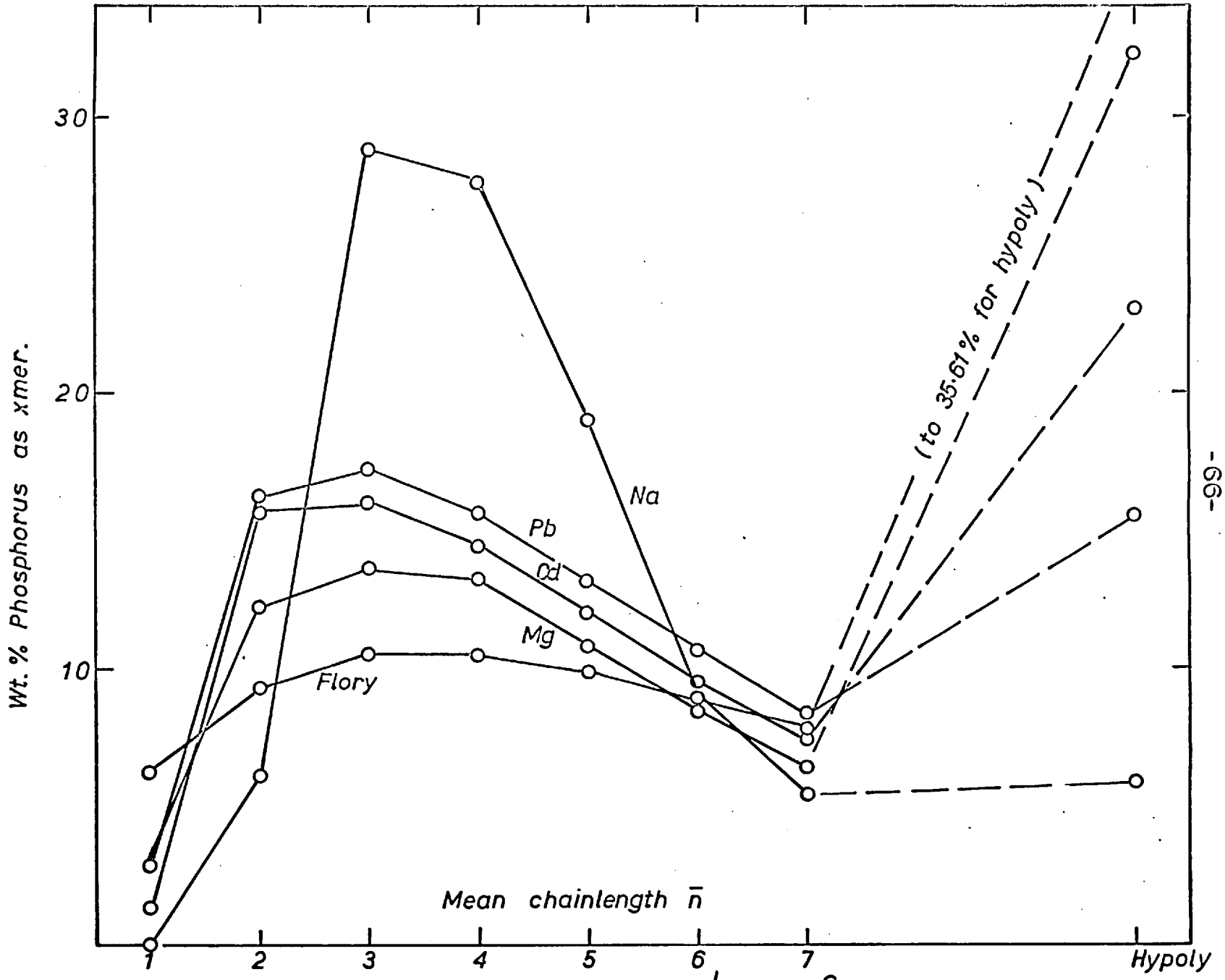

FIG 15 ANION DISTRIBUTION FOR M_2O or $MO/P_2O_5 = 6/4$ GLASSES

FIG. 16

ANION DISTRIBUTION EOR M_2O or $MO/P_2O_5 = 7/5$ GLASSES

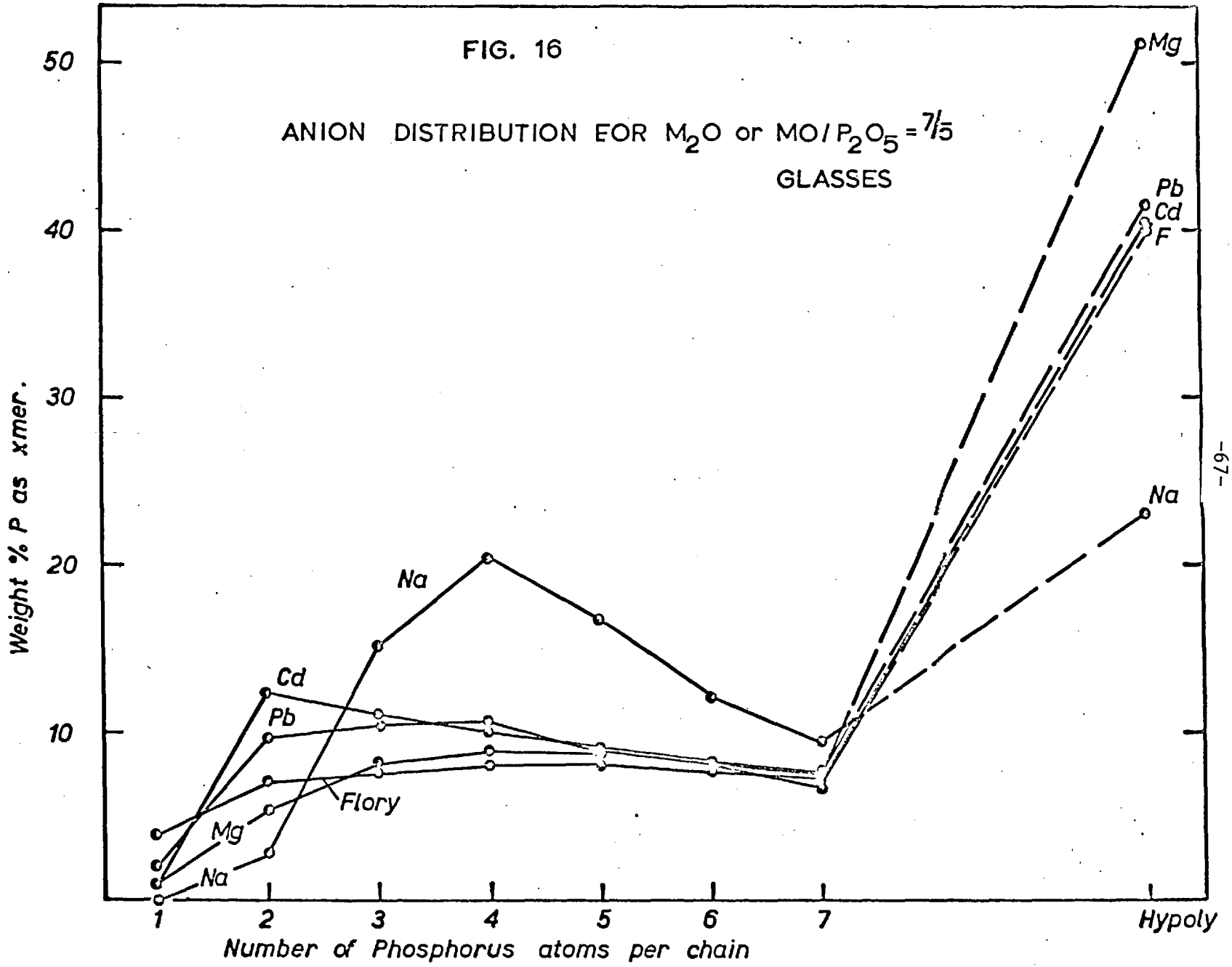

The obtained distributions can be treated in terms of equilibrium constants suggested by Meadowcroft and Richardson (25) which are of the type

$$K_n = \frac{N_{(P_{n+1}O_{3n+4})}^{-n-3} \; N_{(P_{n-1}O_{3n-2})}^{-n-1}}{N^2_{(P_nO_{3n+1})}^{-n-2}}$$

for the equilibria

$$2\,(P_nO_{3n+1})^{-n-2} = (P_{n+1}O_{3n+4})^{-n-3} + (P_{n-1}O_{3n-2})^{-n-1}$$

Since the amounts of anions ortho to heptapoly have been measured it is possible to calculate the equilibrium constants K_2 to K_6. These are given in tables B-5 and B-6 for the various systems at the different compositions. In addition, the mean values for the systems are given when the equilibrium constant does not vary much with the composition.

In table B-7 the distributions for fast quenched sodium phosphates and the values of equilibrium constants calculated therefrom are given. All the results quoted in the tables B-2 to B-4 and B-7 were obtained by taking the average of results obtained from at least six chromatograms on two melts made in the same manner. The standard deviation was calculated for each component on the chromatograms using the formula

$$\sigma = \sqrt{\frac{(x - \bar{x})^2}{N-1}}$$

where $\bar{x}$ is the mean of the result, N is the number of results and σ is the standard deviation. The standard error of the mean for each component was calculated using the formula

$$\text{Standard error} = \frac{\text{standard deviation}}{\text{no. of results}} = \frac{\sigma}{\sqrt{N}}$$

The ranges of the standard deviation and the standard error were found to be functions of metal oxide to phosphorus pentoxide ratio and of the polymer ion and not of the cation. Hence in table B-8 and B-9 the range of the errors are given for the various phosphate composition and chain lengths. These are given as weight per cent of total phosphorus. From these tables it can be seen that each mean result can be taken as $\pm$ 0.5%(wt) of total phosphorus.

Taking the error for each mean result as $\pm$ 0.5%, the error in the values of K_n can be calculated. This gives an error in K_n values of about $\pm$ 10% when the equilibrium involves the dominant anions, for example when n approaches $\bar{n}$, and near $\pm$ 30% when n and $\bar{n}$ differ markedly.

Table B-5

Value of equilibrium products for Sodium and Lead glasses

Cation	$\frac{M_2O \text{ or } MO}{P_2O_5}$	K_2	K_3	K_4	K_5	K_6
Na	$6/4$	negligible	0.23	0.66	0.90	1.15
	$6.25/4.25$	"	0.24	0.68	0.92	1.00
	$7/5$	"	0.28	0.65	0.91	1.11
	means	"	0.25	0.66	0.91	1.08
	M & R means	"	0.26	0.66	0.97*	1.03
Pb	$2/1$	0.07	1.07	0.99	-	-
	$5/3$	0.10	0.96	0.97	1.00	1.07
	$6/4$	0.25	0.97	0.99	1.00	0.99
	$6.4/4.4$	0.30	1.00	1.01	0.98	1.06
	$7/5$	0.29	1.12	1.02	1.12	1.00
	means	0.07 to 0.30	1.02	0.99	1.02	1.03

* Mean of K_5 calculated by M&R from Westman et al and not their results

Table B-6

Values of equilibrium products for Cadmium and Magnesium Glasses

Cation	MO/P_2O_5	K_2	K_3	K_4	K_5	K_6
Cd	$2/_1$	0.09	1.08	1.09	-	-
	$5/_3$	0.08	0.88	1.06	0.99	0.98
	$6/_4$	0.12	0.99	0.97	0.99	1.01
	$7/_5$	0.10	1.04	1.12	0.91	0.99
	means	0.10	1.00	1.08	0.96	0.99
Mg	$6/_4$	0.35	1.00	0.90	1.00	0.98
	$7/_5$	0.40	0.95	0.98	0.96	1.01
	means	0.38	0.98	0.94	0.98	0.99

Table B.7

Distribution in Fast Quenched Sodium Phosphate Glasses

Na_2O/P_2O_5	Orhto	Pyro	Tri	Tetra	Penta	Hexa	Hepta	Hypoly	no. of chains per 100 P atoms	$\bar{n}$
		6.81	29.94	28.67	15.87	8.38	4.69	5.74		
6/4	0	6.81	29.94	28.67	15.87	8.38	4.69	5.74	26.45	3.93
7/5	0	2.65	16.20	20.51	15.49	11.74	8.71	24.68	20.90	4.78

Values of Equilibrium Constants

Na_2O/P_2O_5	K_2	K_3	K_4	K_5	K_6
6/4	negligible	0.25	0.62	1.00	0.99
7/5	negligible	0.24	0.64	1.04	1.00

Table B-8

Errors in Chromatography

Component	$MO / P_2O_5 = 2/1$		MO or $M_2O/P_2O_5=5/3$	
	Standard deviation (wt%)	Standard error (wt%)	Standard deviation (wt%)	Standard error (wt%)
ortho-	0.24-0.98	0.12-0.49	0.28-0.98	0.11-0.40
pyro-	0.74-1.57	0.52-0.88	0.76-1.34	0.31-0.62
tri-	0.59-0.88	0.30-0.62	0.90-1.68	0.34-0.75
tetro-	0.60-1.01	0.35-0.50	0.29-0.81	0.15-0.47
penta-			0.41-0.79	0.16-0.46
hexa-			0.38-0.62	0.19-0.28
hepta-			0.25-0.79	0.11-0.30
hyp-	0.08-0.16	0.05-0.10	0.40-0.98	0.16-0.44

Table B.9

Errors in Chromatography

Component	MO or M_2O/P_2O_5 = 6/4 (wt.%)		MO or M_2O/P_2O_5 = 7/5 (wt.%)	
	Standard Deviation	Standard Error	Standard Deviation	Standard Error
Orhto	0.16 - 0.58	0.07 - 0.24	0.36 - 0.74	0.21 - 0.33
Pyro	0.54 - 0.86	0.22 - 0.43	0.42 - 1.10	0.19 - 0.45
Tri	0.51 - 1.16	0.21 - 0.58	0.40 - 1.12	0.18 - 0.59
Tetra	0.42 - 0.98	0.17 - 0.44	0.78 - 1.36	0.32 - 0.61
Penta	0.31 - 0.70	0.13 - 0.29	0.51 - 0.90	0.21 - 0.40
Hexa	0.24 - 0.68	0.11 - 0.28	0.32 - 0.61	0.13 - 0.25
Hepta	0.44 - 0.88	0.20 - 0.36	0.40 - 0.82	0.16 - 0.33
Hypoly	0.48 - 1.20	0.20 - 0.49	0.50 - 1.36	0.22 - 0.61

Chapter 8

Discussion

(a) Distribution of Glasses Made Under Dry Conditions.

In a phosphate glass containing only chain anions, for example of mean chain length four corresponding to a metal oxide to phosphorus pentoxide ratio of 6/4, the number of phosphorus atoms per 100 phosphorus atoms must be 25, if the glass is of composition intended. Meadowcroft and Richardson[25] observed the number of chain anions in their experimental distributions was always greater than expected from theoretical considerations. Since the phenomenon could not be explained by errors in the chromatography or by hydrolysis during this process, they concluded that it was caused by other factors. The extra anions could be explained by the pressure of 0.29 wt% H_2O in these melts or ascribed to errors in composition arising from such factors as error in starting materials or volatalization of phosphorus pentoxide.

In the present work, to eliminate the possibility of water dissolution in these glasses, the glasses were made under conditions of rigid exclusion of water as described earlier. The distribution obtained for sodium phosphate glasses made in this manner is compared with that of Meadowcroft and Richardson[25], (who made their glasses by melting in air and subsequent quenching)., in

table B-2. The distributions are in good agreement within the experimental errors of the investigations. The values of the equilibrium constant calculable from the distributions are also compared in table B-5, and are also in good agreement.

Usually the partial pressure of H_2O in the muffle atmosphere would be of the order of 10mm to 15mm of Hg. In this investigation the furnace chamber was evacuated to less than 10^{-3} mm of Hg, before being filled with dry argon and hence the p_{H_2O} should not exceed 10^{-3}mm. Hence, changing the p_{H_2O} by a factor of 10^4 has had no influence on the anion distributions of the glasses. However, this change in p_{H_2O} should have produced a big difference in the solubility of water, if any, in these melts and hence in the glasses. It is concluded, therefore, that the extra anions observed by Meadowcroft and Richardson[25] and Cripps-Clark[37] cannot be due to water dissolution in these melts.

The most probable reason for this observed additional anions is that the glasses were not of the composition intended. This composition error could be caused by error in the amounts of starting materials or because of change of composition during melting. Since Analar grade reagents were used after careful drying and great care was taken in weighing it is improbable the error is in the amounts of starting materials.

The observed extra anions could be explained if the compositions were richer in the metal oxide by 0.4 to 1.0 mole % than

those originally intended. This would be caused by vaporisation of P_2O_5 as P_4O_{10} (g) from the melt during melting, since P_2O_5 has a high vapour pressure at these melting temperatures of 1000°C. to 1300°C. Though P_2O_5 sublimes at about 800°C, the extent of volatalization will be considerably reduced by the large negative partial heats and free energies of solution of P_2O_5 in these melts. An idea of the magnitude of the partial heats of solution of P_2O_5 can be had from Meadowcroft and Richardson's[25] data on heats of formation of glasses. At the metal oxide to phosphorus pentoxide ratio of 6/4, the $\Delta\bar{H}_{P_2O_5}$ varies from - 35 k.cals for zinc to - 60 k.cals for sodium.

Hence the loss of P_2O_5 by volatalization will depend to a large extent on the manner in which the solid materials are pretreated beforebeing melted. If the formation of the phosphates is homogeneous in the solid state, without regions richer in metal oxide or P_2O_5, then the vapour losses will be a minimum. Furthermore, the vapour loss will depend on the stability of the phosphate, (given by the heats and free energies of formations) and the temperature of melting. If the metal oxide also has a high vapour pressure then the two effects will counteract each other to give compositions near to that intended. Because of the various factors acting simultaneously it is not possible to make an estimate of the expected composition change due to volatalization losses. However, a glass richer in metal oxide by 0.4 to

1.0 % (mole) than intended is not surprising and in fact the loss of P_2O_5 is much smaller than what one would expect (due to the high volatility of P_2O_5 itself). This as explained earlier is due to the large negative heats and free energies of formation of the phosphates.

(b) Fast Quenching of the Melts.

As described earlier, fast quenching was attempted to freeze the phosphate liquids at a higher temperature, which could give an idea of the change in anionic distribution with change in the glass transition temperature. The distributions obtained for fast quenched glasses and the equilibrium constants calculated therefrom are given in table B-7. It can be seen that these are not significantly different from the distributions for a normal quenched glass of the same composition (cf. table B-2). The values of K are very slightly altered but they are not much outside the possible error in K's of $\pm$ 10% to $\pm$ 30%.

The relatively unchanged distributions could be explained in three ways: (a) the quenching rates were not fast enough. (b) the glass temperature is not altered sufficiently or (c) the distributions are not sensitive to changes in glass temperatures. These will be considered in turn.

Although the splat quenching technique[46] employed here has previously been used for quenching liquid metals and alloys at rates greater than 200,000°C/sec, the same rates may not be attained

with phosphate melts because of the much poorer thermal conductivity of these melts and glasses compared to the metals. This rate of quenching is very difficult to measure and was not attempted. However, it is reasonable to suppose that the rates obtained should nevertheless have been increased by several orders of magnitude when compared to 200-300°C/sec., attainable by quenching between aluminium blocks operated by hand.

The variation of glass transition temperature with quenching rate is not well understood. Ritland[52] has studied this phenomenon in borosilicate glasses and derived an expression,

$$Tg'' = Tg' + {}^{1}/_{k} \ln r''/r'$$

where Tg'' and Tg' are the observed transition temperatures at cooling rates r' and r'' respectively, and k is a constant which for the borosilicate glasses was 0.1192/ °K.

Now if we assume that the heats of disproportionation, $H_n = - RTg \ln K_n$, defined by Meadowcroft and Richardson[25] do not vary with temperature, then as in a regular solution $Tg' \ln K_n' = Tg'' \ln K_n''$. For sodium phosphates, the K_3 value is 0.23 and the experimental error in determining K_3 will be ± 10%. A change in K_3 by 10% would correspond to a change of 33° in the glass temperature, Tg . We can now apply Ritland's analysis to this case assuming the value of k found by him for the borosilicate glasses This gives a value of $r''/r' = 50$, which means that charging the quenching rate from 200°/sec to 10,000°/sec may not produce sufficient change in

distributions to evaluate accurately the change in K. If this reasoning is valid, the quenching rate obtained may not be far above this value of 10,000°/sec. However, it should be pointed out that glasses are far more difficult to obtain in the phosphates than in the corresponding borosilicates. This is because the viscosity of borosilicate melts is about 10^8 poise at 700°C compared tc 10^5 poise for a sodium phosphate melt (Na/P = 1/1) at the same temperature, and hence the relaxation-times 'c' will be much smaller for phosphates than for silicate glasses. This means that a greater change in quenching rates will be needed for the phosphates than for the borosilicates to alter the Tg by the same amount in both cases. If this were the case the quenching rates obtained in this work should be greater than 10,000°C/sec, but still insufficient to produce a significant change in the observed distributions.

More recently Poch[53] and Roye[53a] have changed the distributions in phosphate glasses by the application of pressure. Poch[53] considers that this change in distribution produced could be due to the change in Tg produced by pressure. The application of pressure would increase the melting point and decrease the free volume which could result in the increase in glass temperatures. Hence it seems unlikely that the distributions are not sensitive to changes in glass temperature 'Tg'.

Therefore, the apparent constancy of distribution and the K_n values with quenching rate in this study and that of Cripps-Clark[37]

using a different technique of quenching, seems to be due to the smallness of the changes in glass temperatures produced in these phosphate systems over a wide range of quenching rates. Application of pressure seems to produce a greater effect on the distribution presumably due to increased Tg's and are hence more interesting to investigate in order to prove conclusively the presence of heat effects in these distributions.

(c) Effect of Mean Chain Length ($\bar{n}$) on the Values of Equilibrium Constants.

Meadowcroft and Richardson[25] observed that once the mean chain length, $\bar{n}$, exceeds three, the Flory model could be usefully applied to their glasses, since the equilibrium constants with the possible exception of K_1 and K_2 were nearly independent of $\bar{n}$. Furthermore, the K's above K_4 approached unity as in the Flory model. A study of the variation of K_2 is possible only in the systems with a broad distribution, and thus in which there are measurable amounts of orthophosphate anions. This is the case in PbO - P_2O_5, CdO - P_2O_5 and MgO - P_2O_5 systems and these have therefore been used.

In figure 17 , the values of K_2 are plotted as a function of mean chain length. The value for H_2O - P_2O_5 is that of Jameson,[26] ZnO - P_2O_5 that of Cripps-Clark[37] and CaO - P_2O_5 is from Meadowcroft and Richardson[25]; the values for the other systems are from this study (cf. table B-5 and B-6). It can be seen that

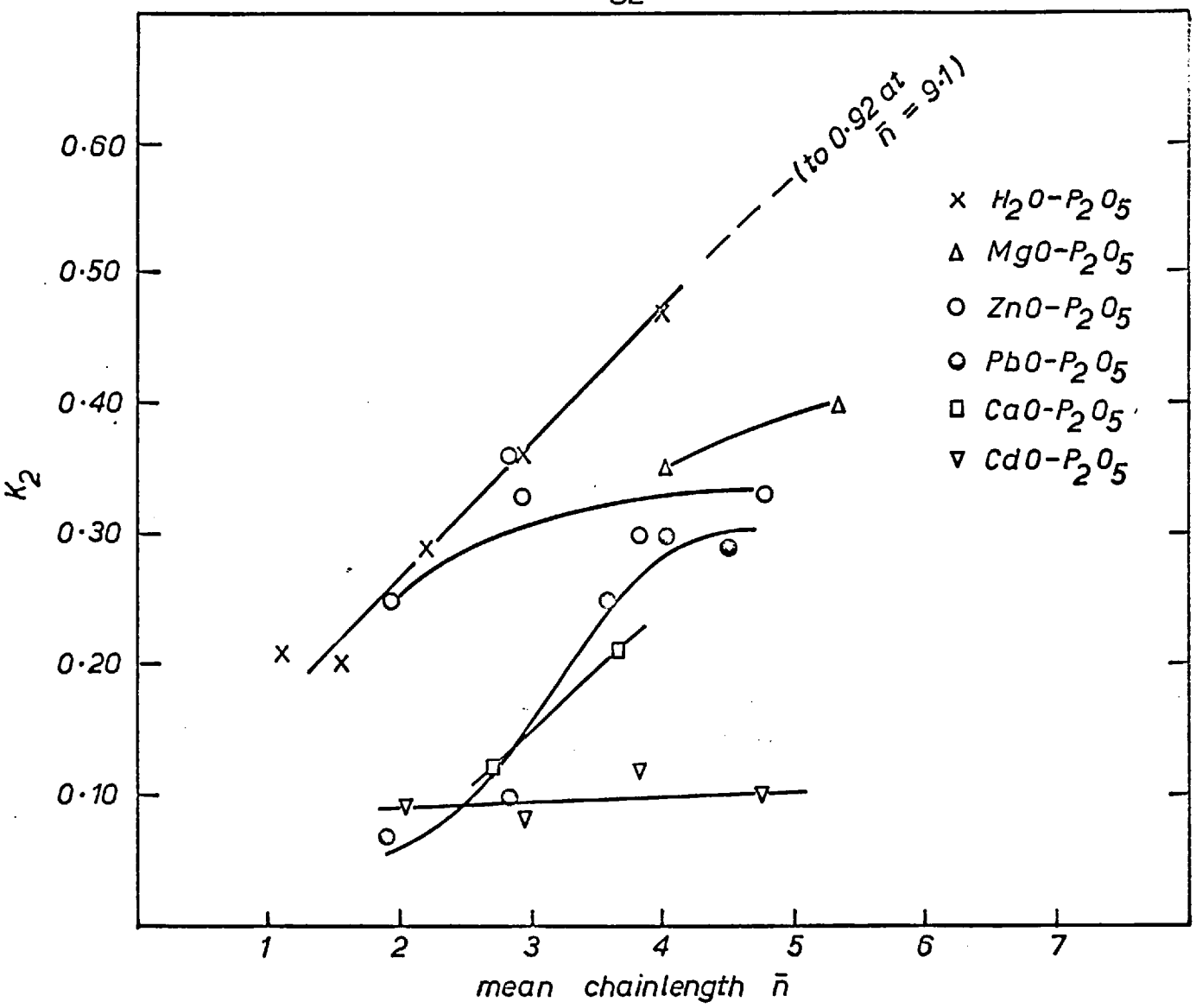

FIG.17 PLOT OF K_2 vs. MEAN CHAINLENGTH $\bar{n}$

K_2 varies with mean chain length to a different extent for the different systems. For CdO - P_2O_5, ZnO - P_2O_5 and MgO - P_2O_5 systems the variation is not much and can be argued to be within the experimental errors involved in the measurements (see page 69). However, for the other systems, namely H_2O - P_2O_5, PbO - P_2O_5 and CaO - P_2O_5 there is a definite increase in the value of K_2 with increase in $\bar{n}$. Hence it seems that variation of K_2 with $\bar{n}$ is to be expected in these systems, whereas, the degree of this variation is dependent on the cation present.

The influence of the cations on the distributions and hence the values of K_2 should be related in some manner to the cation radius to charge ratio,[51] since this determines the cation-oxygen coulombic interactions at the end of the chains. This would be smaller with smaller values of radius/charge ratios of the cation. If we assume that variation of K_2 with $\bar{n}$ is related to the cation radius to charge ratio, then Cd with a similar ratio to Ca, (Cd^{2+} 0.48 and Ca^{2+} 0.49) should show similar variaitons. From figure it can be seen that this is not the case. However, lead (Pb^{2+} - 0.60), has a large value of radius/charge and hence is expected to show greater variations in K_2 with $\bar{n}$ compared to zinc (Zn^{2+} - 0.37) and magnesium (Mg^{2+}-0.33), which is in agreement with observed variaitons. The discrepancy with cadmium and calcium phosphates could be partly because of the difference in ionisation potential of the cadmium and calcium ion.

Calcium being readily ionized would have larger coulombic interaction with oxygen ions than cadmium, though of very similar size.

For all the systems studied values of K_n when $n \geqslant 3$ are constant with $\bar{n}$ (cf. tables B-5 and B-6). Also for systems other than sodium, the values of K_3 to K_6 are nearly unity and are constant with $\bar{n}$. This is in agreement with Meadowcroft and Richardson's view that K's above K_4 are unity for these phosphate systems - based on their studies and Jameson's[26] data for $H_2O - P_2O_5$ system in which K's up to K_{14} are calculable and K_3 to K_{14} are unity.

The ion-exchange chromatography first used by Jameson[26] for $H_2O - P_2O_5$ has the advantage that polymer fractions above chain length seven can be separated, which cannot be done paper chromatographically. This method has been recently extended to the $Na_2O - P_2O_5$ system by the research department of Albright and Wilson[27]. It was possible to analyse a sodium phosphate glass of $Na_2O/P_2O_5 = 7/5$ in their machine, and the results obtained are compared with the analysis done by paper chromatography in table B-10. The values of 'n' in the table refer to the value of 'n' in the general formula $(P_nO_{3n+1})^{-n-2}$ for the chain phosphates.

The distributions obtained by the two techniques are in fair agreement with each other. The small differences in the individual values and hence that in derived values of K are considered to be

Table B-10

Distribution in $\frac{Na_2O}{P_2O_5} = \frac{7}{5}$ Glass.

Values of 'n'	Type of chromatography Ion-Exchange+	Paper++	Kn	Type of chromatography Ion-Exchange+	Paper++
1	0	0	K_2	negligible	negligible
2	2.68	2.82	K_3	0.19	0.28
3	17.20	15.17	K_4	0.79	0.65
4	19.33	20.55	K_5	0.96	0.91
5	16.11	16.84	K_6	1.02	1.08
6	12.28	12.04	K_7	0.94	
7	9.28	9.32	K_8	0.94	
8	7.25		K_9	1.20	
9	5.21		K_{10}	0.87	
10	4.46				
11	3.27				
Hypoly	3.01	23.26			

\+ Albright and Wilson research department

++ This study

because, in iom-exchange chromatography, the intensities which are automatically recorded on chart paper tend to overlap and the peaks corresponding to particular anions are not easy to saparate. This effect is most pronounced at high chain lengths and is considered to be the reason for the scattered values of K_n at high 'n' values. Besides these drawbacks, the results support the view of Meadowcroft and Richardson that K's above K_6 are also unity for the phosphate glasses and hence these distributions can be considered in terms of the Flory model.

(d) Heats of Disproportionation.

If it is assumed that the heats of disproportionation can be calculated from the values of the equilibrium constants K_n, in the Meadowcroft and Richardson manner[25], they will be given by,

$$\Delta H_n = - R\,Tg\,\ln K_n$$

where Tg is the glass transition temperature. Cripps-Clark measured the Tg's of a number of binary and ternary phosphate glasses using the Differential Thermal Analysis technique. He concluded that for a binary system the value of Tg did not vary with the metal oxide to phosphorus pentoxide ratio and in general was three fifths the melting point (in degrees kelvin) of the nearest Crystalline Component. Using this observation, the Tg's of $CdO - P_2O_5$ and $MgO - P_2O_5$ glasses can be estimated to be 703°K and 861°K respectively. For the $Na_2O - P_2O_5$ and $PbO - P_2O_5$ glasses Cripps-Clark determined the transition temperatures to be 543°K and 608°K respectively.

Since K_n is directly related to ΔH_n by the above equation, any variation of K_n with the mean chain length would result in the variation of ΔH_n with $\bar{n}$. The values of ΔH_2, ΔH_3 and ΔH_4 are given in table B-11 for sodium, lithium, calcium, cadmium, lead, zinc and magnesium glasses for different mean chain lengths. The results of lithium, calcium and zinc are taken from Cripps-Clark[37] and Meadowcroft[51] and the remainder from the present work. The errors in the values of ΔH_n are caused by errors in K_n and Tg. Tg for all cases except for Cd and Mg which were estimated as described before, are accurate to $\pm$ 5°C. For cadmium and magnesium the estimated value should be accurate to $\pm$ 50°C, which would mean an error in ΔH_n, of $\pm$ 230 cals for K_n value of ~ 0.10 for cadmium and $\pm$ 100 cals for K_n value of 0.40 for magnesium glasses. The errors in Kn as mentioned before can be from $\pm$ 10% to $\pm$ 30%, which would be an error of $\pm$ 150 cals to $\pm$ 370 cals in ΔH_n. for a K_n value of 0.30 and Tg of 700°K. In the following section the different distributions obtained for the various cation systems will be discussed in terms of these heats of disproportionation.

Table B-11

Heats of Disproportionation

CATION	ΔH_2 (cals)				ΔH_3 (cals)				ΔH_4 (cals)			
	2/1	5/3	6/4	7/5	2/1	5/3	6/4	7/5	2/1	5/3	6/4	7/5
Na	-	-	-	-	-	1,570	1,586	1,373	-	490	448	464
Li*	-	-	-	-	-	930	930	-	-	125	80	-
Ca*	-	3,480	2,540	-	-	670	515	-	-	0	0	-
Cd	3,364	3,528	2,961	3,216	0	0	0	0	0	0	0	0
Pb	3,210	2,780	1,674	1,495	0	0	0	0	0	0	0	0
Zn*	1,960	1,500	1,600	1,550	0	100	130	145	0	0	0	0
Mg	-	-	1,795	1,567	0	-	0	0	-	-	0	0

* Data from Cripps-Clark and Meadowcroft and Richardson

(e) Effects of different cations on the anionic distribution in the phosphate glasses.

Westman and Cartaganis[36] and Meadowcroft and Richardson[25] found that the anionic distributions in the phosphate glasses are a function, not only of the metal oxide to phosphorus pentoxide ratio but also of the cation. Meadowcroft and Richardson[25] put forward the view that there is an enthalpy change involved in addition to an entropy change during the formation of a distribution. This enthalpy change was treated by them in terms of the heats of disproptionation, discussed in the earlier section. The heats of disproportionation are, as seen in the last section, a function of the cation, which according to Meadowcroft[51] can be explained in terms of a) the coulombic interactions between the cation and oxygen at the end of the chains, which would be dependent on the cation radius to change ratio and b) the shape of the heats of formation curves for the binary phosphate glasses

In the systems studied by Meadowcroft and Richardson[25], the relative steepness of the heats of formation curves were increasing with the radius to charge ratio of the cation, as seen in figure 18. In figure 18, the values of heats of formation for the glasses and crystals plotted are those of Meadowcroft and Richardson[54] except the values for orthophosphates of Lead and Magnesium, which were taken from the work of Pitzer[55] and Stevens and Turkdogan[56]

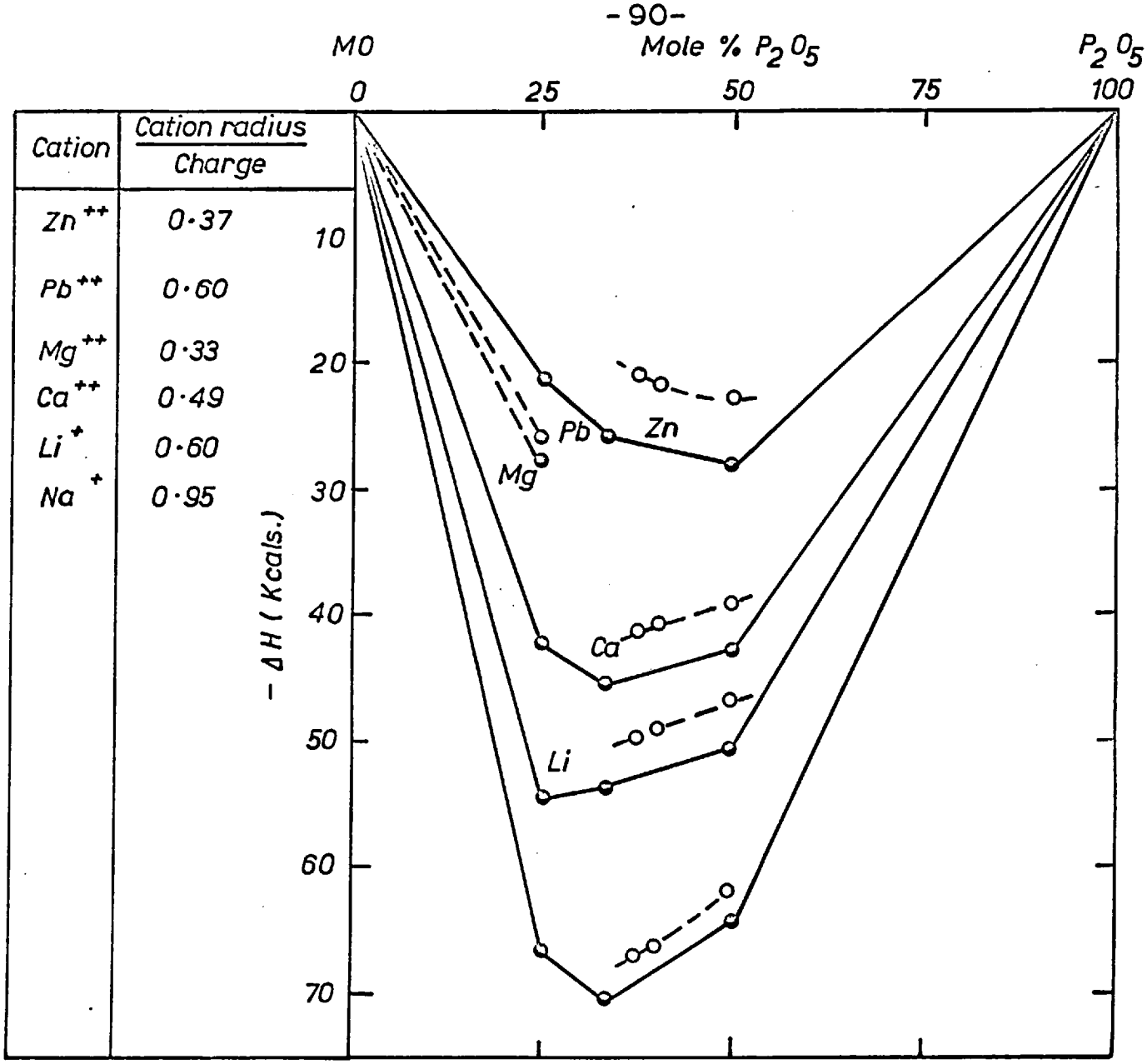

FIG.18 HEAT OF FORMATION OF CRYSTALLINE PHOSPHATES O & GLASSES O IN Kcals/mole OXIDE ($MO + P_2O_5$) AT 35°C

respectively. To check which of the above two factors had an over ruling influence on the observed distributions, it was necessary to choose a system for which the heats of formation and the cation radius to change does not fall in the above order. The available thermodynamic data on the phosphate systems are meagre and the heat of formation of the orthophosphate had to be taken as a guide to the steepness of the heat of formation curve for that system. The lead and magnesium systems were suitable ones to study because the heat of formation of orthophosphate of lead was far less negative than that of Lithium, though the cation radius to charge ratios for the two systems is 0.60, and the heat of formation of orthophosphat of magnesium was more negative than that of zinc though magnesium has a smaller value for the cation radius to charge ratio (cf figure 18). Hence if the distribution is controlled by the cation radius to charge ratio, then lead and lithium phosphates of the same $\bar{n}$ should have the same distributions and magnesium phosphate should have a broader distribution than that of zinc. On the other hand if heats of formation curves is a measure of the breadth of the distribution, then, lead phosphate should have much broader distribution than those of lithium, and zinc phosphate should have a similar distribution to that of the magnesium glasses.

In table B-12, the distributions of Lithium[25], Zinc[25] Lead and Magnesium phosphate glasses of M_2O or MO/P_2O_5 ratio of

Table B-12

Anionic Distributions in Glasses of M_2O or MO/P_2O_5 Ratio of 6:4

Cation	Ortho	Pyro	Tri	Tetra	Penta	Hexa	Hepta	Hypoly
Li*	0.00	12.92	26.26	20.52	14.15	8.83	5.95	11.37
Pb	2.83	16.31	17.26	15.71	13.22	10.68	8.38	15.61
Zn*	3.10	15.04	16.52	14.64	11.66	8.93	8.34	21.77
Hg	2.87	12.21	13.63	13.24	10.81	8.52	6.42	32.35

*Meadowcroft and Richardson[25]

of $6/_4$ are compared. It can be seen that lead glasses have a much broader distribution than that for lithium and near to that of zinc, and magnesium and zinc have similar distributions. The breadth of the distributions can be dealt in terms of the heats of disproportination, discussed in the last section. The sum of $\Delta H_2 + \Delta H_3 + ... \Delta H_n$ will given an idea of the breadth of the distribution. In the following table the $\Sigma \Delta H_n$ is given for the various systems studied by Meadowcroft and Richardson[25], Cripps-Clark[37] and the present author, together with cation radius to charge ratios and the heat of formation of the orthophosphate. The heat of formation of the orthophosphates as mentioned earlier, have been taken as a guide for the steepness of heat of formation curves.

Table B-13

System	Cation Radius / Charge (A)	Heat of formation of orthophosphate (K.cals/mole of oxide)	$\Sigma \Delta H_n$ (cals)
$Na_2O-P_2O_5$	0.95	-66.8	>10,000
$Li_2O-P_2O_5$	0.60	-54.5	>8,000
$CaO-P_2O_5$	0.49	-42.2	3,480
$CdO-P_2O_5$	0.48	?	3,216
$MgO-P_2O_5$	0.33	-27.7	1,654
$PbO-P_2O_5$	0.60	-25.5	1,500
$ZnO-P_2O_5$	0.37	-21.2	1,630

From the above table it can be seen that the breadth of the distributions for the systems studied are directly related to the shape of the heat of formation curves and not to the cation radius to charge ratio. If this is true for all cases then the heat of formation of cadmium orthophosphate should be near that of calcium and this would be interesting to determine.

PART C

THERMODYNAMICS OF PbO, PbO-SiO_2, PbO-B_2O_3 PbO-P_2O_5 and PbO-PbF_2 MELTS

Chapter 9

(i) Introduction

In extraction metallurgy many processes are based on the removal of impurities from metals by equilibration with a slag phase under conditions where impurities are oxidised and their oxides dissolved in the slag. It is therefore of importance to know the activities of the component oxides in metallurgical slags, which are mainly polyanionic melts such as silicates, phosphates and borates. To understand this complex situation it is advantageous to start from simpler binary systems. Though thermodynamic information has been obtained on numerous binary silicates (summarised in Fig.19) little or no information is available for the corresponding phosphate and borate melts. From survey of the literature it seems so far no systems have been investigated in which the same cation was studied in a number of systems with various polyanions.

Often fluorides (particularly fluorspar CaF_2) are added to metallurgical slags to increase their fluidity, by breaking down the anionic networks. The effect of these fluoride ion additions on the oxygen ion activity in the slags is not well understood. This is of industrial importance since strong interactions between F^- and O^{2-} ions in the melt could bring about an

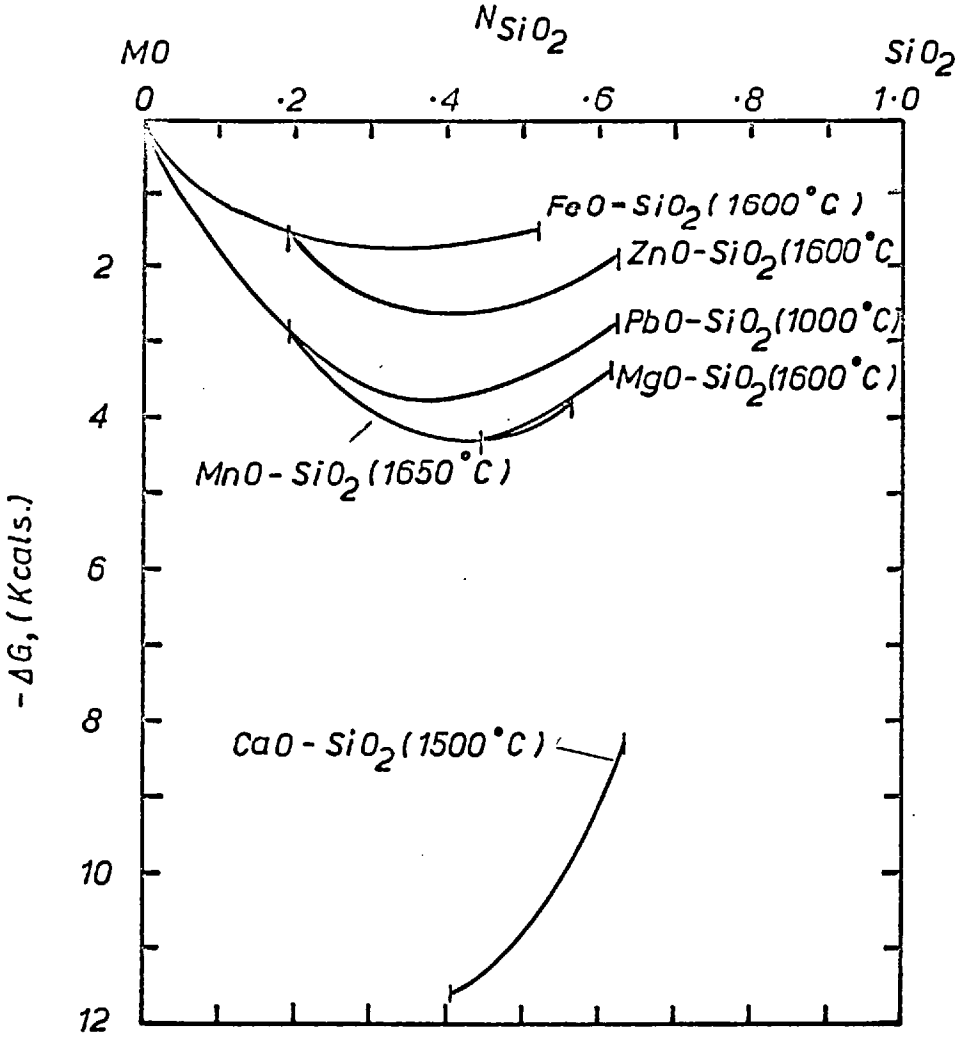

FIG. 19 FREE ENERGIES OF FORMATION OF BINARY SILICATE MELTS

appreciable lowering of the oxygen ion activity, and consequently lowering the sulphide capacities[57] of the slag and therefore the efficiency of refining.

The lead oxide systems were chosen for investigation because of their lower melting points, which made it possible to study them over a wide range of temperatures and compositions, and the possibility of using a simple emf cell for activity measurements.

(ii) Choice of the Method

Ito and Yanagase[35] have measured the lead oxide activities in lead silicate melts using a formation type cell with an oxygen electrode, and obtained values which were in reasonable agreement with earlier equilibration studies of Richardson and Webb[3]. Such an oxygen electrode had been employed in borate melts by Csaki and Dietzel[58] as far back as 1940. They investigated the cell,

$$Pt;H_2 \;\big|\; Na_2O\text{-}B_2O_3 \;\big|\; Pt;O_2$$

and obtained good values for the free energy of formation of the reaction $2H_2 + O_2 = 2H_2O(g)$ at 750-915°C. The use of an oxygen electrode for the silicates was first suggested by Didtschenko and Rochow[59] and later employed by Ito and Yanagase[35] and Minenko and Ivanova[60]. Delimarskii and Andreeva[61] have used an oxygen electrode in $PbO\text{-}Na_2O\text{-}P_2O_5$ melts. Hence it seemed promising to study the various lead binaries by means of a formation cell using an oxygen electrode.

The criteria which have to be satisfied for the

successful operation of a simple cell of the formation type are:-

(1) The melts studied must conduct electricity by ionic conduction only.

(2) The free energy of formation of the metal oxide must be sufficiently smaller than that of the acid oxide, so that the cell reaction is unambiguous.

(3) The solubility of metal in the slag and slag constituents in the metal must be small.

(4) The vapour pressures, liquid ranges and compatability with available refractories and electrode materials of the cell components should be satisfactory.

(5) The electrode reactions must be reversible.

The first criterion has to be fulfilled to obtain a meaningful emf from the cell, If the melt is not completely ionic and has electronic conduction, this would act as a short circuit, and the emf obtained will not be the reversible emf- hence cannot be related to the free energy change for the cell reaction. Bockris and Mellors[62] have shown PbO and PbO-SiO_2 melts to be ionic in nature. It is reasonable to assume the lead phosphate and borate melts would similarly be ionic in character. Lead fluoride has a conductance[63] of 5.7 $ohm^{-1}cm^{-1}$ at 977°C which is in the range for ionic conductors.

The ionic nature of lead oxide systems could be related to the large difference in equilibrium oxygen potential of the lower and higher oxides of lead when compared to the transition

metal oxides. This can be seen from Fig. 20 in which the ΔG^{o} of the oxides of Pb, Fe and Cu are plotted. It will be seen that the introduction of Pb^{3+} ions into a PbO lattice, - hence to produce non-stoichiometry and electronic conduction, - would require far more energy than the corresponding iron and copper cases. Hence it seems unlikely that a formation type cell can be used for measuring transition metal oxide activities in the transition metal oxide systems. This could, of course be overcome by the use of oxide solid electrolytes which ensures pure ionic conduction.

In order to fulfil the second criterion, the standard free energy of formation of PbO should be much less negative than that of SiO_2, B_2O_3, P_2O_5 and PbF_2. This condition was satisfied for all cases except for P_2O_5, for which ΔG^{o} for $P_4O_{10}(g)$ at these temperatures was not very much less than ΔG^{o} for PbO. As described later this led to some unforseen results.

The third criterion, namely the solubility of lead in the slag or the slag constituents in the metal is important as the former would introduce electronic conductivity in the melt and the latter would tend to reduce the lead activity. The effect of electronic conductivity on the emf has been dealt with under criterion one. The reduction of activity of lead by unknown amounts would make the interpretation of the results difficult.

To deal first with the solubility of lead in slags, Meyer and Richardson[64] have shown that at about 1500°C the maximum solubility of lead in lead blast furnace slags would be

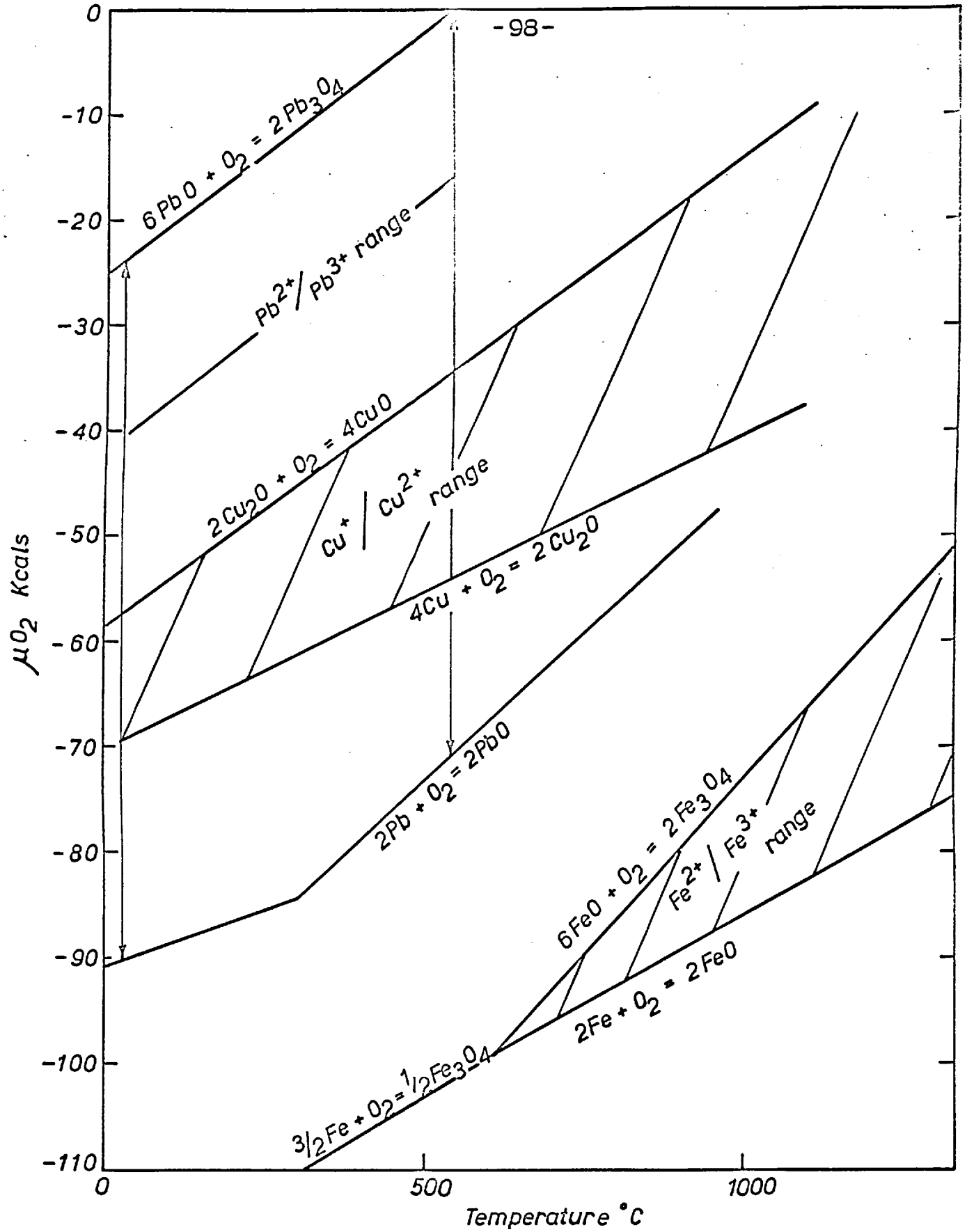

FIG.20 OXYGEN POTENTIALS OF Pb, Fe, Cu OXIDES

around 0.1% wt. This solubility decreases sharply with temperature and since (as seen later) this work was carried out at temperatures not exceeding 1150°C, the solubility in the silicate and the corresponding borates and phosphates can be assumed to be negligibly small. This supported by the fact that there is no appreciable non-stoichiometric range in these melts.

On the other hand halide melts generally dissolve various amounts of the metal. Though no information is available on the solubility of lead metal in lead fluoride melts, data is available for lead solubility in lead chloride[65] and Iodide[66] $PbCl_2$ dissolves 0.123% mole of Pb at 800°C and PbI_2 0.41% mole of Pb at 700°C. Assuming a similar lead solubility in PbF_2 it is unlikely to contribute significantly to the conduction in the melt. This is supported by the fact that for alkali halides[67] contribution to the conductivity by the metal solute decreases greatly going from iodide to the fluoride, i.e. with the size of the halide ion.

Considering next the solubility of the slag constituents in the metal, Hansen[68] reports the solubility in lead of Si-0.02% wt at 1250°C, B-neglibible at 1500°C, and P-negligible. Van Wazer[13] has reported a solubility of 1.5%wt of P in liquid lead. The oxygen solubility at 1000°C is These solubilities are small and they are therefore not likely to affect the lead activity by an appreciable amount in these measurements ($\Delta\bar{G}_{Pb}$ should be less than 50 cals at 1000°C).

It will be seen in the next chapter that criterion four and five were also satisfied by these melts.

In order to determine the activity of lead oxide in $PbO-SiO_2$, $PbO-B_2O_3$, $PbO-P_2O_5$ and $PbO-PbF_2$ melts using the following cell (of Ito and Yanagase's [35] type)

$$Pb \;\big|\; PbO \text{ containing melt} \;\big|\; O_2:Pt$$

it is necessary to know the standard free energy of formation of liquid PbO. Recent measurements of oxygen potentials of PbO have been mainly carried out in the solid state and the measurements on liquid PbO[60][61][69] are not in very good agreement with each other. It was decided therefore to measure the emf of the above cell using pure liquid PbO as the electrolyte. This gives a basis for calculating PbO activities in PbO containing melts without having to use externally derived data. The activity of PbO in these melts can then be calculated from the relationship,

$$-\ln a_{PbO} = \frac{2F(E_2-E_1)}{RT}$$

$$\text{or} \quad \log a_{PbO} = \frac{2F(E_1-E_2)}{4.575T} = 1.008\times10^{4} \times \frac{(E_1-E_2)}{T}$$

where

E_1 - Emf of the cell using PbO as electrolyte

E_2 - Emf of the cell using PbO-containing melt as electrolyte

F - Faraday's constant

R - Gas Constant

T - Temperature in degrees Kelvin.

Chapter 10

Experimental

(a) EMF Measurements

(i) EMF Cell

The construction of the cell used is shown in Fig. 21 The cell assembly was suspended in a cage of "Kanthal 'A' " wire and was so arranged that it could be assembled outside the furnace, which could then be raised into position around the cell without disturbing the relative positions of the cell components. The furnace was heated by a silicon carbide resister and the temperature of the hot zone was controlled to within ± 1°C by means of a proportional band controller operated by a Pt/Pt-13% Rh thermocouple located near the bottom of the crucible. The temperature of the cell was measured by another Pt/Pt-13% Rh thermocouple located at the side of the crucible. This thermocouple was calibrated against a third thermocouple which was immersed in the melt.

The cell consisted of an alumina crucible in which liquid lead was in contact with a pure iron electrode protected from the slag by an alumina sheath. The oxygen electrode consisted of small bore alumina tube with a platinum wire inside it, the end of the tube just dipping into the electrolyte, which floated above liquid lead due to its lower density.

The observation of Webb[70] that alumina ware made by the Royal Worcester Porcelain Company is particularly resistant

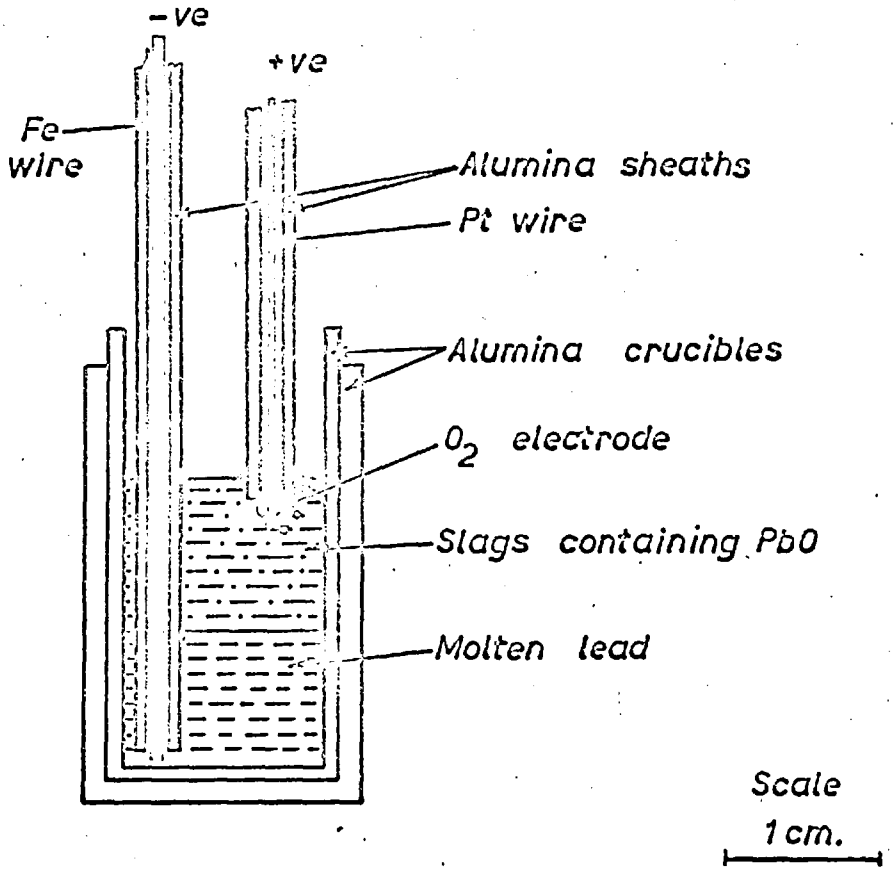

E.M.F CELL

FIG. 21

to attack by PbO containing melts because of their low porosity was confirmed and this grade of alumina was used throughout these experiments. One of the advantages of the type of cell used in these experiments is the rapidity with which it comes to equilibrium. This advantage was fully utilized in case of $PbO-PbF_2$ melts for which the cell life was limited by the rapid penetration of the alumina sheath of the iron electrode by these melts which resulted in the short circuiting of the cell. The rapid attainment of equilibrium enabled a study of this system to be made over the whole composition range at one temperature ($1170^{o}K$) since readings could be obtained within fifteen to thirty minutes from the time the cell was placed in the hot zone. However, after this time the emf would suddenly drop from the steady value, an effect which was attributed to attack of the iron electrode by the melt which had seeped through the alumina sheath. Here again it is worthwhile to note that alumina crucibles made by the Royal Worcester Porcelain Company were dense enough to retain the melts for long periods but that alumina ware bought from elsewhere was not dense enough. In all cases the porosity of the alumina seems to be important in the minimisation of attack. For the other melts, namely $PbO-SiO_2$, $PbO-B_2O_3$, and $PbO-P_2O_5$ this rapid attainment of equilibrium in the cell meant that most experiments at any one composition could be carried out over the whole range of temperatures studied in two to three hours. After such a period of time, no appreciable attack on the refractories by the melt could be

detected either by inspection of sectioned samples or by analysis.

The emf of the cell was normally measured with a potentiometer (made by Croydon Rrecision Instruments Ltd.,) reading to $\pm$ 0.1 mv. and this was periodically checked by taking readings with a high impedance electrometer, to confirm that the potentiometer circuit did not affect the cell voltage appreciably.

(ii) Operation of the Cell.

The iron electrode was placed in position and about 10 g of lead shot placed around it in the crucible. 5-6 g of powdered slag mixture (or PbO), were added and the furnace raised into position. However, for slags of low melting points (e.g. in PbO-PbF_2 and PbO-B_2O_3 systems), the lead had to be pre-melted in the crucible under a nitrogen or argon atmosphere (to prevent oxidation of lead). This was necessary because the slag and metal in such cases melted simultaneously and the slag melt had a preferential affinity to cover the iron electrode and its alumina sheath, thereby preventing any contact of iron with lead, although in theory the slag should float above molten lead. This pre-melting of lead ensured that only molten lead surrounded the iron electrode and the slag added subsequently melted and floated on top of it.

When the crucible contents had melted and reached a steady temperature, the oxygen electrode was slowly lowered until it just touched the surface of the melt. This could be observed by an emf registered in the potentiometer from the completion of the circuit

and also by the small back pressure developed in the flow meter due to the initial resistance of the melt to the oxygen which is flowing around the platinum wire. The exact relative position of the end of the platinum wire and the alumina tube of the oxygen electrode was found to be important. In early experiments the wire was allowed to protrude from the end of the tube and this was found to produce very unsteady emf's which depended on the flow rate of oxygen and the amount the wire was protruding into the melt. These unsteady emf values however oscillated appreciably in a sawtooth manner with periods exactly that of the dis - engagement of the oxygen bubbles from the tube, which could be followed by the small oscillations in the di-butylphthalate level in the flow meter measuring the oxygen flow rate. When the wire was withdrawn so that its end was just inside the tube, a steady emf was obtained. This behaviour of the oxygen electrode will be discussed later (page151).

The furnace atmosphere was found not to be critical for measurements with PbO, PbO-SiO_2, PbO-B_2O_3 and PbO-P_2O_5 melts. However, in the case of PbO-PbF_2 melts an atmosphere of dry nitrogen or argon was maintained inside the reaction tube. The nitrogen or argon was dried by passing successively through silica gel, magnesium perchlorate and P_2O_5. This was done to eliminate the possibility of reaction of PbF_2 with H_2O to give PbO. For the hydrolysis reaction :

$$PbF_2 + H_2O = PbO + 2HF$$

the ΔG^{o} at 1200°K (927°C) is 2.7 K.cals. and hence is likely to occur. This reaction would continuously change the composition by introduction of PbO into the melt and would be especially pronounced in PbF_2 rich melts. The observation that the atmosphere was not critical for other melts indicates a low rate of mass transfer of oxygen through the slag in the crucible, which is a further point in favour of the type of cell used.

(iii) Tests of Cell Reversibility.

The most remarkable feature of the operation of the cell was the speed with which it attained a constant emf. When the cell temperature was changed, for instance, it was found that a constant emf. was obtained within seconds of a steady temperature indication from the thermocouple. In order to determine whether the voltage observed was the true reversible emf of the cell, the following tests of reversibility were carried out:

1. It was established that the same emf was observed when a particular temperature was attained from higher or lower temperature.

2. Emf greater than or less than the equilibrium value were impressed on the cell by an external circuit. On removal of the constraint the cell emf became constant again within a few seconds.

3. The partial pressure of oxygen in the gas was changed and the change in emf of the cell was found to correspond to this

change.

4. The rate of passage of oxygen through the oxygen electrode was varied by a factor of twenty (1 to 20 ml/min) with only very slight changes being observed in the cell emf.

A further point which supports the reversibility of the cell used is the good agreement between the values obtained for the free energy of formation of PbO and PbO activities in PbO-SiO_2 melts in this study and those obtained by earlier workers with other techniques.

(iv) Calibration and Correction.

The potentiometer was checked against an external Weston standard cell. The cell emf was corrected for the thermal emf due to the different leads. The emf of Iron^{+}- Platinum^{-} couple was measured over a range of temperatures and the result is plotted in figure 22 .

(b) Preparation of Slags.

Analar grade lead, lead oxide, ammonium dihydrogen orthophophate (as a source of P_2O_5), reagent grade Boric oxide, lead fluoride and high purity washed quartz powder were used as the raw materials.

In all cases except PbO-PbF_2, which were prepared by mixing the required amounts of PbO and PbF_2 insitu in the cell, the slags were prepared before hand. Weighed amounts of lead oxide and the corresponding acid oxide ($NH_4H_2PO_4$, which loses H_2O and NH_3 on

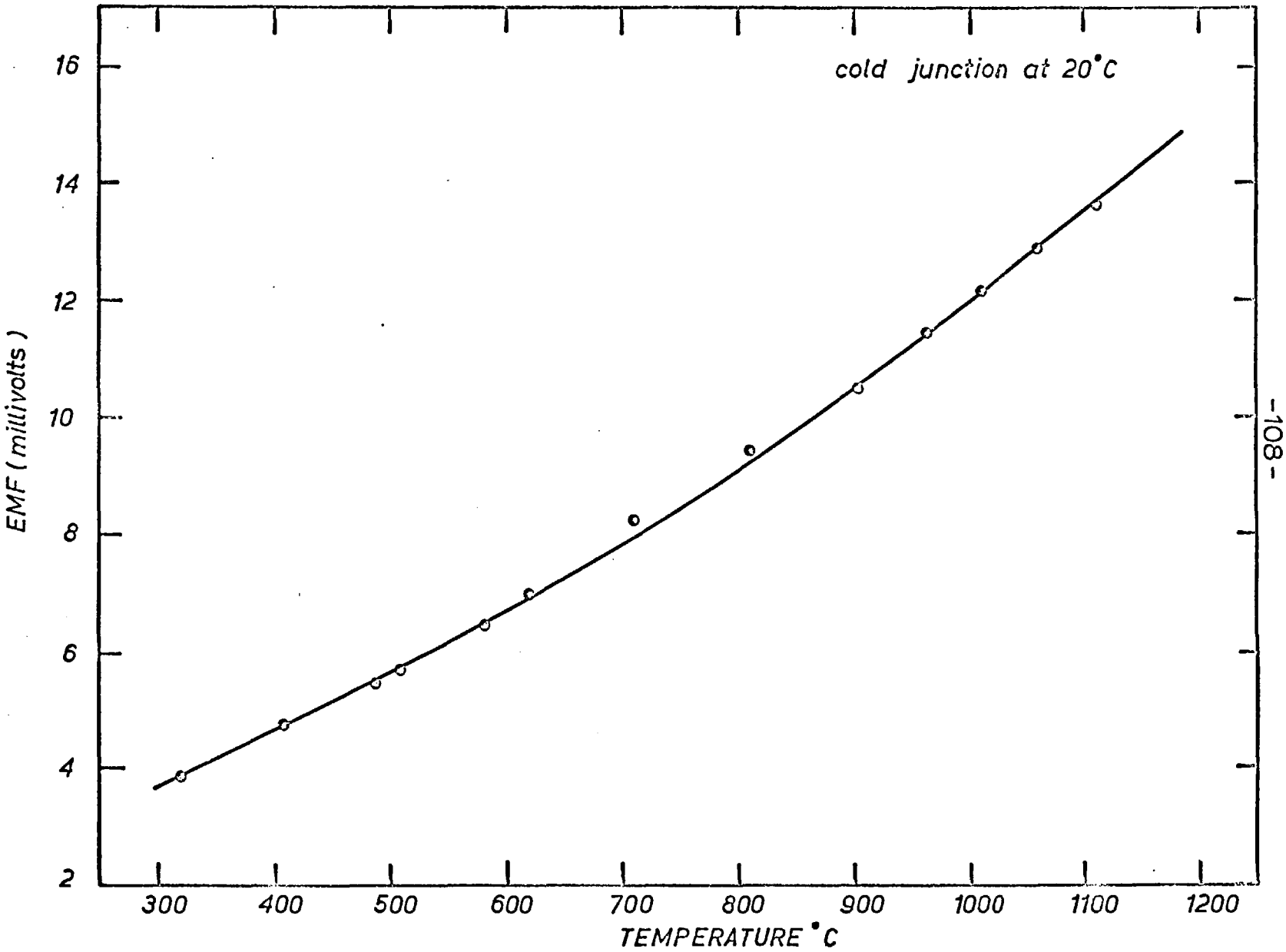

FIG. 22 THERMAL EMF FOR Fe^{+} - Pt^{-} COUPLE .

heating to give P_2O_5, was used as a source of P_2O_5), were mixed in a platinum crucible and melted usually at 1000°C (for compositions of phosphates near the orthophosphate higher temperature up to 1100°C was used). Homogeneous melts were obtained within thirty minutes at these temperatures. The melts were quenched by pouring on to a nickel plate or an aluminium block. The samples were then finely ground and stored in a desiccator. It was difficult to obtain homogeneous glasses in the PbO-SiO_2 system for compositions above $^{N}SiO_2$ = 0.50, due perhaps to the proximity of the silica saturation limit and hence this system was studied from pure PbO to ^{N}PbO = 0.50. When preparing phosphate slags, special care was needed because of attack on platinum crucibles; this has already been mentioned in part B, Chapter 6.

Samples of slags from the emf runs were periodically analysed to check their composition and to check whether they were contaminated with Al_2O_3 from the cell-components. The lead silicates and borates were analysed for PbO by reacting them with hydrofluoric and nitric acids and determining lead in the baked residue gravimetrically as $PbSO_4$. Silica in the silicate was determined on a separate sample by evaporating to dryness with hydrochloric acid heating and extracting with nitric acid. The SiO_2 remaining was washed and ignited. In the case of borates, the B_2O_3 was determined from the difference in weight between the original sample taken and the lead oxide analysed. In case of the phosphates

the sample composition was checked using the paper chromatographic technique (Part B), since the same batch of glass was also used to determine chain length distribution. For some other compositions for which this was not done, the analysis carried out by the Analytical Serviees Laboratory agreed to within 0.5% of the intended composition. When analysing the samples from runs of pure PbO no detectable residue was found, which confirmed the observation that the alumina of the cell was not appreciably attacked. Furthermore, the slag compositions analysed to within 1% of the nominal composition of the starting mixture used and so that it appears that little or no change in composition had taken place in all cases during the experiments.

Chapter 11

Results

(a) Pure Liquid Lead Oxide

The emf of the cell with pure PbO as electrolyte was measured from 900°C to 1080°C, that is from just above the melting point to the temperature where the vapour pressure of PbO becomes sufficiently great for appreciable distillation from the hot zone of the apparatus to take place. The experimental values are given in Table C-1.

Table C-1

Temperature °K	1173	1190	1202	1234	1256	1282	1300	1352
Emf.(m.v.)	513	506	501	488	478	468	461	438

The emf is plotted versus temperature in figure 23. together with the experimental points of Delimarskii and Andreeva[61] and Minenko and Ivanova,[60] who also measured the emf of the cell

$$Pb\ (l)\ /\ PbO\ (l)\ /\ O_2\ (g)\quad Pt$$

The agreement between the values obtained by these workers and that of this study will be discussed in the next chapter.

The best line has been drawn through the experimental points of this study and that of Minenko and Ivanova and the emf can be represented by the equations:

$$E = 0.9936 - 0.4098 \times 10^{-3}\ T \text{ Volts} \quad (C\text{-}2)$$

and $$E = 0.9866 - 0.4098 \times 10^{-3}\ T \text{ Volts} \quad (C\text{-}3)$$

respectively.

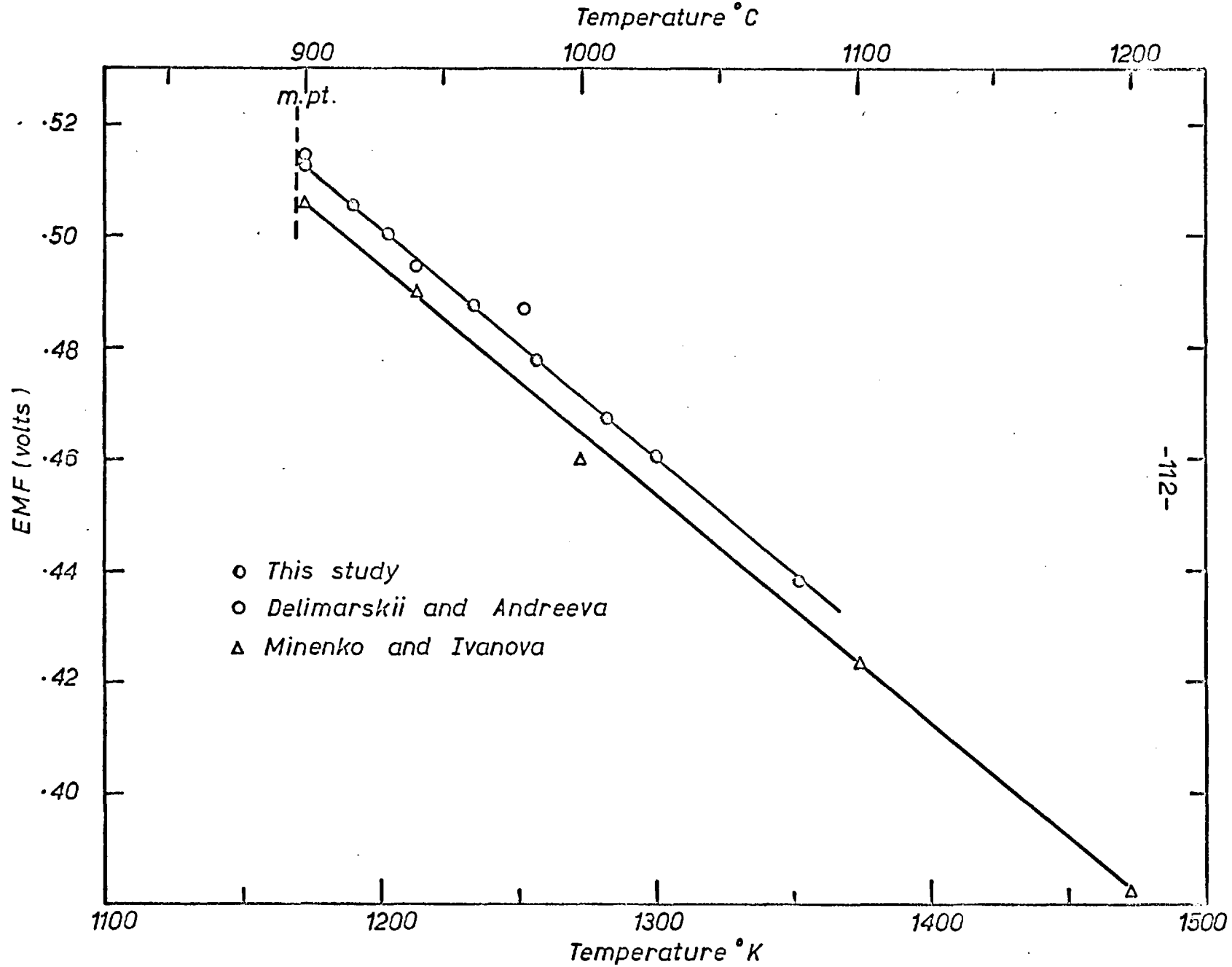

FIG. 23 EMF OF CELL Pb(l) | PbO(l) | O_2(g) : Pt

From these emf values the standard free energy for the reaction:

$$Pb\ (l) + 1/2\ O_2\ (g) = PbO\ (l)$$

can be calculated from the relationship

$$\Delta G^\circ = -2FE = -46{,}126\ E \qquad (C\text{-}4)$$

combining equations C-4 and C-2

$$\Delta G^\circ_T = -45{,}830 + 18.90\ T \text{ Cals/mole PbO} \qquad (C\text{-}5)$$

A comparison of this free energy of formation of liquid PbO with other data is made later. (Page 156).

(b) PbO - SiO_2 Melts

The emf values determined over a range of temperatures for cells containing PbO-SiO_2 melts of various compositions are given in table C-2 and are plotted in figure 24 . In the figure the circles represent the experimental points, and the four crosses the values obtained from Ito and Yanagase[35]'s study by interpolation. Their values could not be compared for other compositions and temperatures because of the limited composition and temperature range of their investigation.

The activities of lead oxide determined directly from these results using equation C-1 (page 100) are shown in figure 25 as a function of composition at 850°C, 950°C and 1050°C. The activities of silica at various compositions in these melts can be calculated using the Gibbs-Duhem relation, which can be expressed in the form:

$$\log a_{SiO_2} = -\frac{N_{PbO}}{N_{SiO_2}} \int d \log a_{PbO} \qquad (C\text{-}6)$$

The necessary integration can be carried out graphically in this particular case from the silica saturation where $^{a}SiO_2 = 1$ (tridymite standard state) to the composition where silica activity is required.

To perform the integration the ^{a}PbO should be known for all compositions up to silica saturation and the silica saturation limit should be well defined. The phase diagram for the $PbO-SiO_2$ system has been studied by Geller, Cremer and Bunting[89] and Krakau, Mukhin and Heinrich.[70a] Though Geller, Cremer and Bunting's phase diagram (figure 49 page 170) is very well defined for the low temperature liquids and solids, their silica saturation composition is not well defined because the liquidus was measured only up to 930°C. However, Krakau etal have measured the liquidus up to 1500°C (figure 26). Richardson and Webb, who measured the oxygen solubility in liquid lead equilibrated with lead silicate melts, found that their function N_{Pb}. At%O , which should become independent of PbO concentration at the silica saturation limits at the various temperatures, did do so at compositions corresponding to Krakau, Mukhin and Heinrich's liquidus. The experimental values of ^{a}PbO which were determined up to $^{N}PbO=0.50$ were extrapolated to these silica saturation limits, which occur around $^{N}PbO = 0.60$, and the Gibbs-Duhem integration carried out. The resulting values for $^{a}SiO_2$ at 850°C, 950°C and 1050°C are also plotted in figure 25 .

Table C.2

EMF as a Function of Temperature for Cells Containing $PbO.SiO_2$ Melts

N_{PbO} = 0.90		N_{PbO} = 0.76		N_{PbO} = 0.70		N_{PbO} = 0.60		N_{PbO} = 0.50	
Temp. °K	EMF Millivolts	Temp. °K	EMF Millivolts	Temp. °K	EMF Millivolts	Temp. °K	EMF Millivolts	Temp. °K	EMF Millivoltd
1140	536	1128	563	1129	580	1123	617	1123	655
1175	522	1139	560	1170	564	1134	612	1168	638
1210	505	1150	554	1205	552	1176	596	1197	628
1243	492	1165	549	1236	538	1193	599	1231	613
1274	480	1200	534	1273	525	1223	576	1240	608
1277	478	1240	518	1316	509	1232	572	1260	600
1300	469	1294	497	1322	505	1284	552	1298	584
1314	463	1316	488	1333	503	1307	544	1301	585
1332	456	1322	487			1314	542	1324	576
						1335	534		

Table C-3

(a) a_{PbO} in $PbO-SiO_2$ melts

N_{PbO}	a_{PbO}			
	850°C	950°C	1000°C	1050°C
0.90	0.85	0.85	0.85	0.85
0.76	0.52	0.53	0.54	0.54
0.70	0.36	0.37	0.38	0.40
0.60	0.17	0.20	0.21	0.22
0.50	0.08	0.095	0.11	0.12

(b) a_{SiO_2} in $PbO-SiO_2$ melts

N_{SiO_2}	a_{SiO_2}			
	850°C	950°C	1000°C	1050°C
0.10	0.0023	0.0032	0.0034	0.0043
0.20	0.0103	0.0130	0.0150	0.0170
0.30	0.064	0.075	0.080	0.084
0.40	0.22	0.24	0.25	0.25
0.50	0.59	0.56	0.55	0.54
0.60	0.98	0.96	0.95	0.91

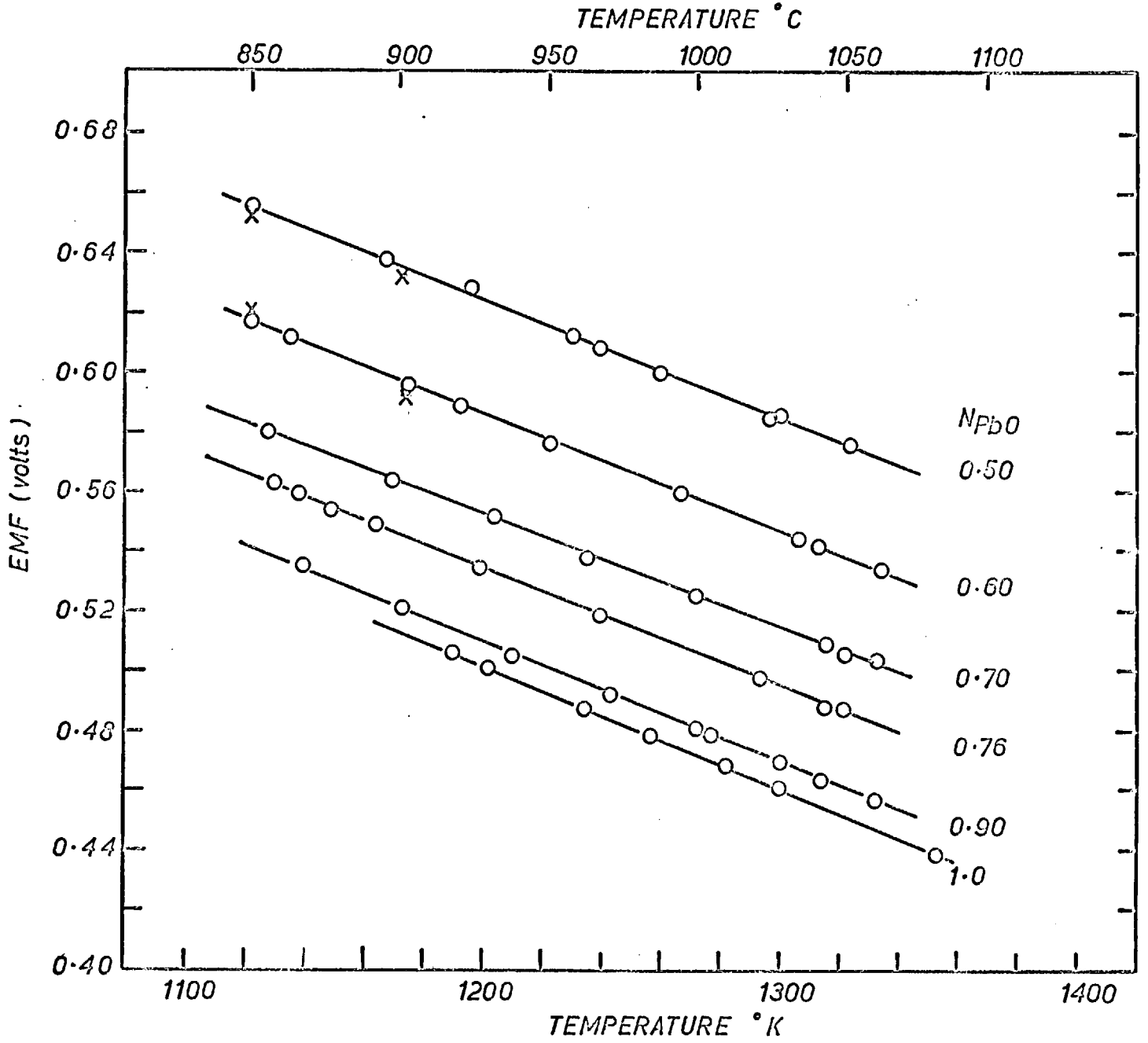

FIG. 24 EMF OF CELL WITH PbO AND $PbO-SiO_2$ MELTS

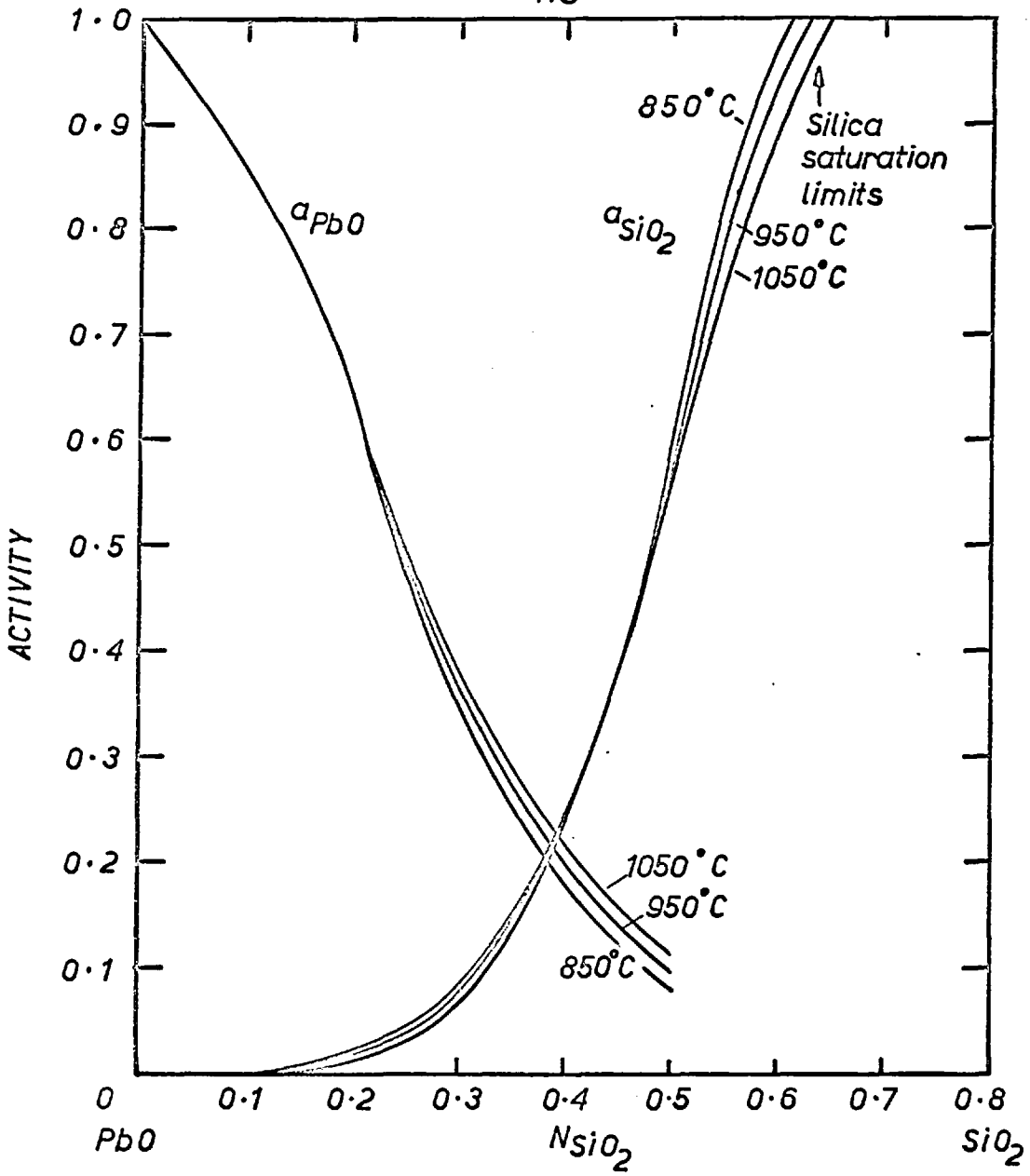

FIG.25 ACTIVITIES OF MOLTEN PbO AND TRIDYMITE IN $PbO-SiO_2$ MELTS

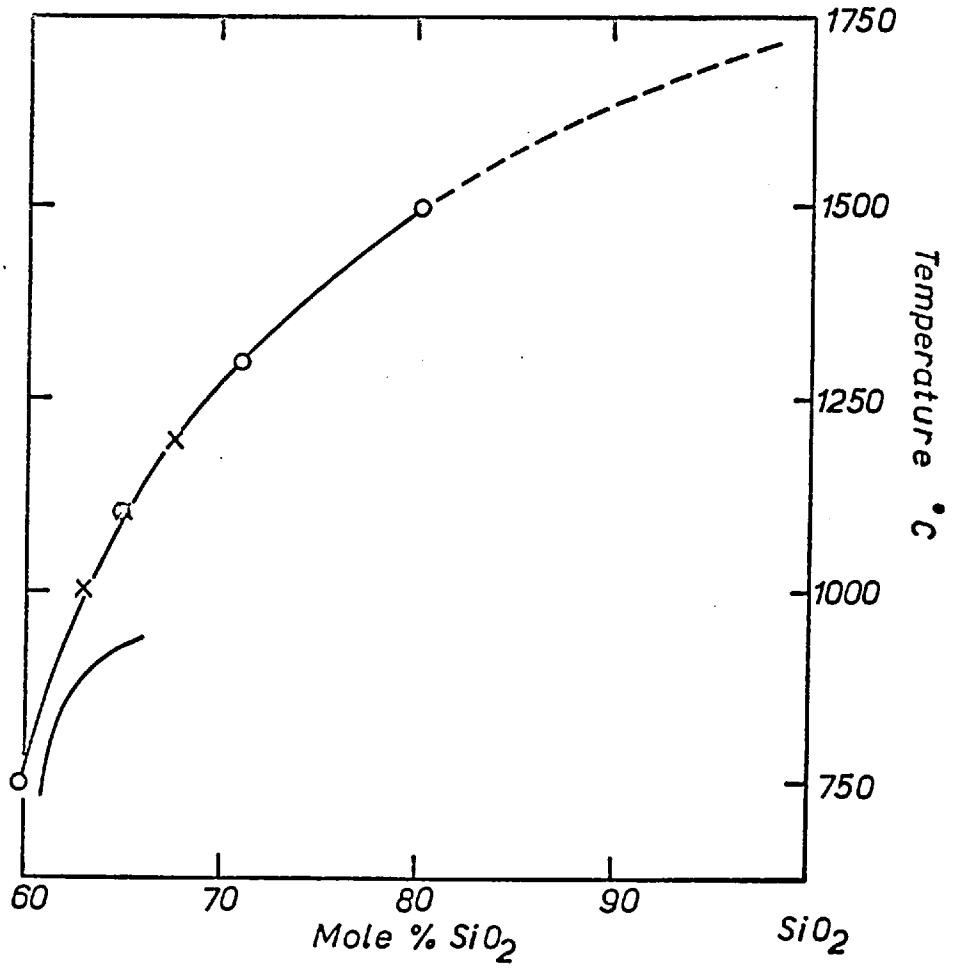

o Krakau, Mukhin and Heinrich x Richardson and Webb
——Geller, Creamer and Bunting

FIG.26 THE LIQUIDUS AT SILICA SATURATION FOR THE SYSTEM PbO-SiO_2

Activities PbO and SiO_2 at 850°C, 950°C, 1000°C and 1050°C are tabulated in table C-3(a) and C-3(b).

(c) $PbO-B_2O_3$ Melts

The emf values determined over a range of temperatures for cells containing $PbO-B_2O_3$ melts of various compositions are given in tables C-4 (a) and C-4 (b) and plotted in figure 27 . The activities of lead oxide were determined from these results using equation C-1 (page 100) and are tabulated in table C-5 (a) for 900°C, 950°C. 1000°C and 1050°C. The activities of B_2O_3 in these melts can be derived using the Gibbs-Duhem relationship, which can be expressed as:

$$\log a_{B_2O_3} = -\int_{N_{B_2O_3}=1}^{N_{B_2O_3}=x} \frac{N_{PbO}}{N_{B_2O_3}} \, d \log a_{PbO}$$

Since in this case a_{PbO} is known over the entire range of composition, the integration can be carried out and the $a_{B_2O_3}$ so obtained at 900°C, 950°C, 1000°C and 1050°C are given in table C-5 (b)..The activities for PbO and B_2O_3 are plotted as a function of composition at 900°C and 1050°C in figure 28 .

(d) $PbO-P_2O_5$ melts

In the case of phosphate melts it was found impossible to extend measurements beyond $N_{PbO} = 0.60$ because of the production

Table C-4(a)

EMF as a Function of Temperature for Cells Containing $PbO-B_2O_3$ Melts

N_{PbO} = 0.95		N_{PbO} = 0.90		N_{PbO} = 0.80		N_{PbO} = 0.725		N_{PbO} = 0.60	
Temp. °K	EMF Millivolts	Temp. °K	EMF Millivolts	Temp. °K	EMF Millivolts	Temp. °K	EMF Millivolts	Temp. °K	EMF Millivolts
1334	452	1340	479	1334	534	1336	555	1336	613
1316	461	1320	488	1301	542	1319	561	1326	617
1275	478	1298	496	1263	554	1280	572	1275	632
1257	485	1278	503	1238	561	1252	580	1240	644
1235	493	1261	509	1201	571	1230	585	1208	653
1230	494	1253	513	1195	573	1209	593	1174	665
1198	509	1242	517	1172	580	1191	597	1140	676
		1223	524	1122	596	1160	602		
		1178	543			1156	608		
		1156	550			1120	620		

TABLE C-4(b)

EMF as a Function of Temperature for Cells Containing $PbO-B_2O_3$ Melts

N_{PbO} = 0.50		N_{PbO} = 0.40		N_{PbO} = 0.30		N_{PbO} = 0.10	
Temp. °K	EMF Millivolts	Temp. °K	EMF Millivolts	Temp. °K	EMF Millivolts	Temp. °K	EMF Millivolts
1340	663	1328	732	1326	797	1334	888
1292	673	1319	735	1303	805	1301	900
1278	678	1298	740	1280	812	1274	912
1242	691	1265	752	1271	816	1248	910
1210	701	1235	761	1239	830	1232	915
1190	707	1205	770	1204	841	1214	921
1160	716	1164	782	1182	849	1198	928
		1148	787	1157	509	1170	950
		1110	799				

Table C-5

(a) ^{a}PbO in $PbO-B_2O_3$ melts

N_{PbO}	^{a}PbO			
	900°C	950°C	1000°C	1050°C
0.95	0.88	0.88	0.88	0.88
0.90	0.55	0.55	0.55	0.55
0.80	0.27	0.26	0.24	0.22
0.725	0.17	0.16	0.15	0.15
0.60	0.051	0.052	0.052	0.053
0.50	0.020	0.020	0.021	0.022
0.40	0.0050	0.0056	0.0062	0.0070
0.30	0.0012	0.0015	0.0019	0.0023
0.10	0.000175	0.00020	0.00033	0.00044

(b) $\log {}^{a}B_2O_3$ in $PbO-B_2O_3$ melts

$N_{B_2O_3}$	$-\log {}^{a}B_2O_3$			
	900°C	950°C	1000°C	1050°C
0.90	0.0540	0.0521	0.0513	0.0511
0.70	0.2616	0.2585	0.2379	0.2294
0.60	0.5838	0.5548	0.5078	0.4878
0.50	1.0711	1.0332	0.9404	0.8765
0.40	1.6200	1.5491	1.4424	1.3604
0.275	2.5937	2.4869	2.3472	2.2249
0.20	3.3200	3.1198	2.9855	2.7745
0.10	5.3640	5.3982	5.3045	5.2760

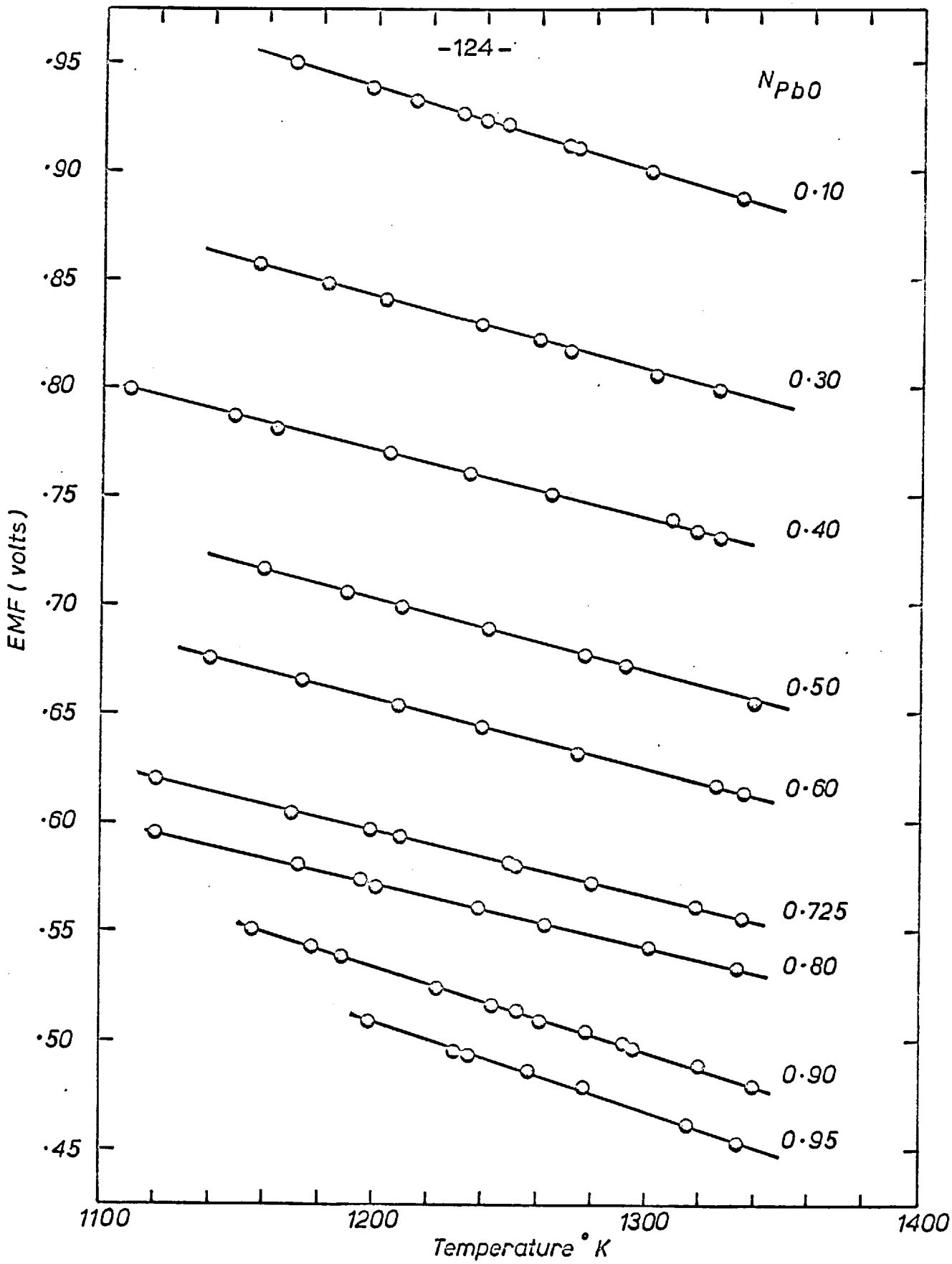

FIG.27 EMF OF CELLS CONTAINING $PbO-B_2O_3$ MELTS

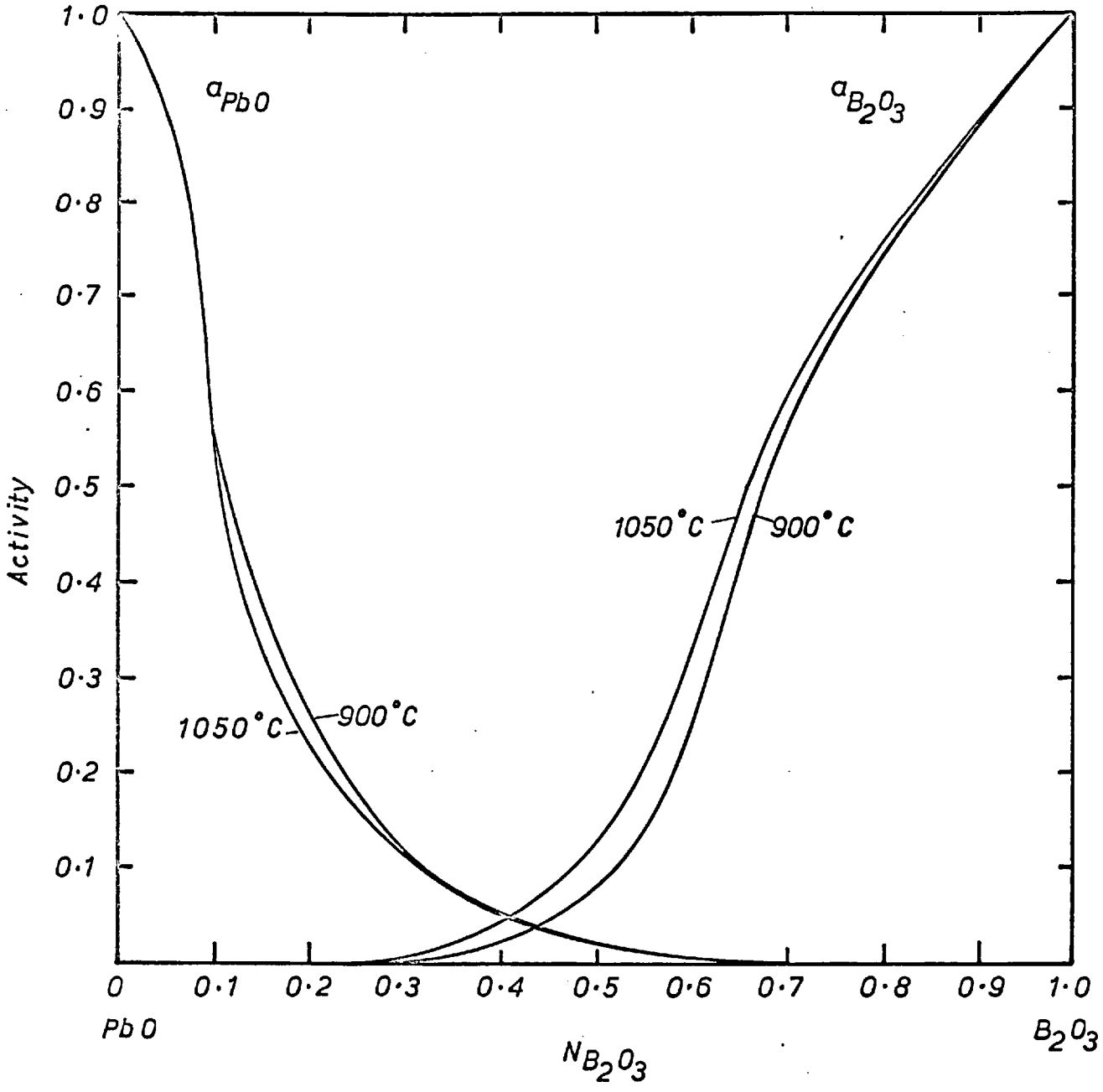

FIG. 28 ACTIVITIES OF MOLTEN PbO AND B_2O_3 IN PbO-B_2O_3 MELTS

of elemental phosphorus. Thus one of the conditions for satisfactory operation of the cell, namely that the free energy of formation of the metal oxide must be sufficiently lower than that of the acid oxide was not completely fulfilled. This would mean that a reaction of the type

$$5\ Pb\ (l) + P_2O_5\ (\text{in melt}) = P_2\ (g) + 5\ PbO\ (\text{in melt})$$

could take place when the activity of PbO in such melts were sufficiently low. Attempts to use a melt of the composition $N_{PbO} = 0.50$ resulted in the production of flashes in the apparatus, which were recognised by Dr. Jeffes as characteristic of burning phosphorus; in fact the activity of PbO in melts of this composition are very low (10^{-4} to 10^{-5}) and such a reaction is likely to take place.

Melts of composition $N_{PbO} = 1$ to $N_{PbO} = 0.60$ were investigated over a temperature range 975°C - 1125°C and the emf of cells with various compositions are given in tables C- 6 and in figure 29 . The activities of PbO determined from these emf values at 975°C 1025°C, 1075°C and 1125°C are given in table C- 7 . The activities of P_2O_5 in these melts were approximately estimated from the above observation of the evolution of phosphorus. For this it was assumed that this reaction commences at a composition $N_{PbO} = 0.55$ and that the phosphorus evolved was at 1 atmosphere pressure. From the equilibrium constant for this reaction at 1025°C, the activity of P_2O_5 referred to 1/2 $(P_4O_{10})_g$

Table C.6(a)

EMF as a Function of Temperature for Cells Containing $PbO.P_2O_5$ Melts

$N_{PbO} = 0.95$		$N_{PbO} = 0.90$		$N_{PbO} = 0.86$	
Temperature °K	EMF Millivolts	Temperature °K	EMF Millivolts	Temperature °K	EMF Millivolts
1184	520	1198	529	1250	545
1219	503	1240	515	1271	535
1237	499	1273	500	1291	525
1267	483	1278	495	1303	519
1285	475	1320	475	1319	513
1304	470	1358	460	1330	506
1325	458	1369	452	1339	505
1345	449	1384	449	1355	499
1380	435	1425	428	1375	489
				1394	478

Table C.6(b)

EMF as a Function of Temperature for Cells Containing $PbO.P_2O_5$ Melts

$N_{PbO} = 0.80$		$N_{PbO} = 0.70$		$N_{PbO} = 0.60$	
Temperature ^oK	EMF Millivolts	Temperature ^oK	EMF Millivolts	Temperature ^oK	EMF Millivolts
1280	670	1259	911	1199	1064
1326	644	1320	877	1210	1057
1361	625	1344	865	1237	1036
1369	621	1362	855	1255	1022
1379	615	1382	842	1280	1015
1423	590	1410	829	1308	994
				1327	982
				1347	968
				1400	935

Table C- 7

Activity of PbO in PbO-P_2O_5 melts

N_{PbO}	a_{PbO}			
	975°C	1025°C	1075°C	1125°C
0.95	0.85	0.85	0.85	0.85
0.90	0.64	0.64	0.64	0.64
0.86	0.31	0.33	0.34	0.36
0.80	Liquidus	0.026	0.033	0.041
0.70	0.00031	0.00046	0.00069	0.00097
0.60	0.000039	0.000064	0.00011	0.00019

Activity of P_2O_5 in PbO-P_2O_5 melts at 1025°C

$N_{P_2O_5}$	0.45	0.40	0.30	0.20	0.10
$-\log {}^{a}P_2O_5$	5.7932	6.2844	7.5134	13.6385	16.4015

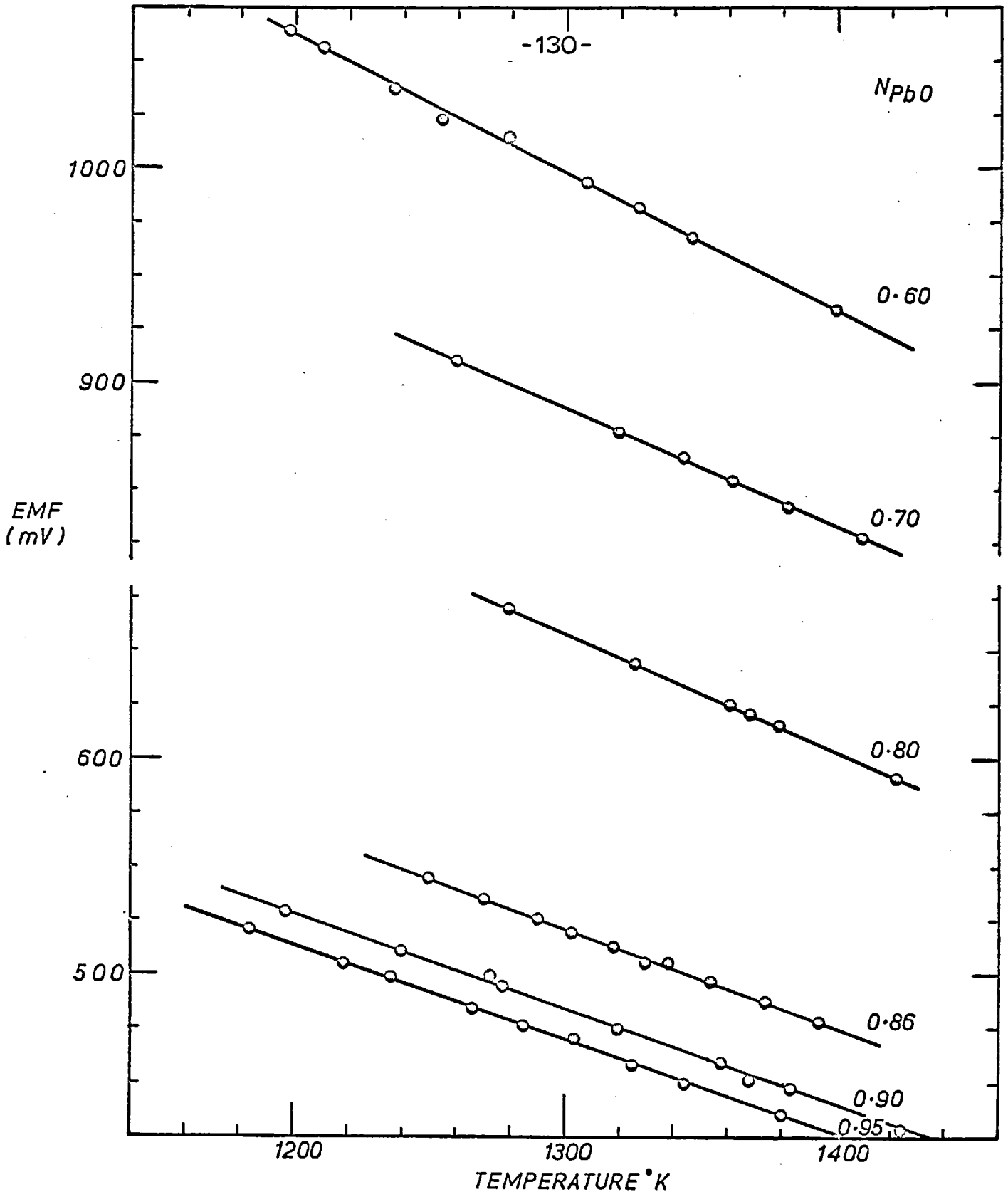

FIG. 29 EMF vs T°K of $PbO-P_2O_5$ MELTS

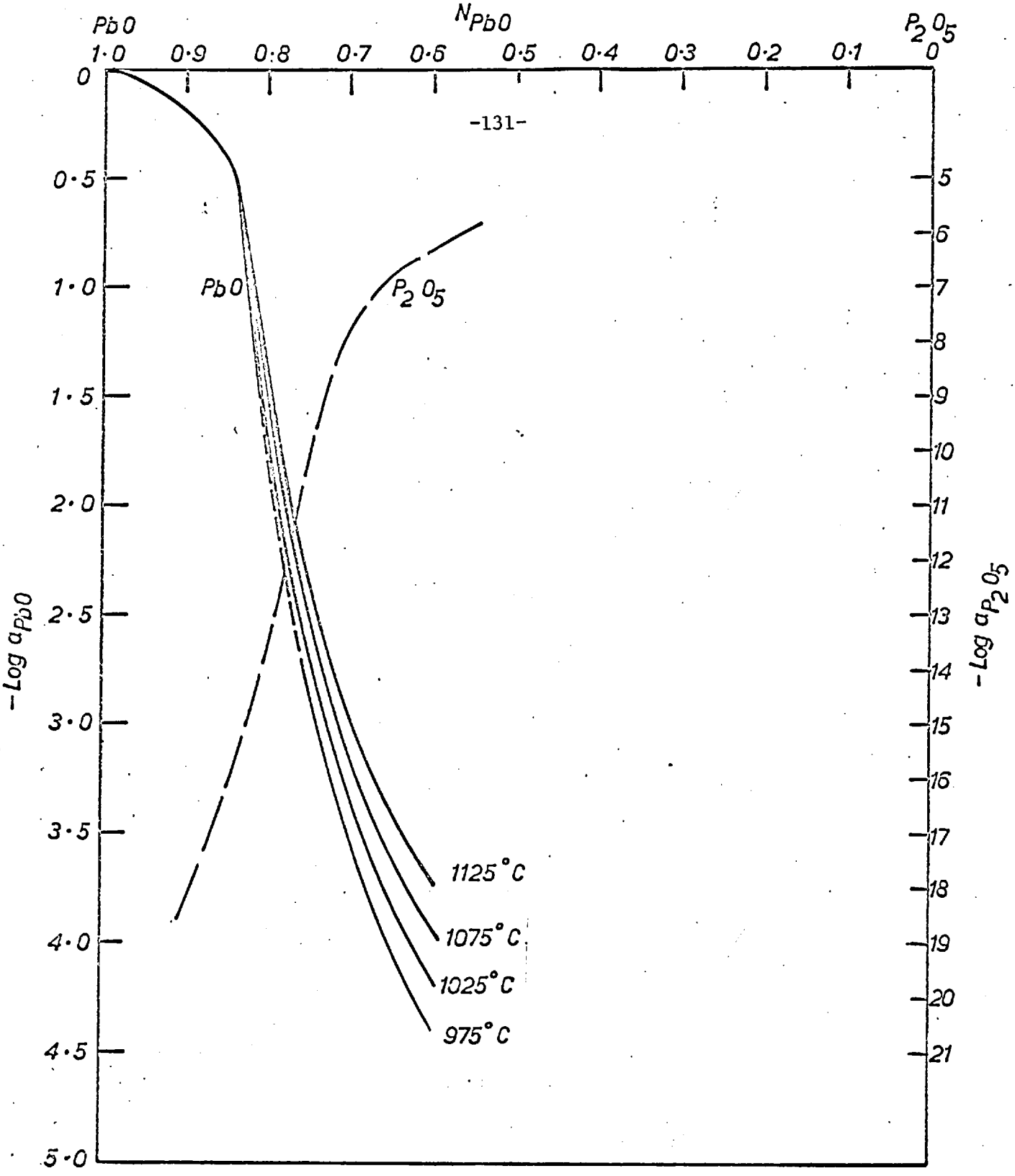

FIG. 30 ACTIVITIES OF PbO & P_2O_5 IN PbO – P_2O_5 MELTS

at 1025°C as the standard state, can be calculated. After fixing the $^{a}P_2O_5$ at $^{N}PbO = 0.55$, the Gibbs-Duhem integration can be carried out and the resulting values for the activity of P_2O_5 are given in table C 7 and plotted together with activities of PbO in these melts in figure 30 . The activity for P_2O_5 is plotted in dotted lines because of the great uncertainty involved in these approximations; the curve does, however, help to give an idea of the magnitude of this activity in these melts.

(e) PbO-PbF_2 melts

As mentioned previously, difficulty was experienced in the case of these melts because of the fast penetration of the alumina sheath round the iron electrode due to their high fluidity. Hence the temperature dependence of emf was only studied for high PbO melts (N_{PbO} 1.0 to 0.70. However, owing to the rapid equilibrium attained by the type of cell used, emf data could be obtained at 1170°K for the entire composition range and these values are tabulated in table C- 8 . The emf as a function of temperature for compositions N_{PbO} 1.0 to 0.70 are given in table C-8 and plotted in figure 31 . The dotted line for pure PbO is obtained from equation C-2 and would correspond to hypothetical liquid PbO. The break in the emf temperature curve for $^{N}PbO = 0.90$ near 1083°K is due to the liquidus at this composition. This agrees fairly well with the value of 1078°K from the phase diagram of PbO-PbF_2 (figure 55 page 185) determined by Sandonnini.[98] The

Table C-8

EMF of cells containing $PbO-PbF_2$ melts

$N_{PbO}=0.90$		$N_{PbO}=0.80$		$N_{PbO}=0.70$		Temp. 1170°K	
Temp°K	EMF (mv)	Temp°K	EMF (mv)	Temp°K	EMF (mv)	N_{PbO}	EMF (mv)
1170	525	1170	539	1170	554	0.90	525
1167	526	1158	544	1144	564	0.80	539
1159	530	1145	549	1125	571	0.70	554
1148	535						
1134	540	1119	559	1105	579	0.60	570
1127	544	1100	567	1091	586	0.50	585
1121	545	1087	572	1075	590	0.40	600
1104	553	1071	578	1060	597	0.30	621
1097	556	1053	586	1040	605	0.20	648
1074	563	1027	597	1025	611	0.10	691

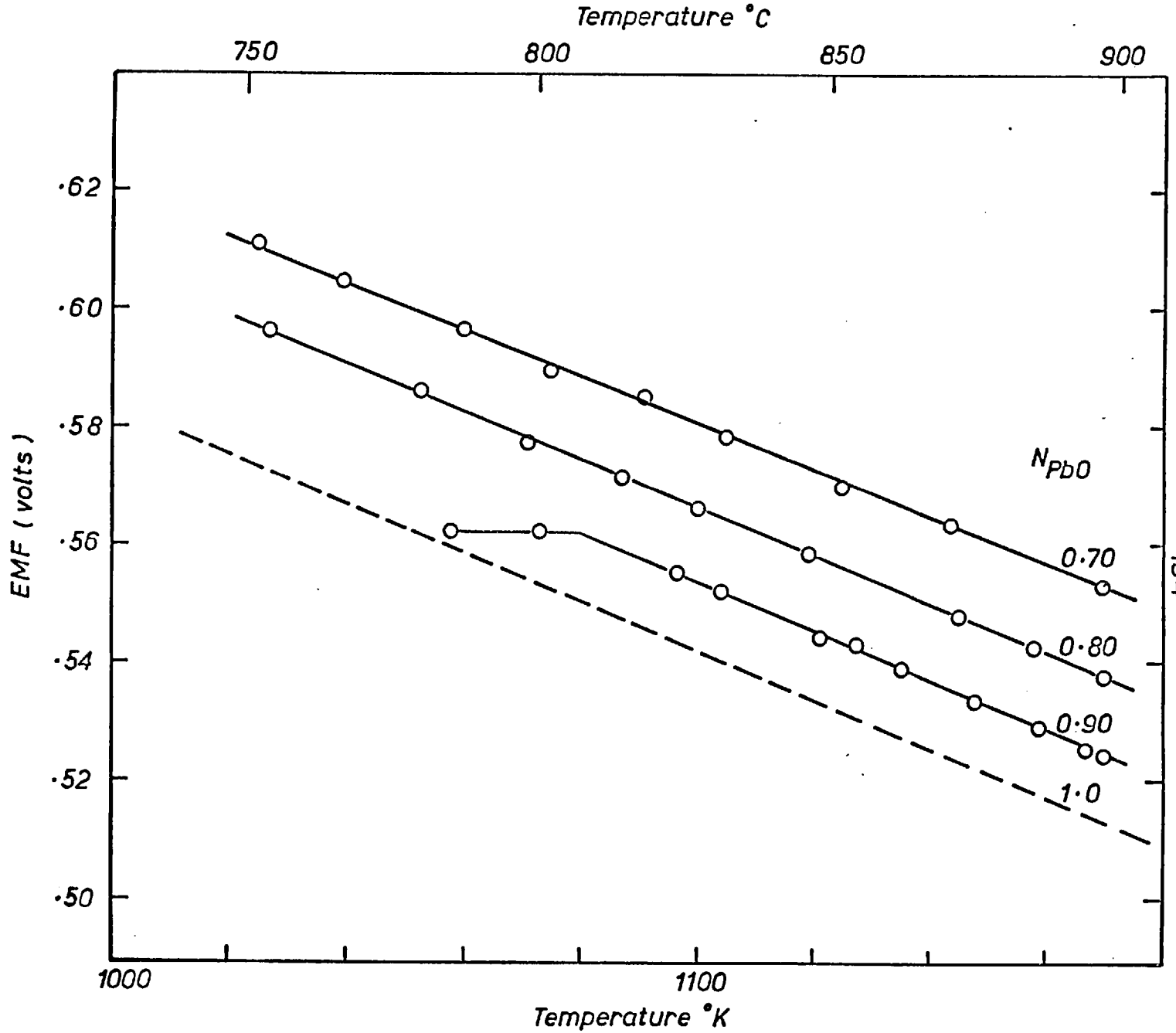

FIG. 31 EMF OF CELLS CONTAINING PbO-PbF_2 MELTS

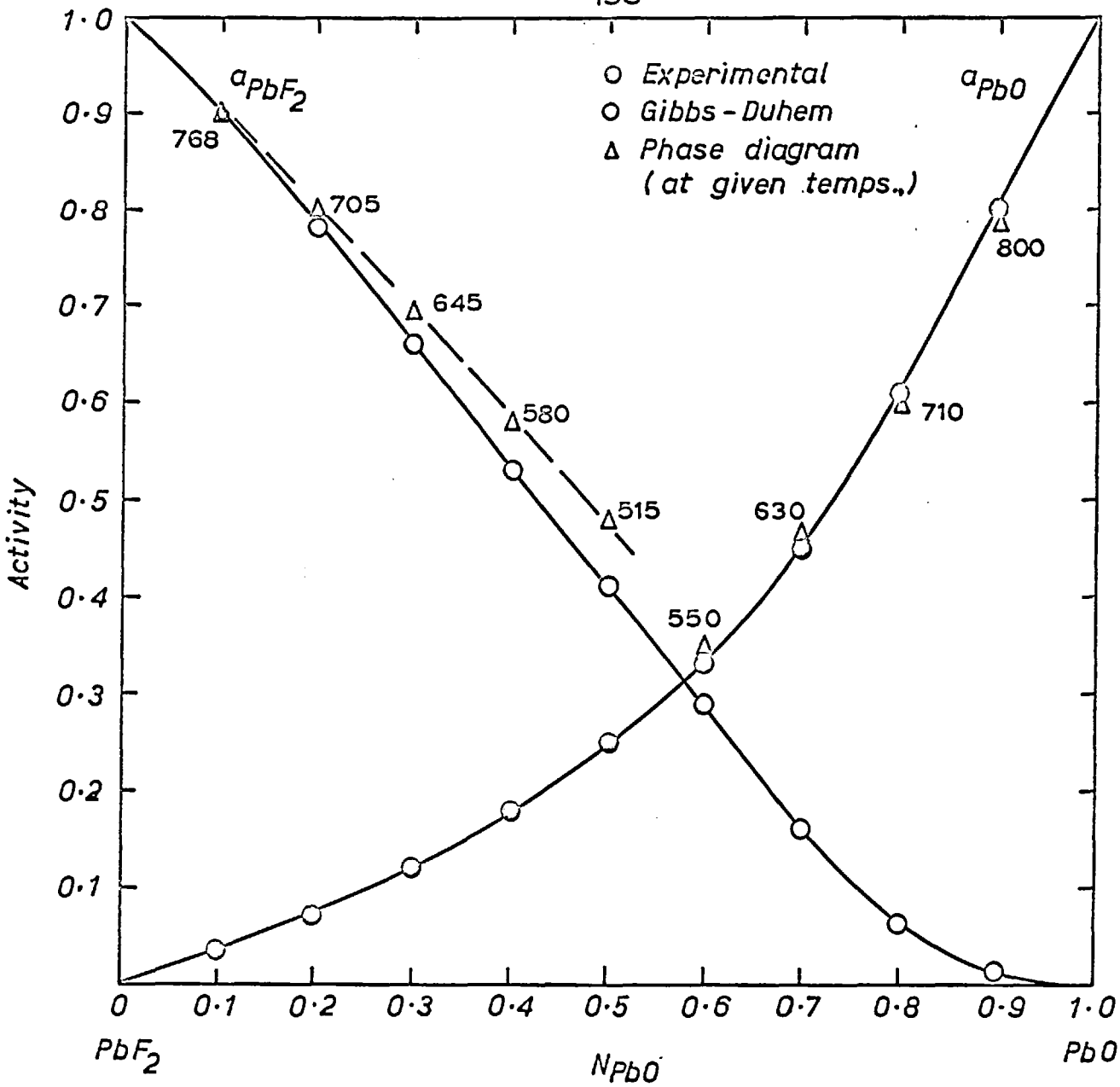

FIG.32 ACTIVITIES OF MOLTEN PbO & PbF_2 IN PbO - PbF_2 MELTS AT 1170°K

derived activities of PbO are plotted as a function of composition at 1170°K in figure 32. The activities of PbF_2 obtained by the Gibbs-Duhem integration are also plotted in figure 32. All these activities refer to pure liquid as the standard state.

(f) Partial Molar Quantities

Lead Silicate, Borate and Phosphate Melts

The activity of PbO in the melts is related to the partial molar free energy of solution of PbO in the melt by the equation

$$\Delta \bar{G}_{PbO} = RT \ln a_{PbO}$$

From the measurement of activity of PbO over a range of temperatures it is possible to derive values for the partial heats and entropies of solution of PbO from the equation

$$\Delta \bar{G}_{PbO} = \Delta \bar{H}_{PbO} - T \Delta \bar{S}_{PbO}$$

assuming that $\Delta \bar{H}_{PbO}$ and $\Delta \bar{S}_{PbO}$ are constant over the range of temperatures studied.

Hence by plotting $\Delta \bar{G}_{PbO/T}$ as a function of 1/T the slope would give the value of $\Delta \bar{H}_{PbO}$. Knowing $\Delta \bar{G}_{PbO}$ and $\Delta \bar{H}_{PbO}$ the value of $\Delta \bar{S}_{PbO}$ can be obtained by substitution in the above equation. Instead of plotting $\Delta \bar{G}_{PbO/T}$, log a_{PbO} can be plotted, in which case the slope will be $\Delta \bar{H}_{PbO}/4.575$ from which $\Delta \bar{H}_{PbO}$ can be calculated.

Since the activities of SiO_2 and B_2O_3 as function of temperature are also known, the corresponding partial heats and entropies of solution of SiO_2 and B_2O_3 in PbO - SiO_2 and PbO-B_2O_3 melts respectively can be obtained from similar plots. These plots of either $\Delta \bar{G}/_T$ against 1/T or log a against 1/T are given in figures 33 to 37 for their respective melts. The values of $\Delta \bar{H}_{PbO}$, $\Delta \bar{H}_{SiO_2}$ and $\Delta \bar{H}_{B_2O_3}$ obtained are plotted as a function of composition in figure 38 . Similarly the variation of $\Delta \bar{S}_{PbO}$, $\Delta \bar{S}_{SiO_2}$ and $\Delta \bar{S}_{B_2O_3}$ with composition in these melts are given in figure 39 .

For PbO - PbF_2 melts $^{a}_{PbO}$ was measured as function of temperature for melts of composition $N_{PbO} = 0.70$ to $N_{PbO} = 1.0$ and these data were used to calculate $\Delta \bar{H}_{PbO}$ and $\Delta \bar{S}_{PbO}$. The values are given in the following table.

Table C 9

N_{PbO}	$\Delta \bar{H}_{PbO}$ cals/mole	$\Delta \bar{S}_{PbO}$ cals/dig.
0.90	30	0.31
0.80	120	0.63
0.70	280	1.26

(g) Integral Molar Quantities

From the partial molar quantities derived above the integral quantities can be obtained using the relationship

$$\Delta G^M = N_1 \Delta \bar{G}_1 + N_2 \Delta \bar{G}_2$$

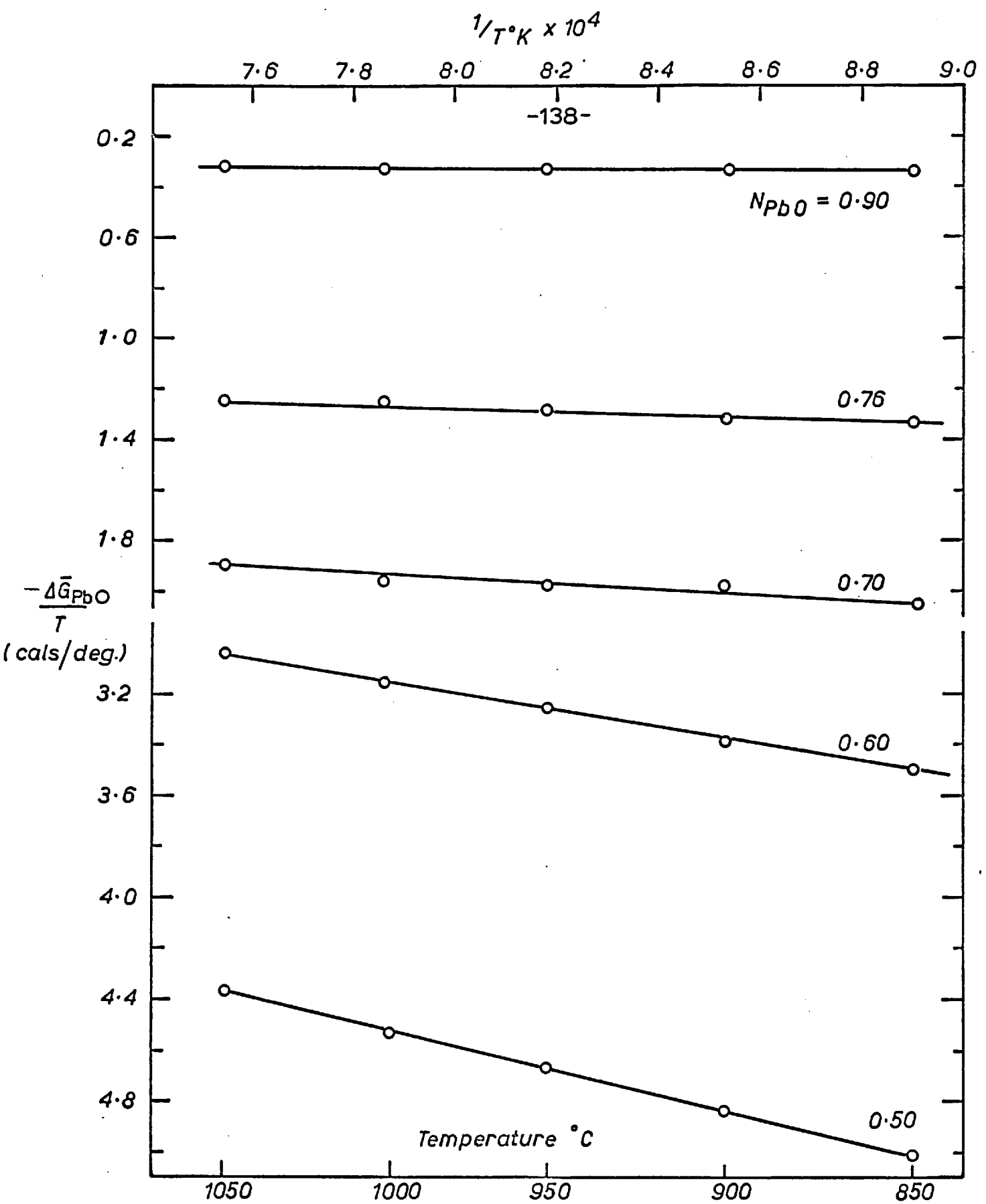

FIG.33 PLOT OF $\frac{\Delta \bar{G}_{PbO}}{T}$ vs $\frac{1}{T°K}$ FOR $PbO-SiO_2$ MELTS

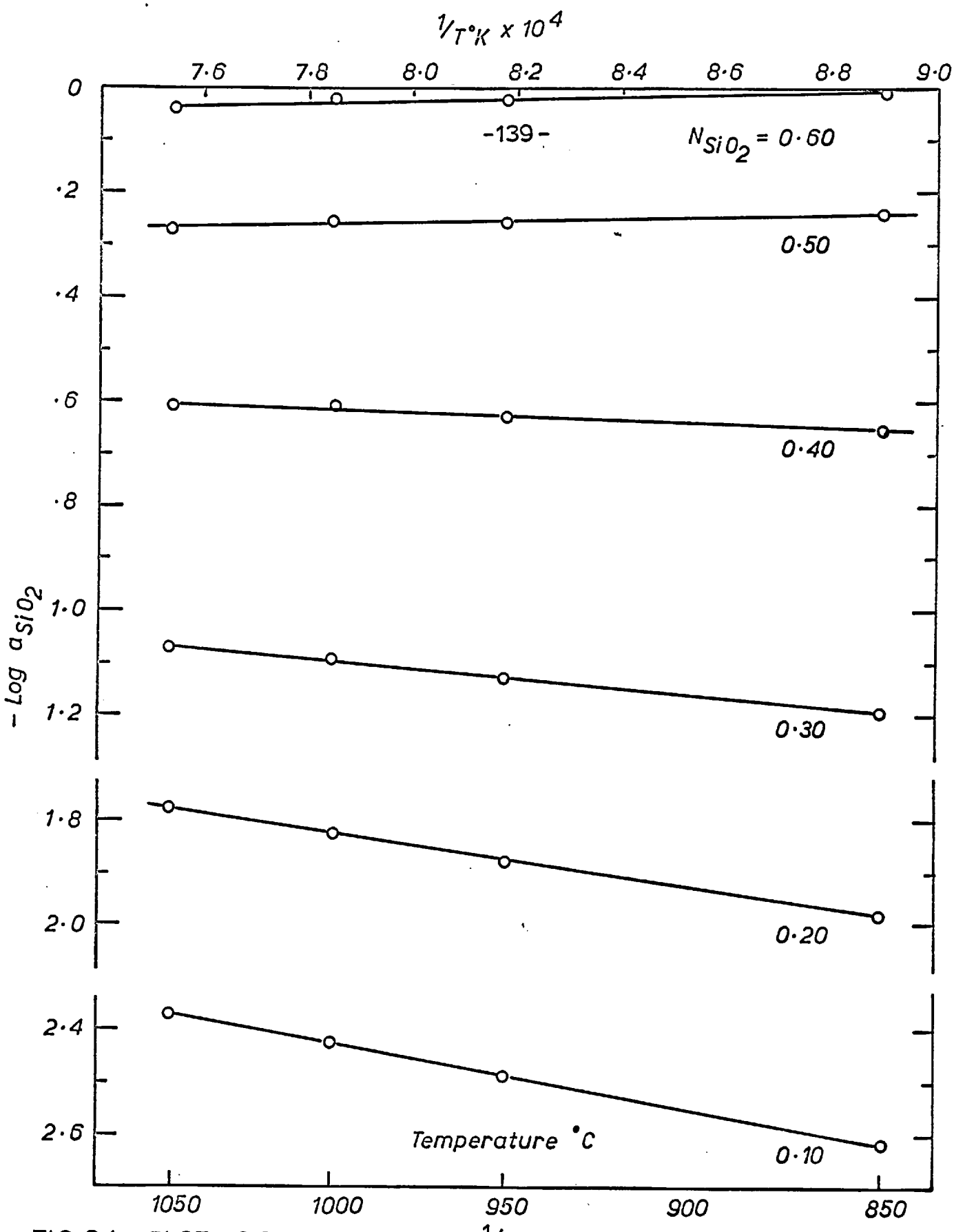

FIG. 34 PLOT OF Log a_{SiO_2} vs $^1/_{T°K}$.

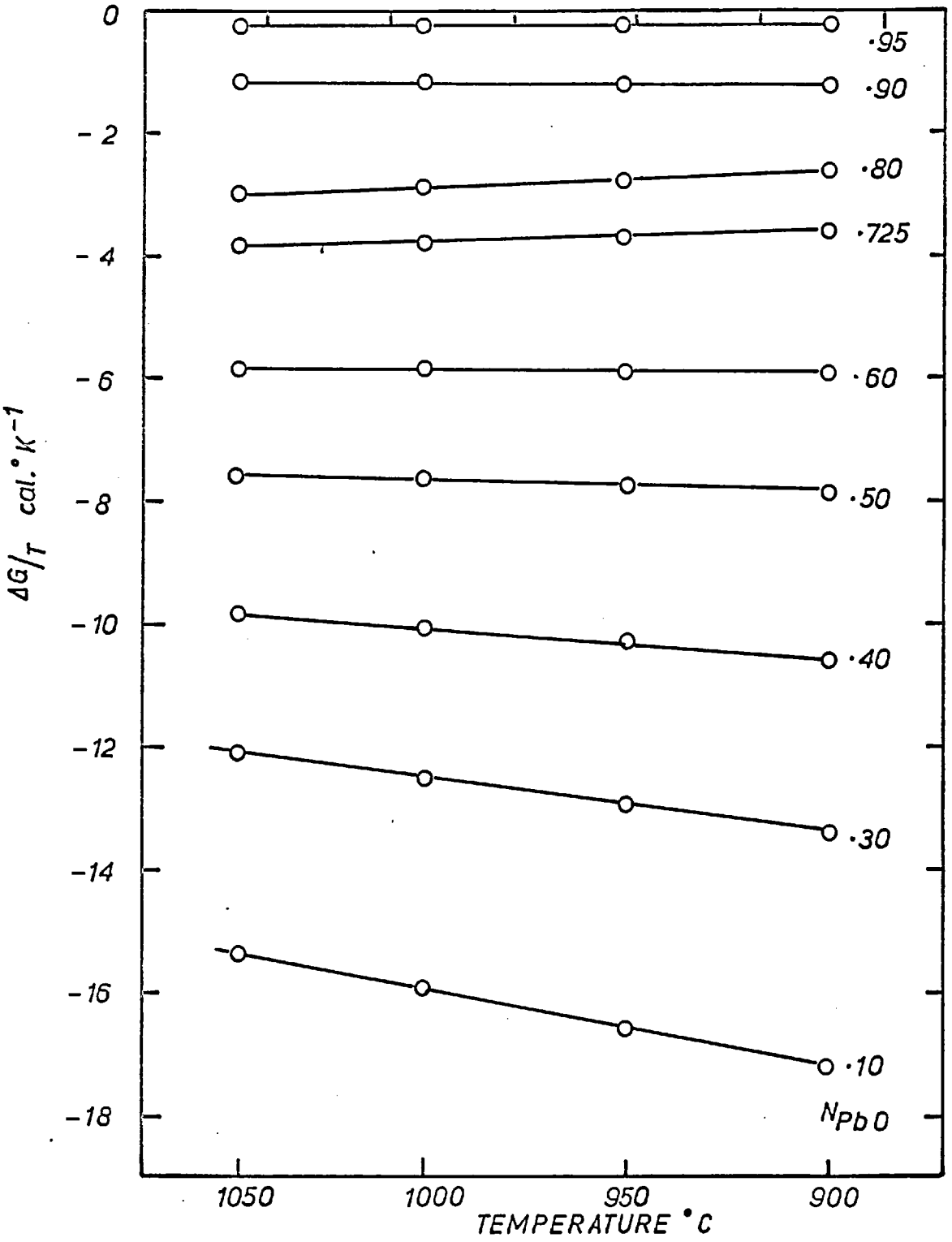

FIG. 35 PLOT OF $\frac{\Delta \bar{G}_{PbO}}{T}$ vs. $^1/_{T°K}$ FOR PbO - B_2O_3 MELTS

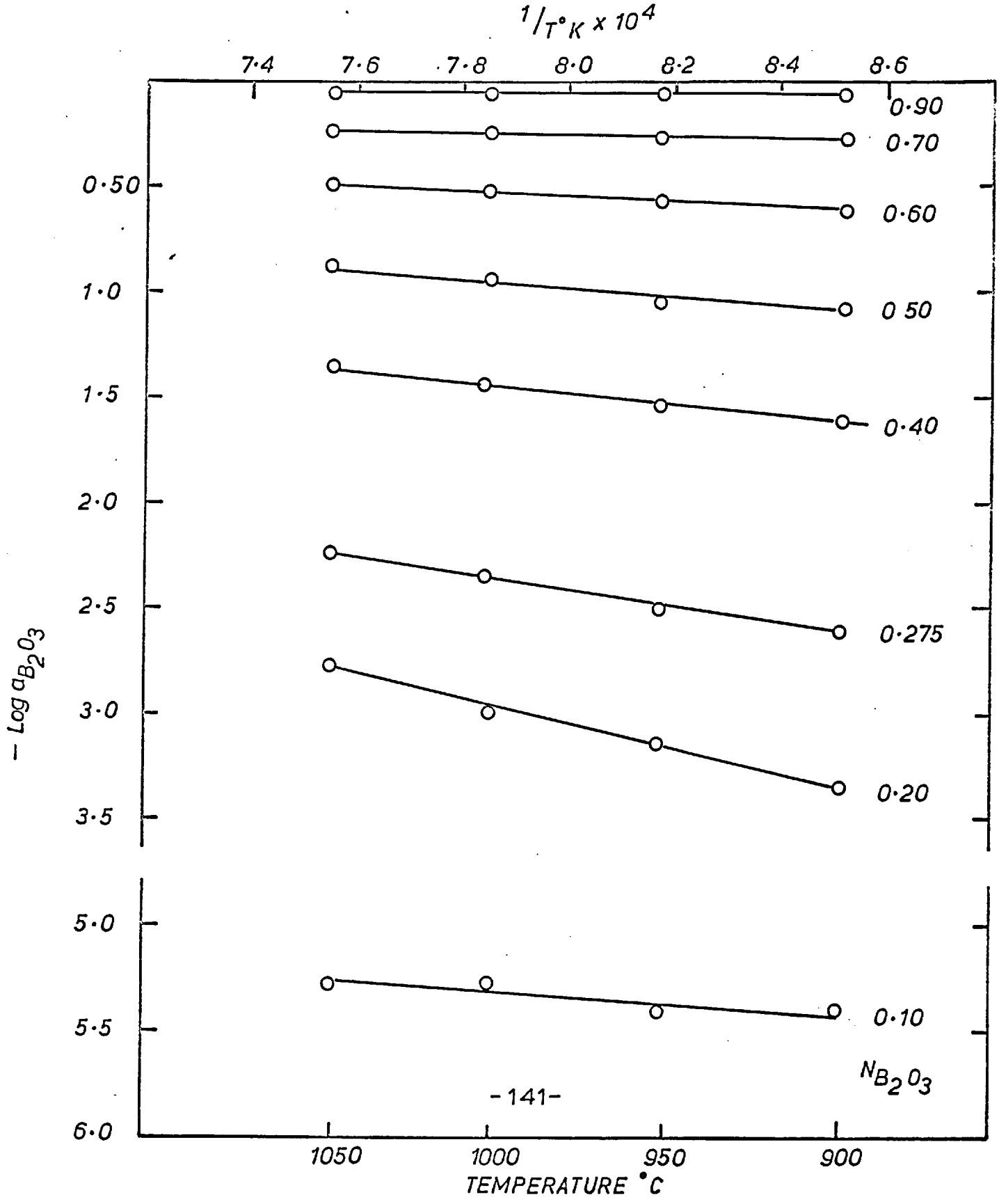

FIG. 36 PLOT OF Log $a_{B_2O_3}$ vs. $^1/_{T°K}$

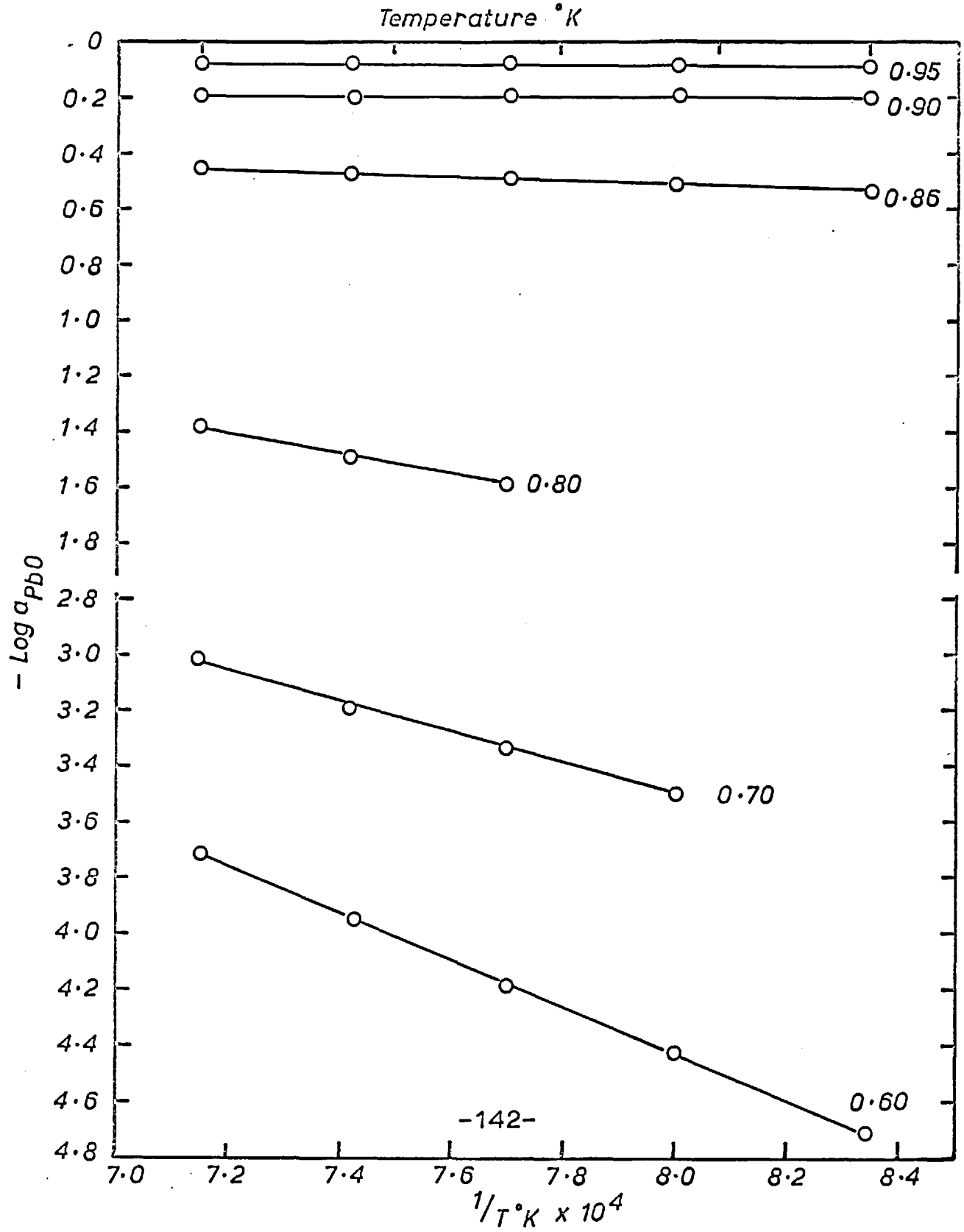

FIG. 37 PLOT OF Log a_{PbO} vs. $1/T$ FOR $PbO-P_2O_5$ MELTS

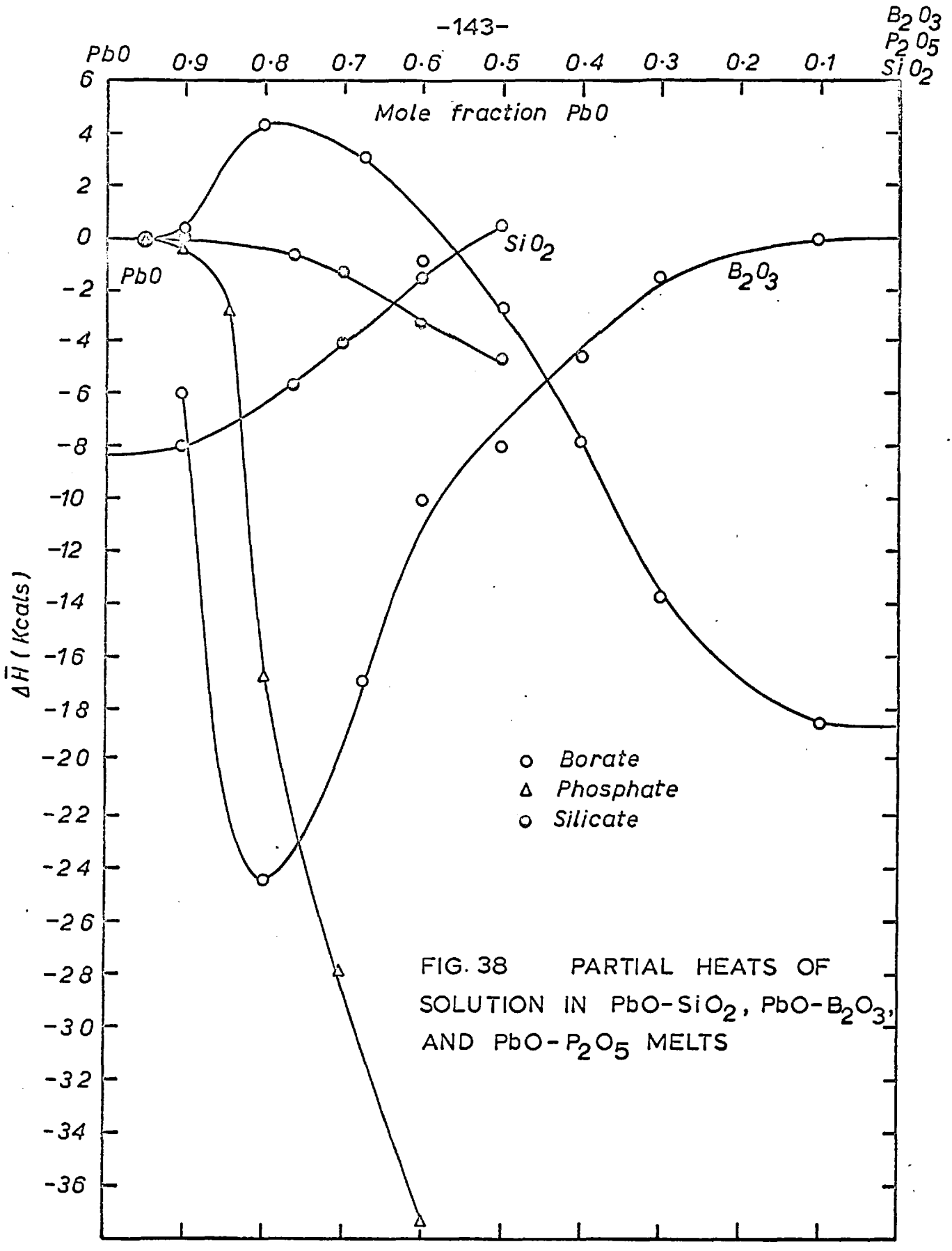

FIG. 38 PARTIAL HEATS OF SOLUTION IN PbO-SiO_2, PbO-B_2O_3, AND PbO-P_2O_5 MELTS

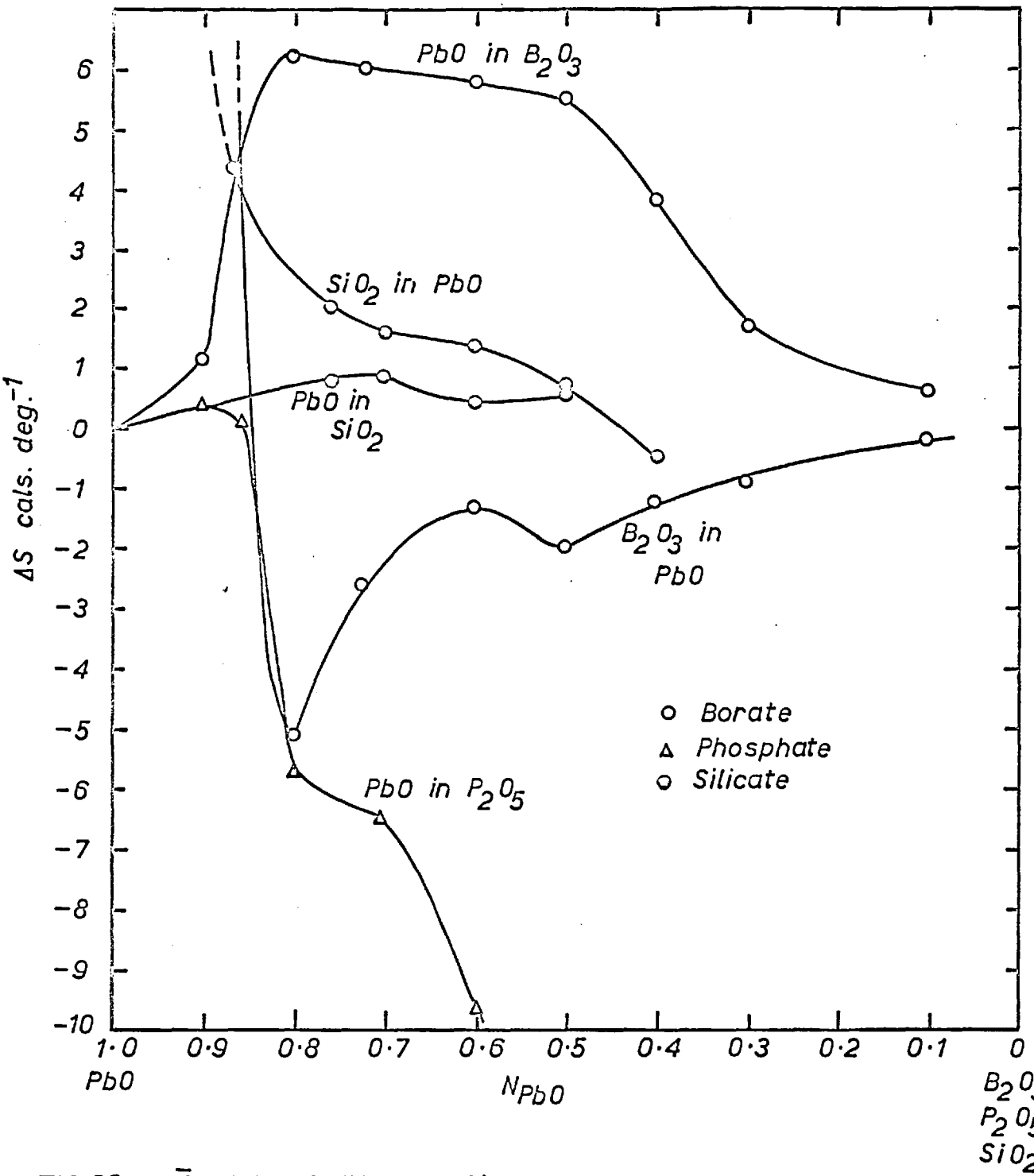

FIG.39 $\Delta\bar{S}$ VALUES IN PbO-SiO_2, PbO-B_2O_3 AND PbO-P_2O_5 MELTS

$$\Delta H^M = N_1 \Delta \bar{H}_1 + N_2 \Delta \bar{H}_2$$

$$\Delta S^M = N_1 \Delta \bar{S}_1 + N_2 \Delta \bar{S}_2$$

where subscript 1 and 2 refer to the two components in question, for example PbO and SiO_2 in PbO-SiO_2 melts.

Since the partial molar free energies, heats and entropies for PbO, SiO_2 and B_2O_3 have been derived in the last section for PbO-SiO_2 and PbO-B_2O_3 melts, the ΔG^M, ΔH^M and ΔS^M for one mole of the melts can be readily calculated and they are given in figures 40 and 41 . In the case of PbO-P_2O_5 melts only the ΔG^M curve is given in figure 42 , since the partial heats and entropies could not be derived for P_2O_5. This was because the derivation of $^aP_2O_5$ itself involved a number of assumptions and the temperature dependence of these activities cannot be relied upon. Though for PbO-PbF_2 melts, we can derive only the $\Delta \bar{H}_{PbO}$ and $\Delta \bar{S}_{PbO}$ over a limited composition region, in Part D, it will be seen that the integral heats and entropies can be obtained for these melts as they seem to exhibit regular solution behaviour and are given in page 214(a).

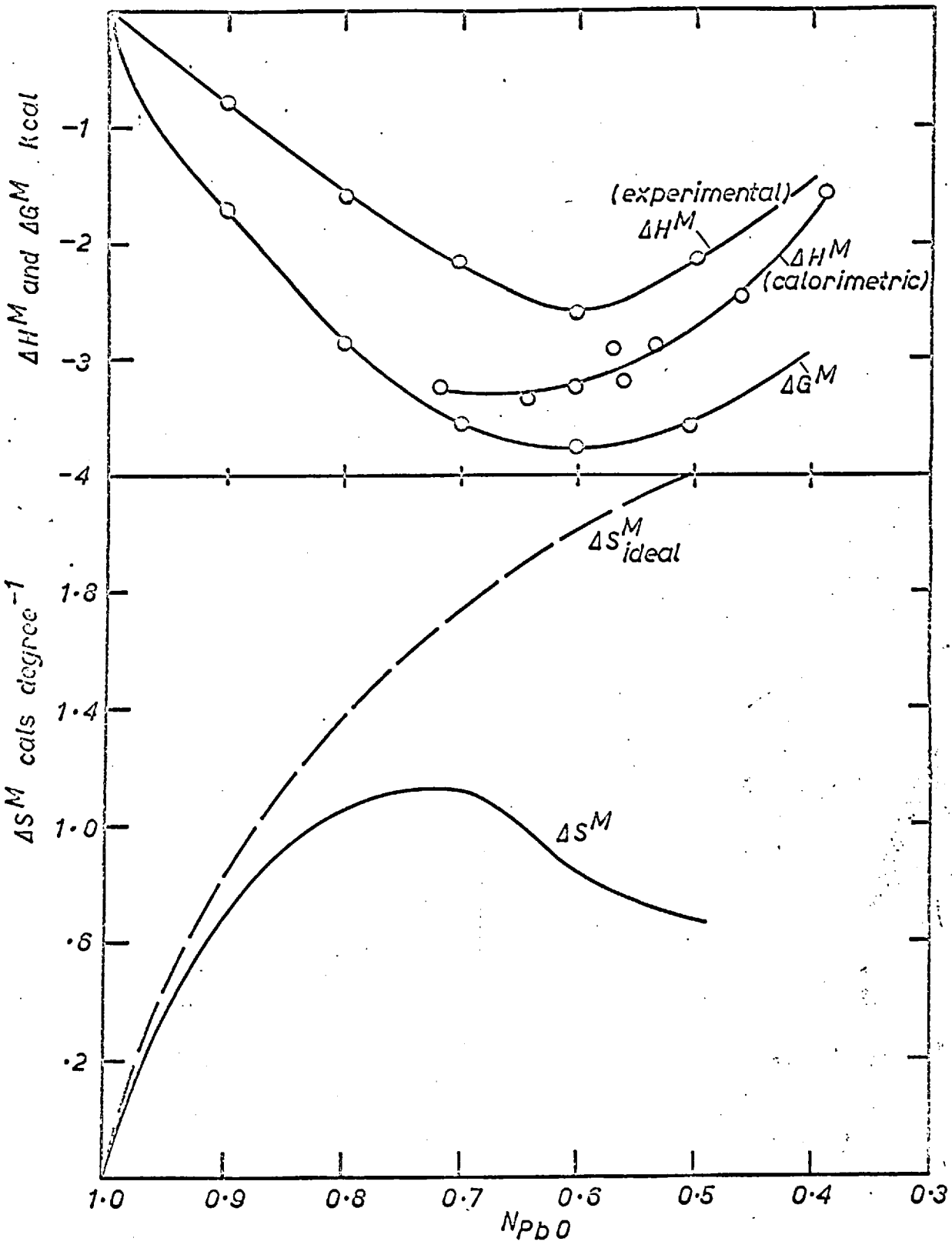

FIG. 40 ΔG^M, ΔH^M & ΔS^M FOR $PbO-SiO_2$ MELTS.

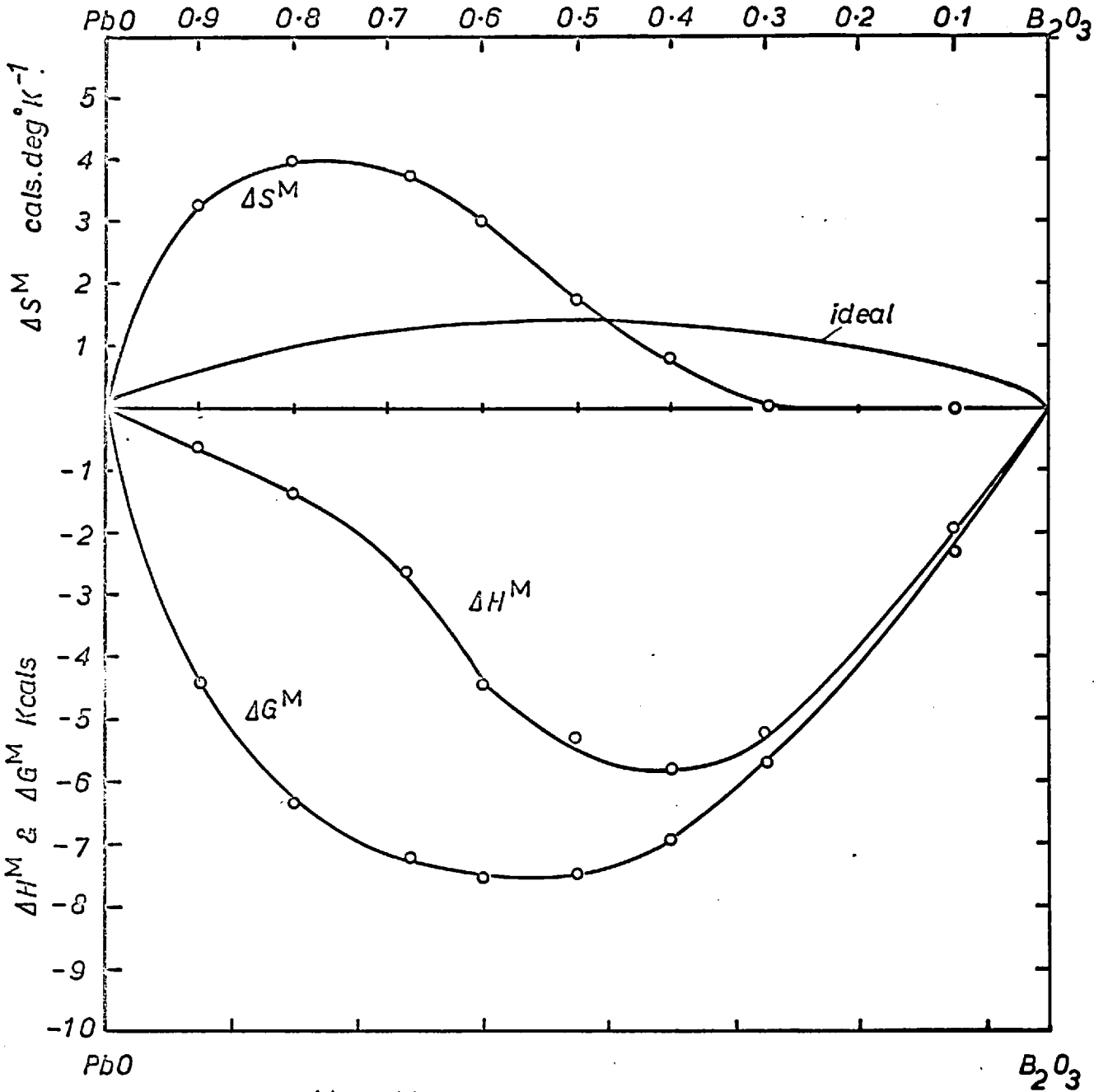

FIG.41 ΔG^M, ΔH^M, ΔS^M FOR PbO-B_2O_3 MELTS FROM LIQUID PbO & B_2O_3

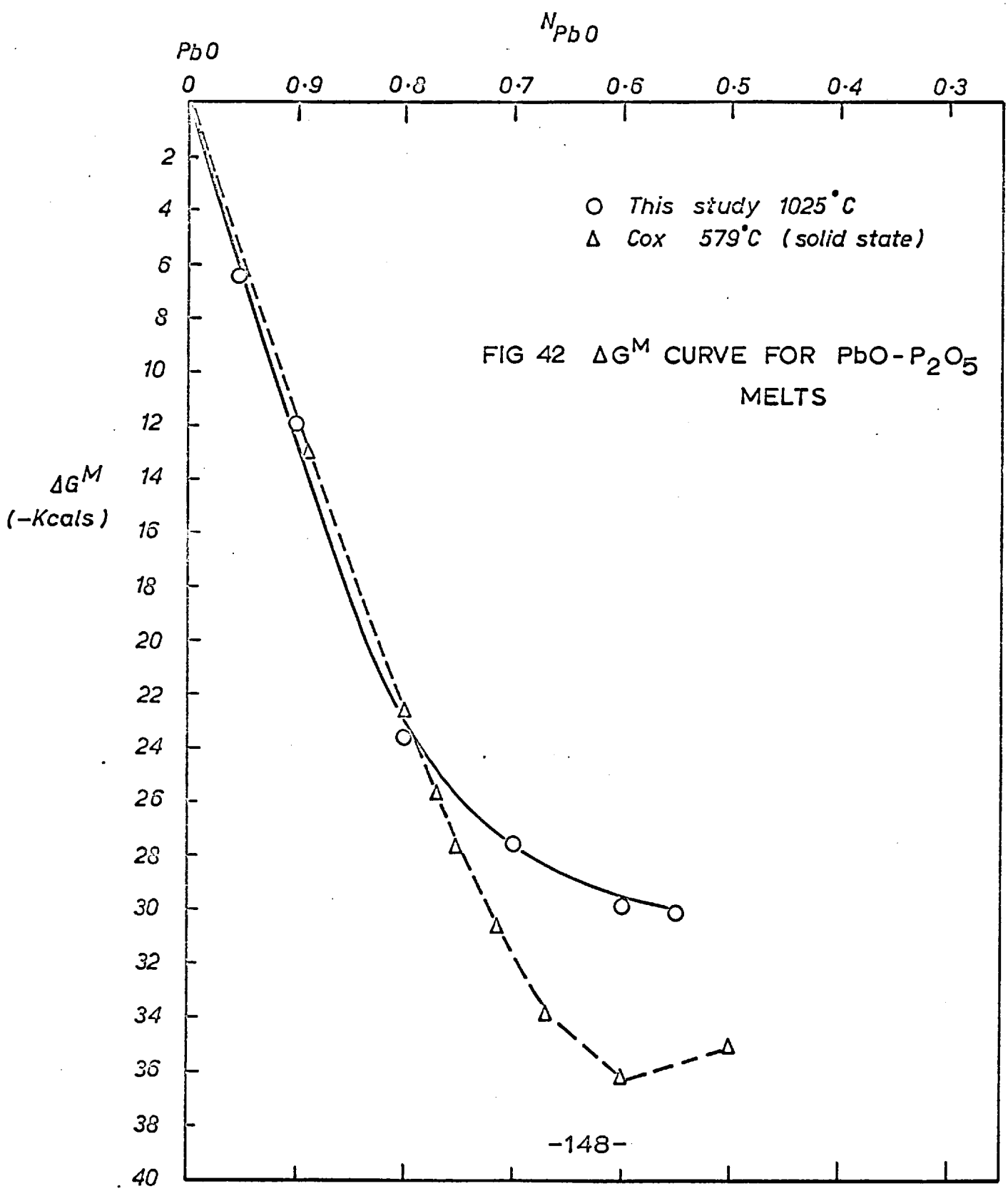

FIG 42 ΔG^M CURVE FOR PbO-P_2O_5 MELTS

(h) Estimation of errors

The reproducibility of the emf of the cells were $\pm$ 2 mv. The partial free energy of solution of PbO, is given by the relation $\Delta \bar{G}_{PbO} = -nF (E_2-E_1)$, where E_1 is the emf of the cell with PbO as electrolyte and E_2 is the emf with PbO containing slags as electrolyte. The error of $\pm$ 2 mv in E_1 and E_2, would result in an error of $\pm$ 2.83 mv in the value for E_2-E_1. Hence the error in $\Delta \bar{G}_{PbO}$ will be $\pm$ 130 cals.

$\Delta \bar{G}_{PbO}$ is related to the activity of PbO by the expression $\Delta \bar{G}_{PbO} = RT \ln {}^{a}PbO$. Therefore, the error in temperature and $\Delta \bar{G}_{PbO}$ would determine the error in ${}^{a}PbO$. The temperature was controlled to $\pm$ 1° C and this would introduce negligible errors on the activity of PbO. Hence the error of $\pm$130 cals in $\Delta \bar{G}_{PbO}$ will mainly determine the error in ${}^{a}PbO$, which corresponds to an error of $\pm$ 5.7%, 5.3% & $\pm$4.9% at 850°C, 950°C and 1050°C respectively in the activity of lead oxide. The activities of SiO_2, B_2O_3 and PbF_2 determined by Gibbs-Duhem integration would be subject to greater error due to the additional errors involved in the graphical integration. Hence the error in $\Delta \bar{G}_{SiO_2}$, $\Delta \bar{G}_{B_2O_3}$ and $\Delta \bar{G}_{PbF_2}$ is likely to be around $\pm$ 150 cals. The integral free energies derived from these partial free energies would be also subject to an error of $\pm$ 150 cals. For the PbO-P_2O_5 system the errors in $\Delta \bar{G}_{P_2O_5}$ and hence the ΔG^{M} is likely to be much greater due to the approximation involved in fixing the ${}^{a}P_2O_5$ at

$N_{PbO} = 0.55$, which was necessary to derive $^{a}P_2O_5$ at other compositions from the Gibbs-Duhem integration.

The errors in partial heats and entropies would also mainly depend on the errors in the partial free energy, since the error in temperature is negligible. The errors in $\Delta \bar{H}$ and $\Delta \bar{S}$ are estimated to be $\pm$ 700 cals and $\pm$ 0.5 cals/deg^{o}K respectively. This means the integral heats and entropies would be subjected to an error of $\pm$ 700 cals and $\pm$ 0.5 cals/deg K respectively.

Chapter 12

Discussion

(a) Behaviour of the Oxygen Electrode

When describing the cell operation (page 104) it was stated that unsteady values for the emf were obtained with a protruberent platinum wire, which was rectified by withdrawing the platinum wire so that its end was just inside the alumina tube. It is considered that the variability of the emf obtained with a protruberent wire was caused by the fact that its tip was in a zone of the melt where the oxygen activity was not unity; this was rectified when the electrode tip was placed where it was always in contact with oxygen gas at one atmosphere pressure. This situation can be diagramatically represented in figure 43 (a) and 43 (b), where figure43 (a) is the condition with the platinum wire protruding from the tube and figure43 (b) is the case when the wire is withdrawn just inside the tube. The three phase contact between platinum, oxygen and melt is through a film of electrolyte which is adhering to the platinum wire. This film is being continuously replenished when, after passage of each bubble, the melt rises into the alumina tube and coats the platinum before being pushed out by the next bubble. This process will be aided by the surface tension effect. In the first case (figure43 (a)), the lower part of the platinum will be always in contact with the

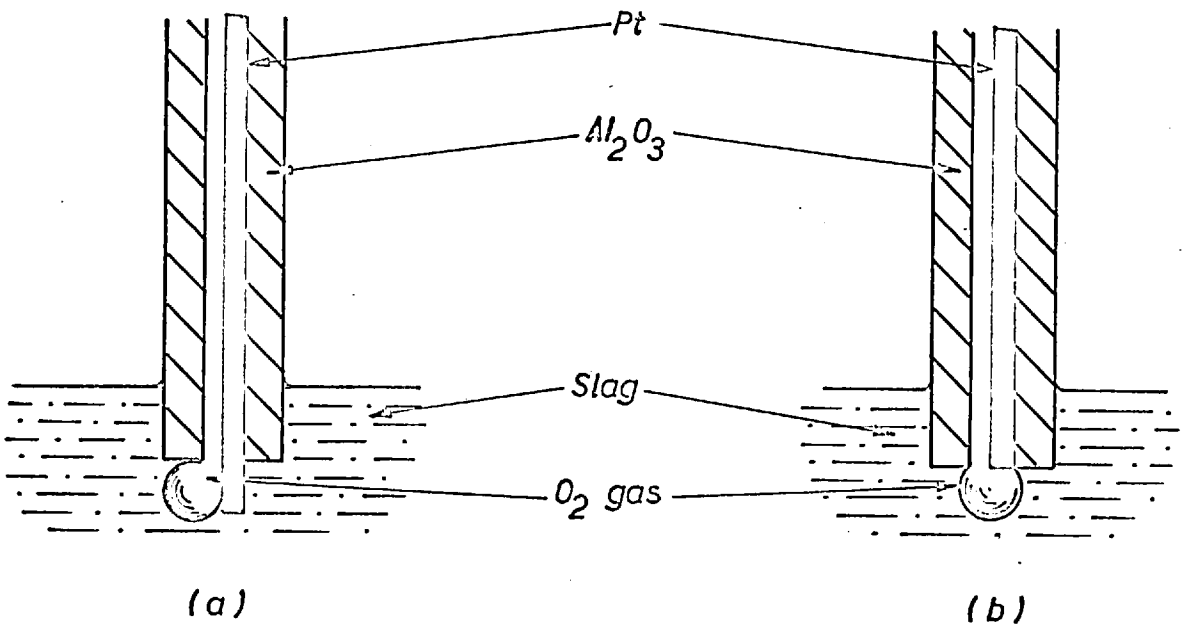

FIG 43 (a) NON-IDEAL & (b) IDEAL OXYGEN ELECTRODES

melt and would not come into contact with oxygen unless a very rapid oxygen flow rate is used.

A survey of the literature on oxygen electrodes used in oxy-anionic melts showed that various workers had used oxygen electrodes of different designs. However, always the design was such that the platinum was in contact with oxygen gas at all times. Didtchenko and Rochow[59], who first introduced oxygen electrode into silicate systems, used a rotating platinum wire, which was continuously kept flushed with a stream of oxygen injected around it. Their observation that rotation of the platinum wire in the melt during measurements, proved advantageous because it promoted the establishment of equilibrium at the platinum-melt-oxygen interfaces supports the present observation for an oxygen electrode of different construction. More recently Delimarskii and Andreva[61], as mentioned in the previous chapter, have used the cell.

$$Pb \;/\; PbO \;/\; O_2 : Pt$$

for measuring the free energy of formation of PbO. Their cell is shown in figure 44(a). For the oxygen electrode they used a platinum tube of 2 mm diameter which was immersed in the melt to a depth of 3 to 5 mm. They report that they were obliged to use a flow rate of 100 ml/min of oxygen to get a steady high emf, whereas in the present study flow rates from 1 to 20 ml/min were used with negligible changes in emf. This suggests that the higher flow

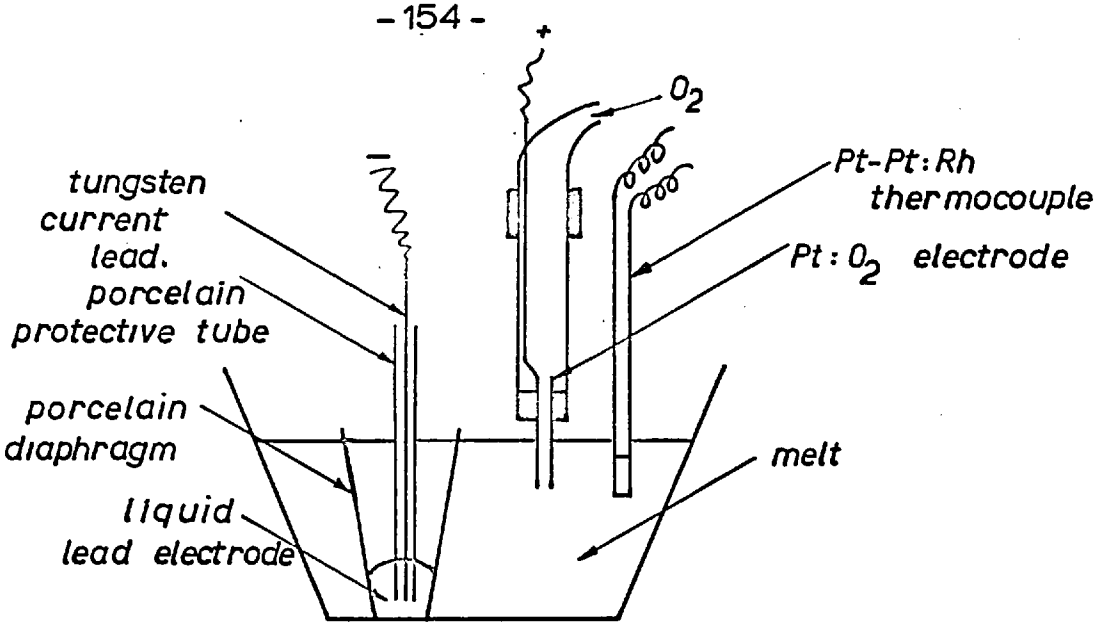

FIG.44 (a)

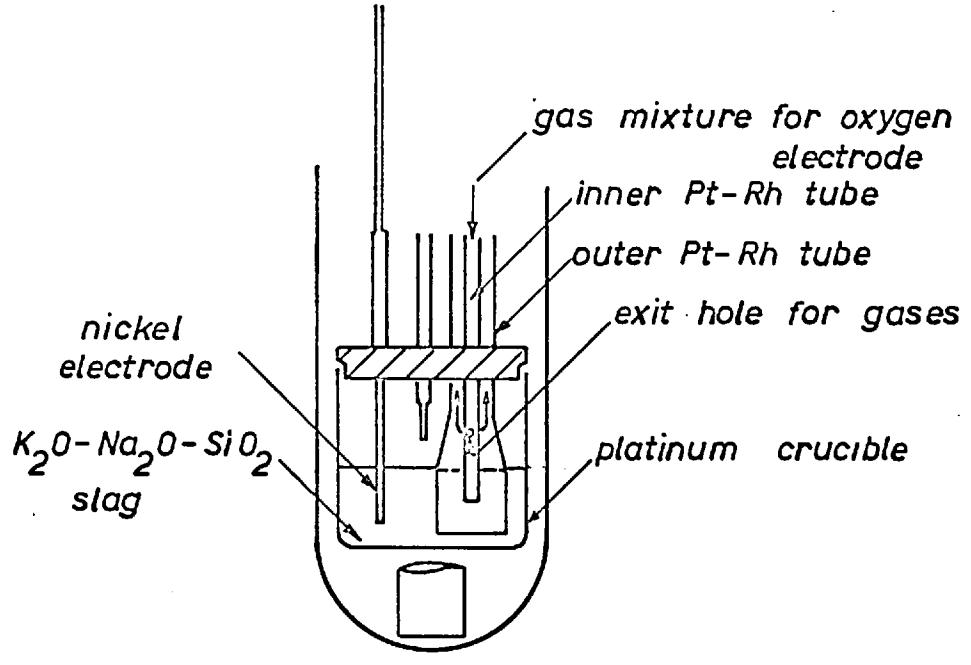

Ranford and Flengas

(b)

rate needed by these workers was to keep all parts of the platinum tube out of direct contact with the melt and flushed by oxygen.

Flood, Forland and Motzfelt[71] used an oxygen electrode in carbonate-sulphate melts with $CO_2 + O_2$ mixtures bubbling around a platinum wire at 1 to 8 ml/min of gas. Their observation that the cell emf comes to equilibrium rapidly supports the present observation. On the other hand, Ranford and Flengas[72] have recently used a Pt - 10% Rh : O_2 electrode in a K_2O-Na_2O-SiO_2 melts, and they observed that their emf varied a great deal when oxygen was bubbled around this electrode and they therefore resorted to a stationary unstirred system (figure 44(b)). This would correspond to the system with a protruding platinum wire of this study, and hence it is not surprising that they observed a very unsteady emf when oxygen was bubbled past the electrode. With a large surface area of the Pt-10% Rh electrode in contact with the melt an extremely fast rate of oxygen would be needed to keep the whole electrode under the same oxygen potential. Hence Ranford and Flengas's electrode seems to be an imperfect one and their results for NiO dissolved in ternary alkali silicate melts should be used with caution; it would be worthwhile to repeat their cell measurements with an oxygen electrode of the type used in this study and thus conclusively prove this point. Hence it seems that the oxygen electrode, when suitable precautions are taken in its

design and use, has a wide applicability in oxy-anionic melts.

(b) Thermodynamics of Pure PbO

The free energy of formation of liquid PbO, obtained from the present results can be represented by

$$\Delta G^{o}_{T} = -45,830 + 18.90\ T \quad (\pm 300)\ \text{cals/mole PbO.}$$

These values are plotted in figure 45 , as a function of temperature, together with values reported by other workers.

The values of Delimarskii and Andreeva[61] obtained from the emf measurements of the cell

$$Pb\ (l)\ /\ PbO\ (l)\ /\ O_2\ (g) : Pt$$

are in good agreement with the present results (also cf Figure 23).

The plotted values for Minenko and Ivanova[60] are those from the free energy equation

$$\Delta G^{o}_{T} = -45,520 + 18.90\ T$$

which was derived from equation C-3 (page 111) obtained from their emf values which they measured using a similar cell to that of Delimarskii and Andreeva[61] and the present study. It can be seen that their values are about 300 cals lower over the entire range studied, but the slope of this free energy temperature curve is in good agreement with that calculated from the present results.

Matsushita and Goto[69] measured the emf of the cell

$$Pb/PbO//\ ZrO_2\ CaO\ //\ NiO/Ni$$

Their results are given in the form of an equation

$$\Delta G^{o}_{T} = -45,675 + 17.82\ T\ (\pm 100)\ \text{cals/mole PbO}$$

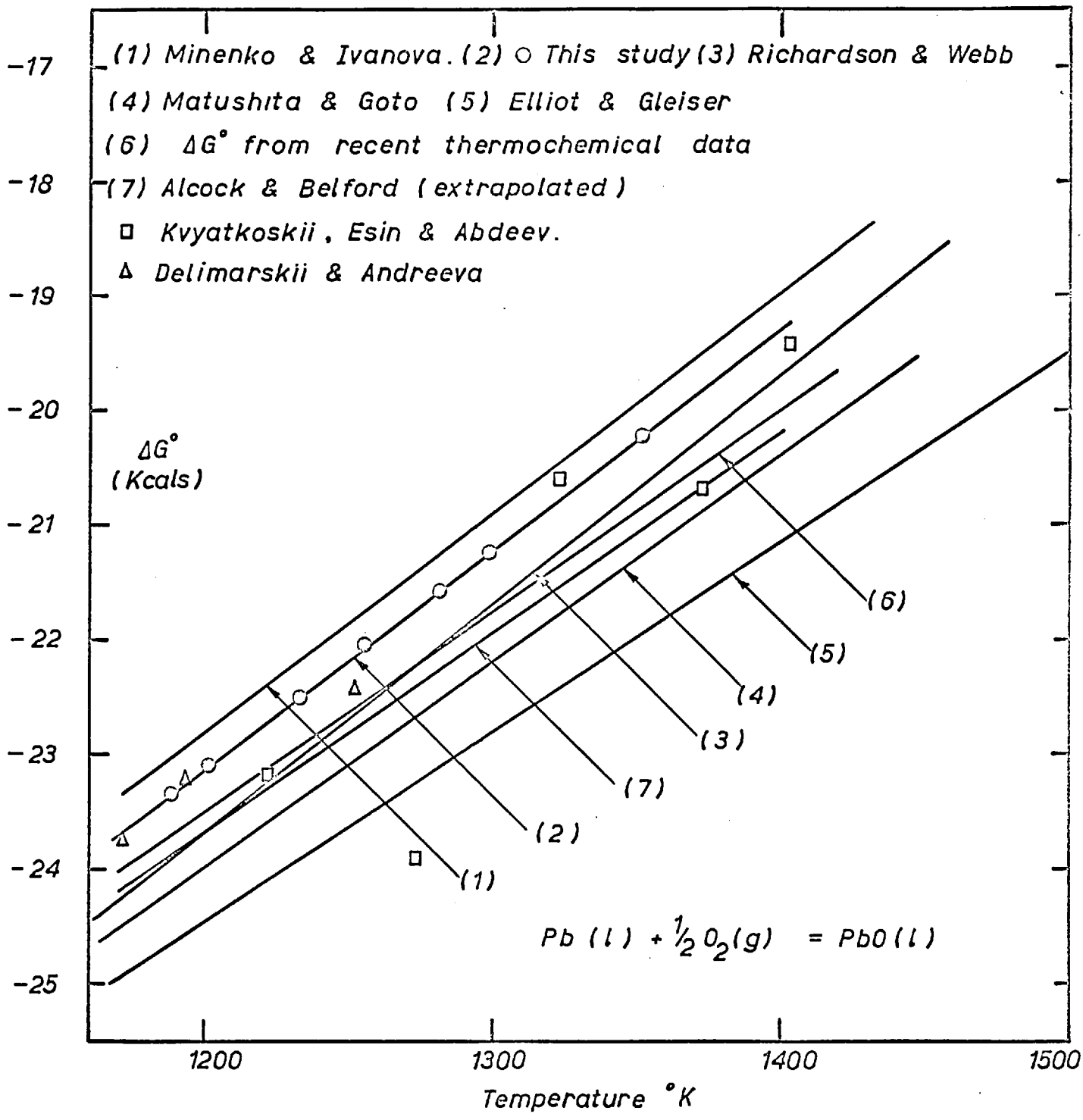

FIG.45 FREE ENERGIES OF FORMATION OF LIQUID PbO

In order to calculate the free energy of formation of PbO from their cell emf these authors had to use the available free energy of formation data for NiO, since Ni/NiO was their reference electrode. They had chosen the Ni/NiO data as assessed by Elliot and Gleiser[73] for this calculation. Steele[74] who has recently measured the emf of the cell

Ni/NiO // Solid Electrolyte // FeO/Fe

and assessed the various available thermo chemical data for the Ni-NiO system, has reported an equation for the standard free energy change of the reaction

$$2\ Ni + O_2 = 2\ NiO$$

as

$$\Delta G^{o}_{(650-1400^{o}K)} = -115{,}240 - 6.558T \log T + 63.57\ T \quad (\pm 300 \text{ cals})$$

This equation gives values for NiO which are 300 to 700 cals more positive than Elliot and Gleiser's value in the temperature range 1200°K to 1400°K. Since Steele's data are considered to be the best data available at present, Matsushita and Goto's values for PbO have been recalculated using this Ni/NiO data. This leads to the equation

$$\Delta G^{o}_{T} = -45{,}736 + 18.10\ T \quad \text{(cals/mole PbO)}$$

for the free energy of formation of liquid PbO. The values of the recalculated data of Matsushita and Goto plotted in figure 45 , are about 1 K.cal more negative than the present results.

Alcock and Belford[75] have measured the emf of the cells

$Pb/PbO \;//\; ZrO_2\ MgO \;//\; Ni/NiO$

and

$Pb/PbO \;//\; ThO_2\ Y_2O_3 \;//\; Ni/NiO$

over the temperature range 450°C to 800°C (i.e. below the melting point of PbO). They have also calculated the data for PbO from then available data on ΔH°_{298}, ΔS°_{298} and C_p for Pb, O_2 and PbO. Their experimental data were in good agreement with the data calculated using the Third Law of Thermodynamics. In their calculations they used the value for ΔG°_{298} of -44,960 cals/mole for yellow PbO given by Spencer and Mote[76] for calculating ΔH°_{298}. The recent National Bureau of Standards publication (270-2) [77] gives a value of -51,940 cals for $\Delta H^\circ 298$ (yellow PbO) which is 150 cals less negative than the older value calculable from Spencer and Mote's data. When the new value of ΔH°_{298} for PbO is used, Alcock and Belford's calculated values for the standard free energy change ΔG° for the reaction

$$Pb\ (s,l) + 1/2\,O_2\ (g) = PbO\ (yellow,\ s.l)$$

may be represented by the equations

$$\Delta G^\circ_{(298\text{-}600^\circ K)} = -52{,}860 + 39.02\,T + 0.2935 \times 10^{-3}T^2 - 5.090T \log_{10}T + 44{,}145\,T^{-1} \qquad (C\text{-}7)$$

$$\Delta G^\circ_{(600\text{-}1170^\circ K)} = -53{,}110 + 24.64\,T - 1.4665 \times 10^{-3}T^2 + 0.622T \log_{10}T + 32{,}645\,T^{-1} \qquad (C\text{-}8)$$

$$\Delta G^\circ_{(1170\text{-}1200^\circ K)} = -50{,}270 + 52.09\,T - 0.1100 \times 10^{-3}T^2 - 9.63T \log_{10}T - 10{,}000\,T^{-1} \qquad (C\text{-}9)$$

The extrapolated value of Alcock and Belford[75] using the fusion data of Rodigina, Gomel'skii and Luginina[78] and those calculated from the above equation (C-7 to C- 9) are also plotted in figure 45 . It can be seen that Alcock and Belford's values are about 500 cals more negative than the present results near the melting point of PbO. The data calculated from ΔH°_{298}, ΔS°_{298} and C_P values are from 300 to 600 cals more negative than this study.

Kvyatkovskii, Esin and Abdeev[79] have measured the emf of the cell

$$C \;/\; Pb \;/\; PbO \;//\; MgO \;//\; Na_2SiO_3 \;/\; CO : C$$

over the temperature range 900°C to 1150°C. From their emf data the free energy of formation of PbO can be calculated using the free energy data for the reaction

$$C + 1/2\ O_2 = CO$$

Coughlin's[80] C-CO data have been used, and the values calculated for PbO are also plotted in figure 45 . The large scatter in Kvyatkovskii et al's data may possibly be caused by the thermoelectric effects arising from temperature variations within the relatively large cell which they employed, and also by the electronic contribution to the conductance of MgO solid electrolyte at these temperatures. Mitoff[81] measured the electronic transport number of MgO and found it to vary from 0.1 to 0.9 under various conditions of temperature, oxygen pressure, and impurity levels. Hence Kvyatkovskii, Esin and Abdeev's data are considered

here to be insufficiently reliable for comparison.

In figure 46 the ΔG^{o} values estimated by Richardson and Webb[3] and those more recently compiled by Elliot and Gleiser[73] are also given. It is interesting to note that estimated data of Richardson and Webb are in closer agreement with recent thermochemical data; Elliot and Gleiser's values are more negative than any experimental or calculated (from third law) data by nearly 1 k. cal and are hence considered to be inaccurate.

The fact that the values obtained using the type of cell employed in this investigation tend to be somewhat less negative than those obtained by other means may indicate that some electronic conduction had taken place in the melt. An electronic transport number of 0.02 would make the results less negative by about 500 cals (i.e. 2% of the total). It is therefore possible that the absolute values of the oxygen potentials of the Pb-PbO system may be up to 500 cal too small if the ionic transport number of liquid PbO is 0.98 - the lower limit of the quoted range of Bockris and Mellors[62]. On the other hand as will be noted in the following discussion on PbO-SiO_2 melts, the excellent agreement of ^{a}PbO obtained by the present cell and the results of Richardson and Webb[3], and the rather poor agreement obtained with solid electrolyte cells, cast some doubts on the precision of the latter - in which case the present results for PbO may indicate an ionic transport number for liquid PbO greater than 0.98.

Also from figure 45, it can be seen that there is a difference in slope between the line obtained from recent thermochemical data . the data of Alcock and Belford[75] (extrapolated using this thermochemical data), and the lines obtained from other values. This could be due to the fact that the former data are strickly valid only up to 1200°K, since the dependence of Cp on temperature for liquid PbO is not available above 1200°K and is therefore assumed to be constant. As all available experimental data including this study for liquid PbO give slopes from 18.10 cals/°K to 18.90 cals/°K, it is likely that the correct value is in this range. It would be worthwhile to study the high temperature heat capacity of PbO above 1200°K to check this point, especially since accurate high temperature data up to 1500°C is necessary for calculations involving lead blast furnace slags containing lead oxide.

(c) PbO - SiO_2 melts

In figure 24, the emf obtained in this study has been directly compared with a few points obtained by Ito and Yanagase[35] (these are values for which comparison is possible and were obtained using a very similar cell to the present one). Since Ito and Yanagase[35] did not measure the emf for a pure PbO cell, they had to use external data for pure PbO to calculate their a_{PbO} in PbO-SiO_2 melts. Thus the data they obtained were only in fair agreement with Richardson and Webb[3], who used a vapour

phase equilibration technique to measure PbO activities in PbO-SiO_2 slags. It is possible to recalculate Ito and Yanagase's values for ^{a}PbO using the present results for pure PbO. The data thus obtained is compared with the present results at 900°C in figure 46 ; which are in excellent agreement. As can be seen from Ito and Yanagase's points, their work was limited to a composition range of $^{N}SiO_2$ = 0.268 to $^{N}SiO_2$ = 0.555 (and between 800°C to 900°C).

Also in figure 46 , are plotted the values of Esin, Sryralin and Khlynov[82] obtained using the cell:

Pb / PbO // MgO // PbO-SiO_2 / Pb

It can be seen that their values are not in agreement with this and Ito and Yanagase's studies. Jeffes[83] has reviewed the use of emf studies for determining activity measurements in silicate melts and suggests that this discrepancy could be due to the non-ionic character of MgO solid electrolyte referred to earlier. This is in agreement with the fact that ΔG° values for liquid PbO determined by Esin and co-workers using MgO are, as mentioned in the last section, not in agreement with any other data.

In figure 47 the values of the activities of PbO at 1000°C are compared with those of other workers. The present results are in excellent agreement with those of Richardson and Webb.[3] The values of Callow[84] were based on weight loss determinations by Preston and Turner[85] and not adequate for this purpose. The

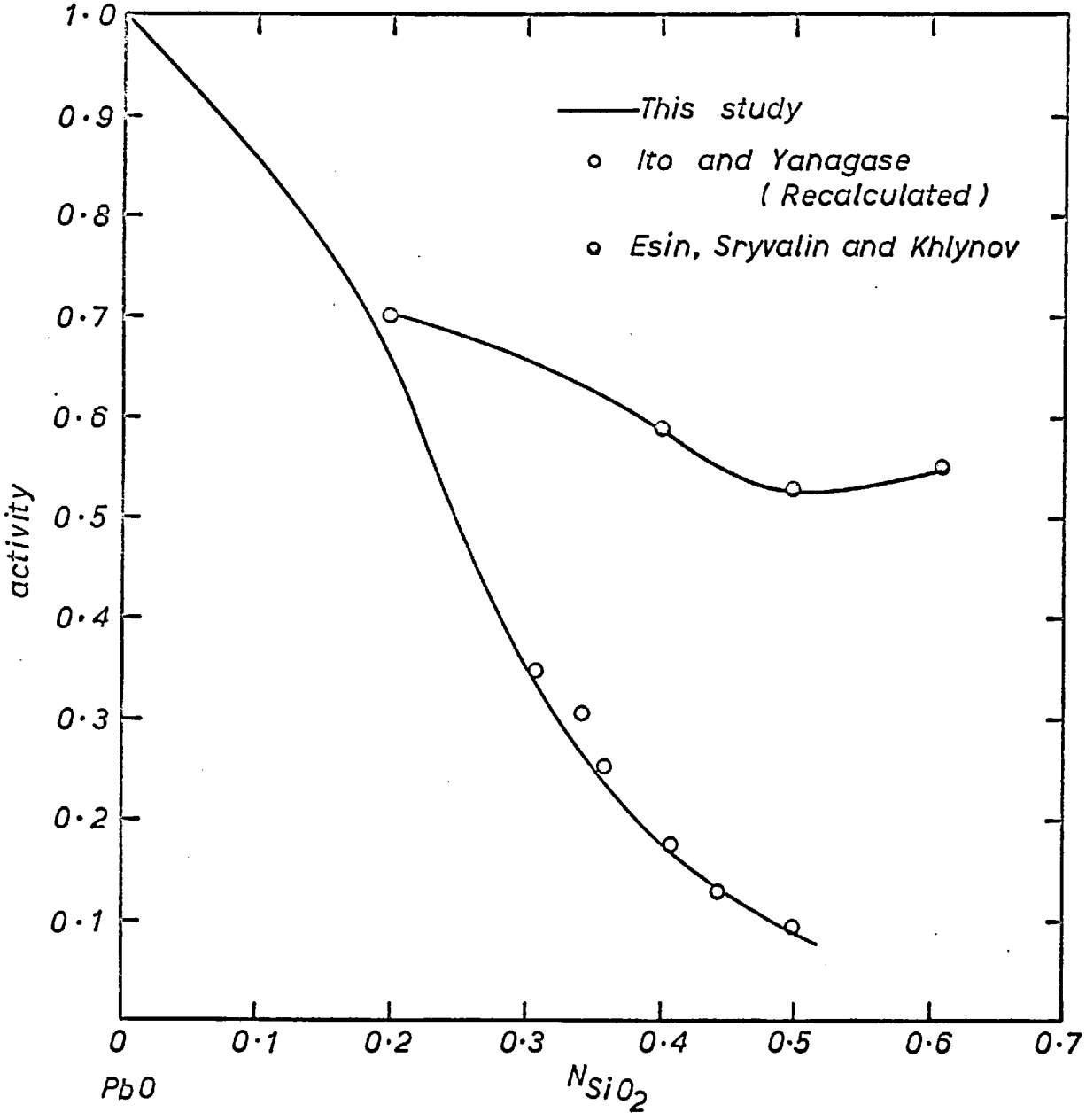

FIG.46 ACTIVITY OF PbO IN PbO-SiO_2 MELTS AT 900°C

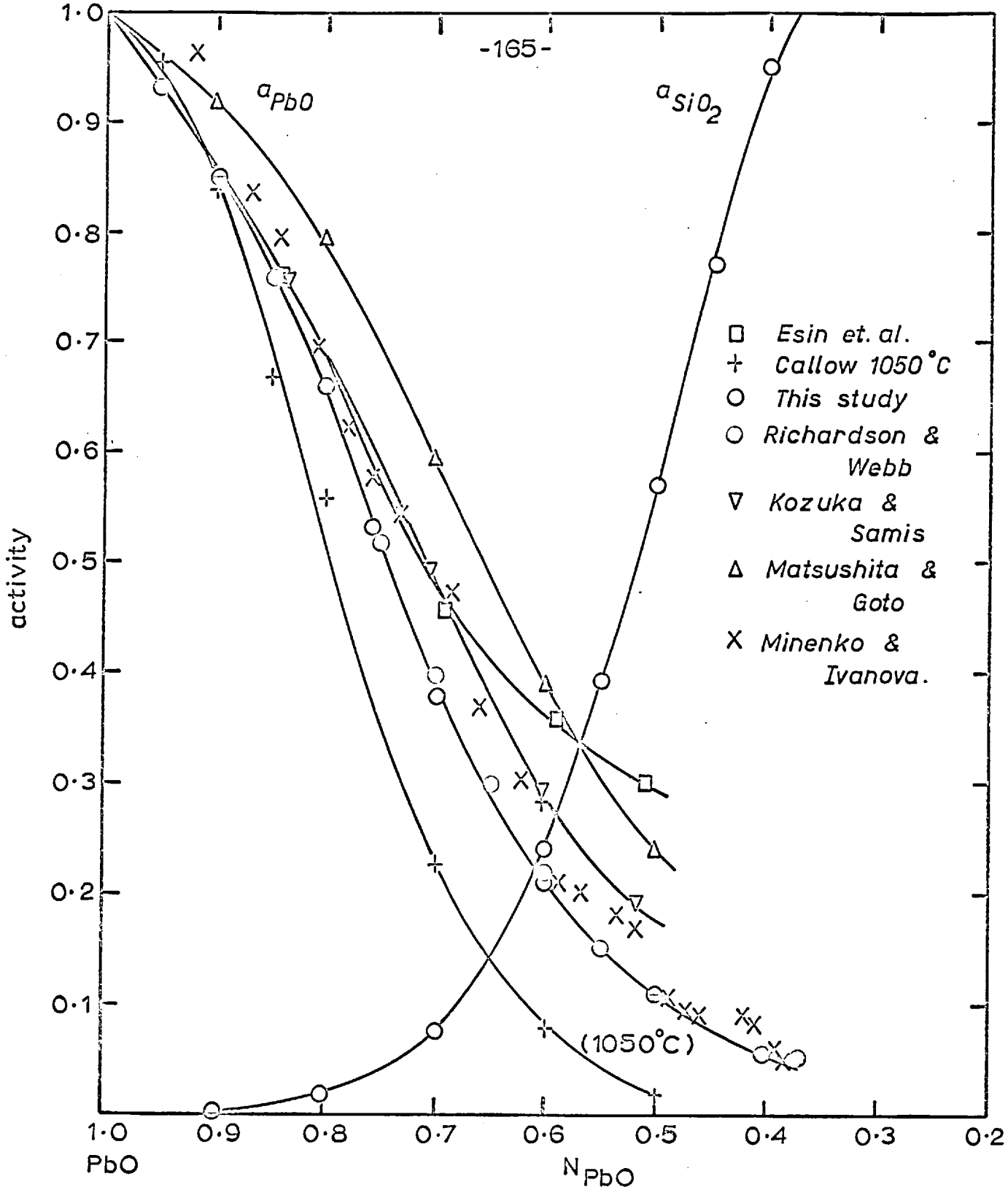

FIG.47 ACTIVITIES OF MOLTEN PbO & TRIDYMITE IN $PbO-SiO_2$ MELTS AT 1000°C

values of PbO activities determined by Matsushita and Goto[69] using the combination of values of cell described in last section, and the cell

$$Pb \;/\; PbO\text{-}SiO_2 \;//\; ZrO_2\ CaO \;//\; NiO \;/\; Ni$$

are considerably higher. Any error in the Ni/NiO data used by them will have no effect in this case since the errors would cancel out. Their higher values for the activity could possibly arise from the developement of a parasitic emf due to the formation of an Fe-FeO electrode at the point of emergence of the iron lead from the solid electrolyte component (cf. figure 48a).

Kozuka and Samis[86] have used cells of the type

$$Pb \;/\; PbO \;//\; ZrO_2\ CaO \;//\; PbO\ SiO_2 \;/\; Pb$$

to measure the activity of PbO in $PbO\text{-}SiO_2$ melts. Their results are also plotted in figure 47 . From the figure it can be seen that there is a fair agreement between the present values and those of Kozuka and Samis up to about $N_{PbO} = 0.80$. As the mole fraction of PbO decreases, the activities they obtained become increasingly higher than those obtained in this study. Figure 48(b), shows their cell system. It can be seen that no precaution had been taken to prevent any PbO distilling into the $PbO\text{-}SiO_2$ compartment via the vapour phase. This could act as a short circuit of the cell (via the gas phase) and hence the cell would be likely to record a lower emf. This phenomenon, if it occurs, would be more pronounced when the compositions of the two cell

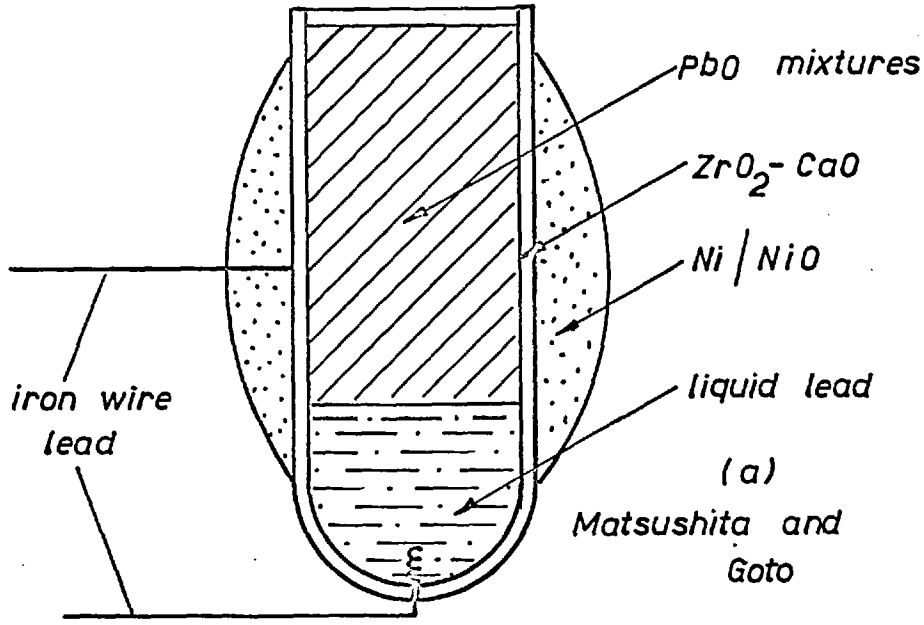
PbO mixtures
ZrO_2- CaO
Ni / NiO
liquid lead
iron wire
lead
(a)
Matsushita and
Goto

FIG.48

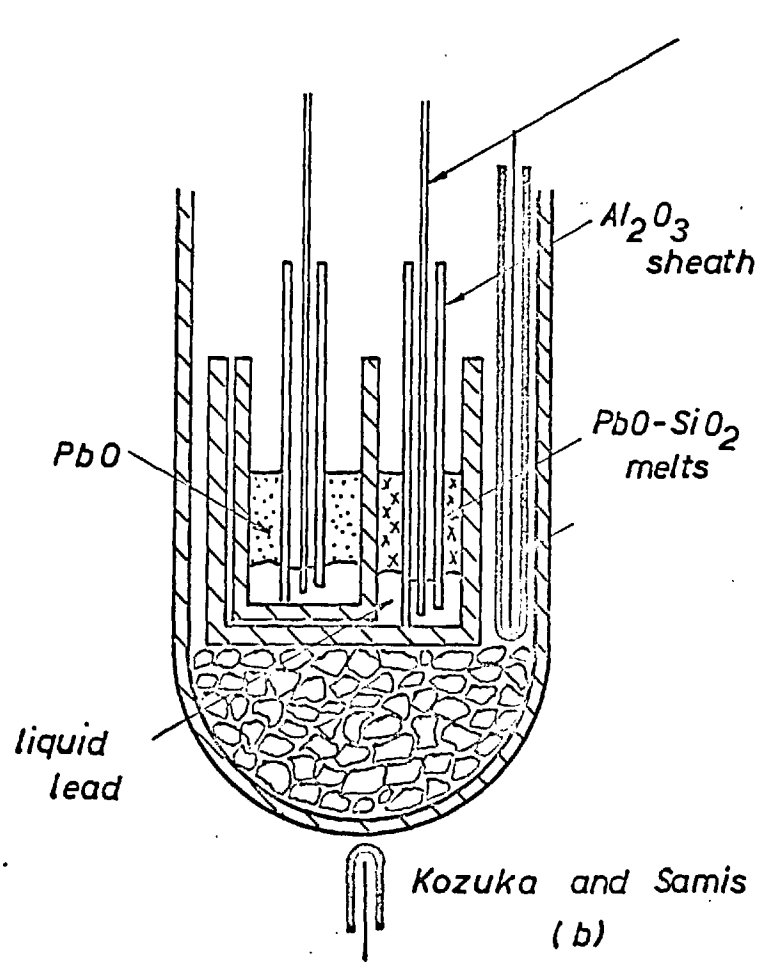
Al_2O_3
sheath
PbO-SiO_2
melts
PbO
liquid
lead
Kozuka and Samis
(b)

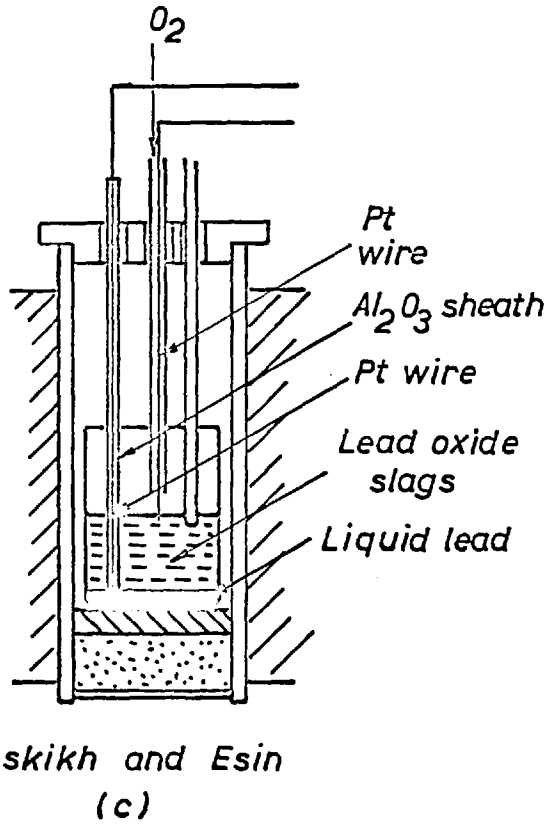
O_2
Pt
wire
Al_2O_3 sheath
Pt wire
Lead oxide
slags
Liquid lead
Lepinskikh and Esin
(c)

Compartments were very different, i.e. with a PbO reference electrode the effect should increase as the silica rich compositions are approached. This seems to be the trend followed by their results. Since PbO has a vapour pressure of about 2 mm of Hg, this effect is therefore likely to be the cause of their higher observed activities than those of the present study at low mole fractions of PbO.

Benz and Schmalzried[87] studied a similar solid electrolyte cell in the solid state and their values agree fairly well with the extrapolated values of Richardson and Webb[3] and of the present study.

Esin, Lepinskikh and Musikhin[88] have used a cell similar to the one employed in this investigation. Hence it would be reasonable to expect a good agreement with this study and those of Ito and Yanagase[35] and Minenko and Ivanova[60]. As already mentioned, Ito and Yanage's values are in good agreement with the present values. However, Esin et al[88] value are not in good agreement. This is considered to be due to the inherent fault in their cell construction (cf figure 48(c)). They used a platinum wire dipping in lead, which would lead to errors caused by solution of platinum in liquid lead; at 1000°C lead dissolves 63 % mole of platinum[68]. Furthermore, their arrangement of the oxygen electrode is considered to be unsatisfactory. The protruberant wire could produce non-equilibrium and unsteady emf values.

Hence, the result of Esin, Lepinskikh and Musikhin.[88] are considered erroneous.

The values reported by Minenko and Ivanova[60] (cf figure 47) are scattered and hence no attempt has been made to draw a line through their points. Since their exact cell construction was not described it is impossible to explain the scattered values with certainty. They have, in fact, drawn a curved line with humps for their activity versus composition plot and point out that these occur near the compositions of metasilicate (PbO/SiO_2 = 1/1), pyrosilicate (PbO/SiO_2 = 3/2) orthosilicate (PbO/SiO_2 = 2/1) and a 4/1 compound, showing the presence of these compounds in these melts. From the structural picture given in this thesis, it is clear that in the melt there would be distribution of anions and not single anions corresponding to a particular compound in the phase diagram. However, it might be noted that their values though scattered are in fair agreement with the present results over the entire composition, which might suggest that perhaps Minenko and Ivanova's values could have been affected by such errors as temperature variation or not a completely ideal oxygen electrode.

The activities obtained experimentally can be partly checked using the phase diagram of Geller, Greamer and Bunting[89] (figure 49). Near the lead oxide end of the diagram the activities can be calculated from the depression in the freezing

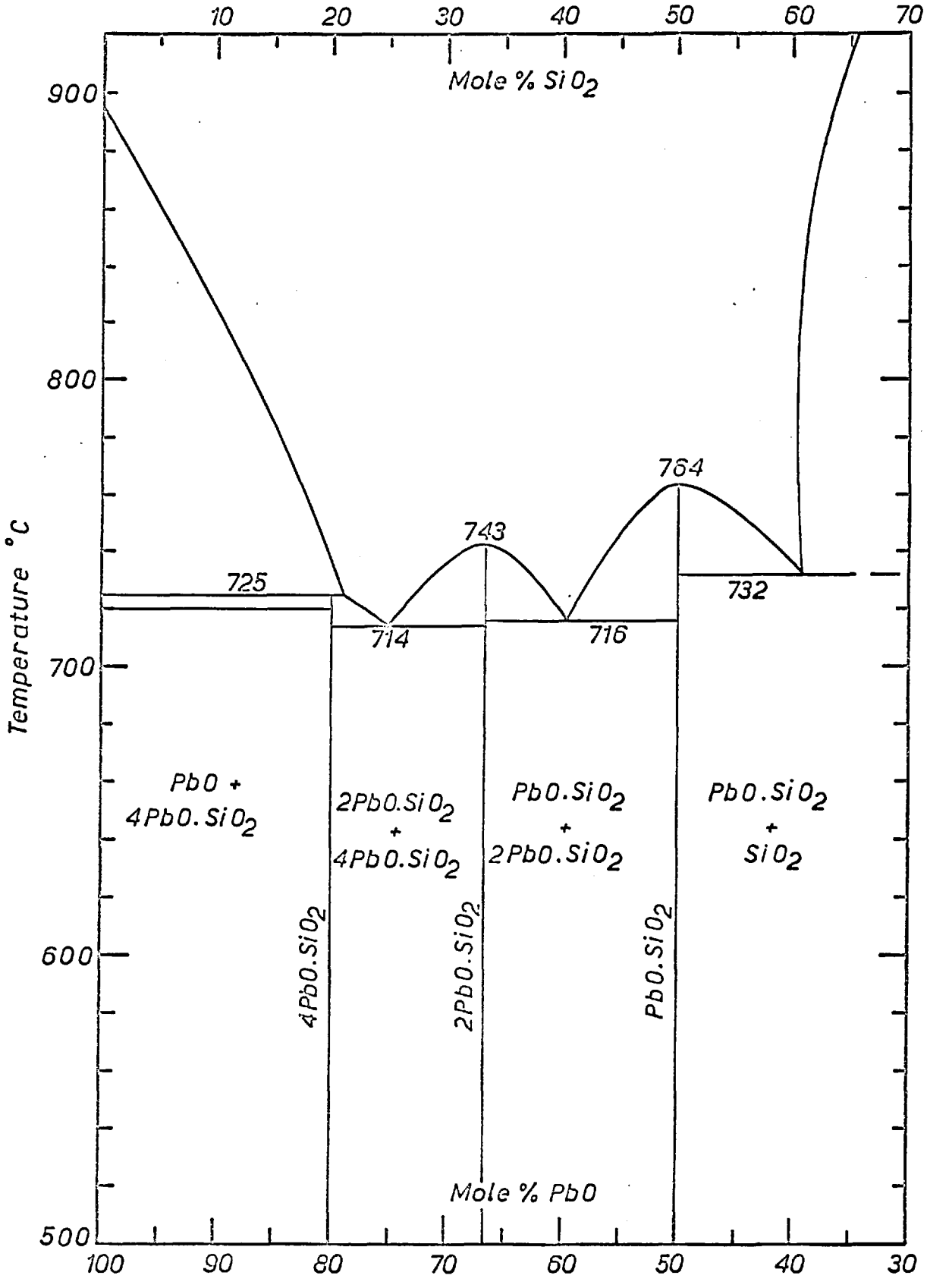

FIG.49 $PbO-SiO_2$ PHASE DIAGRAM

point. For this calculation the T_f and ΔH_f values for PbO of Rodigina, Gomel'skii and Luginina were used. The calculated activities and the observed activities (at 1000°C) are shown below.

Composition N_{PbO}	a_{PbO} (from phase diagram)	a_{PbO} (Experimental 1000°C)
0.95	0.93 at 860°C	0.93
0.90	0.87 at 828°C	0.85
0.85	0.76 at 785°C	0.76
0.80	0.66 at 736°C	0.66

The remarkably good agreement between the observed and calculated activities of PbO in spite of the different temperatures to which they refer, supports the small effect of temperature on a_{PbO} in PbO-rich melts depicted in figure 25.

Another check on the activity values can be made from the fact that at 718°C the function RT ln $a^2_{PbO} \cdot a_{SiO_2}$ should be the same at 59.8% mole PbO and 74.5% mole PbO. This is because the crystalline phase $2PbO.SiO_2$ is in equilibrium with these liquids at this temperature and the Gibbs free energy of formation of $2PbO.SiO_2$ is given by RT ln $a^2_{PbO} \cdot a_{SiO_2}$. This was done by using the activity data at 1000°C and extrapolating to 718°C using the relation ,

$$\ln \frac{a_{PbO\ (718^\circ C)}}{a_{PbO\ (1000^\circ C)}} = \frac{\Delta \bar{H}_{PbO} \times 282}{4.575 \times 1273 \times 991}$$

The values for RT ln $a^2_{PbO} \cdot a_{SiO_2}$ obtained at these compositions

were 10,480 and 10,520 cal/mole of 2 $PbO.SiO_2$. This good agreement suggests that the activities and their dependence on temperatures obtained in this study is of the right order.

It is also possible to compare the partial molar heats and entropies derived from the temperature dependence of activities with those reported by other workers[3,69,86]. In figure 50 the partial heats of solution of $PbO-SiO_2$ melts are compared with those of Richardson and Webb[3], Kozuka and Samis[86] and Matsushita and Goto[69]. The partial heats are in good agreement with those of Richardson and Webb[3], but in poor agreement with those of Kozuka and Samis[86] and Matsushita and Goto[69]. The partial entropies of solution, $\Delta \overline{S}_{PbO}$, (figure 51) are in good agreement with those of Richardson and Webb[3] and Kozuka and Samis from $N_{PbO} = 1.0$ to $N_{PbO} = 0.80$. Below this value there is a sharp divergence in the values of $\Delta \overline{S}$ derived from these three sources, but all show a minimum at about $N_{PbO} = 0.60$- that of Richardson and Webb[3] even showing a change of sign. It should be noted that the partial heats derived from the temperature dependence of activity are generally not very accurate and a better method for determining these quantities would be to measure the heats of solution directly at this temperature. This is possible with the development of high temperature Calvet type calorimeters in the Calvet institute[90] and by Kleppa[91]. These heats in conjuction with the free energies of solution would

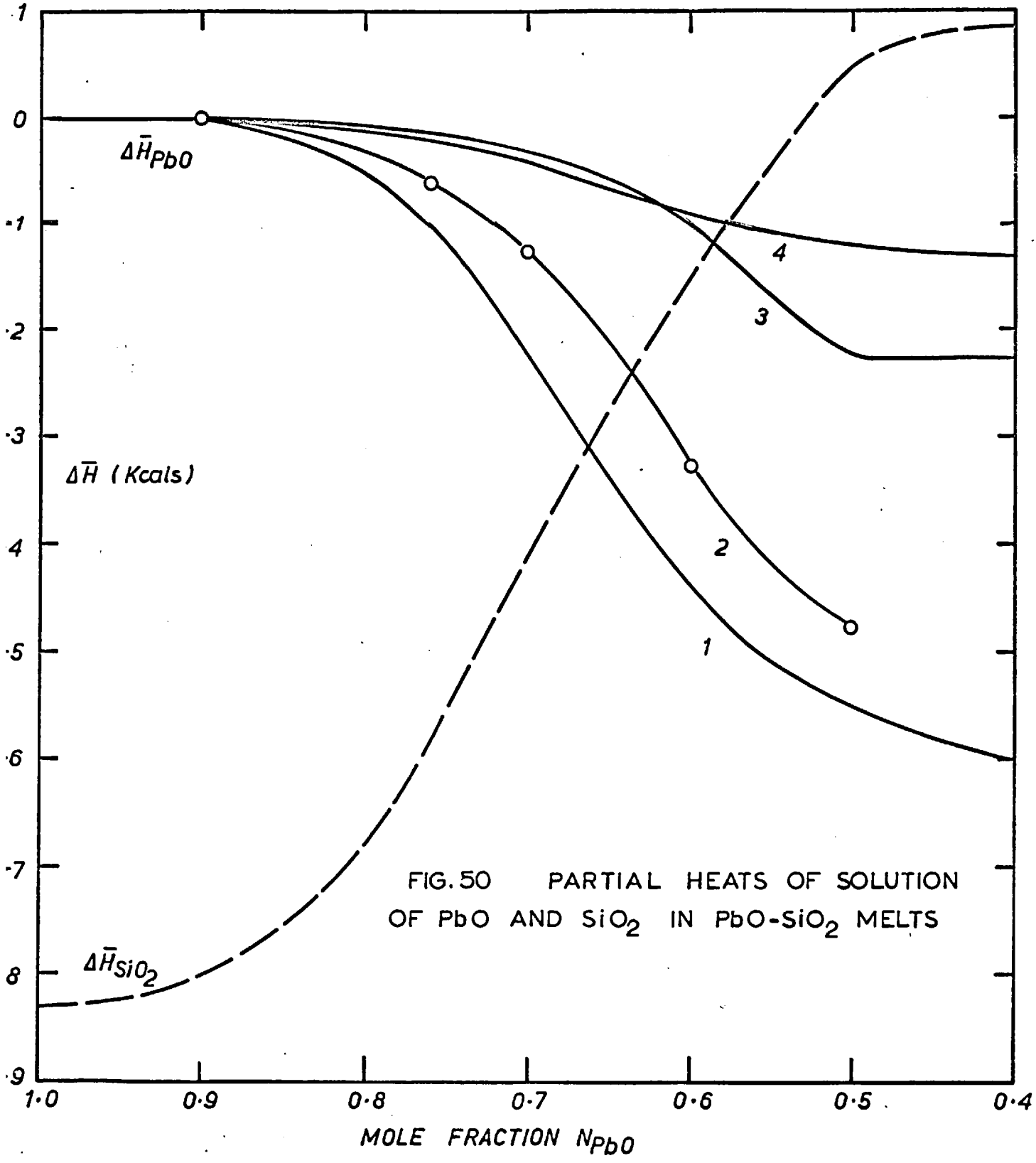

FIG. 50 PARTIAL HEATS OF SOLUTION OF PbO AND SiO_2 IN PbO-SiO_2 MELTS

accurately fix the entropies of solution, which are often employed to check various structural models.

In figure 40, the integral heats of mixing are compared with ΔH^M derived from calorimetric data. These ΔH^M values were derived from measurements of heats of solution of $PbO-SiO_2$ glasses by Shartsis and Newman[92], assuming that $\Delta C_p=0$ for the reaction:

$$X.\ PbO_{(S)} + Y\ SiO_{2(S)} = X.\ PbO.\ Y\ SiO_{2(gl\ or\ l)}$$

and a heat of fusion of 6,110 cals/mole for PbO. The only moderate agreement of these values of ΔH^M is probably due to the incorrections of the assumptions made in their derivations; but they agree within 1 K cal over most of the ranges of compositions.

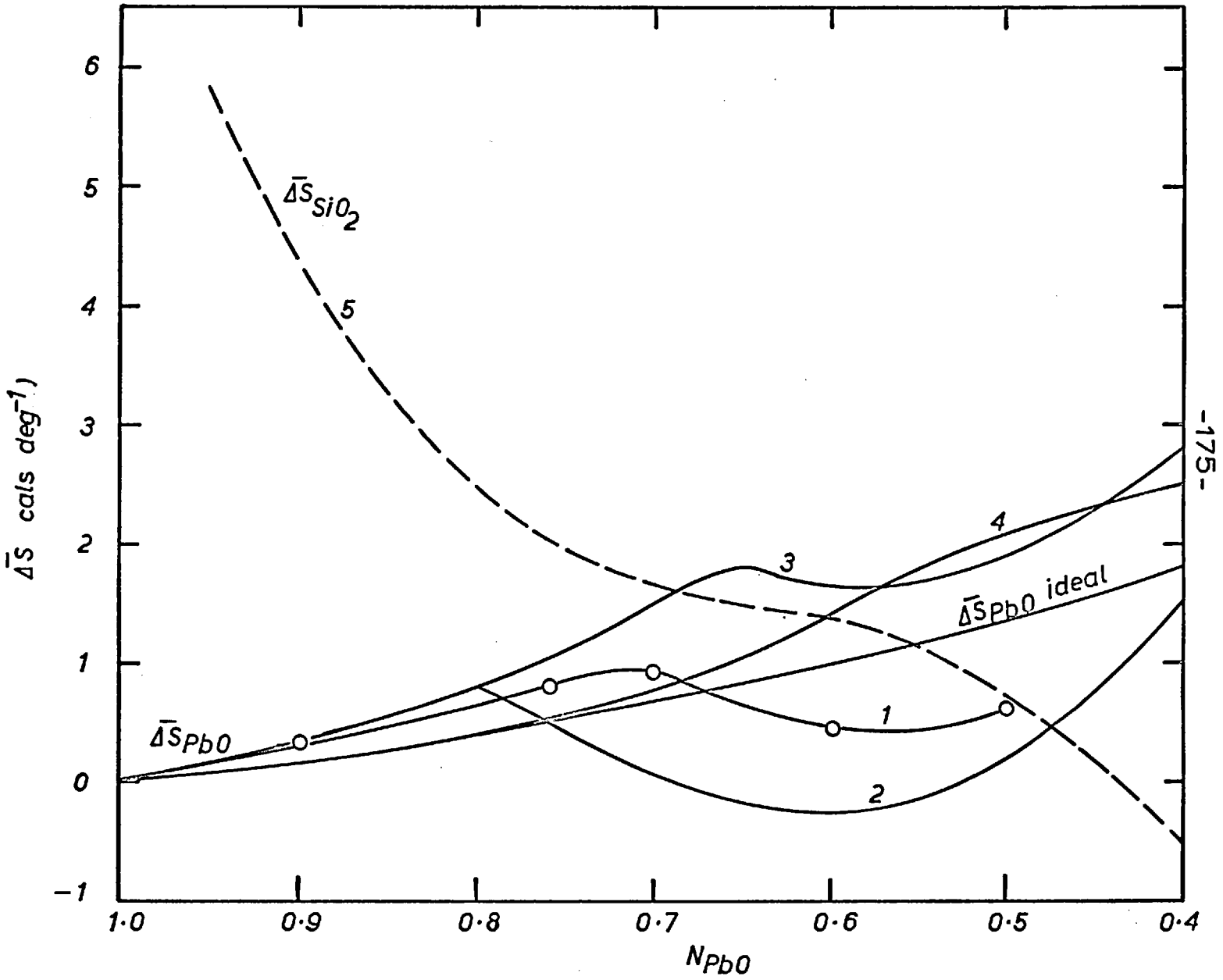

FIG. 51 PARTIAL ENTROPIES OF SOLUTION OF PbO AND SiO_2 IN PbO-SiO_2 MELTS

(d) $PbO-B_2O_3$ melts

Previous studies on $PbO-B_2O_3$ melts have been less extensive than those reported above for the $PbO-SiO_2$ melts, and hence an extensive comparison of the present results with other data is not possible. However, Lepinskikh and Esin[93] have measured the emf of the cell:

$$Pt \;/\; Pb \;/\; PbO-B_2O_3 \text{ melts} \;/\; O_2 : Pt$$

As mentioned already, in the discussion of Esin, Lepinskikh and Musikhin's[88] work on $PbO-SiO_2$ melts employing a similar cell, the use of platinum wire in contact with liquid lead is not ideal due to the big solubility of platinum in lead (63% mole Pt at 1000°C [68]). Also they used an unsatisfactory oxygen electrode with the platinum wire protruding from the alumina tube (refer figure 48). Hence their results must be considered erroneous, and in fact their values for ^aPbO in $PbO-B_2O_3$ melts are again far greater than those obtained in the present study.

Hirayama[94] has measured the rates of weight loss of lead silicate and lead borate melts under comparable conditions. He found that, at comparable temperatures, the volatility of the binary silicate melt is higher than that of the lead borate at corresponding PbO content. If it is assumed that (1) the weight loss is due only to the PbO evolution, which is reasonable in view of the relative vapour pressures of PbO, SiO_2 and B_2O_3 (0.5mm for PbO, 5×10^{-7}mm for B_2O_3 and $< 10^{-8}$mm for SiO_2 at 1000°C) and the

activities of PbO in the melts studied and (2) the rate of evaporation of PbO is proportional to its activity in the melt, one can compare the activities of PbO in borate and silicate melts at N_{PbO}= 0.50. Hirayama measured the rate of weight loss as a function of time and found a small linear decrease in the rate with time for a given composition of lead silicate or borate melt. This linear plot could be extrapolated to zero time to obtain the initial rate of weight loss, since this would be more representative of the vapour pressure of PbO over the melt. Since he had measured the weight loss for borate compositions N_{PbO} = 0.52 and N_{PbO}=0.48 and silicate compositions of N_{PbO}=0.63 and N_{PbO}=0.40, these rates of weight loss at 850°C have been interpolated. The ratio of the rates of weight loss for borate and silicate thus obtained at N_{PbO}=0.50 is 0.019. The ratio of a_{PbO} in borate and silicate from present results is 0.020, which is in good agreement. Since the weight loss measurements of Preston and Turner[85] on lead silicate melts gave results for the activities of PbO in silicate melts in fair agreement with those obtained by other means (cf figure 47 , page 165), it is considered that Hirayama's results afford a valuable corroboration of the present results on lead borates.

In figure 52 , Lepinskikh and Esin's[93] results on $PbO-B_2O_3$ are compared with present results on borate and silicates. If Lepinskikh and Esin's data are correct one would expect a higher

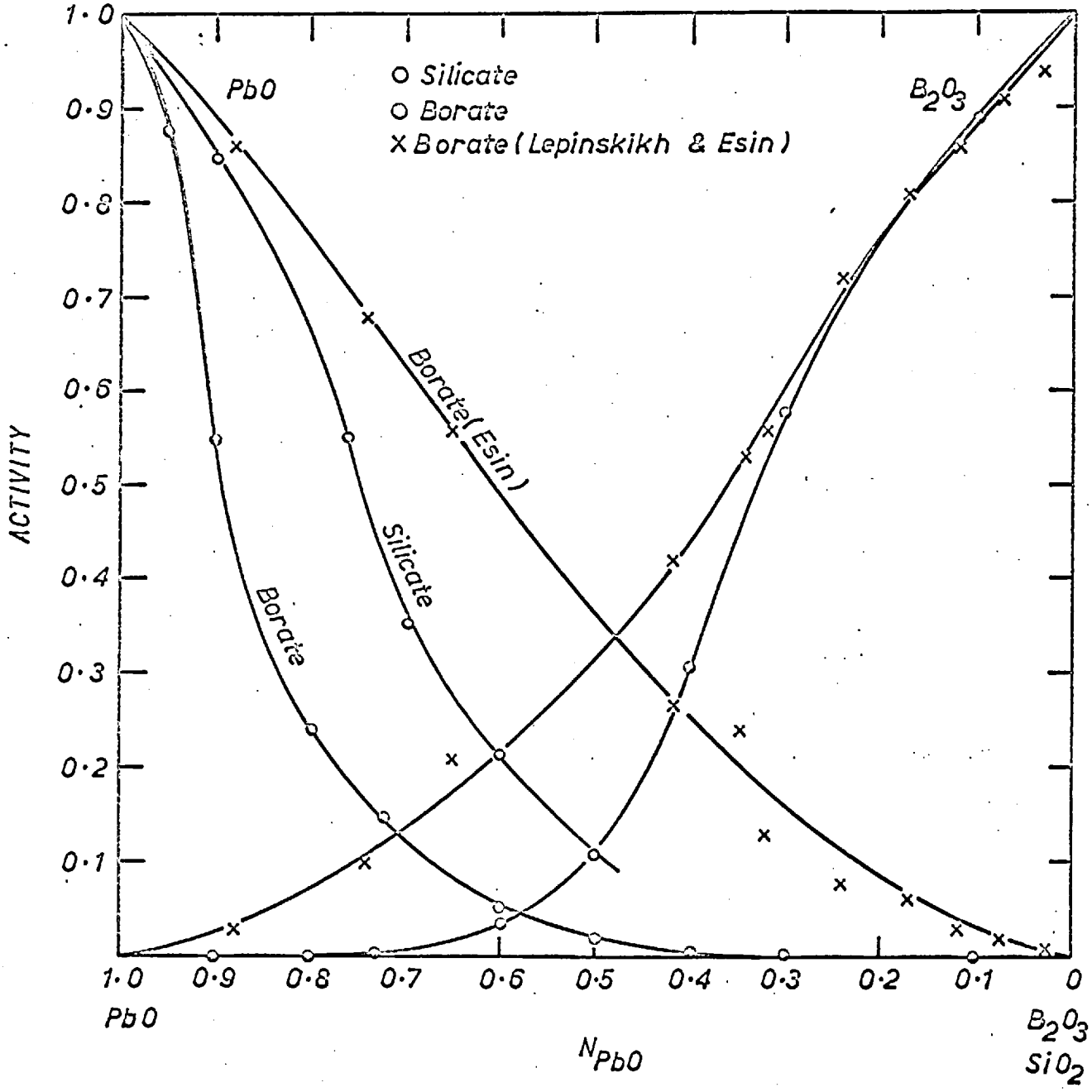

FIG. 52 ACTIVITIES IN $PbO-SiO_2$ & $PbO-B_2O_3$ MELTS AT 1000°C

vapour pressure of PbO in borate than in the silicate and hence a higher volatility of lead borate melts. This is contradictory to the observations of Hirayama[94] for these melts. As mentioned earlier this might have been due to spurious emf in Lepinskikh and Esin[93] cell; which points towards a need for careful examination of the cell system to obtain meaningful results from such high temperature galvanic cells.

The freezing point depression of PbO by addition of B_2O_3 can be used to check the ^{a}PbO in the range N_{PbO}=1 to N_{PbO}= 0.85. This can be done employing the T_f and ΔH_f for PbO of Rodigina, Gomel'skii and Luginina[78] and the phase diagram of Geller and Bunting[95](figure 53). The calculated activities and observed activities (at 1000°C) are shown below

Composition N_{PbO}	^{a}PbO From Phase diagram	^{a}PbO Experimental (1000°C)
0.95	0.88 at 842°C	0.88
0.90	0.62 at 720°C	0.55
0.85	0.39 at 590°C	0.37

These values of the lead oxide activity from phase diagram were derived assuming that ΔH_f is constant over the appropriate range of temperature. The error introduced by this assumption can be minimised by correcting for the variation of ΔH_f and ΔS_f with temperature. Rodigina et al have measured the high temperature

FIG. 53 PHASE DIAGRAM FOR THE $PbO - B_2O_3$ SYSTEM

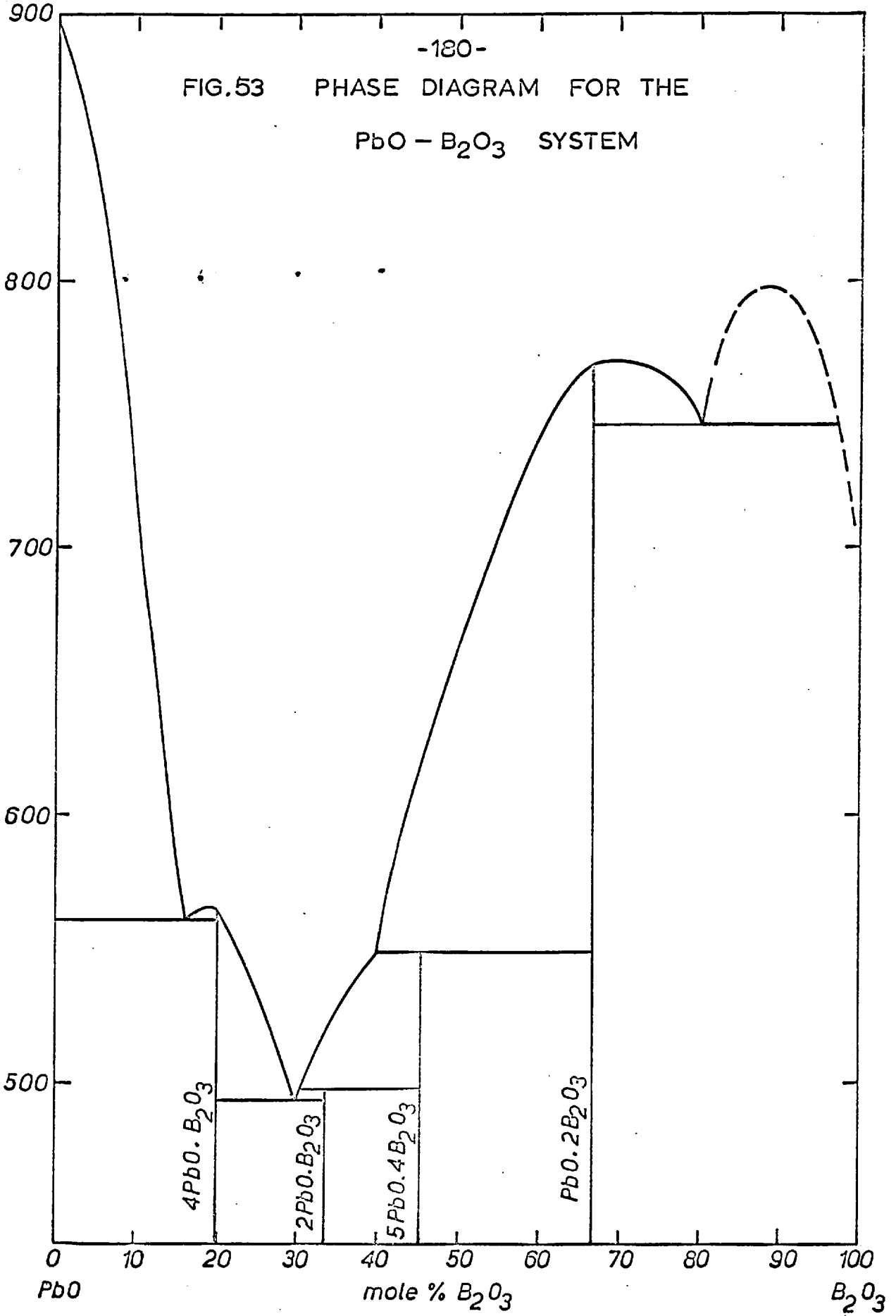

heat capacities of PbO which are represented by the equations:

C_p for liquid PbO = 15.50 cals/deg.

C_p for solid PbO = 11.08 + 2.713 x $10^{-3}T$ - 83,290 T^{-2} cals/deg

For the fusion reaction

PbO (S) = PbO (l)

$$\Delta G^{o}_{T} = 2,840 + 27.45\ T + 1.3565 \times 10^{-3} T^2 - 10.252\ T \log_{10} T - 42,645\ T^{-1}$$

when this correction is applied and ^{a}PbO recalculated at N_{PbO} = 0.85, it results in a value of 0.41 which as can be seen is not very different from that calculated assuming constant ΔH_f and $\Delta C_p = 0$ for the fusion process. Again these phase diagram calculations are in fair agreement with the present results and does not support Lepinskikh and Esin's[93] values.

(e) PbO-P_2O_5 melts

The only comparison which can be made with the present results for this system is with the work of Cox[96], who studied the emf of the cell:

Pb / PbO // ZrO_2 Y_2O_3 // PbO - P_2O_5 / Pb

in the temperature range 500-700°C (in the solid state). In figure 42 , the integral free energy of mixing values of Cox and the present study are compared, and it can be seen that ΔG^{M} values are of the same order. Cox had to use the free energy of formation of 3 PbO. P_2O_5 to calculate the partial

and integral free energy values from his cell emf. To estimate the free energy of formation of $Pb_3(PO_4)_2$ [54], as a function of temperature he assumed the heat capacity dependence on temperature to be the same as that for $Ca_3(PO_4)_2$. From these data he estimated the value of ΔG^o_T for the reaction.

$$3/4\ PbO + 1/4\ P_2O_5 = 1/4\ Pb_3(PO_4)_2$$

which he gave as:

$$\Delta G^o_T = -30.87 + 3.65 \times 10^{-3} T \quad K.cals$$

over the temperature range 700°K - 1000°K. Extrapolating this to 1020°C, i.e. upto the melting point of $3\ PbO.P_2O_5$, we obtain a value of -24.78 K.cals/mole oxides. This value is in extremely good agreement with the value of -24.80 K.cals/mole oxides (cf. figure 42) obtained in the present study. This agreement is better than expected since the derivation of the expression for ΔG^o_T for $3\ PbO\ P_2O_5$, involves a number of assumptions and also the ΔG^M values derived from the present results are based on $\Delta \bar{G}_{P_2O_5}$ values which as discussed in the results sections are only approximate. It might be worth noting that Cox's experimental results near $N_{PbO} = 0.50$ are likely to be unreliable as he should have also experienced the troubles of phosphorus evolution at high P_2O_5 end, observed in the present study.

In the $PbO-P_2O_5$ system, the phase diagram[97] check can be done only upto $N_{PbO} = 0.95$. This was done in a similar manner described for the borate and silicate systems and the value

FIG.54 PHASE DIAGRAM FOR THE $PbO-P_2O_5$ SYSTEM

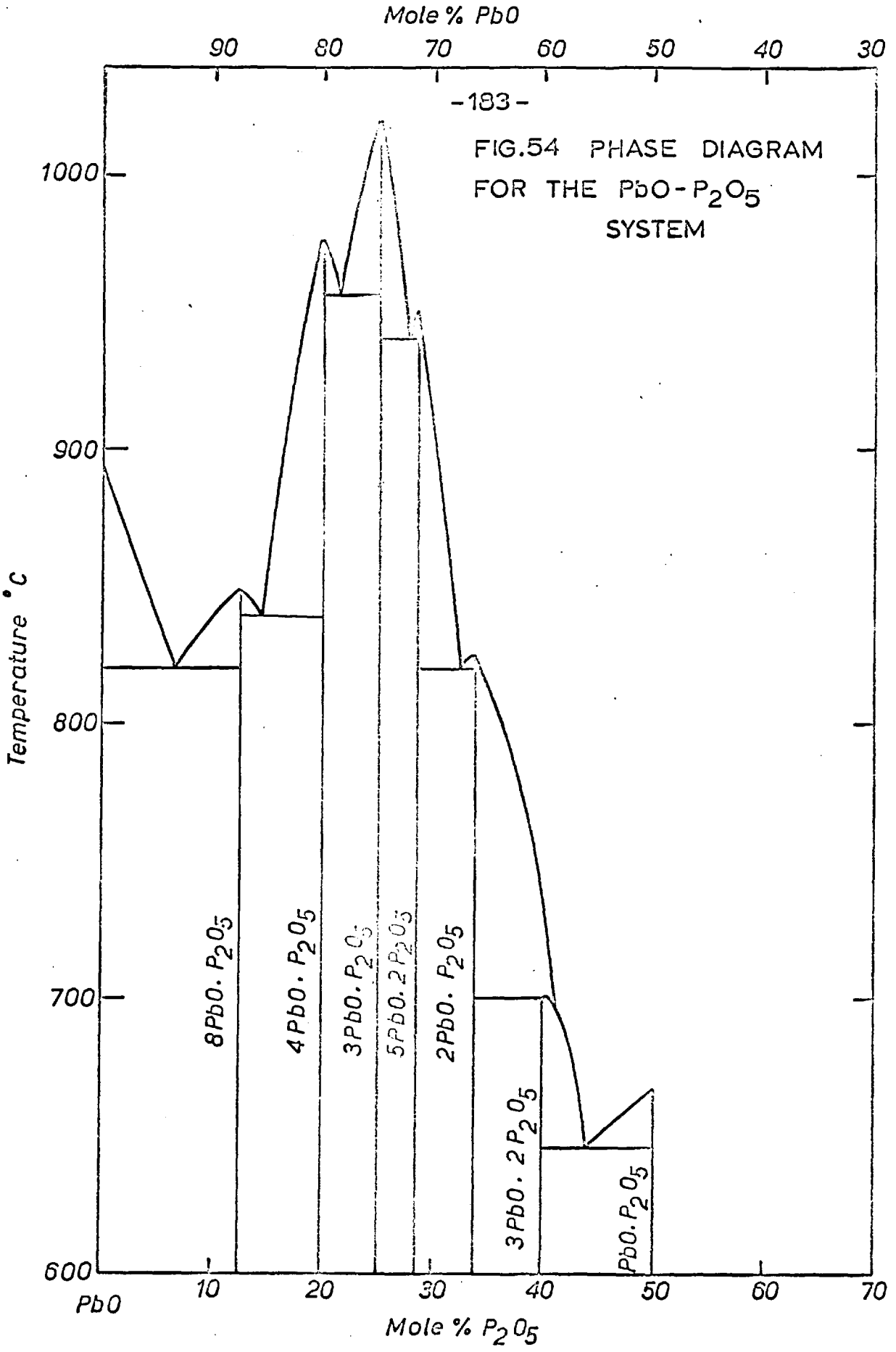

obtained is:

N_{PbO}	a_{PbO} Phase diagram	a_{PbO} Experimental
0.95	0.87	0.85

It can be seen that a_{PbO} obtained from phase diagram is in fair agreement with the value of the present study.

(f) $PbO-PbF_2$ melts

In figure 32 (page 135), the measured activities of PbO in $PbO-PbF_2$ melts are given together with activities of PbO calculated from phase diagram. These calculations were made using Sandonnini's[98] phase diagram for the $PbO-PbF_2$ system given in figure 55 . The values of T_f and ΔH_f for PbO employed for these calculations have been already given in sections (c) and (d). The temperatures dependence of heat and entropy of fusion, was taken into account for these calculations (cf. section (c)). From figure 32 , it can be seen that the experimentally derived activities of PbO and that calculated from phase diagram are in very good agreement, though these are referred to different temperatures. The small values of $\Delta \overline{H}_{PbO}$ derived from the present results (cf. table C- 9), would mean a small effect of temperature on a_{PbO} in these melts. This could be the reason for the rather good agreement of the activities obtained experimentally and from phase diagram.

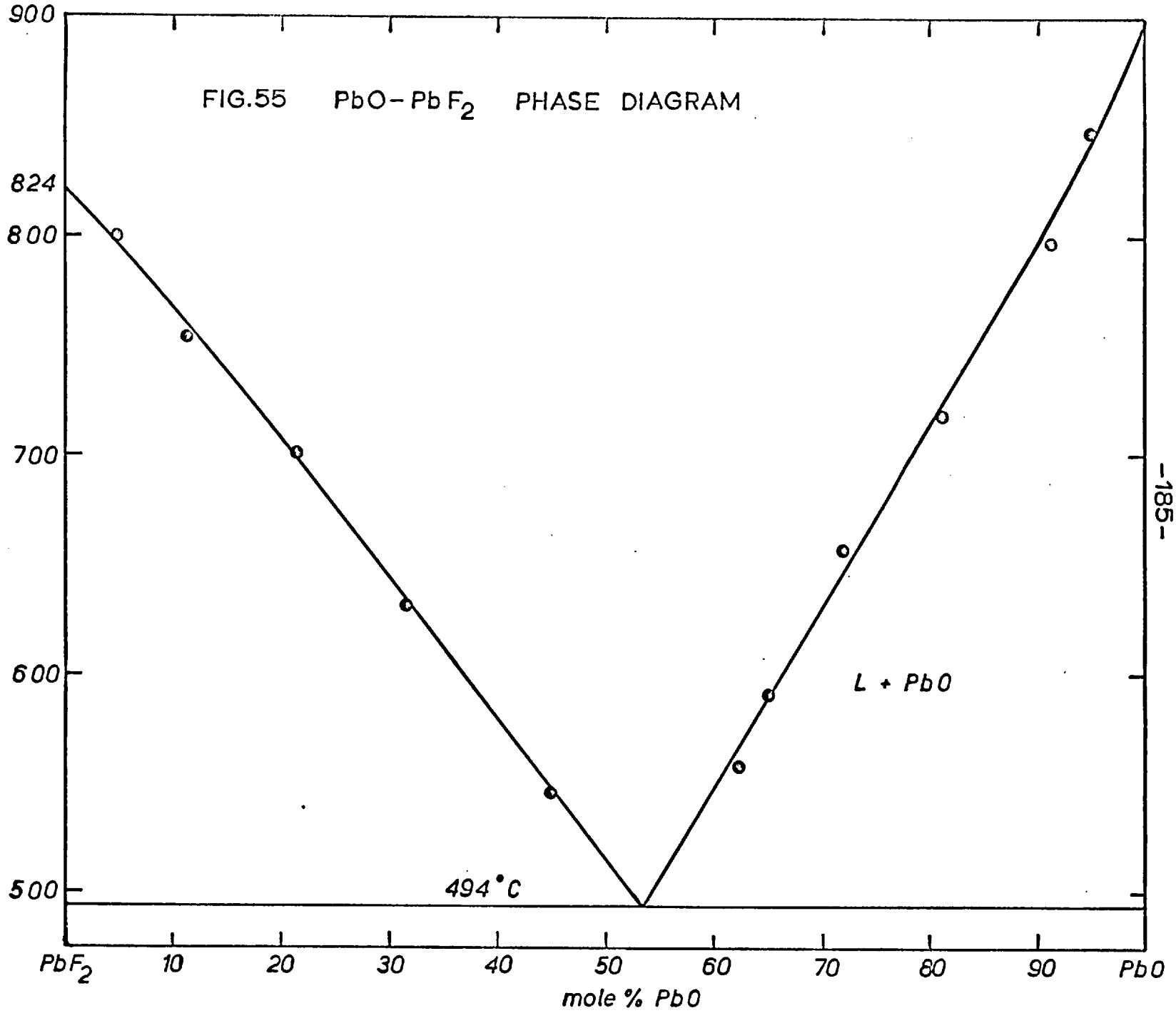
FIG.55 PbO – PbF2 PHASE DIAGRAM
900
824
800
700
600
500
494°C
L + PbO
PbF2
10
20
30
40
50
60
70
80
90
PbO
mole % PbO

The activities of PbF_2 were calculated from the phase diagram using ΔH_f of 4160 cals/mole and T_f of 1091°K for PbF_2, reported by Lumsden[99]. In these calculations the temperature dependence of heats and entropy of fusion was not taken into account. This was because the dependence of Cp on temperature for PbF_2 is not accurately known and can only be estimated. However, ^aPbO derived from phase diagram neglecting the effect of temperature on heat and entropy of fusion, were nearly the same as those obtained taking this correction into account. This may well be valid for PbF_2, and if so the $^aPbF_2$ derived neglecting the temperature dependence of heat and entropy of fusion will not be in error.

In figure 32 , it is seen that the $^aPbF_2$ obtained from phase diagram and that obtained by Gibbs-Duhem integration of experimental ^aPbO, are in fair agreement. The small differences could be due to reasons like, the errors involved in Gibbs-Duhem integration, the exactness of the value of heat fusion PbF_2.

(g) Activities in ternary melts

Delimarskii and co-workers[61,100] have studied the emf of the cells:

$$Pb \;/\; PbO - Na_2B_4O_7 \;/\; O_2 : Pt$$

and

$$Pb \;(\; PbO - NaPO_3 \;/\; O_2 \;:\; Pt$$

From the emf of these cells the ^aPbO in the ternaries Na_2O-PbO B_2O_3 and Na_2O-PbO-P_2O_5 can be derived knowing the emf for the cell

containing pure PbO, in a manner similar to that used in the present study. The study of Delimarskii and co-worker on these ternary melts has been limited to melts with constant Na_2O/B_2O_3 and Na_2O/P_2O_5 ratios, and to a small composition range. However, knowing the activity of PbO in the binary borate and phosphate melts (from the present study), and in the ternary melts from studies of the Russian workers we can get an idea of the variation of ^{a}PbO in the ternary borate and phosphate melts.

In figure 56, the variation of ^{a}PbO in the two ternaries are shown. The lines are shown in dotted as these are based on only two points. It can be seen that the type of variations are similar to those found by Taylor and Chipman[2], in $FeO-CaO-SiO_2$ melts, by Richardson and Pillay[7] in ternary silicates containing PbO and by Abraham, Davies and Richardson[6] in manganese oxide containing ternary silicate melts.

This tendency for the PbO activity to be raised by Na_2O additions in the borates and phosphates seems to suggest that the mixing relationships put forward by Abraham and Richardson[101] in ternary silicates may be valid for phosphate and borate melts. However, a more thorough study over wider composition regions in the ternary is essential for arrival at any final conclusions.

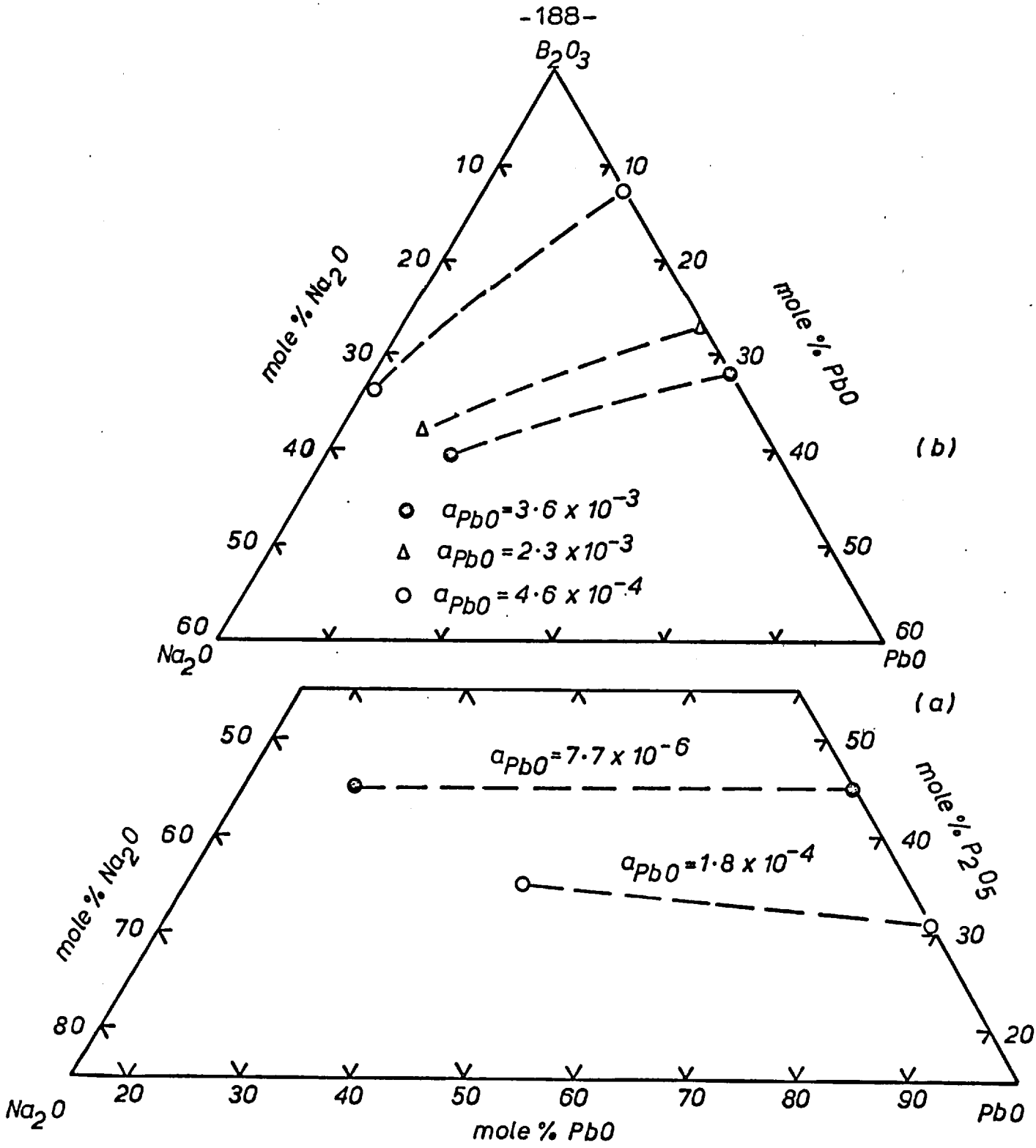

FIG.56 a_{PbO} IN TERNARY PHOSPHATE & BORATE MELTS

PART D

GENERAL DISCUSSION

Chapter 13

(i) Introduction

During the course of this discussion an attempt will be made to derive structural information from the thermodynamic data obtained for melts in the silicate, Phosphate, Borate and the Oxide-Fluoride systems (given in Part C). Also, the possibility of extending the structural information gained on the phosphate glasses (cf. Part B) to other systems and their relation to activity of metal oxide in these melts will be discussed.

The polymeric systems of silicates, phosphates and borates, containing a range of polyanions, and the simple ionic solutions of oxide-Fluoride melts will be dealt with separately. The polyanionic melts are considered first, and have been discussed in terms of 1) The basic metal oxide-rich melts, above the ortho composition, where these melts are expected to be comparatively simple ionic solutions containing predominantly Pb^{2+}, O^{2-} and the corresponding ortho ions. 2) The composition range from ortho to the acid oxide, where these would contain a range of polyanions.

(ii) Polyanionic melts (Silicate, Borate and Phosphate)

(a) Basic-oxide rich (Sub-ortho) melts

The observed activities for PbO in silicate, borate and phosphate melts in the "Sub-ortho" range can be compared with the activities calculated from the Temkin[16] model (cf. page 3) assuming that the only ionic species present are Pb^{2+}, O^{2-} and the corresponding ortho ion, SiO_4^{4-}, BO_3^{3-} and PO_4^{3-} respectively. These are compared in figures 57 and 58 .

In figure 57 , for the silicate melts it will be seen that the observed activity of PbO agrees with that calculated from the Temkin model, which in this case leads to the equation

$$a_{PbO} = \frac{n_{O^{2-}}}{n_{O^{2-}} + n_{SiO_4^{4-}}}$$

down to values of N_{PbO} of about 0.75. As the ortho silicate composition (N_{PbO}= 0.67) is approached, the observed activity of PbO shows a positive deviation from the Tmekin model, (which would indicate a zero PbO activity at this composition), owing to the production of O^{2-} ions presumably by condensation reactions of the type:

$$SiO_4^{4-} + SiO_4^{4-} = Si_2O_7^{6-} + O^{2-}$$

These types of equilibria have been shown to occur in phosphate melts and glasses, as discussed in Part B, and it is not unlikely that such equilibria would also occur in silicate melts.

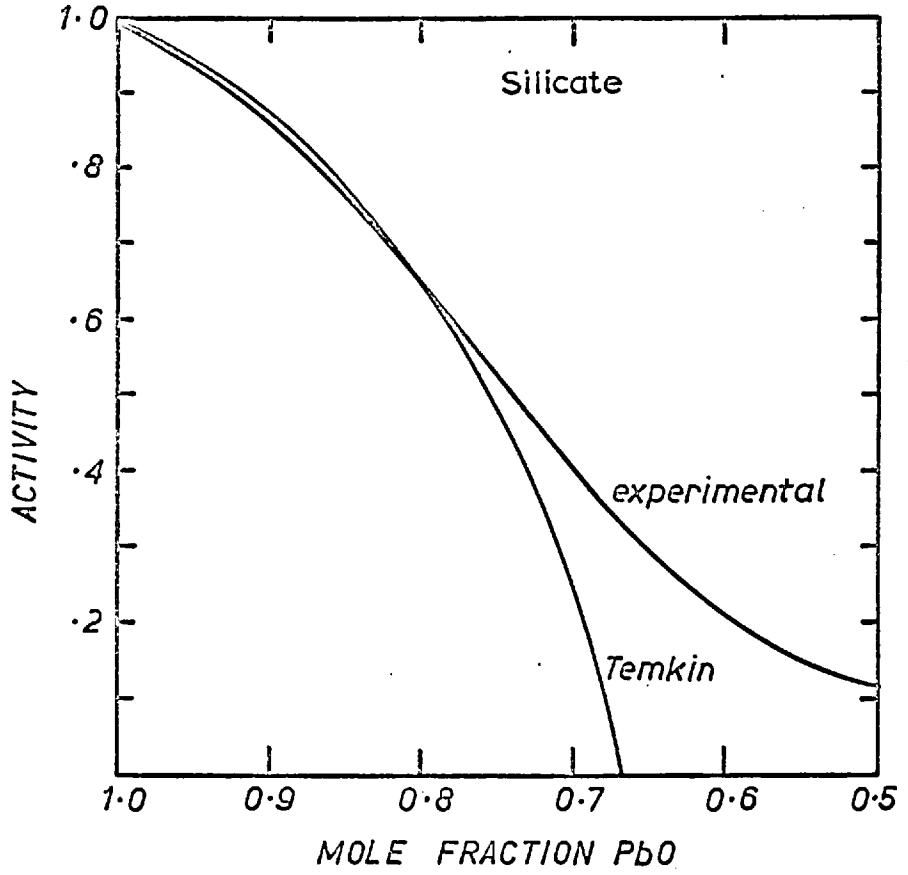

FIG.57 a_{PbO} IN 'SUB ORTHO' MELTS

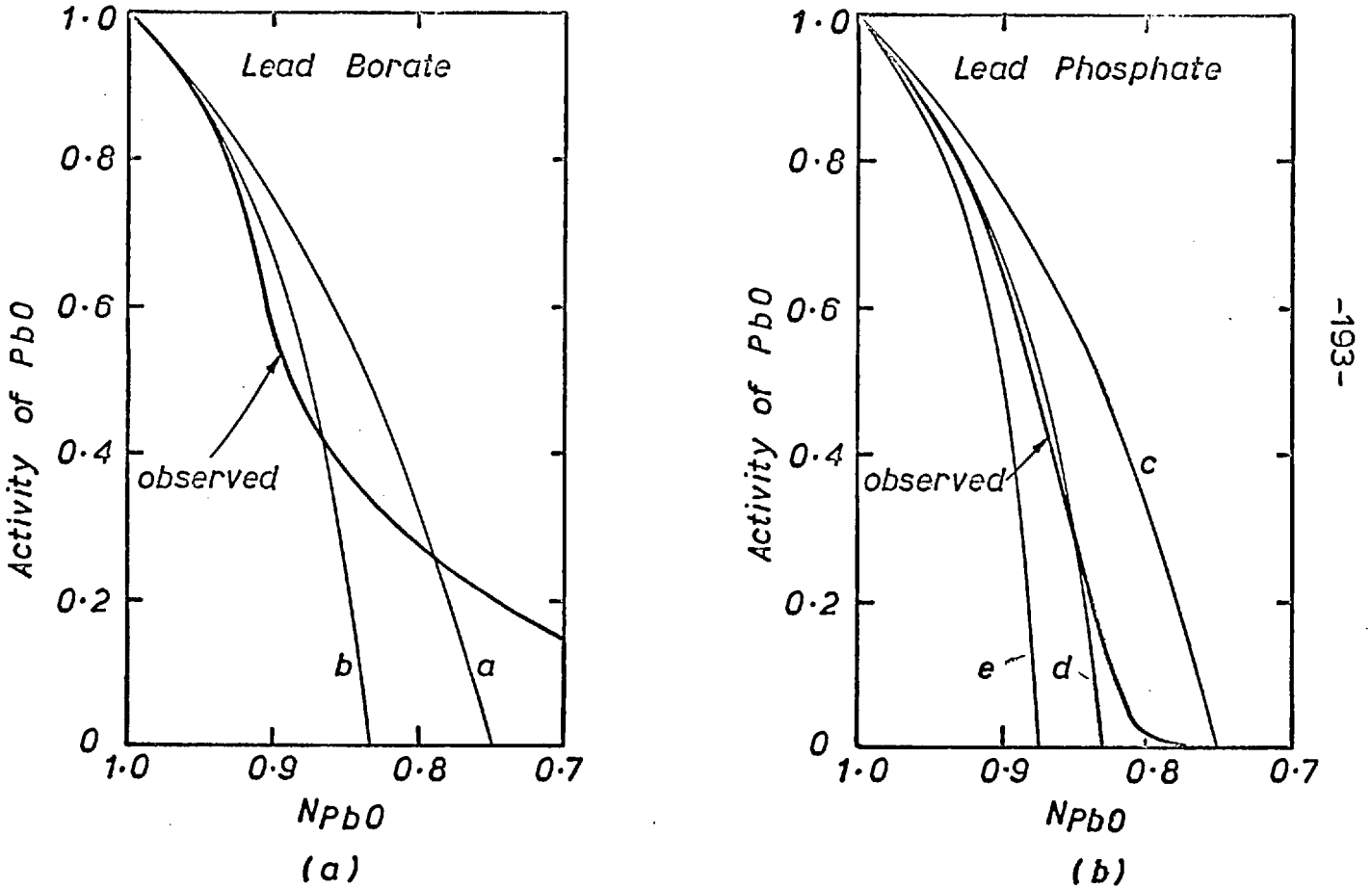

FIG.58 ACTIVITIES OF PbO IN "SUB-ORTHO" MELTS

In the borate melts, a more complex deviation from Temkin model based on the BO_3^{3-} anion is observed (cf. line a in figure 58). In the range of N_{PbO} between 1.0 to 0.78 negative deviations occur before the positive deviation, analogous to that in the silicate melt, takes over near the ortho borate composition.

However, as mentioned in chapter 2, there is evidence that in crystalline borates the boron atoms exist both in four and three co-ordinated configurations. More recently Bray and co-workers[102,103,104] have investiagted the existence of three and four co-ordinated boron atoms in alkali and lead borate glasses, using nuclear magnetic resonance. Their results are given in figure 59 . From the figure it can be seen that, in lead borate glasses, there are a number of boron atoms which are four co-ordinated in the lead oxide rich region. Krogh-Moe[105] employed Infra red spectroscopy for glasses and freezing point depression determinations for melts and confirmed the existence of three and four co-ordinated boron atoms in borate glasses and melts. The integral heats and entropies of mixing curves for $PbO-B_2O_3$ melts (figure 41) obtained in this study can also be interpreted in terms of the presence of three and four co-ordinated boron atoms in the melt. In the lead oxide rich region there is an inflexion in the integral heat curve; this could result from un-mixing caused by the presence of three or

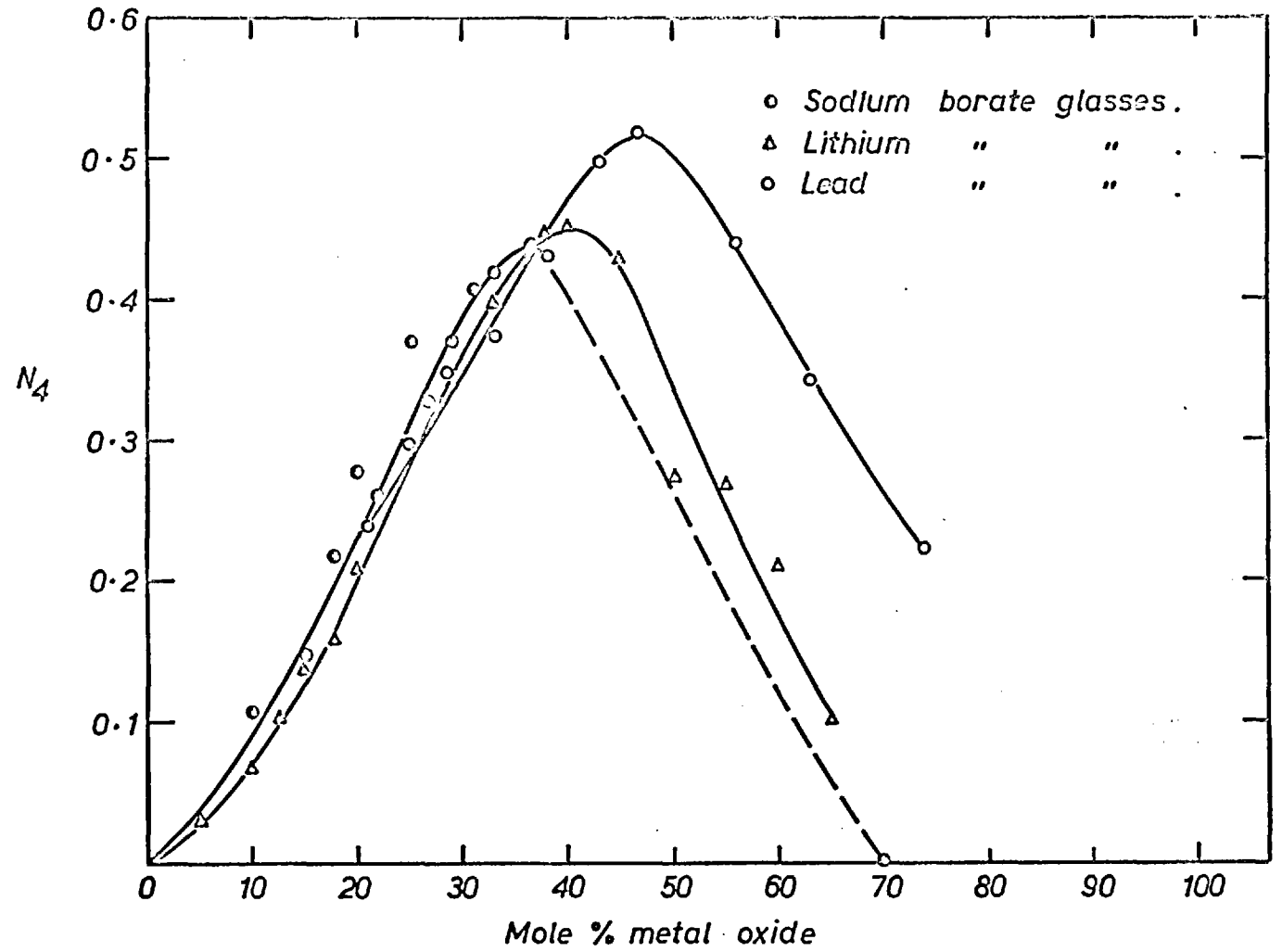

FIG. 59 N_4 - fraction of boron atoms in four co-ordination.

four co-ordinated borons. This would reflect on the entropy of mixing as an increase from ideality, which is seen from figure 41. The higher co-ordination of boron is also indicated by the existence of a crystalline compound $4PbO.\ B_2O_3$ in the PbO-B_2O_3 system (figure 53).

If it is supposed, that in dilute solution in PbO-rich melts, all the borate ions are of type BO_4^{5-}, (i.e. four co-ordinated ortho ion), the Temkin activity for PbO would be indicated by the line 'b' in figure 58 . This is in better agreement with the observed PbO activity than the line 'a', based on BO_3^{3-} ions. The tetrahedral co-ordinated boron will be based on sp^3 hybrid orbitals. It is also worth noting that with a tetrahedral co-ordination the boron would have the octet completed as in inert gases and this could be a reason why boron changes the co-ordination readily from three to four.

As we proceed to the more acid regions the observed activity shows a positive deviation from Temkin activities calculated based on BO_4^{5-} and BO_3^{3-} ions. This can be explained by polymerisation-depolymerisation reactions, of the type indicated for the silicates, occuring in these melts.

In the phosphate melts, the negative deviations shown for the PbO activity from that given by the Temkin model, based on PO_4^{3-} ion (line c figure 58) is displayed over an even wider range of compositions, and the Temkin activity of PbO is only

surpassed at compositions very close to ortho-phosphate. Although no evidence has been found in the literature to indicate that phosphorus can exist as ions showing an oxygen co-ordination number greater than four , there is ample evidence[13] for the formation of PCl_5 by dsp^3 and PCl_6^- by d^2sp^3 bond hybridization with configurations corresponding to a trigonal bipyramid and an octahedron respectively.

If the Temkin model is calculated in terms of PO_5^{5-} and a PO_6^{7-} ion the lines indicated by d and e in figure 58 results, and it is interesting to note that the observed activities of PbO in the melts are not inconsistent with the existence of both these hypothetical ions. The higher co-ordination of phosphorus is also indicated by the existence of crystalline compounds $8PbO.\ P_2O_5$ and $4PbO.\ P_2O_5$ in the $PbO-P_2O_5$ system (figure 54).

(b) Melts more acidic than the ortho composition

It was shown in part B that for phosphate melts, in the region where linear polymers predominate (which is usual for compositions more basic than metaphosphate, $N_{P_2O_5} = 0.5$), the anions can be considered in terms of disproportionation equilibria, as proposed by Meadowcroft and Richardson[25]. For example, their first three equilibrium constants K_1, K_2, K_3 would correspond to the equilibria,

$$2\ PO_4^{3-} = P_2O_7^{4-} + O^2$$

$$2\ P_2O_7^{4-} = P_3O_{10}^{5-} + PO_4^{3-}$$

$$2\ P_3O_{10}^{5-} = P_4O_{10}^{6-} + P_2O_7^{4-}$$

respectively. As described earlier, the values of K_n above n = 2, can be determined by chromatography of the glasses. However, the value of K_1 cannot be determined since the mole fraction of oxygen ions cannot be evaluated by the paper chromatographic method. This difficulty can be overcome to a degree if the activity of the metal oxide is known from other techniques, since

$$K_1 = \frac{N_{O^{2-}} \quad N_{P_2O_7^{4-}}}{N^2_{PO_4^{3-}}} = \frac{a_{O^{2-}} \quad N_{P_2O_7^{4-}}}{\gamma_{O^{2-}} \quad N^2_{PO_4^{3-}}}$$

If we assume $\gamma_{O^{2-}}$ to be constant, then

$$K_1' = \frac{a_{O^{2-}} \quad N_{P_2O_7^{4-}}}{N^2_{PO_4^{3-}}}$$

where $K_1' = K_1 \gamma_{O^{2-}}$

The value of K_1' can be determined if $a_{O^{2-}}$, $N_{P_2O_7^{4-}}$ and $N_{PO_4^{3-}}$ are known at a particular composition. The values of K_1' thus calculated for lead phosphates at various mean chain length from the results of this study are plotted in figure 60 . Similar calculations were made for the $CaO-P_2O_5$ system, using the a_{CaO} values of Schwerdtfeger and Engell[106] and the distribution results of Meadowcroft and Richardson and are given in figure 60 . For the system $H_2O-P_2O_5$, it is possible to obtain

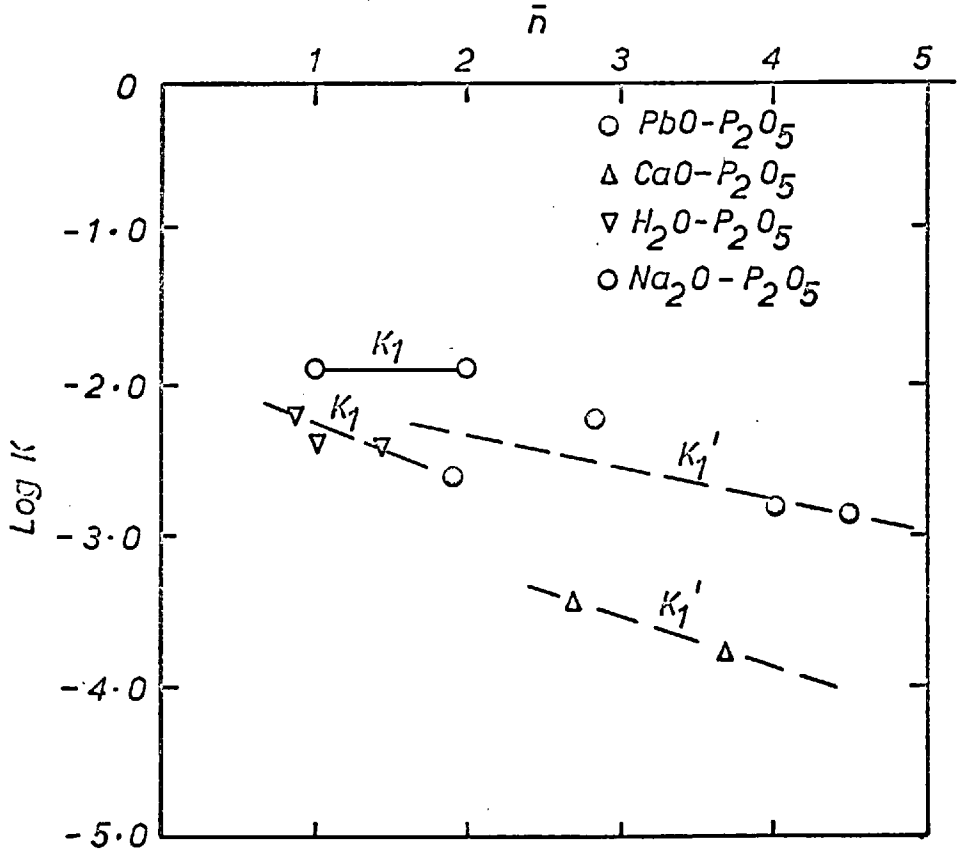

FIG 60 PLOT OF LOG K vs MEAN CHAINLENGTH ($\bar{n}$)

the value of the equilibrium constant,

$$K = \frac{N_{H_2O} \quad N_{H_4P_2O_7}}{N^2_{H_3PO_4}}$$

from the measurements of Hahti and Gartag is[107] and Jameson[26]. This constant would correspond to the equilibrium constant K_1 defined by Meadowcroft and Richardson[25], and is plotted as function of $\bar{n}$ in figure 60 .

In figure 60 , the value of K_1 for Na_2O-P_2O_5 system is that recently reported by Mitchell[108], who used infra red spectrascopy to arrive at this result. He reports a constant value of K_1 of 1.23×10^{-2}, in the composition range $\bar{n} = 2$ to 3. This value is much higher than expected, since $^{a}Na_2O$ in Na_2O-P_2O_5 melts should be much smaller than ^{a}PbO in PbO-P_2O_5 and ^{a}CaO in CaO-P_2O_5 melts at the same composition (ΔH^M curve for Na_2O-P_2O_5, system is much steeper than for CaO-P_2O_5 and PbO-P_2O_5 systems (figure 18), and it is reasonable to assume a similar trend for ΔG^M curve). This discrepancy could have arisen because infra red transmission technique cannot measure $N_{PO_4^{3-}}$ and $N_{P_2O_7^{4-}}$ very accurately and Mitchell calculated his values for $N_{O^{2-}}$ by subtracting the amounts of PO_4^{3-} and $P_2O_7^{4-}$ determined by infra red spectra from the total phosphate concentration in the original solution.

From figure 60 , it can be seen that K_1' varies with $\bar{n}$, and though $K_1' \neq K_1$ the same trend can be expected for K_1. This is supported by the fact that K_1 varies with composition for Na_2O-P_2O_5 system. The constancy of K_1 for Na_2O-P_2O_5 is not taken as conclusive since Mitchell's method of determining K_1, as described above, is by no means accurate.

Hence it seems, in the phosphate systems, that the values of K_1 and perhaps K_2 vary with metal oxide to P_2O_5 ratio, whereas from K_3 onwards the values are constant with composition and in most cases unity. If this variation of K_1 and K_2 were understood then the structure and thermodynamics could be correlated using Meadowcroft and Richardson's approach.

The only drawback of Meadowcroft and Richardson's[25] approach is that it neglects the presence of ring anions and would only be strictly valid in the composition range N_{MO}= 1.0 to near 0.50, where chain anions predominate and the amounts of ring anions is small. This difficulty could be overcome if the equilibria between the chains and rings were also taken into account. A quantitative study of chain-ring equilibria is difficult in the case of phosphates using paper-chromatographic technique, since in composition regions where measurable amounts of rings are present, the number of small chains ($n \leq 7$) which can only be separated by this technique is very small. However, such measurements could be made by using the ion-exchange chromatographic

technique. Carmichael has recently studied the problem of ring-chain equilibria in silicones and this could serve as a guide for studies on phosphate glasses.

In the case of the silicate melts, in the composition region where chain anions are predominant, Meadowcroft and Richardson's[25] approach can be directly extended, and equilibrium constants for equilibria of the type

$$2\ SiO_4^{4-} = Si_2O_7^{6-} + O^{2-}$$

$$2\ Si_2O_7^{6-} = Si_3O_{10}^{8-} + SiO_4^{4-}$$

etc,

can be considered. Since the ΔG^M curves for silicates are far shallower than for the phosphate, the distributions of the chains will be broader than for the corresponding phosphates. This would mean that values of K_n would be unity even for small values of n and perhaps the silicates differ one from the other only in the value K_1. Hence, if one could define the value of K_1 and its variation with composition (if any) then from a measurement of metal oxide activity at one composition, it might be possible to calculate it over a wide range of compositions.

Similarly these observations could be extended to the lead borate melts, in which the distributions should be broader than for phosphates, but more peaked than the silicates, because the ΔG^M curve for lead borate system lies between that for the silicate and phosphate, and could be generally true for other

borate systems.

As mentioned in chapter 3, Toop and Samis[30], and Masson[31] have considered ionic equilibria in silicate melts. Also, Flood and co-workers[32,33,34,] have proposed structures for borate and silicate melts based on phase diagrams and thermodynamic data. Since all the results of the present work have been discussed above in terms of Meadowcroft and Richardson's[25] model, it was thought to be interesting to determine how this compares with these other models.

Toop and Samis[30] have used Fincham and Richardson's[57] suggestion that a probable equilibrium

$$2\,O^- = O^{2-} + O^0$$

occurs in silicate melts, where O^-, O^0 and O^{2-} refer to singly bonded, doubly bonded and non-bonded oxygen ions. The equilibrium constant for such a reaction, in terms of moles, is given by:

$$K = \frac{N_{O^0}\ N_{O^{2-}}}{N^2_{O^-}}$$

From charge and material balance considerations, Toop and Samis derived the relation:

$$4K = \frac{\left[4N_{SiO_2} - N_{O^-}\right]\left[2 - 2N_{SiO_2} - N_{O^-}\right]}{N_{O^-}{}^2}$$

relating N_{O^-}, K and composition. For given values of K and N_{SiO_2}, the equation gives values of N_{O^-}.

They derived values for N_{O^-} in this manner, for constant values of K, as a function of N_{SiO_2} and claim that these curves have the characteristic shape of Integral free energy of mixing curves for binary silicates. However, this is not exactly true, because tangents to the N_{O^-} versus N_{SiO_2} curves near $N_{SiO_2} = 0$ and 1 do not tend to minus infinity.

The two approaches of Meadowcroft and Richardson[25] and Toop and Samis[30], can be compared by taking an ideal Flory distribution for the phosphate anions, and evaluating the respective equilibrium constants. This has been done for phosphates of mean chain lengths two and five. The number of moles of O^- and O^o (singly and doubly bonded oxygen) were determined from the summations Σ (n + 2) moles of P_nO_{3n+1} and Σ(n-1) moles of P_nO_{3n+1} respectively. The calculated value of Toop and Samis's equilibrium constants were 0.0625 and 0.0207 at $\bar{n}$ = 2 and 5 respectively, compared to the constant value of unity for Meadowcroft and Richardson's constants. Thus even in the ideal case the two methods of approach differ markedly, as in one case the equilibrium is a function of $\bar{n}$ and in the other it is not and hence they cannot be directly compared. However, Meadowcroft and Richardson's model is superior to that of Toop and Samis, since with values of equilibrium constants, one can calculate the exact amounts of the various anions present by the former model, which is not possible using the latter approach.

Masson[31] on the other hand has considered equilibria of the type

$$SiO_4^{4-} + SiO_4^{4-} = Si_2O_7^{6-} + O^{2-} \qquad (K_{1,1})$$

$$Si_2O_4^{4-} + Si_2O_7^{6-} = Si_3O_{10}^{8-} + O^{2-} \qquad (K_{1,2})$$

$$SiO_4^{4-} + Si_3O_{10}^{8-} = Si_4O_{13}^{10-} + O^{2-} \qquad (K_{1,3})$$

etc.

The first equilibrium constant $K_{1,1}$ of Masson is the same as K_1 defined by Meadowcroft and Richardson. The second equilibrium constant $K_{1,2}$ of Masson is $K_1 \times K_2$ defined by Meadowcroft and Richardson. Hence $K_{1,n}$ of Masson will be $K_1.K_2.K_3.....K_n$ of Meadowcroft and Richardson. For relating the distributions, and the values of $K_{1,n}$ to the thermodynamic data Masson has assumed that

$$K_{1,1} = K_{1,2} = K_{1,3} = ... = K$$

and that Temkin's model is valid for these melts for which $a_{O^{2-}} = N_{O^{2-}}$. By using these assumptions Masson has derived the equation

$$N_{SiO_2} = 1 \Big/ \left[3 - K + \frac{a_{MO}}{1-a_{MO}} + \frac{K(K-1)}{\frac{a_{MO}}{1-a_{MO}} + K} \right]$$

relating K, N_{SiO_2} and the activity of the metal oxide in a binary silicate melt.

When values are substituted in the above equations, at all

values of $N_{SiO_2} \geqslant 0.50$, $a_{MO} = 0$, for $K > 0$. For $K = 0$, $a_{MO} = 0$ at $N_{SiO_2} = 0.67$. This anomaly of this theory is due to the fact that Masson[31] has assumed only the pressure of chain anions and at $N_{SiO_2} = 0.50$, the mean chain length of the silicate anion should be infinity and the amount of O^{2-} ions would be negligible. On application to data, Masson finds that it provides a good fit for the systems $FeO-SiO_2$, and $CaO-SiO_2$ but does not fit the $PbO-SiO_2$ data. He considers that for such systems perhaps more than one equilibrium constant have to be defined.

Masson's equilibrium constants are equivalent to the product of Meadowcroft and Richardson's equilibrium constants and when even one of Meadowcroft and Richardson's K's varies with composition all Masson's K's will vary with composition. Except for these differences Masson's and Meadowcroft and Richardson's model are similar and the former should have as wide an applicability as the latter.

Flood and co-workers[32,33,34] have put forward structural models to fit activity data calculated from phase diagrams and those available from thermodynamic property measurements. Knapp and Flood[32] have evaluated the ionic species existing in $CaO-B_2O_3$ melts. They put forward the existance of the ions BO_3^{3-} and $B_2O_5^{4-}$ in the region between the compositions $Ca_3(BO_3)_2$ and $Ca_2B_2O_5$, and ions $B_2O_5^{4-}$ and $(BO_2)_3^{3-}$ in the region between $Ca_2B_2O_5$ and $Ca(BO_2)_2$ and $(BO_2)_3^{3-}$ and $B_4O_7^{2-}$ (or B_4O_6) ions in the region

between $Ca(BO_2)_2$ and CaB_4O_7. Hence they have accounted for the activities assuming four ionic species present in these melts. However, the present state of knowledge on phosphate systems show that, even at basic compositions near the pyrophosphate composition (N_{MO}= 0.67), there are a large variety of anions present, and when we proceed to the more acidic glasses there are a yet greater range of anions, and certainly more than Flood's four or five types.Hence, it seems that this type of approach is unlikely to give us a true picture of these polyanionic melts.

In the particular case of the $PbO-SiO_2$ melts, Flood and Knapp[34] have used Richardson and Webbs[3] data for a_{PbO} and put forward a structural model which would fit these activities.

(iii) Lead oxide - Lead fluoride mixtures

It is reasonable to assume that these melts are simple ionic solutions containing Pb^{2+}, O^{2-} and F^- ions. Information about the structures of these melts may be derived by interpreting the thermodynamic data obtained in the present study (cf. Part C), in terms of various models of melts discussed in chapter One.

According to the Temkin's[16] model for ideal ionic solutions, the activity of PbO in $PbO-PbF_2$ melts will be given by

$$a_{PbO} = N_{Pb^{2+}} \; N_{O^{2-}} = N_{O^{2-}}$$

since $N_{Pb^{2+}} = 1$

Therefore $$a_{PbO} = N_{O^{2-}} = \frac{n_{O^{2-}}}{n_{O^{2-}} + n_{F^-}}$$

Similarly a_{PbF_2} in $PbO-PbF_2$ melts according to this model will be,

$$a_{PbF_2} = N^2_{F^-} = \left[\frac{n_{F^-}}{n_{F^-} + n_{O^{2-}}} \right]^2$$

where $N_{Pb^{2+}}$, $N_{O^{2-}}$ and N_{F^-} are the ionic fractions of Pb^{2+}, O^{2-} and F^- ions and $n_{O^{2-}}$ and n_{F^-} the number of oxygen and fluorine ions.

Flood, Forland and Grjotheim's[17] model on the other hand gives,

$$a_{PbO} = N^1{}_{O^{2-}} = \frac{2\, n_{O^{2-}}}{2n_{O^{2-}} + n_{F^-}}$$

for the activity of PbO in the oxide- Fluoride mixtures where $N^1{}_{O^{2-}}$ is the equivalent ionic fraction and other symbols are as defined for Tomkin's case. For the activity of PbF_2, this model gives

$$a_{PbF_2} = N^1_{F^-} = \frac{n_{F^-}}{2n_{O^{2-}} + n_{F^-}}$$

In table D-1, the observed activities are compared with those calculable from these two models and are plotted in figure 61 . It can be seen that the experimental data are in better agreement with the Temkin's model than the Flood, Forland and Grjotheim model. It is interesting to note that for a mixture of

Table D-1

a_{PbO} and a_{PbF_2} for $PbO-PbF_2$ melts at 1170°K

N_{PbO}	a_{PbO}			a_{PbF_2}		
	Experimental	Temkin	Flood et al	Experimental (Gibbs-Duhem)	Temkin	Flood et al
0.90	0.80	0.82	0.90	0.013	0.033	0.10
0.80	0.61	0.67	0.20	0.065	0.11	0.20
0.70	0.45	0.54	0.70	0.16	0.21	0.30
0.60	0.33	0.43	0.60	0.29	0.33	0.40
0.50	0.25	0.33	0.50	0.41	0.44	0.50
0.40	0.18	0.25	0.40	0.53	0.56	0.60
0.30	0.12	0.18	0.30	0.66	0.68	0.70
0.20	0.07	0.11	0.20	0.78	0.79	0.80
0.10	0.03	0.05	0.10	0.90	0.90	0.90

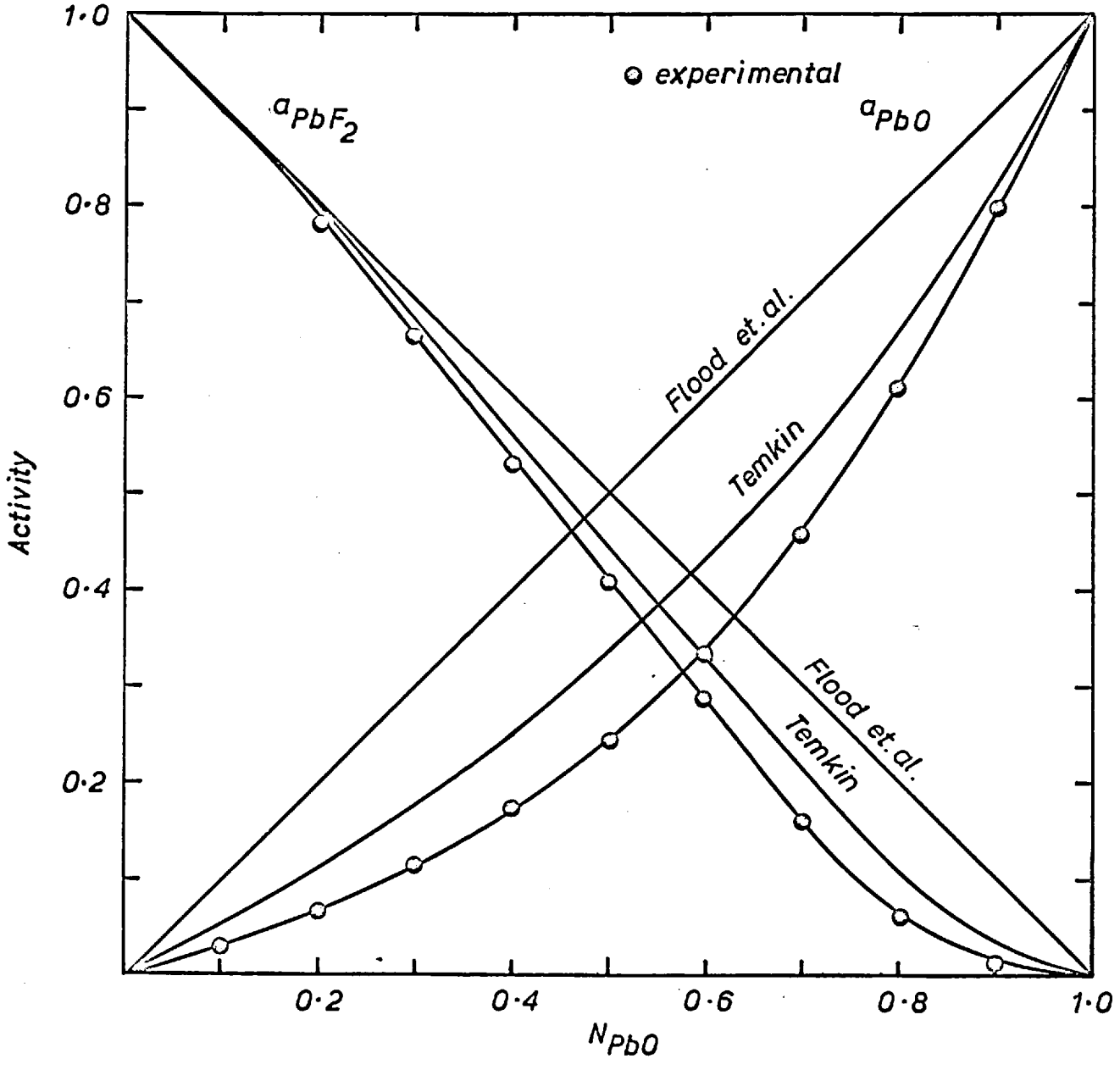

FIG. 61 a_{PbO} & a_{PbF_2} IN $PbO-PbF_2$ MELTS

the type XY and XZ_2, with X^{2+}, Y^{2-} and Z^- ions, the activity of XZ_2 predicted by Temkin is not very different from that according to Flood et al, specially in the XZ_2 rich melts. However, the two activities of XY would differ markedly even in XY rich melts. Hence the determination of a_{XY} in XY + XZ_2 melts is useful to understand the Temkin or Flood behaviour of such melts, but to arrive at any definite conclusion by the study of a_{XZ_2} in these melts, investigation has to be carried out over a wider range of compositions. Also the study of the partial entropies serves to check which model fits the observed data.

In table D-2, the partial entropies of solution of PbO in PbO + PbF_2 melts, derived from the temperature dependence of experimental a_{PbO} are compared with those expected from Temkin[16] and Flood, Forland and Grjotheim[17] models.

These two models give $\Delta \bar{S}_{PbO}$ as,

$$\Delta \bar{S} = - R \ln N_{O^{2-}}$$

$$\Delta \bar{S} = - R \ln N^{1}_{O^{2-}}$$

respectively.

Table D-2

N_{PbO}	$\Delta \bar{S}_{PbO}$, cals/°K		
	Experimental ($\pm$ .5)	Temkin	Flood et al
0.90	0.31	0.40	0.21
0.80	0.63	0.81	0.44
0.70	1.26	1.23	0.67

Thus for $PbO-PbF_2$ melts, $\Delta \bar{S}_{PbO}$ seems to agree with Temkin's model more closely in the composition range studied. However, it may be argued that this conclusion is not strictly valid on account of the error of $\pm$ 0.5 cals/deg. in the experimental $\Delta \bar{S}_{PbO}$. This would have been more conclusive had it been possible to study the temperature dependence of $\Delta \bar{G}_{PbO}$ over the whole range of the binary.

Since the $PbO-PbF_2$ melts seem to be Temkin type solutions with ideal entropies of mixing, it is interesting to see whether the small deviations of the observed activities from those predicted by Temkin's model are due to heats of mixing of the O^{2-} and F^- ions. In figure 62 , the function RT ln $\gamma_{O^{2-}}$ is plotted against $N_{F^-}^2$. The $\gamma_{O^{2-}}$ was calculated by dividing the observed activity of oxygen ions, by Temkin's mole fraction $N_{O^{2-}}$. It would appear that RT ln $\gamma_{O^{2-}}$ is a linear function of $N_{F^-}^2$ if the allowance is made for the experimental scatter. From the plot, RT ln $\gamma_{O^{2-}}$ can be related to $N_{F^-}^2$ by the equation:

$$RT \ln \gamma_{O^{2-}} = -1{,}460 \; N_{F^-}^2$$

However, Forland[17a] considers that in an ionic salt mixture of the type XZ_2 and YZ, the energy of mixing is related to the equivalent fractions defined by Flood, Forland and Grjotheim[17] and the partial energy of mixing of component YZ in the mixture can be represented by

$$\Delta \bar{H}_{YZ} = K \; N'^2_X$$

In Na_2CO_3-$CaCO_3$ mixtures, Forland[17a] concludes that $\Delta \bar{H}_{Na_2CO_3}$ is a linear function of N'^2_{Na} and not of N^2_{Na} though the entropy of mixing agrees with Temkin's model. This he attributes to the fact that the number of cations currounding a cation as next nearest neighbours will decrease as one goes from Na_2CO_3 to $CaCO_3$. In figure 62 RT ln $\gamma_{O^{2-}}$ is also plotted as a function of N'^2_F and it can be seen that the linearity of this plot is not improved as claimed by Forland for Na_2CO_3-$CaCO_3$ melts. However, the slope of the best line drawn through these points is not far different from that of the line drawn through the points of N^2_F- plot.

Hence it seems that, PbO-PbF_2 mixtures are regular solutions and if so $\Delta \bar{H}_{PbO}$ for these melts will be equal to RT ln $\gamma_{O^{2-}}$. The values of $\Delta \bar{H}_{PbO}$ derived experimentally (given in table C-9, page 137) at N_{PbO} of 0.90, 0.80 and 0.70 are in good agreement with values derived from the above equation for RT ln $\gamma_{O^{2-}}$ as shown in the following table D-3.

Table D-3

N_{PbO}	$\Delta \bar{H}_{PbO}$ cals Experimental	RT ln $\gamma_{O^{2-}}$
0.90	30	50
0.80	120	160
0.70	280	310

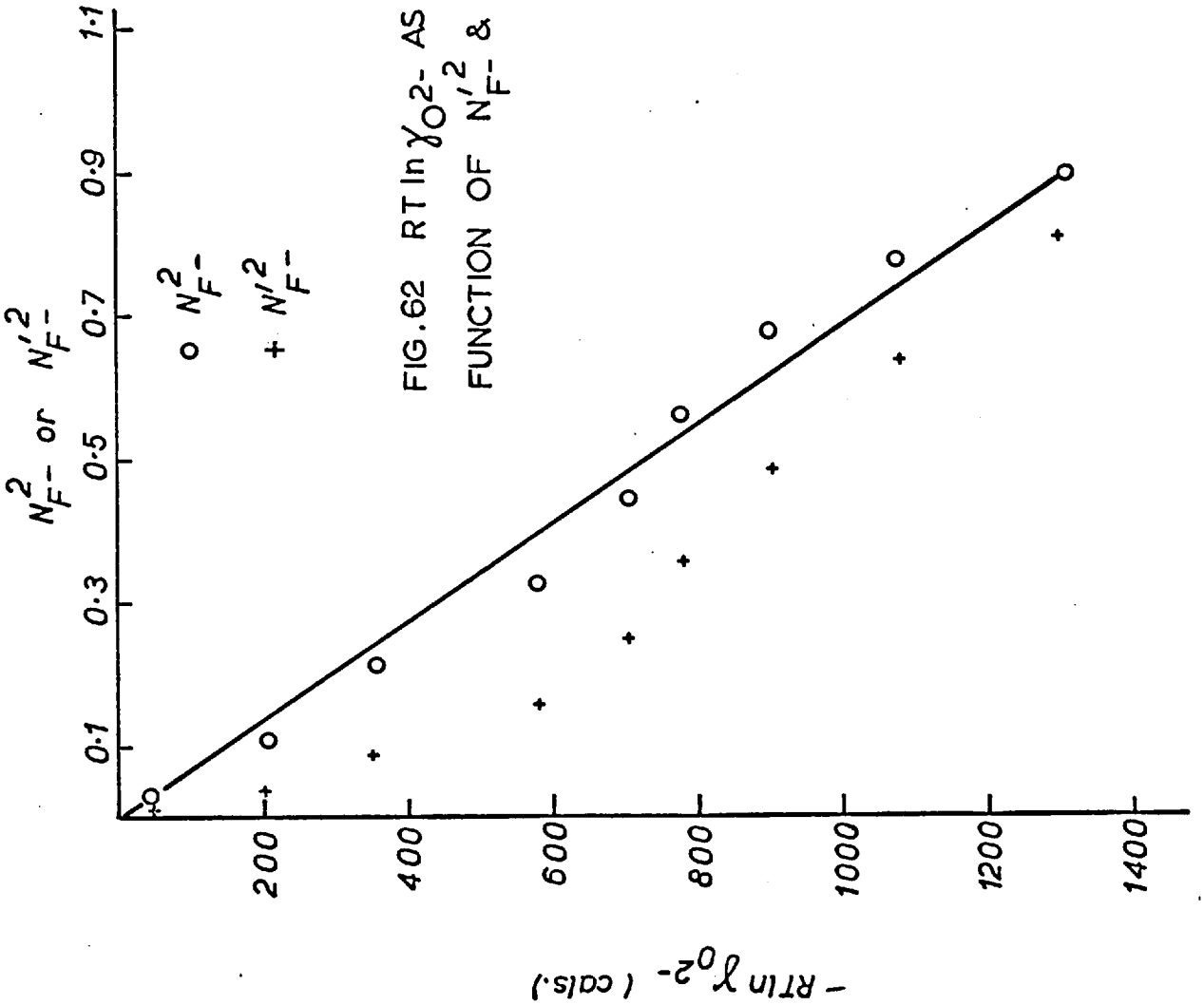

FIG.62 RT ln $\gamma_{O^{2-}}$ AS A FUNCTION OF $N'^2_{F^-}$ & $N^2_{F^-}$

In figure 63 , the values of ΔG^M, ΔH^M and ΔS^M are plotted for $PbO-PbF_2$ melts at 1170°K. The ΔS^M is that for a Temkin solution, and ΔH^M is derived from the experimental value of ΔG^M and ΔS^M (of Temkin) by the relation,

$$\Delta H^M = \Delta G^M + T \Delta S^M$$

The assumption that the entropy of mixing is ideal made in the above treatment may not be valid in the entire binary. However, this seems to be a reasonable assumption on the basis of the data obtained as already explained. This can be checked conclusively if exact heats of mixing are available from calorimetric data, because ΔH^M would define precisely the entropy of mixing from the measured ΔG^M values.

If the entropy of mixing as defined by Temkin is valid for these solutions, as the present study seems to indicate, then in $PbO-PbF_2$ melts the F^- and O^{2-} ions mix randomly even though they are of different charges. The failure of Flood, Forland and Grjotheim's model, which assumes that a O^{2-} ion is equivalent to a vacancy and a F^- ion may be due to the fact that in melts there are already a large number of vacancies (or holes), and creation of a vacancy according to the following scheme,

$$O^{2-} + \square = 2\,F^-$$

does not contribute to the entropy and hence to the free energy of mixing. This is in agreement with Forland's observation

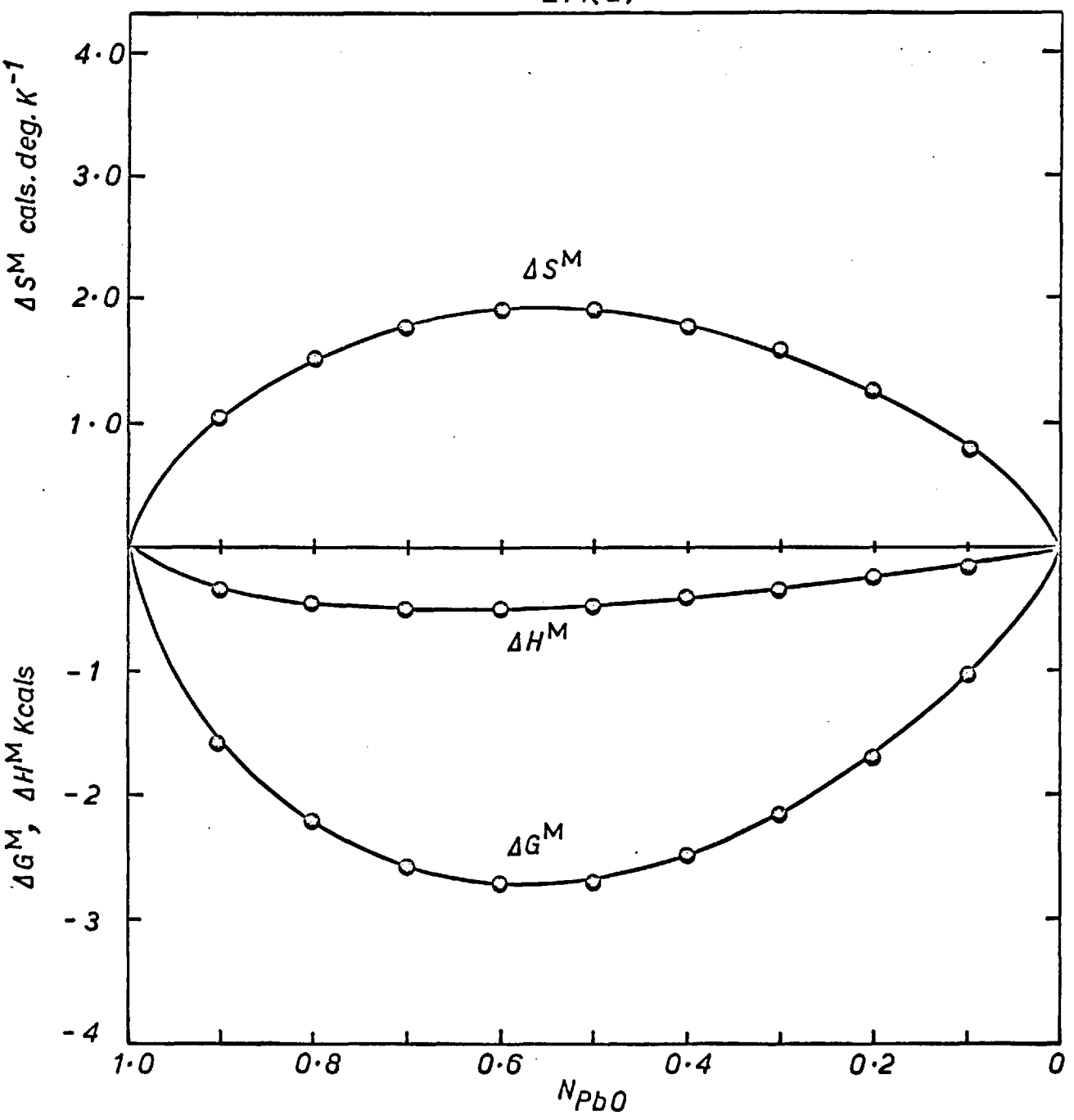

FIG.63 ΔG^M, ΔH^M & ΔS^M PER MOLE ($PbO + PbF_2$) FOR $PbO - PbF_2$ MELTS

that the system $AgCl-PbCl_2$, $Na_2CO_3-CaCO_3$ and $K_2CO_3-CaCO_3$, containing a mixture of mono and divalent cations have entropies of mixing as predicted by Temkin's model. According to Forland[17a] the systems $Na_2CO_3-CaCO_3$ and $K_2CO_3-CaCO_3$ are regular solutions with Temkin entropies of mixing. From the present study it appears that the system $PbO-PbF_2$ exhibits a similar behaviour.

As mentioned, in chapter one, Lumsden[20] has calculated the heats of mixing of alkali halides with a common anion, by estimating the polarization and London forces involved in such mixtures. Similar considerations can be extended to mixtures with a common cation and different anions[99]. However, the situation with $PbO-PbF_2$ mixtures is different as this involves a common cation surrounded by anions of different valencies, namely F^- and O^{2-}. To calculate the contribution of London forces to the heats of mixing of such solutions, in the Lumsden's manner, it is necessary to know the London constants for like ions, $O^{2-}-O^{2-}$, unfortunately this is not known and hence this contribution by London forces for the $PbO-PbF_2$ system cannot be calculated.

On the other hand to calculate the contribution of polarization forces to the heats of mixing, we have to know the Pb-O and Pb-F distances and the polarizability of the Pb^{2+} ion. Frank gives the polarizability of Pb^{2+} ion to be $4.34.\ A^3$. The Pb^{2+} to F^- distance in PbF_2 is given to be 2.57 A. The Pb^{2+}

to O^{2-} distance in PbO is not easy to fix, as it is 2.30 A in the low temperature tetragonal red lead oxide, and it is 2.21 A and 2.49 A in the high temperature orthorhombic yellow lead oxide. The calculation of the polarization energy involved in a PbO-PbF_2 mixture is not straight forward as that for alkali halide mixtures. Hence to make this calculation, it is necessary to assume that the polarization involved for the system

$$O^{2-}Pb^{2+}\begin{matrix}F^-\\F^-\end{matrix} \quad \text{is similar to} \quad X^+ \cdot Z^- \quad Y^+$$

interactions considered by Lumsden[20] for alkali halides. However, there will be a difference on account of the divalent nature of the cation and if this is taken into account the following expression can be derived,

$$K_p = -8\alpha N e^2 \left[\frac{1}{r^2_{Pb-O}} - \frac{1}{r^2_{Pb-F}} \right]^2$$

where K_p is the polarization constant, N the avagadro's number, the polarizability of Pb^{2+} ions and r_{Pb-O}, and r_{Pb-F}, the Pb^{2+} to O^{2-} and F^- distances in PbO and PbF_2 respectively.

Taking the value of 2.49 A for Pb-O distance, the above expression gives -1,100 cals for value K_p and for a Pb-O distance of 2.35 A (i.e. mean of 2.49 A and 2.21 A for yellow PbO) one gets a value of -9,700 cals for K_p. Hence it seems that unless the Pb^{2+} to O^{2-} distance is exactly fixed, one cannot evaluate accurately the energy involved due to polarization.

However, if the distance Pb-O is near 2.49 A in the melt, (may not be unreasonable as Pb^{2+} is 1.20 and O^{2-} is 1.40), then the energy of mixing of 1,100 cals is in good agreement with the experimental value of 1,460 cals obtained in the present study. This would mean that the London force contribution is very small, As mentioned before, we are not in a position to evaluate the London force contribution, but this is likely to be small due to the similar size of the O^{2-} and F^{-} ions. Hence it seems that Lumsden's[20] approach is not easy to apply for systems containing ions of different valencies. Besides application of Lumsden's theory to ionic solutions containing elements belonging to groups other than one and seven is made more difficult due to lack of data on the London constants and distance of separation between ions in these mixtures.

Chapter 14

Conclusions

The present study of the anionic distributions in sodium, cadmium, magnesium and lead phosphate glasses, confirms the views of Westman and co-workers and Meadowcroft and Richardson[25] that anion distribution is a function of both the metal oxide to phosphorus pentoxide ratio and the cation. The width or the broadness of the distribution is directly related to the shape of the heat of formation curve for the binaries, and to the radius to charge ratio of the cations to the extent that these determine the heat of formation.

The making of the glasses under dry conditions instead of in the laboratory atmosphere has no effect on the observed distributions. Also large increases in quenching rates had no effect on the anionic distributions.

When the experimental distributions are treated in terms of equilibrium constants defined by Meadowcroft and Richardson[25] (cf. equation B-10), it is seen that the values of K_n for $n \geq 3$, are constant for a particular system and are not a function of mean chain length $\bar{n}$. Also for all the systems studied, values of K_n, for $n \geq 4$, are unity and hence the different systems vary from one another in values of K_n where $n \leq 4$. Though values of K_n for $n \geq 3$ are constant with $\bar{n}$, it is found that K_2 varies with $\bar{n}$ for most of the systems. Also the values of K_1 (defined in

page 198, calculated using the experimental activity and distribution data is not constant with $\bar{n}$. Hence it seems that if one could relate the variation of K_1 and K_2 with $\bar{n}$ and fix K_3, then the activity of the metal oxide could be calculated over the whole composition range of the binary, given the activity at one composition.

The study of the thermodynamics of the systems PbO + SiO_2, PbO + B_2O_3, PbO + P_2O_5 and PbO + PbF_2, employing the emf technique has confirmed the usefulness of the emf technique for such investigations and the wide applicability of the oxygen electrodes in oxy-anionic melts. The results obtained indicate a strong interaction of PbO with SiO_2, B_2O_3 and P_2O_5 in that order. The results for PbO + B_2O_3 melts can be interpreted, in terms of three and four co-ordinated boron atoms in these melts. Similar considerations indicate that, in PbO rich PbO + P_2O_5 melts, the phosphorus atoms may be five co-ordinated with oxygen. When the present results for the activity of PbO in lead borate and phosphate melts are compared with the values of ^{a}PbO determined in Na_2O + PbO + B_2O_3 and Na_2O + PbO + P_2O_5 melts by Delimarskii and co-workers[61,100], it appears that mixing relationships, suggested by Richardson[19] for ternary silicate melts may also be applicable to these ternary borate and phosphate melts.

The data for PbO + PbF_2 melts suggest that these are regular solutions with an ideal Temkin[16] entropy of mixing. The

evidence available suggests that the heats of mixing in these melts are due to the polarization energy involved in mixing O^{2-} and F^- ions in a Pb^{2+} matrix. This energy is a function of the polarizability of the cation Pb^{2+} and the inter-ionic separation of each cation and the neighbouring anion. Hence in a $CaO + CaF_2$ mixtures, which are of industrial importance, the polarization energy involved is likely to be lower and the F^- and O^{2-} ions would mix nearly ideally with very small heats (if any) of mixing.

As mentioned in chapter 2, the structures of silicates are similar to that in the phosphates and hence the structural information gained on the phosphate glasses can be extended to the silicates. Also, in general the binary silicates seems to have much shallower heats and free energies of mixing curves, than the corresponding borates and phosphates. This would mean a much broader distribution of anions in case of the silicates compared with those in the borates and phosphates. From the review of various models proposed to inter-relate the structure of these polyanionic melts with the thermodynamic properties, it seems that Meadowcroft and Richardson's[25] model is the only one capable of relating quantitatively these two properties for such melts. However, if this model is modified to take into consideration the presence of both chain and ring polyanions, instead only of the chains, it would have an even wider applicability for melts richer

in acid oxide and would be more useful for application to the silicate systems. In many cases metallurgists are interested in basic silicate slags and Meadowcroft and Richardson's model can be usefully applied to these systems, if the anionic distribution in silicates could be determined. As will be seen in the appendix attempts at elucidating the structures from silicate crystals and glasses were unsuccessful.

ACKNOWLEDGEMENTS

I wish to express my gratitude to Dr.J.H.E. Jeffes, who supervised this work, for his interest, guidance and encouragement throughout the course of this work. I am also indebted to Professor F.D. Richardson, for the provision of laboratory facilities and many helpful discussions I have had with him during the course of this work. I am thankful to Dr. P.S. Rogers for the suggestions, criticisms and help during the preparation of this thesis.

I wish to acknowledge M/S Albright and Wilson, for the financial support which enabled this work to be carried out and the staff members of the research department of this company for their continued interest.

I wish to thank, Mr. C. Morcombe, Mr. J. Fecamp, researchers in room 401 and other members of the Nuffield Research Group for their help and suggestions. My thanks are also due to Mr. A.J. Tipple and Mr. V. Ramaswamy for their assistance in the preparation of this thesis.

References

1. Fetters K.L. and Chipman. J. Trans. A.I.M.E., 145, 95 (1941)

2. Taylor C.R. and Chipman J. Trans. A.I.M.E., 154, 228 (1943)

3. Richardson F.D. and Webb L.E. Trans. Inst. Mining Metal 64, 529 (1955)

4. Schumann R. and Ensio P.J. Trans. A.I.M.E., 191 401 (1951)

5. Sharma R.A. and Richardson F.D. J. Iron Steel Inst., 200, 373 (1962)

6. Abraham K.P., Davies M.W. and Richardson F.D. J. Iron steel Inst. 196, 82 (1960)

7. Richardson F.D. and Pillay T.C.M. Trans. Inst. Mining Metal 66, 309 (1957)

8. Rein R.H. and Chipman J. Trans. A.I.M.E. 233, 415 (1965)

9. Bockris J.O.M., Kitchener J.A.,Ignatowicz S. and Tomlinson J.W. Trans. Farad. Soc. 48, 75 (1952); Disc. Farad. Soc. 4, 265 (1948)

10. Bockris J.C.M., Kitchener J.A and Davies A.E. Trans. Farad. Soc. 48, 536 (1952).

11. Bockris J.O.M. and Lowe D.C. Proc. Roy. Soc. A226 ,423 (1954)

12. Bockris J.O.M. and Mellors G.W. J. Phys. Chem. 60 , 1321 (1956)

13. Van Wazer J.R. Phosphorus and its Compounds . Vol. 1. Interscience Publishers, New York (1964)

14. Herasymenko P. Trans. Forad. Soc. 34, 1245 (1938)

15. Flood H. Forland T. and Grjotheim K. Physical Chemistry of Melts, Inst. Mining Metal. London (1953)

16. Temkin M. Acta Phy. Chem. U.R.S.S. 20, 411(1945)

17. Flood H, Forland T. and Grjotheim K. Z. Anorg. Chem. 296, 369(1954)

17a, Forland T. Disc. Farad. Soc. 32 122(1961)

18. Flood H, Forland T. and Grjotheim K., Z. Anorg. Chem. 276, 289(1954)

19. Richardson F.D. Trans. Farad. Soc. 52, 1312(1956)

20. Lumsden J. Disc. Farad. Soc. 32, 138(1961)

21. Lumsden J. Physical Chemistry of Process Metallurgy, Part 1, Interscience. N.Y. 263(1961)

22. Wells A.F. Structural Inorganic Chemistry. Oxford Univ.Press. London, 1962.

23. Eitel W. Silicate Science, Vol.1. (Silicate Structures), Academic Press, 1964

24. Richardson F.D. The Vitreous State, Glass delegacy of the University of Sheffield, p.63.1955

25. Meadowcroft T.R. and Richardson F.D. Trans. Farad Soc. 61, 54(1965)

26. Jameson J.F. J. Chem. Soc. 752 (1959)

27. Private Communication from the research department of Albright and Wilson Ltd.,

28. Lentz C.W. Inorg. Chem. 3 574(1964)

29. Richardson F.D. Physical Chemistry of Steelmaking, M.I.T., Symposium, p.55,(1958)

30. Toop G.W. and Samis C.S. Trans. A.I.M.E. 224, 878(1962)

31. Masson C.R. Proc. Roy.Soc. A287, 201(1965)

32. Knapp W.J. and Flood H. J. Amer. Ceram.Soc. 40; 246(1957)

33. Knapp W.J. and Flood H. ibid. 40, 262(1957)

34. Flood H. and Knapp W.J., ibid. 46 61(1963)

35. Ito. H and Yanagase T., Trans. Japan Inst. Metals. 1 115(1960)

36. Westman A.E.R. and Gartaganis P.A., J. Amer. Ceram. Soc. 40, 293(1957)

37. Cripps-Clark C.J., Ph.D. Thesis, University of London, 1965.

38. Flory P.J. J. Amer. Chem. Soc., 64, 2205(1942)

39. Van Wazer J.R. and Holst K.H., J. Amer. Chem Soc. 72 644(1950)

40. Park J.R. and Van Wazer J.R. J. Amer. Chem. Soc., 79 4890(1957)

41. Van Wazer J.R., Goldstein M. and Faber E. J. Amer. Chem. Soc. 75, 1563(1953)

42. Matula D.W.,Groenweghe L.C.D. and Van Wazer J.R. J. Chem. Phys. 41,3105(1964)

43. Jost K.H. and Wodcke F. Makromol Chem., 53, 1(1962)

44. Westman A.E.R. and Beatty R., J. Amer. Ceram. Soc. 49, 63 (1966)

45. Jeffes J.H.E. and McKerrel H., J. Iron.Steel Inst., 202, 666(1964)

46. Duwez P. and Willens R.H. Trans. A.I.M.E. 227, 362(1963)

47. Gaydon A.G. and Hurle I.R. "The Shock tube in high temperature chemical Physics". Reinhold Press.N.Y.(1963)

48. Westman A.E.R. and Crowther J.P., J. Amer. Ceram. Soc. 37 420(1954)

49. Westman A.E.R.,Smith J. and Garataganis P.A., Can J. Chem. 37, 1764(2959)

50. Smith J. Anal. Chem., 31, 1023(1959)

51. Meadowcroft T.R. Ph.D. Thesis, University of London (1962)

52. Ritland H.N., J. Amer. Ceram. Soc., 37, 370(1954)

53. Poch W., Glastech Ber. 39, 45(1966)

53a. Roye M.P., Private communication.

54. Meadowcroft T.R. and Richardson F.D., Trans. Farad. Soc. 59,1564(1963)

55. Pitzer K.S., Smith W.V. and Latimer W.M. J. Amer. Chem. Soc., 60, 1829(1938)

56. Stevens C.G. and Turkdogan E.T. Trans. Farad. Soc., 50, 370(1954)

57. Fincham C.J.B. and Richardson F.D. Proc. Roy. Soc., A223, 40(1954)

58. Csaki P. and Deitzel A., Glastech. Ber., 18, 33(1940)

59. Didtschenko R and Rochow E.G., J. Amer. Chem. Soc., 76, 3291(1954)

60. Minenko V.I. and Ivanova N.S. Ukr. Khim. Zh., 29, 1160(1963)

61. Delimarskii Yu.K. and Andreeva V.N., Russ J. Inorg. Chem., 5, 873(1960)

62. Bockris J.O'M. and Mellors G.W., J. Phy. Chem. 60,1321(1956)

63. Janz G.J., Ward A.T. , Rensselaer Polytechnic Institute, Troy, N.Y. (1964)

64. Meyer H.W. and Richardson F.D., Trans Inst. Mining Metal, 71, 201(1962)

65. Corbett J.D. and Winbush S.V., J. Amer. Chem. Soc., 77, 3964(1955)

66. Corbett J.D., Winbush S.V. and Albers F.C., J. Amer. Chem. Soc., 79, 3020(1957)

67. Bredig M.A., Molten Salt Chemistry, Ed. Blander Interscience, 1964, p.367

68. Hansen M., Constitution of Binary Alloys, McGraw Hill,(1958)

69. Matsushita Y. and Goto K., J. Fac. Engng. Tokyo Univ. Ser.B. 27,217-80 (1964)

70. Webb L.E., Ph.D. Thesis. University of London, (1953)

70a. Krakau K.A.,Mukhin E.J. and Heinrich M.S., C.R. Acad.Sci. U.R.S.S.(Dokl), 14, 281(1937)

71. Flood H. Forland T. and Motzfelt K., Acta Chem. Scand. 6 257(1952)

72. Ranford R.E. and Flengas S.N., Can. J. Chem. 43, 2879(1965)

73. Elliot J.F. and Gleiser M. Thermochemistry for Steelmaking, Oxford, Pergamon Press (1960)

74. Steele B.C.H., Ph.D. Thesis, Univ. of London. (1965)

75. Alcock C.B. and Belford T.N., Trans. Farad. Soc. 60, 822(1964)

76. Spencer H.M. and Mote J.E., J. Amer. Chem. Soc., 54,4618(1932)

77. Wagman D.D. etal. Selected values of chemical thermodynamic properties. Tech. Note. Natn.Bur.Stand. 270-2,May 1966

78. Rodigina E.N., Gomel'skii K.Z. and Luginina V.F., Russ. J. Phy. Chem. 35, 844(1961)

79. Kvyatkovskii A.N. Esin O.A. and Abdeev M.A., Russ. J. Phy. Chem. 34, 1162(1960)

80. Coughlin J.P., U.S. Bureau of Mines Bulletin 542 (1954)

81. Mitoff S.P., J. Chem. Phy. 36, 1383 (1962)

82. Esin O.A. Sryvalin I.T. and Khlynov V.V., R.J. Inorg. Chem. 2 237 (1957)

83. Jeffes J.H.E. 8th Commonwealth Mining & Metallurgical Congress, Melbourne, 1965

84. Callow R.J. Trans. Farad. Soc., 37, 370(1951)

85. Preston E. and Turner W.E.S. J. Soc. Glass Technol. 19,2960(1935)

86. Kœuka Z. and Samis C.S., Private Communication.

87. Benz. R. and Schmalzried H., Z. Phys. Chem. Frankf. Ausg. 29, 77(1961)

88. Esin O.A. Lepinskikh B.M. and Musikhin V.I., Izvest.Akad. Nauk. S.S.S.R. 4, 47(1959)

89. Geller R.F. Creamer A.S. and Bunting E.N., J.Res.Natn.Bur. Stand. 13, 237(1934)

90. Calvet E and Prat H. Microcalorimetrie, Masson et cie, Paris, (1956)

91. Kleppa O.J. and Yokokawa T. Inorg. Chem. 4, 1806(1965)

92. Shatsis L. and Newman E.S. J.Res.Natn.Bur.Stand., 40,471(1948)

93. Lepinskikh B.M. and Esin O.A., Russ. J. Inorg. Chem. 6, 625(1961)

94. Hirayama C., J. Amer.Ceram.Soc. 43, 505(1960)

95. Geller R.F. and Bunting E.N.,J. Res.Natn.Bur.Stand. 18, 585(1937)

96. Cox. J, Private Communication.

97. Paetsch H.H. and Dietzel A., Glastech.Ber. 29,348(1956)

98. Sandonnini C., Atti.Accad.naz.Lincei.Rc., 23,959(1914)

99. Lumsden J., Thermodynamics of molten salt Mixtures, Academic Press. London. (1966)

100. Delimarskii Yu.K. and Nazarnko G.D., Ukr.Khim.Zh. 27, 458(1961)

101. Abraham K.P. and Richardson F.D., same as reference 21, page 263 (1961)

102. Bray P.J. and O'Keffe J.G.,Phys. and Chem. of Glasses. 4, 37(1963)

103. Bray P.J.,Leventhal M and Hooper ibid. 4, 47(1963)

104. Leventhal M and Bray P.J. ibid 4, 113(1965)

105. Krog-Moe J., ibid 3, 1(1962); 3,101(1962)

106. Schwerdtfeger K and Engell H.J., Arch. Eisenhut. 34, 647(1963)

107. Huhti A.L. and Gartaganis P.A., Can. J. Chem. 34,785(1956)

108. Mitchell A., Trans. Farad. Soc., 62, 3470(1966)

109. Janz G.J., Estimation of thermodynamic properties of organic compounds, Academic Press. N.Y. (1958)

Appendix-I

Study of Silicate Structures

The present state of knowledge of the structure of silicate melts is derived from studies of structure sensitive properties of these melts and from the investigation of constitution of phosphate glasses. However, it is desirable to have a knowledge of the exact distribution of silicate anions in these melts and glasses. Lentz[28] has recently reported some work on extracting structures from silicate minerals.

In his method Lentz extracts the structures as a trimethyl silyl derivatives. This is done by treating the finely ground minerals with a previously homogenised mixture of concentrated hydrochloric acid and hexamethyl siloxane $[(CH_3)_3 Si]_2 O$. It is presumed that HCl liberates the silicate anion from the mineral which reacts with mono functional organosilicon compound $(CH_3)_3 SiCl$ or $(CH_3)_3 SiOH$ to give the trimethyl silyl derivative. The reaction sequence can be illustrated with the following equations:

$$Mg_4 SiO_4 + {}_4 HCl = H_4 SiO_4 + 2 MgCl_2$$

$$H_4 SiO_4 + \begin{matrix} 4\ (Me)_3 SiCl \\ \text{or} \\ 4\ (Me)_3 SiOH \end{matrix} = (Me_3 Si)_4 SiO_4 + \begin{matrix} 4\ HCl \\ \text{or} \\ 2\ H_2O \end{matrix}$$

where Me is (CH_3) group.

The $Me_3 SiCl$ or $Me_3 SiOH$ for the trimethylsilylation reaction is derived from the interaction of HCl with $(Me_3 Si)_2 O$.

$$(Me_3 Si)_2 O + HCl = Me_3 SiCl + Me_3 SiOH$$

Table Ap-1

Summary of Silicate Structures Derived from Minerals.

Mineral	% Si Recovered as				
	SiO_4	Si_2O_7	Si_3O_{10}	$(SiO_3)_4$	Total
olivine, $(Mg,Fe)_2SiO_4$	70.0	11.1			81.1
Hemimorphite, $Zn_4(Si_2O_7)(OH)_2.H_2O$	22.0	77.6	2.4		102.0
Sodalite, $Na_8(AlSiO_4)_6Cl_2$	76.0	8.7	2.5		87.2
Natrolite, $Na_2(Al_2Si_3O_{10}).2H_2O$	10.0	13.1	67.5		90.6
Lammontite, $CaAl_2Si_4O_{12}.\ 4H_2O$	-	-	-	80.9	80.9

It is not known which species is the trimethylsilylating reagent. Either one is probably capable of reacting with silicic acid.

Though Lentz[28] claims that he is extracting the structures intact, this is not exactly true, as can be seen from table Ap-1, where some of his results are summarized. It can be seen that the recovery is not 100%, but it is believed that this could be improved by adjusting the concentration. The more severe drawback is the possibility of not only hydrolysis but also polymerisation taking place. This is to be expected as silicates unlike the phosphates rapidly polymerise and depolymerise in aqueous solutions and the species in the solution is unlikely to be representative of the sample. This is well borne out in the fact that olivine an ortho-silicate (cf. table Ap-1) produces 11.1% pyro ion and Hemimorphite, a pyrosilicate gives 22% of ortho and 2.4% tripolysilicate by this method. Therefore, it can be seen that this was not a suitable method for studying silicate glass structures as the distribution obtained will not be representative of the glass. Another drawback of the Lentz method was that the gas-liquid chromatography which is used to separate the organosilican derivate into various fractions cannot separate trimethyl silyl silicates containing more than four silicon atoms. This is because the present day gas-liquid chromatographs cannot operate much above 250°C, and with increasing number of silicon atoms, the derivatives have large molecular weights and low volatilities. Some preliminary studies using

Lentz's technique using crystalline and glassy sodium silicates confirmed the above observations.

The obvious solution to this problem appeared to be to produce a lower molecular weight derivative and to avoid any aqueous phase polymerisation or depolymerisation. Since the existence of polymethyl silicates are well established, it was logical to attempt at making a methyl derivative. The available methylating agents were the methyl halides, dimethyl sulphate and diazomethane in the order of increasing reactivity. Dimethyl sulphate was chosen as a compromise between reactivity and toxicity. The thermodynamics of the methylation process was interesting to be looked into. The survey of literature revealed that the heat of formation of a common methylating agent, dimethyl sulphate, is not known. Hence it was estimated using the bond energy consideration as follows:

For H_2SO_4

$$2H_2 + S_2 + O_2 = 2\,H_2SO_4$$

$$\Delta H_f = -4\,E_{(H-O)} - 2\,E_{SO_2} + 2\,E_{(H-H)} + 4\,E_{(O-O)} + E_{(S-S)}$$

Janz[109] give the energy of bonds $E_{(H-O)}$, $E_{(H-H)}$, $E_{(O-O)}$ to be 109.4, 103.2, and 34 K. cals respectively.

Substituting for ΔH_f of H_2SO_4 (-200.0 K.cals)

$$E_{S-S} - 2\,E_{SO_2} - = -105.0 \text{ K.cals.}$$

with a value for $E_{(S-S)} - 2\,E_{SO_2}$ we can estimate the ΔH_f for $(CH_3)_2 SO_4$

For $(CH_3)_2 SO_4$

$$4C + 6H_2 + 4O_2 + S_2 = 2\,(CH_3)_2 SO_4$$

$$\Delta H_f = -12\,E_{(H-H)} - 4\,E_{(C-O)} + 2\,E_{SO_2} + 6\,E_{(H-H)} + 4\,E_C + 4\,E_{(O-O)} + E_{(S-S)}$$

Jantz gives a value of 98.2 and 79.0 K.cals for bond energies $E_{(C-H)}$, and $E_{(C-O)}$, respectively. Substituting these values,

$$\Delta H_f = -165.\ \text{K.cals/mole (for dimethyl sulphate)}$$

A similar estimate for the heat of formation of ethyl sulphuric acid resulted in a value of 184.0 K.cals. compared to -208 K.cals reported in the literature. Though this method of estimation gives heats of formation of the right order, it is not very accurate.

Using the estimated value of ΔH_f for $(CH_3)_2 SO_4$, the heat change for the reaction

$$2\,(CH_3)_2 SO_4 + Na_4SiO_4 = (CH_3)_2 SiO_4 + 2\,Na_2 SO_4$$

iscalculated as -570 K.cals taking the following values for the heats of formation for the compounds Na_4SiO_4 -88.85 K.cals; $(CH_3)_4 SiO_4$ -300.0 K.cals,and Na_2SO_4 -688.9 K.cals.

Even if this estimate is of the right order the methylation reaction should take place with a large evolution of heat. However, all attempts at methylating the silicates failed. Even the combination

of high pressure and temperature studied by Mr. Roye did not yield any results. Also attempts at using diazomethane in ether was also unsuccessful in methylating the silicate. Therefore, it was not possible to elucidate the structure of the silicate glasses in a manner analogous to the phosphate, using a chemical treatment followed by chromatographic separation of the anionic species.